

**FLOW BEHAVIOUR OF BIOPOLYMER SOLUTIONS
AND EFFECT ON SALTINESS PERCEPTION**

By

Anne-Laure Koliandris BSc. MSc

Thesis submitted to the University of Nottingham
for the degree of Doctor of Philosophy

Division of Food Sciences
School of Biosciences
University of Nottingham
Loughborough
LE12 5RD

November 2010

TABLE OF CONTENT

Table of content	i
Abstract	v
Acknowledgments	vii
List of abbreviations and symbols	ix
Chapter 1 Introduction	1
1.1 Reduction of sodium in food products	4
1.2 Fundamentals of flavour perception and saltiness perception.....	7
1.2.1 Taste and flavour perception.....	7
1.2.2 In-mouth processes.....	11
1.3 Taste perception in viscous systems.....	14
1.3.1 Flow parameters relevant to taste perception	17
1.3.2 Mechanisms underlying taste perception in viscous solutions.....	19
1.4 Flow behaviour.....	23
1.4.1 Introduction	23
1.4.2 Fundamentals	25
1.4.3 Filament break-up.....	29
1.4.4 Micro-contraction flow device	32
1.5 Thesis organisation.....	34
Chapter 2 Materials and methods	36
2.1 Materials.....	37
2.2 Rheological methods.....	37
2.2.1 Thin film rheology	37
2.2.2 Small amplitude oscillatory shear	40
2.2.3 Filament break-up.....	40
2.2.4 Micro-contraction flow	41
2.3 Sensory methods.....	44
2.3.1 Attribute difference test.....	44
2.3.2 Triangle tests.....	46
2.3.3 Rank rating.....	46
2.4 Other methods.....	47

Chapter 3 Effect of shear flow behaviour on saltiness perception.....	48
3.1 Introduction.....	49
3.2 Materials and methods	50
3.2.1 Materials and preparation of the polysaccharide solutions	50
3.2.2 Characterisation of polysaccharide solutions	52
3.2.3 Experimental designs and sensory analysis.....	53
3.3 Results and discussion.....	63
3.3.1 Study A: Is high shear or low shear viscosity relevant to saltiness perception?.....	63
3.3.2 Study B: Is the <i>zero</i> shear viscosity or viscosity measured at <i>low</i> shear (10-50 s ⁻¹) relevant to saltiness perception?.....	69
3.3.3 Study C: To which extent is saltiness perception affected by polymer concentration?	73
3.3.4 Mouthfeel perception.....	81
3.4 Conclusions	85
Chapter 4 Food grade Boger fluids	86
4.1 Introduction.....	87
4.2 Materials and methods	90
4.2.1 Newtonian solvents.....	90
4.2.2 Elasticity imparting polymers.....	90
4.2.3 Additives	91
4.2.4 Sample preparation and compositions.....	91
4.2.5 Rheological characterisation.....	93
4.2.6 Sensory methods.....	96
4.2.7 Qualitative analysis of sample mixing with oral fluids.....	98
4.3 Results and discussion.....	99
4.3.1 Sample Rheology	99
4.3.2 Saltiness and mouthfeel perception.....	110
4.3.3 Mixing experiment	117
4.4 Conclusions	119
Chapter 5 Shear and extensional rheology of polysaccharide solutions of various molecular structures.....	120
5.1 Introduction.....	121
5.2 Polysaccharides used in this research	123
5.2.1 Galactomannans.....	123

Table of content

5.2.2	Xanthan gum.....	124
5.2.3	Dextran.....	125
5.2.4	Pullulan.....	126
5.2.5	Methylcellulose.....	127
5.2.6	Xyloglucans.....	128
5.2.7	Konjac Mannan.....	129
5.3	Polymer conformation and solution properties.....	130
5.3.1	Introduction.....	131
5.3.2	Polysaccharide chain flexibility.....	133
5.3.3	Concentration dependence of polymer solution behaviour.....	136
5.4	Extensional flow behaviour of polymer solutions.....	141
5.4.1	Characterisation of solution viscoelasticity using a filament break-up device.....	143
5.4.2	Characterisation of solution viscoelasticity using Micro-contraction flow.....	145
5.5	Materials and methods.....	151
5.5.1	Materials.....	151
5.5.2	Sample preparation.....	152
5.5.3	Rotational rheology.....	154
5.5.4	Filament break-up.....	155
5.5.5	Micro-contraction flow.....	155
5.5.6	Molecular weight.....	156
5.5.7	Density.....	157
5.5.8	Surface tension.....	157
5.6	Results and discussions.....	158
5.6.1	Molecular behaviour.....	158
5.6.2	Large deformation shear behaviour.....	166
5.6.3	Viscoelastic behaviour of polysaccharide solutions.....	170
5.7	Conclusions.....	196

Chapter 6 Emulsion interface stabilisation by chemical cross-linking of adsorbed protein..... 199

6.1	Introduction.....	200
6.1.1	Bovine serum albumin as emulsifier.....	201
6.1.2	Cross-linking of proteins.....	203
6.1.3	EDC mediated cross-linking of protein-polysaccharides.....	208
6.1.4	Competition protein/surfactant at the interface as a tool to investigate interfacial cross-linking of BSA.....	210
6.1.5	Duplex emulsions.....	212
6.2	Materials and methods.....	214

Table of content

6.2.1	Materials	214
6.2.2	Method to demonstrate successful cross-linking.....	215
6.2.3	Single emulsion preparation	216
6.2.4	Duplex emulsions preparation	219
6.2.5	Quantification of BSA in the serum	220
6.2.6	Measurement of emulsion droplet size.....	222
6.2.7	Optical light microscopy	224
6.2.8	Rheology	224
6.2.9	pH adjustment	225
6.2.10	Statistical analysis.....	225
6.2.11	Experimental plan	225
6.3	Results and discussion.....	227
6.3.1	<i>Reference conditions</i> : displacement of BSA from the interface by Tween® 20 without pH adjustment.....	227
6.3.2	Effect of pH on the displacement of BSA from the interface by Tween® 20 233	
6.3.3	Effect of the presence of pectin on the displacement of BSA from the interface by Tween® 20.....	241
6.3.4	Effect of the presence of PGPR on the displacement of BSA from the interface by Tween® 20.....	245
6.3.5	Duplex emulsions	249
6.4	Conclusions.....	254
Chapter 7 Overall general conclusions.....		258
7.1	Implications of this thesis.....	259
7.1.1	Work on thickened aqueous solutions	259
7.1.2	Emulsions	263
7.2	Future directions	264
7.3	Summary of the findings.....	266
Bibliographic references.....		267
Appendices to chapter 2.....		293
Appendices to chapter 3.....		300
Appendices to chapter 4.....		303
Appendices to chapter 5.....		304

ABSTRACT

In order to improve public health, active measures are taken to lower the salt (sodium chloride) consumption of the population. However, significant effort is required to reduce salt content in processed foods without adversely affecting taste, flavour and consumer preference. This research aimed at investigating how the saltiness efficiency of sodium chloride could be improved.

The first approach investigated the relationship between rheology and taste perception to evaluate whether it is possible to enhance saltiness perception through careful design of product rheology. The objective was to identify the flow parameters correlating to saltiness perception. The shear rate relevant to saltiness perception was investigated using a range of typical solution flow behaviour (Newtonian, shear-thinning, yield behaviour). It was found that saltiness perception is related to viscosity measured at low shear ($1-10 \text{ s}^{-1}$) and not to zero shear or high shear viscosity. An enhancement of saltiness perception was found for very high polymer concentrations, which could be explained by the increased osmolality of these solutions. Subsequently, food grade Boger fluids (Newtonian fluids of high elasticity) were formulated and characterised to investigate whether extensional viscosity impacts saltiness perception. As no clear effect was reported, hypothesised to be due to the unfavourable mouthfeel of the relatively thick fluids, an alternative approach using

low viscosity polysaccharide solutions of identical shear behaviour but of different extensional behaviour was taken. Extensional behaviour of polysaccharide solutions in large deformation flow has received very little attention compared to shear flow behaviour and was characterised here using the techniques of filament break-up and microfluidics as preliminary work for future sensory studies. Large differences in elasticity among polysaccharides and singularities of polysaccharides compared to synthetic polymers were found.

As a second approach it was investigated whether duplex emulsions could be stabilised by chemical cross-linking of proteins adsorbed at the oil-water interface. The interest in duplex emulsions is based on the hypothesis that increase in the salt concentration in the continuous product phase of an emulsion-based food may increase saltiness perception. Formulation of stable food duplex emulsions is challenging and here it was shown that chemical cross-linking of Bovine Serum Albumin (BSA) adsorbed at the oil-water interface improved stability towards coalescence and emptying out of the internal water phase. The interface of single oil-in-water emulsions was also successfully cross-linked.

Both the industrial impact and fundamental interest of this research were discussed.

ACKNOWLEDGMENTS

Those three years of PhD were a fantastic journey during which I have never felt alone but always guided and accompanied by many great people I would like to thank here.

First of all, I would like to thank my supervisors Dr. Bettina Wolf and Prof. Andy J. Taylor for entrusting this fascinating project to me and for their guidance, support and many fruitful discussions. I am in particular indebted to Bettina for introducing me to the great world of Rheology.

I must thank the Technology Strategy Board's Collaborative Research and Development programme for their financial support and all the partners in that project: Unilever, Fluent-Ansys and the University of Birmingham, in particular Dr. Serafim Bakalis. From the 'Nottingham team', I would like to thank Dr. Louise Hewson for her help with the sensory part, Dr. Mita Lad for providing me the surface tension data and specially Dr. Cecile Morris for her great contribution in the project. Her experience, pertinence and friendship were really valuable. I also would like to express my gratitude to Dr. Jason Stokes for his interesting comments and discussions. Thanks to Danisco, Dainippon Sumitomo Pharma and Shimizu for kindly providing some of the polysaccharides.

I shall also express my gratitude to all the staff in Sutton Bonington. There was always someone there to discuss any particular issue: to Dr. Joanne Hort for her guidance through the sensory work, to Dr. Rob Linforth for his help with experimental design, to Dr. Gordon Morris for his insights on biopolymer flexibility and practical help with molecular weight determination, to Dr. Tim Foster for his great knowledge of polysaccharides and to Prof. John Mitchell for the great discussions we had on various aspects of the projects. I also shall thank all the technical staff in SB for their support and help! I had that 'special link' with the UoN for the last 5 years of my life, and I

Acknowledgments

really feel that I am indebted to all of you for the outstanding scientific formation you gave me.

I had the fantastic opportunity to spend a month in at the University of Queensland (Brisbane, Australia) to carry out the microfluidics work. I would first of all like to thank Prof. Justin Cooper-White for welcoming me in his lab and sharing with me his understanding of polymer solutions. I would also like to warmly thank Dr. Elisabeth Rondeau and Dr. Edeline Wong for taking the time to help me in the lab. Finally, I would like to thank the School of Bioscience of the University of Nottingham and U21 committee for their financial support.

I would like to express my gratitude to the students that directly worked on this project: Feng Miao for biopolymer characterisation, Christophe Michon for the osmolality work and Ruodan Jiang for the CaBER commissioning. It would be a mistake not to thank all those who participated to the sensory tests (from the University of Nottingham's external sensory panel and from the students and staff in Food Science) for their kindness to try weird salty solutions. Thanks to them also for their constructive feedback on all the new cakes recipes I have tested on them as a reward for their help!

During my time in Nottingham I have made numerous good friends which gave an enjoyable lively atmosphere at work. Listing them all will be difficult as many left and many arrived so a big thanks to all of them (you know who you are).

Finally, I want to express a great thanks to my parents and my husband Andreas, for their continuous love and support. If I hadn't met Andreas, I would most likely *not* be writing this thesis. You were always there for me, and your encouragements always helped me move forward again when things were difficult.

LIST OF ABBREVIATIONS AND SYMBOLS

BSA	Bovine serum albumin
BCA	Bicinchoninic acid
CaBER	Capillary break-up extensional rheometer
DSD	Droplet size distribution
EDC	1-(3-Dimethylaminopropyl)-3-ethylcarbodiimide hydrochloride
EI	Elasticity number
FSA	Food standard agency
HPMC	Hydroxypropyl methylcellulose
IEP	Isoelectric point
LBG	Locust bean gum
MC	(or MCellulose) Methylcellulose
Na-Alg	Sodium alginate
NaCl	Sodium chloride, 'salt'
Na-CMC	Sodium carboxymethyl cellulose
PEO	Polyethylene oxide
PGPR	Polyglycerol polyricinoleate
Re	Reynolds number
SAOS	Small angle oscillatory shear
SDS	Sodium dodecyl sulfate

List of abbreviations and symbols

SEC-MALS	Size exclusion chromatography-multi-angle light scattering
TRC	Taste receptor cells
Wi	Weissenberg number

List of symbols

$c \cdot [\eta]$	Degree of coil occupancy
$d(t)$	Mid-point diameter of the filament as a function of time (filament break-up experiment)
η_s	Shear viscosity
η_e	Extensional viscosity
η_{SP}	Specific viscosity
$[\eta]$	Intrinsic viscosity
$\dot{\gamma}$	Shear rate
λ	Characteristic time scale for viscoelastic stress growth in uniaxial elongational flow or simply 'relaxation time'
ρ	Fluid density
Q	Volumetric flow rate in the channel (micro-contraction flow device)
w_c	Width of the contraction (micro-contraction flow device)
h	Height of the channel (micro-contraction flow device)

CHAPTER 1
INTRODUCTION

This PhD project was embedded in a UK Government sponsored Technology Programme project entitled 'Complex microstructures and processes for reduction of salt' (TP/6/DAM/6/S/K3004C). The project was led by Unilever UK and with Ansys, the University of Nottingham and The University of Birmingham as further partners. The aim of the project was to develop and demonstrate advanced technologies that allow significant salt (NaCl) reduction in semi-liquid processed foods. The technological approach investigated at Nottingham included seeking routes to enhance saltiness perception through manipulation of the in-mouth delivery profile of salt to the taste buds. This was thoroughly tested by delivering different temporal profiles of salt and the main conclusion was that saltiness perception was governed by the overall amount of salt delivered in the profile, not by the actual profile (Morris et al., 2009; Morris et al., 2010). As a result of this finding, the project focus moved on to increasing the concentration and, thus, the saltiness efficiency of salt in the external aqueous phase of food products. This is achievable in oil-in-water emulsion based foods by increasing the oil fraction to concentrate the salt in the external aqueous phase as it has previously been shown (Malone, Appelqvist and Norton, 2003b). However, high fat products are also not desirable. Inclusions of water within the oil droplets (water-in-oil-in-water emulsion or duplex emulsion) allow a concurrent reduction of the fat content and an increase of the salt concentration in the external water phase. The problem with duplex emulsions, however, is microstructure instability, as 'emptying out' of the oil droplets is commonly observed in the presence

of ionic species (Garti, Aserin and Cohen, 1994). This PhD research included evaluation of chemical cross-linking of interfacially adsorbed protein as a mechanism to manufacture duplex emulsions stable in complex food formulations. The major part of this PhD research, however, was concerned with the effect of food thickeners on saltiness perception. Nearly all processed semi-liquid foods contain some sort of thickener and the fundamental question asked here was: *can an informed choice of a food thickener, exhibiting specific flow behaviour, enhance saltiness perception of the thickened solution, thus allowing a reduction of salt content in foods without loss of flavour?* It is known that saltiness perception is affected by flow properties of foods, however the flow parameters correlated to saltiness perception remain to be determined. It was thus hypothesised that a more thorough understanding of the relationships between flow behaviour of foods and saltiness perception would enable guidelines to be offered which could optimise low salt products formulations. A wide range of flow behaviour was studied and characterised over a large range of shear and extensional deformation. A substantial amount of sensory work was conducted in order to ‘record’ saltiness perception in various thickened solutions. This introductory chapter is organised as follows: firstly (1.1), the motivations for sodium reduction in food product will be presented. The literature on taste perception in viscous systems will be reviewed in 1.3 after an introduction to the fundamentals of flavour perception (1.2). Finally, fundamental elements on flow behaviour will be presented in 1.4.

1.1 REDUCTION OF SODIUM IN FOOD PRODUCTS

Sodium (Na^+) is one of the main ions present in plasma, whereas intracellular fluids are low in sodium and rich in potassium (K^+). This imbalance is essential to many physiological mechanisms such as muscle and nerve activity and therefore sodium is an essential component of the human diet (Morris, Na and Johnson, 2007). The ancestral diet, mainly based on fruits and vegetables, was rich in potassium but quite poor in sodium (Laplaize, 2007). Mammals thus may have developed the ability to identify sources of sodium through saltiness perception (Kilcast and Angus, 2007; Morris et al., 2007). Even for humans today, experimental evidence of salt craving following sodium depletion exists (Beauchamp et al., 1990; Leshem, Abutbul and Eilon, 1999).

Humans, like other mammals, are genetically adapted to consume a very small amount of salt (0.25 g/day). About 5000 years ago, the Chinese discovered that salt could be used to preserve foods and salt intake gradually increased, reaching an average of 18 g/day in the 19th century in Europe (Kilcast and Angus, 2007). With the invention of the refrigerator, salt was no longer required as a preservative and salt intake declined. However, with the increased availability of processed foods in the 20th century, salt intake increased dramatically as many processed foods contain high amounts of salt. The main reasons for adding salt to processed foods is as flavour enhancer, preservative and processing agent (Kilcast and Angus, 2007). In semi-liquid

products, such as soups and sauces, sodium is essential to improve the sensory perception. Not only does it impart a primary salty taste but it is an essential ingredient to optimise the overall flavour balance (Beauchamp, Bertino and Moran, 1982; Bertino, Beauchamp and Engelman, 1982; Hutton, 2000). Some soups contain as much as 3 g salt per portion (350 g serving).

The vast majority (77%) of salt consumed comes from processed foods, whereas only 11% is added by the consumer during cooking or eating (the remaining 12% is naturally occurring in foods) (Jacobson, 2005). Nowadays, the average salt intake in most countries around the world is approximately 9 to 12 g/day, whereas 2 g/day may be sufficient. This overconsumption of salt impacts on the health of the population therefore increasing health care costs.

There is substantial evidence that excess consumption of salt is the major cause of high blood pressure (hypertension) and that a reduction in salt intake lowers blood pressure (Mohan and Campbell, 2009; He and MacGregor, 2010). High blood pressure is one of the key cardiovascular disease risk factors accounting for nearly two-thirds of all strokes and a half of all coronary heart diseases. Along with hypertension, atherosclerosis, osteoporosis, kidney damage and stomach cancer have also been associated with excessive sodium intake. The physiology underlying the association with excessive sodium intake is detailed elsewhere (He and MacGregor, 2010).

Cardiovascular diseases are the single largest risk factor for early death both in developed and developing countries and high blood pressure is considered as the leading cause of preventable illness and death after smoking. It is therefore considered that a reduction in salt intake would result in a major improvement in public health and it was estimated to be at least as cost-effective as tobacco control (He and MacGregor, 2010). This is why health authorities in most developed countries are aiming to reduce the salt intake to 4-6 g/day, by informing consumers of the risk and setting the food industry targets to reduce salt in processed foods (He and MacGregor, 2010).

Food companies have been urged to reduce salt in processed foods to meet the health agencies guidelines for salt reduction. Simple removal of salt from product formulation is possible in small quantities as this may be undetected by the consumer. However, large reduction of salt content to meet the governmental targets will be difficult as taste, flavour and consumer's preference are likely to be adversely affected. A different approach is to match the salty flavour of the original formulation, while reducing the actual amount of sodium chloride. This can be achieved by using salt replacers such as potassium chloride (KCl), salt enhancers which enhance the salty taste in combination with NaCl (such as monosodium glutamate) or by enhancing the salt efficiency (Kilcast and Angus, 2007; Dotsch et al., 2009). The objective of the later

approach is to increase the availability of sodium chloride at the place of being tasted to optimise delivered saltiness and was the focus of this PhD.

1.2 FUNDAMENTALS OF FLAVOUR PERCEPTION AND SALTINESS PERCEPTION

The perception of flavour results from the cognitive combination of two senses, the sense of smell and the sense of taste. The sense of smell, or aroma, results from the perception of volatile compounds by the olfactory epithelium whereas non-volatile compounds are sensed by the taste buds on the tongue (taste). The flavour perceived while eating a food product is determined by the nature and quantity of the flavour components (aroma and tastants), the availability of these components to the sensory system which is influenced by in-mouth processing of the food and cognitive mechanisms. These different factors are briefly reviewed in the following sections where the focus is on perception of salty taste.

1.2.1 TASTE AND FLAVOUR PERCEPTION

The anatomical units of taste detection are taste receptor cells (TRCs). As depicted in Figure 1.1, TRCs are assembled into taste buds, which are distributed across the tongue's papillae. Each TRC is tuned to one or multiple taste modalities (salty, sweet, bitter, sour or umami) (Yoshida and Ninomiya, 2010). In addition, it is now believed

that there is no tongue 'map' but that responsiveness to the five basic tastes is present in all areas of the tongue (Chandrashekar et al., 2006).

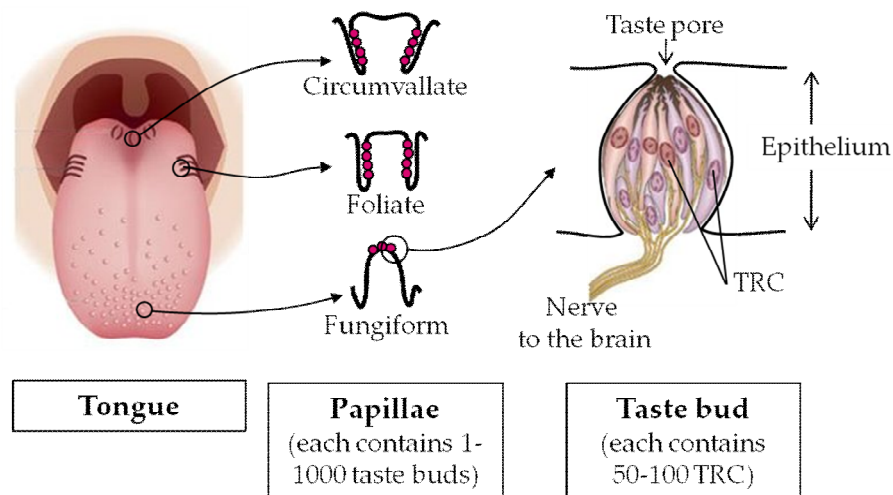


Figure 1.1: Taste receptor cells, buds and papillae (modified from Chandrashekar et al. (2006) and Breslin and Spector (2008)).

The salt 'receptors' in the TRCs and the molecular mechanisms of saltiness transduction remain controversial (Chandrashekar et al., 2006; Breslin and Spector, 2008; Stahler et al., 2008; Ishimaru, 2009). A simple model is depicted in Figure 1.2. Saltiness perception is mediated by ion channels. Na^+ penetrates the TRCs through Na^+ channels located at the mucosal side of the cell ('outside of the tongue'). Such channels are called 'amiloride sensitive' as their activity is inhibited by amiloride. The influx of Na^+ induces a depolarisation of the cell and ultimately results in the release of neurotransmitters which activate gustatory nerve fibres. However in contrast to rodents, the amiloride sensitive sodium channel is not the only transducer of salt taste

in humans (Ossebaard and Smith, 1995). Amiloride insensitive channels are present in the serosal side of the epithelium so that solutes have to diffuse through the 'tight junctions' linking the TRCs to penetrate the cells through amiloride insensitive channels (Stewart, DeSimone and Hill, 1997; Michlig, Damak and Le Coutre, 2007). The size of anion in Na^+ salts will affect the diffusion through the tight junctions, which is thought to explain the differences in salty taste of the various Na^+ salts (Schiffman, McElroy and Erickson, 1980; Ye, Heck and Desimone, 1991; Delwiche, Halpern and Desimone, 1999).

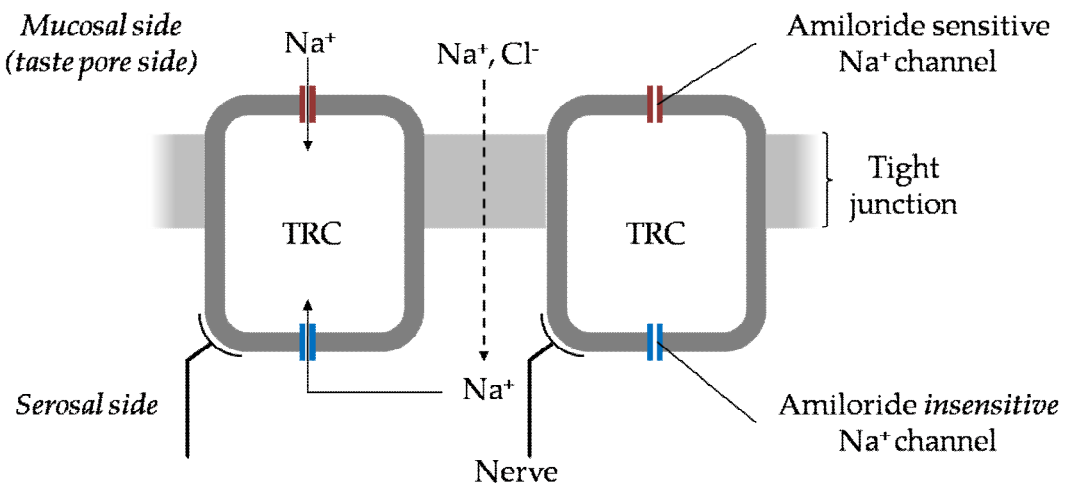


Figure 1.2: Diagrammatic representation of the transduction of saltiness at the cellular level.

Taste receptor cells are designed to respond to changes compared to 'resting conditions' in mouth. For example, it has been shown that an increase in Na^+ concentration in saliva impairs saltiness sensitivity (Delwiche and Omahony, 1996),

and that the neuronal response to Na⁺ stimulation increases for hyperosmotic (relative to saliva) solutions (Lyll et al., 1999). As salivary Na⁺ concentration and osmolarity at rest differ across individuals, this, together with other genetic differences, may explain the large inter-individual variability of saltiness sensitivity reported (Johansson et al., 1973).

The perception of saltiness naturally depends on the concentration of tastant as described by Stevens's law (Stevens, 1969) but is also time-dependent as the perception follows a time-intensity profile and continuous exposure leads to adaptation (Lawless and Heymann, 1997). In addition, saltiness perception is strongly affected by the presence in the food matrix of other flavour compounds (aroma or tastants). Binary taste-taste interactions (Keast and Breslin, 2003) and aroma-taste interactions (Noble, 1996; Djordjevic, Zatorre and Jones-Gotman, 2004; Bult, de Wijk and Hummel, 2007; Stevenson and Tomiczek, 2007) are well documented and represent a strategy for salt reduction in food. For example, addition of monosodium glutamate (Roininen, Lahteenmaki and Tuorila, 1996) or aroma associated with salty food such as ham or cheese (Kostyra and Barylko-Pikielna, 2007; Lawrence et al., 2009) to low-salt products was reported to enhance the perceived saltiness.

Understanding taste perception is of the utmost importance as there is evidence that taste perception 'drives' overall flavour perception: a reduction in taste perception is

sufficient to induce a reduction in aroma perception, even if the aroma concentration remains unchanged (Hollowood, Linforth and Taylor, 2002; Cook et al., 2003a; Koliandris et al., 2007). In this research, NaCl was used in absence of other flavour compounds to avoid any taste-taste or taste-aroma interactions and to focus on the effect of rheological behaviour of semi-liquid foods on taste perception. In order to be perceived, tastant molecules are transferred from the food matrix to the saliva surrounding the taste buds as a result of in-mouth processing of the food.

1.2.2 IN-MOUTH PROCESSES

Food samples undergo several phenomena when placed in the mouth for consumption. First, the sample's temperature changes to reach body temperature, 37 °C. This has dramatic consequences on the flavour perception of products such as ice cream, chocolate or gelatin-based gummy sweets as it induces melting. For semi-liquid products, however, the effect of temperature change on taste and flavour perception is weak (Rosett et al., 1997; Engelen et al., 2003). Any food -liquid or solid- will also be mixed with saliva in the mouth. Among other functions (Humphrey and Williamson, 2001), saliva is essential to taste perception as it conveys the tastants to the taste buds and patients with xerostomia (dry mouth syndrome) have a diminished sense of taste (reported in Davies et al. (2009)). The rheology of saliva as affected by food consumption is currently the object of many studies (Park et al., 2007; van Aken, Vingerhoeds and de Hoog, 2007; Davies et al., 2009). Upon mixing with saliva, the

viscosity of the more viscous foods decreases whereas it increases for low viscosity foods. The efficiency of mixing is likely to depend on the viscosity and the microstructure of the food (Desse et al., 2010), the residence time of the sample in the mouth (Parkinson and Sherman, 1971), as well as the relative volume of both saliva and food products. It is also extremely dependent on the forces applied by the jaws and the tongue.

The forces exerted in the mouth during consumption have been the object of many studies but are still debated. A more complete review can be found elsewhere (Van Vliet, 2002). For many years, the magnitude of the forces applied in the mouth were estimated through perception of thickness: the correlation between thickness perception and shear flow viscosity was considered to be best for the shear rate occurring in the mouth. The well renowned '50 s⁻¹' was obtained by Wood (1968) using this method with semi-liquid products. Other authors found that thickness perception was better correlated to shear viscosity at 10 s⁻¹ (Cutler, Morris and Taylor, 1983) or to complex viscosity at 50 rad.s⁻¹ (Richardson et al., 1989). According to Shama and Sherman (1973), the forces exerted on a food depend on the product consistency. They found that sensory evaluation of thickness in fluids samples was a function of the shear rate developed for a constant shear stress (~10 Pa), whereas for thicker samples, sensory evaluation of thickness was a function of the shear stress developed at a

constant shear rate (10 s^{-1}). Later, Takashi and Kakazawa (1991) confirmed with experimental data that palatal pressure varies with product viscosity.

As thickness perception does not necessarily occur at average forces exerted in the mouth, models were established. Kokini and co-workers proposed a calculation for the oral shear stress (Kokini, Kadane and Cussler, 1977; Kokini and Cussler, 1983; Kokini, 1985). The so-called Kokini oral shear stress is a theoretical calculation of the shear stress applied to the fluid at the tip of the tongue. This calculation assumes a 'parallel-plate model', with a cylindrical plug of fluid compressed between the tongue and the roof of the mouth. In this model, the rheological properties of the food are considered using power law parameters. Thanks to computer simulation, in-mouth processing of foods was revisited by Nicosia and Robbins (2001). Based on assuming squeeze flow conditions (as before by Sharma and Sherman (1973) and Kokini et al. (1977)) these authors found that the transient shear rate in the mouth could be as high as 10^5 s^{-1} , more than 4 orders of magnitudes higher than 50 s^{-1} , generally considered as the in-mouth shear rate. This recent numerical analysis has triggered growing research interest in product rheology at very high shear rates or in thin films (tribology) (Gans, Watson and Tabak, 1990; de Vicente, Stokes and Spikes, 2006; Stokes et al., 2008).

The construction of an accurate model for in-mouth processes during food consumption is a very difficult task. The squeeze flow model has been criticised as

tongue and palate are not two parallel plates. In addition, the flow may be turbulent (Parkinson and Sherman, 1971) and is likely to be time-dependent. Finally, a combination of forces is exerted in mouth: squeeze flow, shear flow and plug flow, thus a combination of shear and extensional flow. Presence of extensional flow components during in-mouth processing has often been suggested, but not conclusively proven.

1.3 TASTE PERCEPTION IN VISCOUS SYSTEMS

The effect of viscosity on taste perception, mostly sweetness, has been studied for more than 50 years, see Table 1.1. In most cases model foods were used, however, some reports based on 'real' food products such as tomato juice (Pangborn, Gibbs and Tassan, 1978), chicken broth (Rosett et al., 1996), soups (Kremer, Mojet and Kroeze, 2005) or mayonnaise (Kostyra and Barylko-Pikielna, 2007) can also be found.

The effect of sample's viscosity on taste perception has been reported to be taste-specific. Pangborn and Trabue (1973) and Moskowitz and Arabie (1970) found that perception of the different taste modalities was lowered when the viscosity was increased, but saltiness was the taste modality the least affected by viscosity. Other researchers reported that increasing viscosity significantly decreased saltiness and sweetness perception but not sourness and bitterness (Lynch et al., 1993; Cook et al., 2002). The effect of cooling the tongue (Green and Frankmann, 1987) or coating it with

oil (Lynch et al., 1993) prior to sensory testing was also found to have different effects on the four basic taste modalities. In the following, literature on taste perception in viscous solutions will be reviewed. The focus will be on saltiness perception, yet results from other taste modalities will be reported since the majority of the relevant literature was concerned with sweetness perception.

Table 1.1: Summary of papers studying the effect of viscosity on taste perception ordered chronologically

Source	Tastant and aroma					Polymers	Experimental design	Flow behaviour /viscosity
	Salty	Sweet	Acid	Sour	Volatile			
1	-	X	-	X	-	MC	Water vs. MC, only 1 concentration	n/a
2	-	X	-	-	-	Starch**, MC, Na-CMC ^{is} , gum tragacanth	Fixed polymer concentration, so necessarily samples differ in viscosity	Reported but not correlated to sensory data
3	-	X	-	-	-	Starch**, guar, Na-CMC ^{is}	Viscosity matched at 0.5 rpm (very low shear rate)	Reported but not correlated to sensory data
4	0.36-10% Unrealistic for food products	X	X	X	-	Na-CMC ^{is}	Viscosity matched at 57 rpm but only one polymer (equivalent to range of concentration)	n/a
5	0.1-0.65%	X	X	X	-	HPC, Na-CMC ^{is} (2 Mw), Na-Alg ^{is}	Fixed polymer concentration, so necessarily samples differ in viscosity	n/a
6	-	X	-	-	X			
7	0.3-4.6%	X	-	-	-	Na-CMC ^{is} (3 Mw)	Viscosity matched at a specific shear rate, data of different Mw are not compared (equivalent to range of concentration)	n/a
8	-	X	-	-	X	Guar (3 Mw)	Range of polymer concentration	Sensory data correlated to $c[\eta]$
9	0.1-0.2%	-	-	-	-	κ -carr ⁱ , Xant ⁱ , LBG, guar	Fixed polymer concentration, so necessarily samples differ in viscosity	n/a
10	<0.14%	-	-	-	-	Xant ⁱ , LBG		
11	<0.23%	-	-	-	-	Na-CMC ^{is} , xant ⁱ , guar, LBG, starch**		
12	0.35%	X	X	X	X	HMPC, guar, λ -carr ⁱ	Paired comparison of 2 samples thickened with different concentrations of the same polymer	n/a
13	-	X	-	-	X	HPMC	Range of polymer concentration	n/a
14	-	X	-	-	X	Guar, HPMC, λ -carr ⁱ	Range of polymer concentration	Power law parameters. Sensory data correlated to Kokini oral shear stress, η_0 , $\eta(50s^{-1})$, $\eta(100s^{-1})$ and c/c^*
15	0.2-0.35%	-	-	-	-	HPMC, λ -carr ⁱ	Paired comparison of 2 samples thickened with different concentrations of the same	n/a

							polymer		
16	-	-	X	-	-		Guar	Range of polymer concentration	Sensory data plotted in function of η_0 and η_∞
17	0.5%	-	-	-	X		HMPC, starch**	Viscosity matched at 50 s ⁻¹	n/a Sensory data plotted in function of Kokini oral shear stress and $\eta(50s^{-1})$

1: (Mackey, 1958)

2: (Stone and Oliver, 1966)

3: (Vaisey, Brunon and Cooper, 1969)

4: (Moskowitz and Arabie, 1970)

5: (Pangborn and Trabue, 1973)

6: (Pangborn and Szczesniak, 1974)

7: (Christensen, 1980)

8: (Baines and Morris, 1987)

9: (Rosett et al., 1994)

10: (Rosett et al., 1995)

11: (Rosett et al., 1996)

12: (Cook et al., 2002)

13: (Hollowood et al., 2002)

14: (Cook et al., 2003a)

15: (Cook, Linforth and Taylor, 2003b)

16: (Malone et al., 2003b)

17: (Ferry et al., 2006a)

Na-CMC^{is} sodium carboxymethyl cellulose

MC

methylcellulose

Na-Alg^{is} sodium alginate

HPMC

hydroxypropyl methylcellulose

LBG locust bean gum

HPC

hydroxypropyl cellulose

Xant^l xanthan gum

Mw

Molecular weight

-carr carrageenan

n/a

not available

^l: ionic polymer, which may have affect the results based on the results published by Rosett et al. (1996)

^s: polymers used as the sodium-salt form, therefore containing large amount of endogenous sodium, which may have affect the results based on the results published by Rosett et al. (1996)

** : starches are indicated in purple as it was later shown that the degradation by amylase in mouth may have affected the results (Ferry et al., 2006b)

Increasing viscosity was found to increase the threshold for detection of sodium chloride. Paulus and Haas (1980) found that the recognition threshold for sodium chloride in guar gum solution of 1 Pa.s was more than twice of the threshold in water (1.55 g.l⁻¹ vs. 0.82 g.l⁻¹ in water). Increasing viscosity, which is obtained by increasing the solution concentration of the viscosifying agent, is typically reported to result in a decrease in taste perception at supra-threshold levels of NaCl (Moskowitz and Arabie, 1970; Christensen, 1980; Baines and Morris, 1987; Cook et al., 2002; Hollowood et al., 2002; Cook et al., 2003a; Cook et al., 2003b; Malone et al., 2003b; Ferry et al., 2006a). However, this relationship is non-linear as viscosity has only a limited effect on taste perception at low solution concentrations whereas the impact increases abruptly for

concentrations above the coil overlap concentration, c^* (Baines and Morris, 1987; Hollowood et al., 2002; Malone et al., 2003b). c^* is defined as the critical concentration above which intermolecular interactions (such as coil overlapping) between neighbouring polymer chains occur (see also 5.3.3). The flow behaviour of solutions below c^* is mainly Newtonian, i.e. the viscosity is shear rate-independent. At higher solution concentrations, however, the molecular characteristics of the viscosifying agent become important as it results in a variety of flow behaviours. Thus, it is important to understand which flow parameter relates to taste perception - the central research question of this PhD. There is a considerable body of relevant literature which is reviewed in the following section.

1.3.1 FLOW PARAMETERS RELEVANT TO TASTE PERCEPTION

In early works unfortunately, sensory data were not discussed in relation to flow behaviour (see Table 1.1) (Stone and Oliver, 1966; Pangborn and Trabue, 1973; Pangborn and Szczesniak, 1974; Rosett et al., 1994; Rosett et al., 1995; Rosett et al., 1996). Vaisey et al. (1969) worked with samples that were matched in viscosity at very low shear rate and concluded that reduction in sweetness perception was more pronounced for weakly shear-thinning samples. However, the less shear-thinning samples exhibited a viscosity more than two decades higher over most of the shear rate range applied for sample characterisation and this higher viscosity level may well have been the origin of the reduction in taste perception.

Subsequent publications feature taste perception data from solutions of variable polymers, and their concentration and their correlation to flow parameters. Baines and Morris (1987) found that sweetness perception data from guar gum solutions of different molecular weights could be successfully scaled using the degree of coil occupancy, $c \cdot [\eta]$, a parameter that is related to zero shear viscosity (see 5.6.1.2). Following on, Cook et al. (2003a) studied sweetness perception from guar gum, HPMC and λ -carrageenan solutions and found that sensory data were better correlated to the Kokini oral shear stress (see in 1.2.2), though the same data could be predicted almost as well by the ratio of c/c^* , the zero shear viscosity, the viscosity measured at 50 s^{-1} , or the viscosity measured at 100 s^{-1} . In a different study using only guar gum of a given molecular weight, sour perception was reported to be linearly correlated to viscosity at infinite shear rates (Malone et al., 2003b). Ferry et al. (2006a; 2006b) investigated samples matched in viscosity at 50 s^{-1} . The samples were based on three different types of starches (wheat, waxy maize and a physically modified waxy maize) as well as a hydrocolloid, hydroxypropylmethyl cellulose (HPMC). Differences in taste perception were observed and related to differences in the efficiency of mixing of the thickened solutions with saliva in the mouth, a hypothesis previously formulated by Baines and Morris (1987). Since it has been recognised that mixing may involve extensional flows (Connelly and Kokini, 2004), Ferry et al. (2006a; 2006b)

suggested that extensional flow behaviour of viscous solutions may correlate to taste and mouthfeel perception. Unfortunately, to-date this hypothesis has not been tested.

The literature review illustrates that, to-date, the flow parameters relevant for saltiness perception (or even taste perception) are still unknown, rendering it difficult to compare different thickeners. In particular, the link between high shear rheology or extensional flow behaviour and sensory perception (taste and mouthfeel) remains to be investigated.

1.3.2 MECHANISMS UNDERLYING TASTE PERCEPTION IN VISCOUS SOLUTIONS

The evidence of decrease in taste perception in viscous solutions is overwhelming, but the mechanisms are not well understood. Several theories have been formulated. With the exception of the cognitive theory, all theories are based on the idea that the reduction in taste perception is due to a reduction in the availability of tastant molecules to the taste buds.

Cognitive interactions

As mentioned above (in 1.2), taste perception is dependent on the processing of the sensory information by the brain. The cognitive theory suggests that the quantity and availability of the tastants is not altered by the viscosity but that the perceived

reduction in taste is attributed to the brain processing of the signal. It therefore suggests a taste-texture interaction at the perceptive level. This theory has been proposed for taste perception in gels (Weel et al., 2002), but not explicitly for semi-liquid products.

Restricted diffusion

The earliest reported theory for viscosity-taste dependence was the diffusion theory (Kokini et al., 1982; Kokini, 1985). It hypothesises that a stagnant layer of sample exists on the tongue, through which tastants diffuse. Theoretically, the diffusion coefficient is proportional to the inverse of the square root of solution viscosity and therefore in thickened solutions, diffusion is slowed down, leading to a reduction in taste perception. This theory was also suggested after the findings that a coating of the tongue with oil reduces taste perception (Lynch et al., 1993).

This theory is now largely rejected as data showed that thickeners have negligible influence on diffusion process at the polysaccharide concentrations typically used in foods (Andersson and Oste, 1994). Restricted diffusion also appeared unlikely as taste perception is not lower in solutions thickened with a large number of short chain polymers compared to solutions of identical viscosity thickened with a small number of long chain polymers (Baines and Morris, 1987). In addition, diffusion is a very slow

process that seems inconsistent with the rapid reaction time to a salty stimulus (about 800 ms) (Kelling and Halpern, 1988).

Chemical binding

Another possibility is that reduction in taste perception is a consequence of a 'direct effect' of the hydrocolloids on tastant molecules. In particular for saltiness perception, electrostatic binding of Na^+ to charged anionic thickeners was argued to be the reason for lower saltiness perception (Rosett et al., 1994; Rosett et al., 1995), supported by NMR data showing that sodium ions were less mobile in solutions thickened with anionic polysaccharides compared to non-ionic polysaccharides.

The binding theory could explain the reduction of saltiness perception in solutions thickened with anionic polysaccharides but it fails to justify the reduction of saltiness also observed in non-anionic polysaccharide solutions, as well as the reduction of other taste modalities. In addition, binding is hypothesised to depend on the thickener used, which contrasts with the reduction of taste perception in a variety of thickener solutions (see Table 1.1). Though the binding of tastants to polymer chains is unlikely to be the only mechanism underlying reduction of taste perception in viscous solution, binding of Na^+ is a physical reality (Schmidt and Ayya, 1989), which is why caution should be applied in generalising the results of perception studies based on charged

polysaccharides, in particular their sodium salt form (such as carboxymethyl cellulose used frequently for taste perception studies as seen in Table 1.1 or sodium alginate).

Surface area stimulation

This theory is based on psychophysical studies of taste perception showing that taste intensity is influenced by the surface contact area between the sample and the tongue or by the sample volume (McBurney, 1969; Smith, 1971; Omahony et al., 1982; Slotnick, Wittich and Henkin, 1988). It postulates that increasing viscosity reduces the contact area between the sample and the tongue as the sample 'spreads' less. This theory was mentioned by Malone et al. (2003b) as well as Saint-Eve et al. (2006).

Restricted mixing

Initially suggested by Baines and Morris (1987), the reduction of taste perception in viscous solutions may be due to restricted mixing with saliva. Indeed, the tastants must reach the saliva to access the taste buds (1.2) and with increasing viscosity, the efficiency of mixing with saliva is likely to decrease and to slow down the replenishment in tastant at the food-saliva interface. This hypothesis, also defended by Malone et al. (2003b), has been experimentally probed by visual observation of the mixing efficiency between a coloured hydrocolloid solution and water (Ferry et al., 2006a; Ferry et al., 2006b; Koliandris et al., 2007). A granular starch system and a gelatin solution of identical viscosity at 50 s^{-1} exhibited much better mixing with water

than HPMC and locust bean gum (LBG). This was associated with a higher release of sodium ions into water compared to the HPMC/LBG solutions (Koliandris et al., 2007) leading to higher taste perception (Ferry et al., 2006a) in those samples.

Though these theories fail to explain why taste perception in viscous solutions is reported as dependent on the taste modality studied (see above in 1.3), restricted mixing and restricted surface area of stimulation are, to date, the two most likely mechanisms explaining the reduction in taste perception in viscous solutions. It has been postulated that extensional properties may control the efficiency of mixing with saliva and therefore taste perception (Ferry et al., 2006b). Yet, literature on extensional properties of polysaccharide solutions is almost nonexistent and this has been a focus of the work reported here in Chapter 5 of this thesis. The concepts of elasticity and extensional viscosity are introduced in the following section.

1.4 FLOW BEHAVIOUR

1.4.1 INTRODUCTION

When shear stress is applied to an ideal liquid it will flow (or deform) and energy is dissipated. On removal of the stress, there is no recovery of deformation (also referred to as strain) as the energy has been lost during flow (Figure 1.3a). In contrast, the deformation of an elastic solid takes place instantaneously on application, and

disappears completely and instantaneously on withdrawal of the deforming stress (Figure 1.3b). When a stress is applied to a solid, energy is stored by the bonds between the molecules. When the stress is removed, the bonds release this energy and the material returns to its origin shape. The ability to store energy elastically is therefore a property of solids whereas liquids dissipate energy when flowing. The flow behaviour of most biopolymer solutions is viscoelastic which is somewhat in between purely viscous and purely elastic behaviour, see Figure 1.3c. Viscoelastic materials partially store energy during deformation (corresponding to the recoverable strain when stress is removed) but energy is also dissipated as the recovery of the strain is not complete. Famous effects resulting from viscoelastic properties are the rod climbing effect and the tubeless siphon effect (pictures and videos can be found on the site of Prof. McKinley group, <http://web.mit.edu/nmf/>). Examples of viscoelastic liquids relevant to food science include saliva, melted cheese, mayonnaise and yogurts.

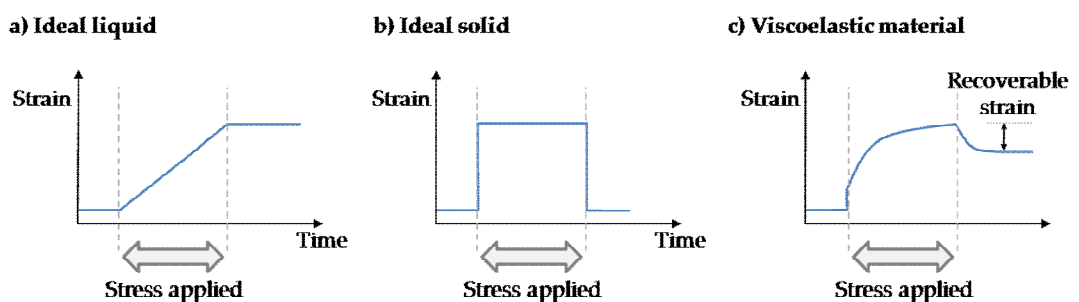


Figure 1.3: Sketch of strain-time plot on the application of a stress for a) an ideal liquid, b) and ideal solid and c) a viscoelastic material.

Viscoelasticity can be observed in all types of deformation: shear, compression or extension. In shear flow, small deformation and large deformation flows are applied depending on whether the interest of the rheological characterisation is to establish parameters relevant to the state of rest of the material or to behaviour in flow processes. A typical small deformation shear experiment is the small angle oscillatory shear (SAOS) test, performed in the limits of linear-viscoelastic deformation, in which the elastic modulus G' (also referred to as the storage modulus) and the viscous modulus G'' (loss modulus) are measured. Elastic flow effects in large deformation shear flow are quantifiable via normal stress growth measurements.

Food handling in the mouth probably includes a strong extensional component in addition to a shear component. As elastic effects are often more pronounced in extensional flow situations than in shear flows, characterisation of viscoelasticity in extensional flow fields was included in this PhD research.

1.4.2 FUNDAMENTALS

The effect of deformation on polymer chains clearly differs in shear and extensional flows. In shear flow, the velocity profile causes the molecules to rotate and gradually align in the direction of flow, whereas molecules are orientated and stretched in extensional flow. The stretching induces a large tension in the polymer chains, which requires more energy than a simple rotation (Petrie, 2006b; Petrie, 2006a). Extensional

flows are therefore much more sensitive to polymer presence and polymer structure than shear flows. Polymer solution relaxation times obtained from extensional flow measurements are always considerably higher than those obtained from SAOS data or from zero shear viscosity data (Liang and Mackley, 1994; Clasen et al., 2006; Tirtaatmadja, McKinley and Cooper-White, 2006; Rodd et al., 2007).

The coil overlap concentration, c^* , is generally defined based on shear flow measurements. For $c < c^*$, interactions between neighbouring polymer chains are negligible, so that the rheological response of the fluid is solely governed by the sum of the deformations and hydrodynamic interactions of isolated coils and solvent. As mentioned above, polymer chains are stretched in extension and the interaction volume increases, which results in chain-chain interactions even for concentrations below c^* (Clasen et al., 2006). Thus in extensional flow, solutions of concentration below c^* may be semi-dilute rather than dilute.

The resistance to flow in extension can exceed the resistance in shear by several orders of magnitudes and it is therefore important to quantify this resistance as extensional viscosity. In this research, for sake of clarity, 'extensional viscosity' refers to uniaxial extensional viscosity not to biaxial extensional viscosity. Uniaxial extensional viscosity characterises the resistance of a material to stretching. Its visible manifestation is the long lifetime of a thread of fluid, such as saliva, the stringiness or ropiness of yogurts

or melted cheese and the qualification of 'long texture' (McKinley et al., 1999). A large number of industrial processes involve extensional flows (mixing, extrusion, compression or sheeting) as well as food handling by the consumer such as spreading and in-mouth processing. Yet uniaxial extensional viscosity has been less frequently studied than shear viscosity because it is difficult to generate pure uniaxial extensional flow fields and steady state is rarely achieved (Petrie, 2006a).

Extensional viscosity was first mentioned by Trouton under the name of 'coefficient of viscous traction' when he established in 1906 that the extensional viscosity of Newtonian fluids equal 3 times their shear viscosity. The ratio between extensional viscosity and shear viscosity has been termed the Trouton ratio (Equation 1.1).

$$Tr = \frac{\eta_e(\dot{\epsilon})}{\eta_s(\dot{\gamma})} \text{ where } \dot{\gamma} = \sqrt{3} \dot{\epsilon} \text{ (Sridhar et al., 1991)} \quad (1.1)$$

where Tr is the Trouton ratio, η_e [Pa.s] the extensional viscosity, $\dot{\epsilon}$ the extensional rate [s⁻¹], η_s [Pa.s] the shear viscosity and $\dot{\gamma}$ [s⁻¹] the shear rate.

Trouton ratio equals 3 for Newtonian fluids or viscoelastic fluids at very small extension rates (Petrie, 2006a). For elastic fluids it can be as high as 10⁴ at high strains (Anna and McKinley, 2001). The conformation of the polymer (rigid, flexible, semi-rigid) affects the strain dependence of the Trouton ratio (Ng et al., 1996).

Another useful parameter to characterise the viscoelasticity of a solution is its relaxation time. This refers to the time it takes for polymer chains to return to equilibrium after being disturbed in some manner. For dilute solutions, the Zimm theory offers a theoretical framework to calculate relaxation times based on zero shear viscosity data (Tirtaatmadja et al., 2006). For semi-dilute and concentrated solutions, the relaxation time can also be determined in shear flow, either using SAOS (Malkin, 2002) or primary normal stress growth in large deformation shear (Cable and Boger, 1978; Mackay and Boger, 1987). The relaxation time in extensional flow can be obtained from filament stretching data as detailed below. The different methods for obtaining relaxation time data may lead to quite different results. As mentioned above, the relaxation time determined in extensional flow is often several times higher than that calculated based on shear flow data (Liang and Mackley, 1994; Clasen et al., 2006; Tirtaatmadja et al., 2006; Rodd et al., 2007). This is why it is important to determine relaxation time from flow conditions (shear or extension) relevant to the application desired.

In order to characterise material behaviour as a result of extensional deformation, it is essential to create a controlled free surface flow so that no shear deformation is applied to the material. The ability to measure polymer solutions in extensional flow significantly improved at the end of the 20th century. Filament stretching (Tirtaatmadja and Sridhar, 1993; Papageorgiou, 1995; McKinley et al., 1999) and filament break-up

rheometry (Stelter and Brenn, 2000; Anna and McKinley, 2001) are the most commonly used techniques nowadays. Other devices designed to characterise material behaviour in extensional flow include the opposed-jet apparatus (Fuller et al., 1987), spine-line rheometers or drop pinch-off set-ups (Tirtaatmadja et al., 2006). More recently, micro-contraction flows devices have been used to characterise low viscosity polymer solutions in extension (Rodd et al., 2005a; Rodd et al., 2007). Results using two of these methods, filament break-up and microfluidics are discussed in this thesis.

1.4.3 FILAMENT BREAK-UP

In this research the commercially available filament break-up device 'CaBER' ('capillary break-up extensional rheometer', Thermo Haake GmbH, Karlsruhe, Germany) was used. The principle is depicted in Figure 1.4 and is analogous to a step-strain experiment in a conventional rotational rheometer. A volume of sample is placed between two horizontal parallel plates. The plates are rapidly separated to a certain distance forming a filament, which then thins until it breaks. The decreasing mid-point diameter of the filament is measured as a function of time using a laser micrometer.

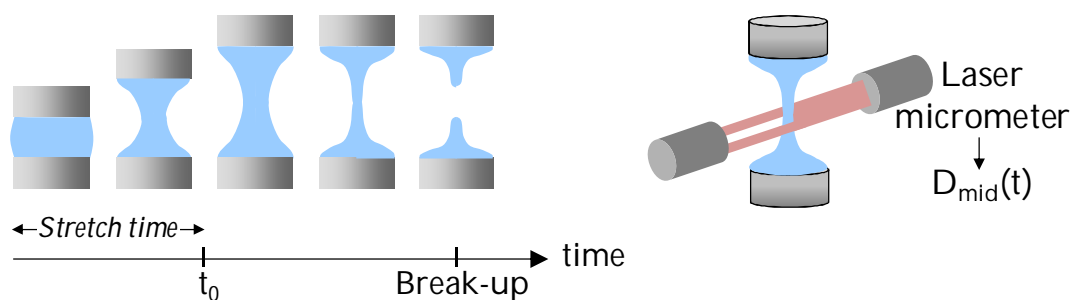


Figure 1.4: Schematic representation of the filament break-up device. The sample is represented in blue.

The filament break-up technique has previously been used to characterise polysaccharide solutions such as of chemically modified guar (Tatham et al., 1995; Duxenneuner et al., 2008), casein-starch mixtures (Chan et al., 2007; Chan et al., 2008) and galactomannans (Wunderlich et al., 2000). The vast majority of the literature, however, concerns synthetic polymers.

Whereas the filament diameter decays linearly with time for purely viscous Newtonian fluids (Papageorgiou, 1995; Anna and McKinley, 2001), the decay is exponential for elastic fluids, leading to a longer break up time compared to inelastic solutions (Anna and McKinley, 2001; James and Yogachandran, 2006). The relaxation time of the fluid (or more rigorously called ‘characteristic time scale for viscoelastic stress growth in uniaxial elongational flow’) can be calculated from the rate of decay (Liang and Mackley, 1994; Stelter and Brenn, 2000). When stretching polymer solutions, a transition from exponential to linear decrease of the diameter with time is observed for the aged filament (i.e. at high strain) (Stelter and Brenn, 2000). This is

interpreted as a quasi Newtonian state, for which the polymer coils are aligned and stretched to the maximum in solution. The apparent steady state extensional viscosity can be obtained from this domain. In addition to extensional viscosity, many other factors such as the surface tension of the fluid, inertial and geometrical forces affect the filament thinning and break-up time (McKinley, 2005) but stretch time and stretch distance have been reported not to affect the actual measurements for polymer solutions (Miller, Clasen and Rothstein, 2009).

Stelter et al. (2002) observed that the extensional viscosity of polymer solutions could be scaled using the relaxation time and data from different polymers fell onto two mastercurves depending on their conformational behaviour (flexible or rigid). The effect of polymer conformation on filament thinning was also reported by Miller and Cooper-White (2009) and prediction of filament thinning based on different polymer theories or fluids models can be found in literature (FENE, Oldroyd-B, ...) (Bazilevskii et al., 1997; Entov and Hinch, 1997; Bhatnagar et al., 2002).

Several issues have been reported regarding the use of filament stretching to characterise flow behaviour in extension, the main problem being lack of controllability (Petrie, 2006a). The operator does not control the strain applied to the sample and must rely on a balance of viscous, elastic and capillary forces to maintain the sample in a near cylindrical shape. This is particularly a problem for low viscosity,

low elasticity fluids. Inertia effects such as beads-on-a-string morphology of the filament, oscillation of the droplets attached to the endplates (Rodd et al., 2005b) and not axially uniform flow (Anna and McKinley, 2001) have been reported for inelastic/low viscosity fluids. Rodd et al. (2005b) established that Newtonian fluids of viscosity lower than 70 mPa.s could not successfully be measured using the filament break-up technique. Since, even if the shear viscosity criterion is satisfied, polysaccharide solutions are weakly elastic compared to synthetic polymers, it might be beneficial to use a different technique to analyse their behaviour in extensional flow, such as micro-contraction flows.

1.4.4 MICRO-CONTRACTION FLOW DEVICE

Microfluidics is 'the science and technology of systems that process or manipulate small amount of fluids (10^{-9} to 10^{-18} litres), using channels with dimensions of tens to hundreds of micrometers' (Whitesides, 2006). Current applications are mainly for bioanalyses and cell biology but research also focuses on manipulation of multiphase flows (Rondeau and Cooper-White, 2008; Wong et al., 2009) which could allow creation of highly reproducible microstructure for food products (gelled particles, duplex emulsions, ...). In addition to requiring only small sample volumes, microfluidics devices present a number of advantages for industrial applications such as short response time and low cost of fabrication of the devices (Squires and Quake,

2005; Whitesides, 2006). In this thesis, results from microfluidics devices are reported as they were used to characterise flow behaviour, that is to say for ‘microrheometry’.

Compared to classic rheometry, microrheometry presents numerous advantages including the absence of free surface (no edge failure), very low inertia and probing of fresh sample at every instant (Kang, Lee and Koelling, 2005; Squires and Quake, 2005; Pipe and McKinley, 2009). Micro-contraction flow devices are characterised by a sudden contraction of the channel width as depicted in Figure 1.5, which induces large deformation rates at very low inertia. The flow at the centreline in the contraction is essentially extensional (Gulati, Muller and Liepmann, 2008), thus the elastic response can be monitored while inertia is minimal because of the small dimensions of the channel. Some difficulties nonetheless exist for fluid mechanics analysis in particular the three dimensional nature of the flow (Kang et al., 2005; Oliveira et al., 2008; Pipe and McKinley, 2009).

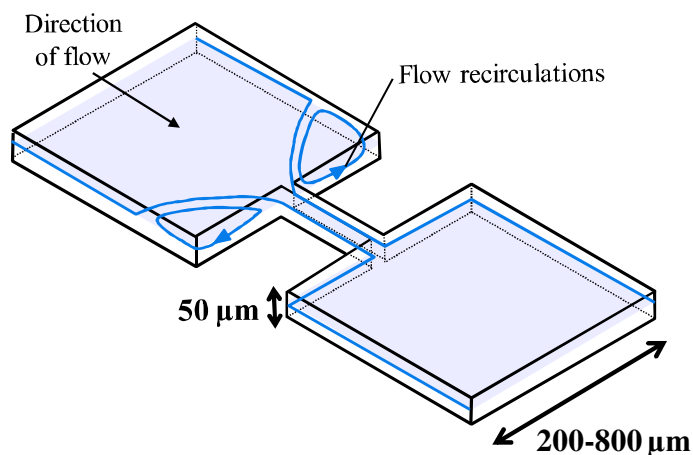


Figure 1.5: Representation of a micro-contraction flow device.

The flow in a microfluidics device can be characterised by measuring the pressure drop in the channel, by visualising streak lines and by using velocimetry techniques to obtain precise flow profiles (for example particle image velocimetry) (Bayraktar and Pidugu, 2006). In particular, visualisation of flow pattern and measurements of excess pressure drop can be interpreted in terms of solutions elasticity as reviewed in detail in Chapter 5.

1.5 THESIS ORGANISATION

The decrease in saltiness perception with increasing viscosity had been extensively reported in the literature, yet it is not well understood which viscosity –measured at which shear rate- is relevant and what are the mechanisms involved. The aim of the research reported in this thesis was to better characterise flow parameters impacting on saltiness perception, in order to establish design rules allowing product formulation at a lower salt content but identical saltiness perception. As illustrated in Figure 1.6, the relationship between shear viscosity and saltiness perception as investigated is reported in Chapter 3, whereas Chapter 4 and 5 report on the understanding generated of the effect of elasticity (or extensional viscosity) on saltiness perception. Two different approaches were employed. In Chapter 4, work on saltiness perception in Boger fluids (elastic fluids of constant shear viscosity) compared to Newtonian fluids is detailed. In Chapter 5, elasticity data of solutions of

polysaccharides of variable structure and preliminary work to compare saltiness perception in these different solutions are presented. Since the vast majority of food products are emulsions, optimising saltiness perception in aqueous systems is only one option among others. Duplex emulsions are complex microstructures that could play a role in salt reduced foods, as described at the beginning of Chapter 1, chemical cross-linking as a novel approach of stabilising food duplex emulsions was investigated and this is reported in Chapter 6.

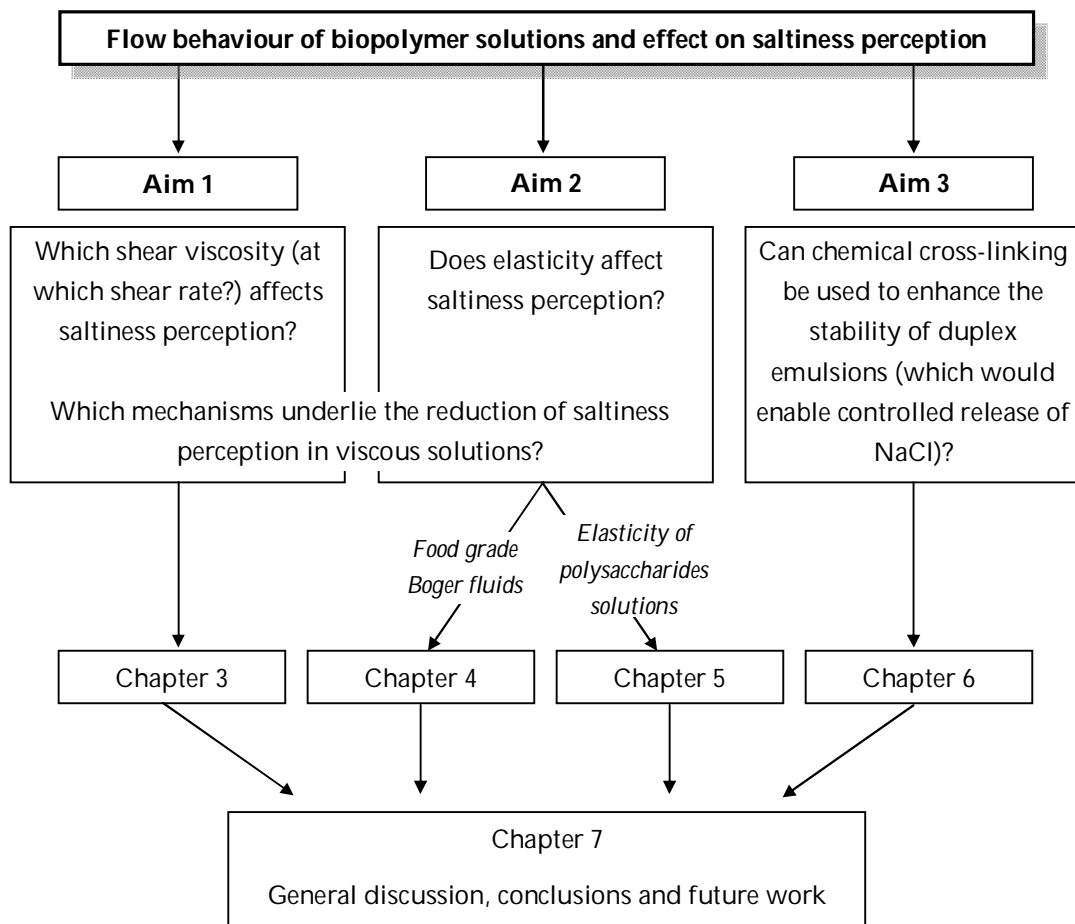


Figure 1.6: Diagram illustrating the organisation of the thesis.

CHAPTER 2

MATERIALS AND METHODS

2.1 MATERIALS

All solutions to be used for sensory analysis were prepared with bottled water (Evian, Danone, France; brand chosen for its low ion content). Sodium azide (0.02% w/v) was added to distilled water as a preservative for samples prepared for instrumental measurements. Sodium chloride was added as 'Table salt' (bought in a local supermarket). Other materials will be described at the beginning of each chapter.

2.2 RHEOLOGICAL METHODS

All rheological measurements were conducted at 20 °C using a rotational rheometer (MCR301, Anton Paar, Austria).

2.2.1 THIN FILM RHEOLOGY

Steady state viscosity data were acquired up to shear rates in the order of 10^6 s^{-1} using a smooth parallel plate geometry (50 mm diameter) following a published protocol for thin film rheology (Davies and Stokes, 2008). Low shear data can be generated at classic gap height (0.5 mm) whereas acquisition of high shear data requires narrow gaps to reduce inertia effects. For each sample, data were collected at the different nominal gap heights 500, 50 and 30 μm for shear rates between of 10^3 - 10^1 , 10^3 - 10^5 and 10^5 - 10^6 s^{-1} , respectively. Data were corrected for non-Newtonian behaviour and gap error using Excel (Microsoft Inc., USA).

2.2.1.1 Determination of the gap error

The top and bottom plates of a geometry are never perfectly flat nor perfectly parallel. Therefore, when the zero gap is set, the two surfaces are never fully in contact. During measurement, the gap height is thus not identical across the sample and the actual gap size differs from the nominal gap size by a gap error ε , usually 30-50 μm . As in classic rheology with parallel plates gap heights of more than 500 μm are typically used, gap errors can be neglected as a 10% error hardly affects the viscosity values calculated from the data. In thin film rheology, gap size and gap error are of similar magnitude and errors have to be quantified. Here, the method described by Kramer et al. (1987) was employed.

Equation 2.1 ('Kramer equation') expresses the gap error ε as a function of the measurement parameters in a shear rate controlled experiment (nominal shear rate $\dot{\gamma}_{R\text{com}}$ and gap height h_{com}) and measurement results (shear stress τ and viscosity η).

Plotting $\frac{h_{\text{com}}\dot{\gamma}_{R\text{com}}}{\tau}$ over h_{com} results in a straight line with a slope of $\frac{1}{\eta}$ and a y-axis

intercept of $\frac{\varepsilon}{\eta}$ allowing a determination of the gap error ε . An example of such a plot

is depicted in Appendix 2.2 and the derivation of Equation 2.1 is given in Appendix 2.1. In practice, the Kramer regression was performed on data collected at five different gap heights (1000, 500, 250, 125 and 50 μm) with 100 cS silicon oil (Dow Corning, purchased from Sigma-Aldrich).

$$\frac{h_{com}\dot{\gamma}_{R\ com}}{\tau} = \frac{1}{\eta}h_{com} + \frac{\varepsilon}{\eta} \quad (2.1)$$

where h_{com} is the nominal gap height, h_{real} the actual gap height, $\dot{\gamma}_{R\ com}$ the nominal shear rate at the outer radius R, τ the shear stress, η the viscosity at R based on the actual shear rate $\dot{\gamma}$ and ε the gap error.

For the fluids of interest in this research, viscosity data had to also be corrected for the non-Newtonian behaviour which is why no equation for calculating the corrected viscosity, η , considering solely the gap error is provided here.

2.2.1.2 Correction for non-Newtonian behaviour considering the gap error

In a parallel plate geometry, shear rate is not uniform across the geometry (zero in the centre and maximal at the rim). The nominal shear rate value indicated by the rheometers software corresponds to the shear rate at the rim. This differs from the shear rate applied *on average* to the sample. Here, a single point correction previously suggested to be the most suitable for fluids fitting the Cross model (as for the fluids in this research) was applied (Shaw and Liu, 2006). In this correction, the average shear rate is considered to be equal to 4/5 of the shear rate at the rim. Because of the gap error ε , the actual shear rate at the rim $\dot{\gamma}_{R\ real}$ differs from the nominal shear rate $\dot{\gamma}_{R\ com}$ leading to Equations 2.2 and 2.3 for corrected shear rate and viscosity, respectively. The complete derivation of these equations is provided in Appendix 2.3 and an example of data before and after correction can be found in Appendix 2.4. In the

following, 'shear rate' and 'apparent shear viscosity' for thin film rheology data will implicitly relate to data corrected for non-Newtonian behaviour and gap error.

$$\dot{\gamma}_{corrected} = \frac{4}{5} \times \frac{\dot{\gamma}_{R\ com}}{1 + \frac{\varepsilon}{h_{com}}} \quad (2.2)$$

where $\dot{\gamma}_{corrected}$ is the corrected shear rate, $\dot{\gamma}_{R\ com}$ the nominal shear rate, h_{com} is the nominal gap height and ε the gap error.

$$\eta_{corrected}(\dot{\gamma}_{corrected}) = \frac{\tau}{\dot{\gamma}_{corrected}} \quad (2.3)$$

where $\eta_{corrected}$ is the corrected viscosity, $\dot{\gamma}_{corrected}$ the corrected shear rate and τ the shear stress

2.2.2 SMALL AMPLITUDE OSCILLATORY SHEAR

Small amplitude oscillatory steady state shear data were acquired using a smooth cone-plate geometry (50 mm, 2 °) and an MCR rheometer fitted with the Direct Strain Oscillation option for enhanced accuracy of strain values (Lauger, Wollny and Huck, 2001). Strain sweeps (0.1 – 100% strain) were performed at 10 rad.s⁻¹. Unless otherwise stated, frequency sweeps were performed from 100 rad.s⁻¹ to 0.1 rad.s⁻¹ at 5% strain.

2.2.3 FILAMENT BREAK-UP

Flow properties in extension were quantified using a capillary break-up extensional rheometer (Thermo Haake GmbH, Karlsruhe, Germany) (CaBER, 2003). The principle

behind such an instrument is following the thinning of a fluid filament generated by rapidly stretching a small volume of sample fluid to a given length (see 1.4.3). In the CaBER filament thinning is estimated via a laser micrometre by the midlength diameter of the filament irrespective whether this is the point of the thinnest filament diameter. The experimental procedure was as follows. Initially, a sample droplet was placed between the bottom and upper plates (6 mm diameter, 3 mm separation) using a 1 ml syringe fitted with a needle. Extra care was taken to obtain a convex meniscus of fluid exempt from entrapped air. In the actual stretching experiment, the top plate was moved up rapidly (in 50 ms) to form a filament of 10 mm length. Due to self-thinning the diameter d of the filament will decrease from the initial diameter d_0 at t_0 as a function of time t until it breaks (t_0 corresponds to the instant the top plate reaches its final position). At least 9 replicate measurements were performed on each sample and three representative set of data were averaged. Such data can be used to calculate solution relaxation time and apparent extensional viscosity using methods detailed in the respective Chapters showing experimental data (Chapter 4 and 5).

2.2.4 MICRO-CONTRACTION FLOW

Microfluidics channels including an abrupt contraction-expansion of the channel were used here to probe the viscoelastic properties of polysaccharide solutions at low inertia and high deformations. The dimensions of the planar abrupt contraction-expansion device used in this research are depicted in Figure 2.1. Its contraction ratio,

defined by the ratio of the width upstream of the contraction to the width of the contraction equals to 16. The channel section is rectangular (square in the contraction) and the depth is constant throughout the device ($50\ \mu\text{m}$).

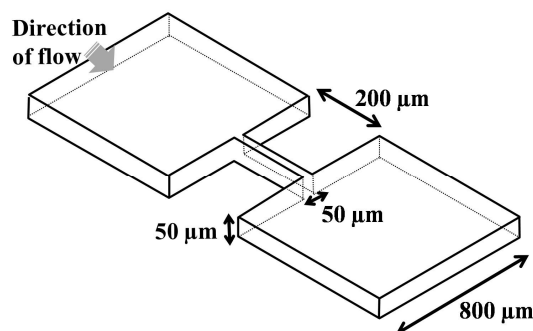


Figure 2.1: Schematic diagram of the planar micro-fabricated contraction-expansion (not to scale).

Channels were fabricated in polydimethylsiloxane (PDMS, Sylgard 184, Dow Corning) using soft-lithography techniques. Photo-resistant moulds were fabricated using a high-resolution chrome mask following standard photo-lithography procedures (further details can be found in Rodd et al. (2005a)). PDMS channels were bound to PDMS-covered glass slides as described elsewhere (Rodd et al., 2007).

The experimental set-up is depicted in Figure 2.2. A motor-driven syringe pump (PHD 2000 Harvard) linked to the syringe through polyethylene tubing (internal diameter $0.58\ \text{mm}$) was used to induce flow of the sample in the contraction. Flow rates between 0.1 and $9\ \text{ml}\cdot\text{hr}^{-1}$ were investigated. Two pressure taps were positioned in side channels located $3\ \text{mm}$ upstream and $3\ \text{mm}$ downstream of the contraction,

respectively, and pressure drop was measured using a differential pressure transducer (Honeywell 24PCB). The pressure transducer was calibrated using a manometer and pressure drop developed by water was measured every day of measurement as a control. Channels were washed with water and ethanol in between samples.

Analysis and representation of microfluidics data are detailed in Chapter 5, showing experimental data.

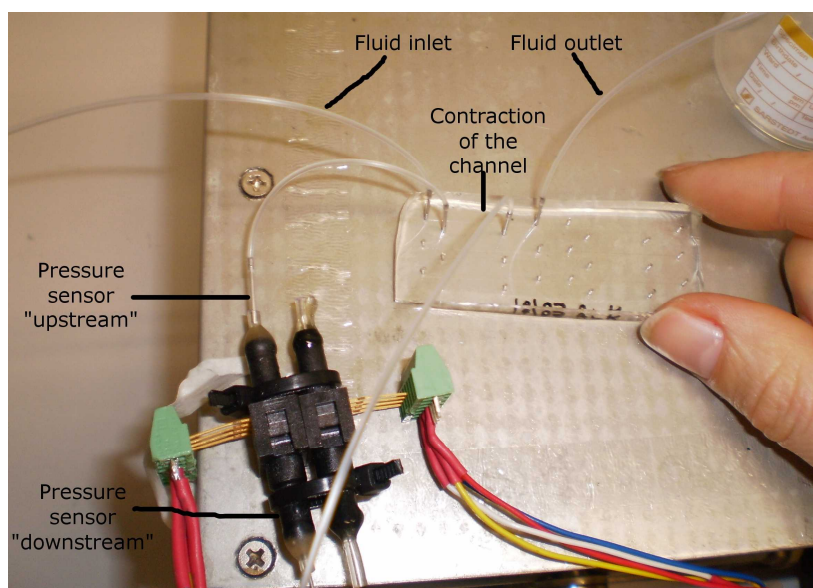


Figure 2.2: Picture of the microfluidics device including a slide containing 6 contraction-expansion channels, pressure sensor, tubing to pressure taps, fluid inlet and fluid outlet. For reference, the width of the glass slide is 25 mm.

2.3 SENSORY METHODS

The sensory experiments carried out in this research were approved by the Medical School Ethics Committee of The University of Nottingham. All subjects gave informed written consent before attending any sessions. Tests were conducted in individual booths, lit with northern hemisphere lighting, in a quiet, air-conditioned room (20 °C). Still mineral water (Evian, Danone, France) and unsalted crackers (99% Fat Free, Rakusen's, UK) were provided as palate cleansers. All samples were coded with random three digit numbers and data were collected using the computerised data acquisition system Fizz (Biosystèmes, France). Samples were served at room temperature and presented on dessert spoons (2 ml of sample).

Sensory experiments were conducted either with untrained panellists or with a panel selected and trained for this research (9 women, aged 48 to 72 years), as specified for each test. Selection and training procedures are reported in Chapter 3.

2.3.1 ATTRIBUTE DIFFERENCE TEST

In attribute difference tests (ISO 5495) samples are compared on a single attribute, e.g., saltiness. If only two samples are compared, the test is called 'paired comparison'. If more than two samples are compared, the test is called 'multiple paired comparison'.

2.3.1.1 Paired comparison

In a paired comparison test, also called 2-alternatives forced choice, each subject was presented with two coded samples and had to indicate which sample appeared the saltiest. The forced choice method was used, meaning that panellists were not allowed to report 'no difference'. An example of the panellists' scoresheet is shown in Appendix 2.5. Panel responses for each test pair were tallied and significant differences between samples judged against tabulated critical numbers of correct answers (two-sides paired comparison test for differences, $\alpha = 0.05$ (Meilgaard, Civille and Carr, 2006)).

2.3.1.2 Multiple paired comparison

In multiple paired comparison tests, each subject was presented with all possible sample pairs, one pair at a time in random order. In reality, this test corresponds to a series of paired comparisons as described above (2.3.1.1). Panel judgments on each pair of samples were pooled and tabulated. The results were subjected to Friedman analysis (Meilgaard et al., 2006). Rank sums representing relative saltiness were presented on a line scale. Significant differences between samples were identified by calculating the honestly significant difference (HSD) value for comparing two rank sums (Meilgaard et al., 2006). An example of data pooling and Friedman analysis can be found in Appendix 2.6.

2.3.2 TRIANGLE TESTS

Triangle tests (ISO 2004c) are designed to show whether subjects can detect *any* difference at all between two samples. Panellists were presented with three coded samples in a specific order whereby two were identical and one was different. All six possible combinations, that is when comparing sample A to B the six triangle tests ABB, BAB, BBA, AAB, ABA, BAA were presented to the subjects albeit in random order. They were instructed to taste (also smell and examine) the samples and to identify the odd sample. The correct number of responses (panellists having correctly identified the odd sample) was tabulated against the number of total response to obtain the level of significance for the test (Meilgaard et al., 2006). An example of the panellists' scoresheet is shown in Appendix 2.7.

2.3.3 RANK RATING

The tests mentioned above only provide *relative* differences between samples. This is in contrast to rating samples for a specific attribute on a continuous intensity scale, anchored at the extremes with references (for example, 0.4% NaCl in water for low saltiness and 0.6% NaCl in water for high saltiness). In this research, differences in saltiness between samples were quite subtle and therefore rank rating was used as it has been shown to improve the discrimination ability of panellists (Ishii, Chang and O'Mahony, 2007). Here, panellists were asked to rank the samples, presented in random order, for increasing saltiness before rating them on an intensity scale. The

attributes examined as well as the anchors of the scales were determined by the panel as reported in Chapter 3. Data analysis is also reported in Chapter 3.

2.4 OTHER METHODS

Density and osmolality of the samples were also measured. Solution density was measured in triplicate using a density meter (DMA500, Anton Paar, Austria), operating on the principle of the oscillating u-tube (20 °C). The osmolality is defined as the number of moles of solute particles in a given mass of solvent and is given in mOsm.kg⁻¹. Osmolality is distinct from molarity as it measures moles of solute *particles* rather than moles of solute and some solutes (such as NaCl) dissociate when they dissolve into several particles (for NaCl, into two particles, Na⁺ and Cl⁻). It was measured in triplicate using an osmometer using the depression of freezing point method (Advanced® Model 3300 Micro-Osmometer, Advanced instruments Inc., Norwood, USA).

CHAPTER 3

EFFECT OF SHEAR FLOW BEHAVIOUR ON SALTINESS PERCEPTION

3.1 INTRODUCTION

In this Chapter, the results of exploring the relationship between low, intermediate and high shear rate viscosity of polysaccharide solutions and saltiness perception are reported. Solutions were thickened using the food hydrocolloids guar gum, dextran and xanthan gum to cover a range of typical solution flow behaviour. Guar gum solutions are shear-thinning and exhibit a zero shear plateau, dextran solutions are Newtonian and xanthan gum solutions are highly shear-thinning often interpreted as showing yield behaviour (Lapasin and Pricl, 1995). More information on the polymers can be found in Chapter 5. In particular, guar gum/xanthan gum mixtures were used as they exhibit weak gel behaviour (Tako and Nakamura, 1985; Shatwell et al., 1991; Schorsch, Garnier and Doublier, 1997; Casas, Mohedano and Garcia-Ochoa, 2000; Khouryieh et al., 2007). At low frequency, the mixture exhibits solid-like properties but behaves essentially like a guar gum solution at high frequencies (Schorsch et al., 1997).

In a first study (study A), saltiness perception was evaluated in solutions of varying molecular weights and concentrations of guar gum and dextran to conclude which viscosity – measured at a low (in the range of 0-50 s⁻¹) or at a high (3000 s⁻¹) shear rate – is relevant to saltiness perception. Two further studies were conducted to firm up the findings of study A. Study B was designed to narrow down the value of the low shear rate at which viscosity correlates to saltiness perception using solutions containing

guar gum and xanthan gum. Indeed, the guar gum or dextran solutions used in study A displayed an extended zero shear plateau so that the effect of *zero* shear viscosity and *low* shear viscosity ($\sim 50 \text{ s}^{-1}$) could not be distinguished. In contrast, the viscosity of guar gum/xanthan mixtures can decrease by one order of magnitude between 1 s^{-1} and 10 s^{-1} (Casas et al., 2000). Thus, in study B it was possible to determine whether *zero* shear or *low* shear ($10\text{-}50 \text{ s}^{-1}$) viscosity is relevant to saltiness perception. An effect of polymer concentration on saltiness perception became obvious during study A, thus an appropriate series of tests was performed on dextran solutions (study C). In the two studies investigating the shear rate relevant to saltiness perception (studies A and B), mouthfeel perception data were also acquired to evaluate whether mouthfeel and saltiness perception were correlated to viscosity at similar shear rate.

3.2 MATERIALS AND METHODS

3.2.1 MATERIALS AND PREPARATION OF THE POLYSACCHARIDE SOLUTIONS

Guar gum used was of the type Meyprodor in the grades Meyprodor[®]30, Meyprodor[®]100 and Meyprodor[®]400 (Danisco, Denmark) with a nominal molecular weight of 420 kDa ('G_L'), 1640 kDa ('G_M') and 2660 kDa ('G_H'), respectively. Three dextran samples of pharmaceutical grade (Pharmacosmos, Denmark) with a nominal molecular weight of 10 kDa ('D_L'), 40 kDa ('D_M') and 500 kDa ('D_H'), respectively, were

used. Xanthan gum was of the type Keltrol®RD (CP Kelco, San Diego, USA). Sodium chloride and sucrose were added as 'Table salt' and 'sugar' (bought in a local supermarket). Silicon oil (100 cSt, Dow Corning) was used as a Newtonian reference fluid to evaluate the gap error in the thin film viscosity measurements as outlined in Chapter 2 (2.2.1). Aqueous solutions were prepared with bottled water (Evian, Danone, France), simply referred to as 'water' in the following.

Initially, stock solutions of each polysaccharide at the highest concentration applied in this study were prepared by dispersing the dry powder in water using a magnetic stirrer. Dextran was fully dissolved after stirring for 3 h at room temperature. Guar gum and xanthan gum dispersions were stirred at 80 °C for 1 h followed by continued mixing overnight on a roller mixer at 4 °C to avoid microbial growth. Samples were stored at 4 °C and used within one week. Preliminary experiments showed that the guar gum solutions contained a small amount of insoluble impurities (cell debris and insoluble proteins) which were removed by centrifugation for 45 min at 5000 g and 4 °C after which the samples appeared less cloudy. Stock solutions were diluted with water containing the appropriate amount of salt to obtain desired viscosity values at specific shear rates and placed for a further 2 h onto the roller mixer. The polymer concentrations are expressed in % w/w of dry powder as provided by the suppliers.

3.2.2 CHARACTERISATION OF POLYSACCHARIDE SOLUTIONS

All rheological measurements were conducted at 20 °C using a rotational rheometer (MCR301, Anton Paar, Austria). Steady state viscosity data for guar gum and dextran solutions were acquired up to shear rates of 10^5 s^{-1} using thin film rheology and data were corrected for gap error as well as non-Newtonian behaviour (see 2.2.1). The corrected apparent viscosity is simply referred to as 'viscosity' in the following. As guar gum/xanthan mixtures (study B) displayed yield stress behaviour, the flow behaviour of these samples was characterised in a stress-controlled test. Shear stress was varied from 0.1 to 100 Pa, allowing 5 s per point and 15 points per decade logarithmically spaced. A pre-shear protocol was utilised to erase sample filling effects as a possible source of errors. During 15 s a shear stress of 100 Pa was applied after which the actual flow curve measurement was started after a one minute rest. For the less viscous solutions, samples D and E, the pre-shear was performed at 10 Pa. A serrated parallel plate geometry (50 mm diameter, gap 1 mm) was used to avoid slippage.

Density and osmolality of the samples were also measured as described in 2.4.

3.2.3 EXPERIMENTAL DESIGNS AND SENSORY ANALYSIS

3.2.3.1 Study A: Is high shear or low shear viscosity relevant to saltiness perception?

3.2.3.1.1 Design and flow behaviour of the samples

This study was designed to investigate whether the decrease in saltiness perception reported with increasing viscosity (see 1.3) was related to high shear or low shear viscosity. Dextran and guar gum solutions were matched in viscosity measured at zero shear and 3000 s^{-1} , respectively, by adjusting polysaccharide concentration and using polymers of different molecular weights. Viscosity levels were chosen so that all concentrations were above c^* , to ensure a significant effect of viscosity on taste perception (see 1.3) (Baines and Morris, 1987). Although 3000 s^{-1} is significantly lower than shear rates recently suggested to be of relevance to in-mouth processing of foods (see 1.2.2), it was the highest shear rate attainable for concentrations above c^* taking into account the considerable degree of shear-thinning of the high molecular weight guar gum sample. Samples contained a constant salt concentration on a weight total basis (0.6% w/w salt), however, based on the results, a repeat of study A was performed with samples containing a constant salt concentration on a volume basis (0.6% w/v salt).

The experimental set was composed of eight samples denoted by two letters referring to the polymer type and a numeral denoting the zero shear viscosity. Zero shear viscosity was matched at viscosity of 0.03 Pa.s and 0.09 Pa.s (samples G_L0.03, G_H0.03, D_M0.03, D_H0.03 and G_L0.09, G_H0.09, D_H0.09, respectively). Samples G_L0.09, D_H0.03 and D_M0.03 also matched at viscosity of 0.03 Pa.s at 3000 s⁻¹. An eighth sample, G_H2, was added to the design as a further high shear viscosity matched sample. It was formulated with a significantly higher zero shear viscosity to enable clear differentiation between the impact of zero shear and high shear viscosity, respectively, on saltiness perception. Sample details are provided in Table 3.1 and the viscosity behaviour is shown in Figure 3.1.

Table 3.1 : Samples of study A. All samples contained 0.6% w/w NaCl and polymer concentrations are based on dry powder as received from the manufacturer.

Sample	Viscosity matching	Polymer (% w/w)	Density (g/cm ³)	c/c*	c[η]	Salt (% w/v) All contain 0.6%w/w
G _H 0.03	0.03 Pa.s at 0 s ⁻¹	0.215	1.0052	1.4	3.9	0.603
G _L 0.03	0.03 Pa.s at 0 s ⁻¹	1.00	1.0086	1.6	3.6	0.605
D _H 0.03	0.03 Pa.s at 0 s ⁻¹ 0.03 Pa.s at 3000 s ⁻¹	10.25	1.0446	1.6	4.6	0.627
D _M 0.03	0.03 Pa.s at 0 s ⁻¹ 0.03 Pa.s at 3000 s ⁻¹	20.50	1.0875	1.5	3.7	0.653
G _H 0.09	0.09 Pa.s at 0 s ⁻¹	0.31	1.0057	2.0	5.6	0.603
G _L 0.09	0.09 Pa.s at 0 s ⁻¹ 0.03 Pa.s at 3000 s ⁻¹	1.50	1.0102	2.4	5.3	0.606
D _H 0.09	0.09 Pa.s at 0 s ⁻¹	14.50	1.0639	2.3	6.5	0.638
G _H 2	0.03 Pa.s at 3000 s ⁻¹	0.70	1.0070	4.5	12.6	0.604

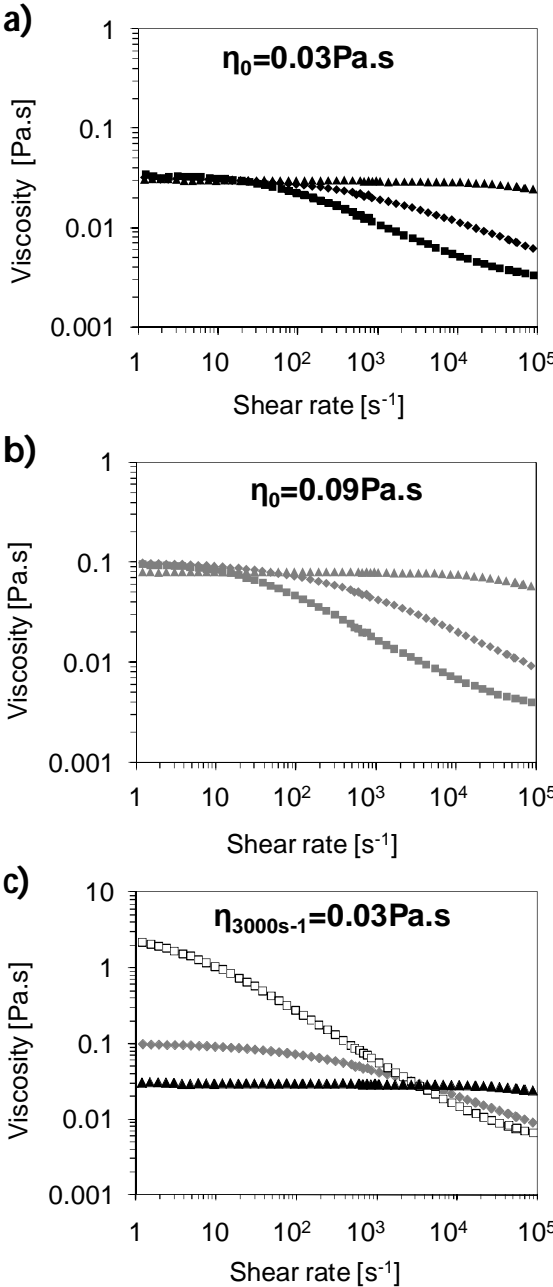


Figure 3.1 : Viscosity curves of samples from study A, inset in plots refers to the criterion of viscosity matching. Symbols refer to the polymer type: G_L (◇), G_H (□), D_M (○), D_H (△) and zero shear viscosity is differentiated by 'colour': 0.03 Pa.s (black), 0.09 Pa.s (grey) and 2 Pa.s (void).

Polymer concentrations ranged from 0.31 to 20.5 %w/w. The dextran molecule is very compact in solution and can therefore be described as an 'ineffective thickener' as a result of which the concentration required to obtain a given zero shear viscosity was at least 10 times higher than for guar gum. Consequently, the density of dextran solutions was also higher (Table 3.1) and salt concentration based on % w/v differed across the sample set, ranging from 0.605% w/v for G_H0.03 to 0.653% w/v for D_L0.03 (Table 3.1). Dextran solutions exhibited Newtonian flow behaviour (Figure 3.1; the viscosity curves for the dextran samples D_M0.03 and D_H0.03 overlap) whereas guar gum solutions were shear-thinning. The degree of shear-thinning increased with increasing molecular weight and increasing concentration (Figure 3.1), which has previously been reported (Morris et al., 1981; Robinson, Ross-Murphy and Morris, 1982). As a result, samples matched in viscosity at zero shear and at 3000 s⁻¹ exhibited markedly different high shear ($G_H < G_L < D_L = D_H$) and low shear ($G_H > G_L > D_L = D_H$) viscosity, respectively. With exception of sample G_H2, an extended zero shear viscosity plateau was observed (up to about 50 s⁻¹).

3.2.3.1.2 *Sensory analysis methods*

An experienced panel was trained to rate attributes they themselves generated and defined through discussion. Nine healthy volunteers were recruited on the basis of their ability to discriminate between samples varying in viscosity or salt concentration. Training was carried out over 4 sessions, each lasting 2 h, using a sub-set of 4 samples and consisted of the following: (i) initial attributes generation (the panellists were

instructed not to consider colour or flavour); (ii) selection of final list of attributes; (iii) Definition of attributes and anchor terms as defined in Table 3.2.; (iv) practise scaling; and (v) monitoring trial on computer in booths and validation of panellist performance. After training was completed, data were collected in triplicate on three different days. Samples were presented in 30 ml cups and a dessert spoon was provided to transfer the samples to the mouth. Panellists were instructed to be as consistent as they could in terms of sample volume and in-mouth handling. Saltiness attributes were rated using a rank-rating approach, whereby panellists were asked to rank the samples for increasing saltiness before rating them on the intensity scale. After a 15 min break, panellists were presented with samples monadically to score the mouthfeel attributes. The rating was performed on a continuous line scale anchored at the extremes with loose ends, and the marks were converted to a score between 0 and 10. The extremes had been defined by the panel during the attribute generation step. For saltiness attributes, references provided to the panellists were NaCl in water (0.4% w/w and 0.6% w/w) and for mouthfeel attributes, references were based on the viscosity extremes of the design (water and sample G_{H2}), see Table 3.2. The rank-rating experiment was repeated with 8 members of the same trained panel for samples salted on a weight-volume basis (0.6% w/v instead of 0.6% w/w), only considering the attribute *initial saltiness*. The rank-rating was performed on two groups of 4 samples with identical zero shear viscosity (0.03 Pa.s and 0.09 Pa.s). The order of presentation within each group and the order of the two tests were randomised.

Table 3.2 : Attributes and their descriptions as defined by the panel.

	Attribute	Definition	Scale	References
Saltiness	Initial saltiness	Immediate saltiness intensity when the product is place in mouth		
	In-mouth saltiness	Saltiness intensity after a few seconds with the product in mouth	Low to high	<i>Low</i> : 0.4% NaCl <i>High</i> : 0.6% NaCl
	Lingering saltiness	Saltiness intensity after swallowing		
Mouthfeel	Thickness	Overall thickness perception	Thin to thick	Based on the
	Lubrication	Smooth, slidy, glidy behaviour of the product in mouth	Least to most	subset of
	Stickiness	Force to separate the tongue from the palate	Least to most	samples during the training: <i>low</i> : water
	Residues	Amount of residues left in mouth after swallowing	Least to most	<i>high</i> :G _{H2}

Data were subjected to an analysis of variance, ANOVA, with two factors (*sample* and *panellist*) and potential interaction between the factors using the software package SPSS (SPSS Inc, Chicago, USA). Where appropriate, Tukey's HSD test (Meilgaard et al., 2006) was used to identify which samples were significantly different to others ($\alpha=0.05$). A stepwise linear regression was applied to identify which of the following factors is most relevant to saltiness perception: polymer concentration (% w/w), density, salt concentration (% w/v), ratio c/c^* , degree of coil occupancy $c \cdot [\eta]$, viscosity

at zero shear, at 50 s^{-1} , at 3000 s^{-1} and at $50,000 \text{ s}^{-1}$. A contour plot was produced using the software package Design Expert (Stat-Ease, Minneapolis, USA). Pearson's correlation coefficients were also calculated.

3.2.3.2 Study B: Is the zero shear viscosity or viscosity measured at low shear ($10\text{-}50 \text{ s}^{-1}$) relevant to saltiness perception?

3.2.3.2.1 Design and flow behaviour of the samples

The results of study A indicated that saltiness perception was related to viscosity measured at a low shear rate. However, the experimental design was such that it could not be established whether the *zero* shear viscosity or the *low* shear viscosity ($10\text{-}50 \text{ s}^{-1}$) was relevant to explain saltiness perception. A new experimental set of five samples based on guar gum (G_M) alone and mixtures of guar gum with xanthan gum was prepared. Samples were either matched in viscosity at very low shear ($<0.5 \text{ s}^{-1}$), considered to be the zero shear viscosity, or at moderately low shear rates ($\sim 50 \text{ s}^{-1}$) by adjusting polysaccharide concentrations. The composition of the samples and the flow behaviour can be found in Table 3.3 and in Figure 3.2, respectively. The salt concentration was set constant at 0.6 % w/v (volume basis).

Table 3.3: Composition of the samples containing guar gum and xanthan gum. The salt concentration was set constant at 0.6% w/v.

Sample	A	B	C	D	E
Xanthan [% w/w]	0.20	0.05	0	0.16	0.05
Guar G_M [% w/w]	0.70	0.90	0.95	0.35	0.40

The effect of the addition of xanthan gum on the flow behaviour is evident when comparing the samples A, B, C. Sample C contained guar gum only and displayed an extended zero shear plateau whereas the samples containing xanthan gum displayed a reduced zero shear plateau and a high degree of shear-thinning, characteristics of weak gel behaviour.

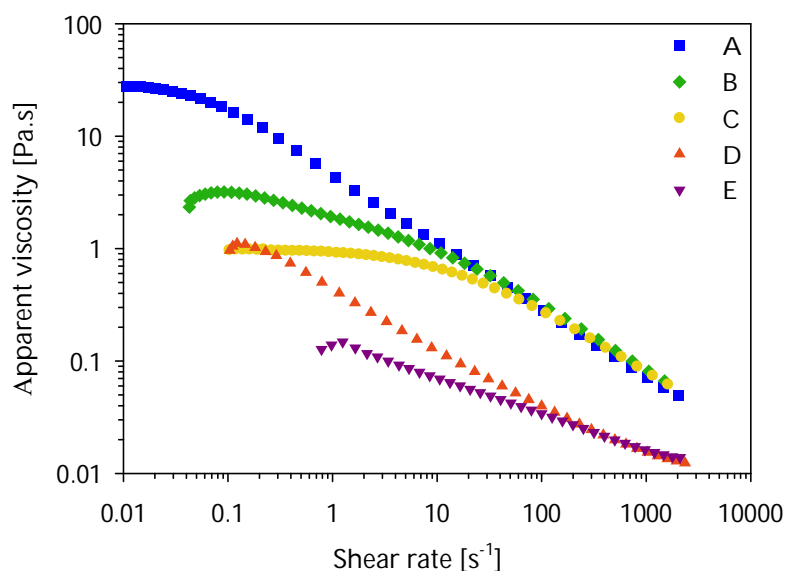


Figure 3.2: Viscosity curves for the guar gum/xanthan gum mixtures (study B). Samples A (■), B (◆), C (●) form the first sub-set and samples C (●), D (▲) and E (▼) to the second sub-set. Samples were subjected to a pre-shear (3.2.2).

As seen in Figure 3.2, samples A, B and C were matched in viscosity at moderately high shear rates ($>15 \text{ s}^{-1}$). At very low shear rates ($<0.2 \text{ s}^{-1}$), the viscosity of samples C and D was matched. Finally, the samples D and E were matched in viscosity at high shear rates ($>100 \text{ s}^{-1}$).

3.2.3.2.2 Sensory analysis methods

Sensory perception of the samples was compared using multiple paired comparisons for two attributes: *initial saltiness* and *thickness*. Samples were compared in two separate sets of three samples: samples A, B and C and samples C, D and E. The two sets were evaluated on the same day with the same panellists. Untrained panellists (N=22) were used.

3.2.3.3 Study C: To which extent is saltiness perception affected by polymer concentration?

To firm up the findings of study A, the effect of polymer concentration on saltiness perception was further investigated using Newtonian dextran solutions (shear rate dependent viscosity was no longer a factor). Samples of identical viscosity (30 mPa.s) and salt concentration (in weight basis or volume basis) were prepared using dextran of different molecular weights. As the thickening power of dextran increases with molecular weight (Tirtaatmadja, Dunstan and Roger, 2001), samples differed in polymer concentration: 10.25% w/w for D_H, 20.5% w/w for D_M and 30% w/w for D_L.

Four different sensory tests were performed (Table 3.4). To ensure the validity of the results, it was verified that the samples could not be distinguished on the basis of their intrinsic taste (due to the thickeners) or their mouthfeel (test C1, samples not containing any tastant). In tests C2 and C3, saltiness perception in dextran solutions was investigated. In test C2, saltiness perception of the two extreme samples (D_L and D_H) was compared when 2 g of sample was given to the subjects, and the effect of the type of NaCl concentration (*weight* basis or *volume* basis) was investigated (Table 3.7). In test C2a, the salt concentration was fixed on a *volume* basis, so that samples differ in total amount of NaCl delivered. In test C2b, the salt concentration was fixed on a *weight* basis, both samples delivering the same total amount of NaCl to the subjects but the salt concentration in *volume* basis differed. To extend the results of test C2, saltiness perception in dextran solutions of three different molecular weights was compared in test C3. The results from tests C2 and C3 clearly demonstrated the effect of polymer concentration on saltiness perception. In order to identify the underlying mechanisms, it was investigated in test C4 whether *sweetness* perception was equally enhanced by high polymer concentrations or if the effect of polymer concentration was taste-specific.

Table 3.4: Sensory experiment performed on the dextran samples to investigate the effect of polymer concentration (study C).

Test	C1	C2a	C2b	C3	C4
Tastant added	None	NaCl 0.65% w/v	NaCl 0.6% w/w	NaCl 0.6% w/v	Sucrose 5% w/v
Samples compared	D _L , D _M , D _H	D _L , D _H	D _L , D _H	D _L , D _M , D _H	D _L , D _M , D _H
Type of test	Triangle tests (all possible combinations)	Paired comparison	Paired comparison	Multiple paired comparison	Multiple paired comparison
Attribute specified		Saltiness	Saltiness	Saltiness	Sweetness
Number of panellists	27	40	26	33	27

3.3 RESULTS AND DISCUSSION

3.3.1 STUDY A: IS HIGH SHEAR OR LOW SHEAR VISCOSITY RELEVANT TO SALTINESS PERCEPTION?

Table 3.5 shows the p-values of the ANOVA and the mean sample scores for sample set with varied and matched high shear and low shear viscosity as described in 3.2.3.1 (see Table 3.1 for composition and Figure 3.1 for flow behaviour of the samples). It is evident that the factor *sample* was significant for all three saltiness attributes ($p < 0.0001$), however, the interaction *panellist*sample* was never significant. The time-

aspect of saltiness perception was not significant as the three attributes *initial saltiness*, *saltiness in mouth* and *saltiness after swallowing* were strongly correlated ($r^2 > 0.99$). Only *initial saltiness*, simply referred to as 'saltiness', will be considered in the following as consumers are very likely to judge saltiness immediately.

Table 3.5 : ANOVA p-values and mean sample scores from the main study. Samples contained 0.6% w/w NaCl. Samples with the same letter code in any one column are not significantly different ($p < 0.05$).

	Initial saltiness	Saltiness in mouth	Saltiness after swallowing	Thickness	Lubrication	Stickiness	Residue
	p-values						
Product	<0.0001	<0.0001	<0.0001	<0.0001	<0.0001	<0.0001	<0.0001
Panellists	0.736	0.53	0.017	<0.0001	<0.0001	<0.0001	<0.0001
Product*							
Panellists	0.086	0.045	0.359	0.091	0.221	0.005	0.308
	Mean samples scores						
G _H 0.03	4.52 _{b,c,d}	4.22 _{b,c}	4.4 _{b,c}	1.97 _a	1.95 _a	1.01 _a	1.31 _a
G _L 0.03	3.07 _{a,b,c}	3.07 _{a,b}	3.2 _{a,b}	3.01 _{a,b}	3.81 _{b,c}	2.2 _a	2.69 _a
D _H 0.03	6.26 _{d,e}	6.27 _d	6.27 _{c,d}	4.04 _b	5.33 _{c,d}	4.65 _b	4.91 _{c,b}
D _L 0.03	7.84 _e	8.47 _e	8.1 _d	3.95 _b	5.11 _{b,c}	4.15 _b	4.57 _b
G _H 0.09	3.72 _{a,b,c}	3.75 _{b,c}	3.12 _{a,b}	3.46 _b	3.72 _b	2.04 _a	2.34 _a
G _L 0.09	4.48 _{b,c,d}	4.53 _{b,c,d}	4.16 _{b,c}	5.9 _c	6.69 _{d,e}	5.31 _b	6.2 _{c,d}
D _H 0.09	5.82 _{c,d,e}	5.86 _{c,d}	6.25 _{c,d}	7 _c	7.59 _e	7.5 _c	7.82 _e
G _H 2	2.04 _a	1.93 _a	1.52 _a	8.6 _d	8.23 _e	7.1 _c	7.24 _{d,e}

Samples scores for *initial saltiness* ranged between 2.0 and 7.8 although all samples contained 0.6% w/w NaCl (Table 3.5). For a given type of polymer, lower saltiness scores were found with increasing polymer concentration (associated with an increase in viscosity) as it has been reported for concentrations above c^* (Christensen, 1980; Baines and Morris, 1987; Cook et al., 2002). For example, G_H0.03 was saltier than G_H0.09, which itself was saltier than G_H2 with scores of 4.5, 3.7 and 2, respectively.

However, only the difference between $G_{H0.03}$ and G_{H2} is significant. The results obtained for zero shear viscosity matched low and high molecular weight guar gum samples did not reveal significant differences. In contrast, high shear matched guar gum samples ($G_{L0.09}$ and G_{H2}) differed significantly in saltiness with G_{H2} assessed as significantly less salty than $G_{L0.09}$. In addition, dextran samples appeared consistently saltier than guar gum samples.

The observations so far can be generalised by modelling saltiness perception data using a stepwise linear procedure, initially including nine factors detailed in the Materials and Methods section of this chapter (3.2.3.1.2). Saltiness perception was successfully explained by two factors only: *polymer concentration* and *zero shear viscosity* ($R^2 = 0.90$; $p=0.004$ and $p=0.05$, respectively). The corresponding surface-response model is depicted in Figure 3.3. Lack of results in the top right hand quadrant of the graph can be explained by the underlying experimental design in which the factors plotted on the abscissa and ordinate had not been considered. Plotting the model clearly demonstrates that high shear viscosity (quantified at 3000 s^{-1}) is not a good predictor for saltiness perception. Correlation is found at the other end of the viscosity curve, however, it cannot be concluded whether viscosity at *low* shear ($10\text{-}50\text{ s}^{-1}$) or at *zero* shear governs saltiness perception as the viscosity of the guar gum and dextran samples is almost constant for shear rate $< 50\text{ s}^{-1}$. Indeed, saltiness perception can be predicted equally well by polymer concentration and viscosity measured at 50 s^{-1}

($R^2=0.90$) as viscosity at zero shear and at 50 s^{-1} are closely correlated. Thus study B was designed, see 3.3.2 for the results.

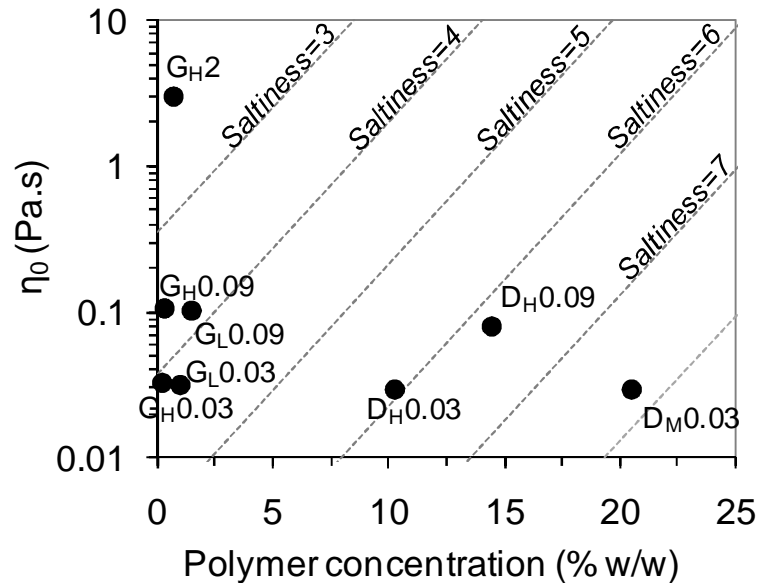


Figure 3.3: Surface-response model of saltiness as affected by polymer concentration and zero shear viscosity ($R^2=0.90$). The dashed lines indicate iso-saltiness as predicted by the model.

When samples were salted at 0.6% w/w, the polymer concentration was found to have a significant effect of saltiness perception, as dextran samples were found saltier than guar gum samples and $D_M0.03$ saltier than $D_H0.03$. Samples containing high polymer concentrations were denser and the salt concentration on volume basis (% w/v) was consequently higher (Table 3.3). To investigate whether the higher salt concentration in volume basis was the underlying phenomena explaining the effect of polymer concentration on saltiness perception, study A was repeated setting the salt concentration on volume basis constant.

3.3.1.1 Saltiness of samples salted at 0.6% w/v (weight-volume basis)

Panellists were given a fixed volume of sample (2 ml) so that salt concentration (0.6% w/v) and total amount of salt delivered (12 mg) were constant across samples. Sensory test methods were slightly different since only 4 samples were presented at a time: 4 samples matched at zero shear viscosity of 0.03 Pa.s ($G_L0.03$, $G_H0.03$, $D_L0.03$ and $D_H0.03$) and of 0.09 Pa.s ($G_L0.09$, $G_H0.09$, $D_H0.09$ and $D_L0.09$), respectively, were ranked for saltiness followed by rating on the scale developed for the initial study (Table 3.2). The mean scores can be found in Table 3.6. ANOVA on the attribute *initial saltiness*, performed on the rating data of both sets separately, showed that the factor *sample* was significant at $p=0.01$ and $p=0.001$ for viscosity matching at 0.09 Pa.s and 0.03 Pa.s, respectively. In both cases, there was no significant *panellist*sample* interaction.

$G_H0.03$ and $G_L0.03$ were not significantly different, in agreement with the previous results at 0.6% w/w. In contrast, significant differences in saltiness were observed between $G_L0.09$ and $G_H0.09$ salted at 0.6% w/v (Table 3.6). It is hypothesised that the significant difference in saltiness perception between $G_L0.09$ and $G_H0.09$ may be due to stimulus errors, as the 'off' taste of guar L is slightly more pronounced than that of G_H . Dextran solutions of similar viscosity ($D_M0.03$ and $D_H0.03$; $D_M0.09$ and $D_H0.09$) were also not significantly different in saltiness, though D_M seems to appear saltier. Finally, dextran samples appeared saltier than guar gum samples, as observed when samples

were salted at 0.6% w/w, despite the fact that the salt concentration in w/v and the amount of NaCl delivered was identical for all samples.

Table 3.6 : Mean sample scores from rank-rating. All samples contained 0.6% w/v NaCl.

$\eta_0=0.03$ Pa.s			$\eta_0=0.09$ Pa.s		
Sample	Sum of rank	Score	Sample	Sum of rank	Score
G _H 0.03	37.0 ^a	4.29 ^a	G _H 0.09	47.0 ^a	3.82 ^a
G _L 0.03	59.0 ^{a,b}	5.48 ^{a,b}	G _L 0.09	59.0 ^{a,b}	6.2 ^b
D _H 0.03	65.0 ^c	6.17 ^{b,c}	D _H 0.09	59.0 ^{a,b}	4.95 ^{a,b}
D _M 0.03	79.0 ^c	7.61 ^c	D _M 0.09	75.0 ^b	6.75 ^b

3.3.1.2 Discussion

Overall, saltiness perception studied on guar gum samples was independent of the shear-thinning behaviour and affected only by the zero shear viscosity, or low shear viscosity in this case since viscosity values at low shear and zero shear are nearly identical due to the nature of the viscosity curve (Figure 3.1). This is corroborated by work of Baines & Morris (1987) who found that sweetness scores of guar gum solutions of different molecular weights were explained solely by the degree of space occupancy $c \cdot [\eta]$, which is correlated to the zero shear viscosity (Morris et al., 1981). Cook et al. (2003a) also reported that Kokini oral shear stress, ratio c/c^* , zero shear viscosity and viscosity at 50 s^{-1} were all successfully modelling sweetness perception ($R^2 > 0.85$), all those parameters correlated with low shear viscosity, not high shear

viscosity. It should be noted, however, that significant differences in saltiness were obtained only for relatively large differences in zero shear viscosity. Thus study B asking whether the viscosity at *zero* shear or at *low* shear (10-50 s⁻¹) governs saltiness perception was designed, see 3.3.2 for the results.

As a general trend, dextran samples appeared saltier than guar gum samples of identical zero shear viscosity (Table 3.5 and Table 3.6), whether the salt concentration was set constant on weight basis or volume basis. This may be due to difference in intrinsic taste between the guar gum and dextran samples. Alternatively, it can be hypothesised that the molecular structure of the polymer impacts on saltiness perception. Guar gum is a more rigid polymer than dextran due to the β -1→4 linkage of the backbone (Lapasin and Pricl, 1995), resulting in higher elastic properties than dextran (see Chapter 5). Finally, it is possible that the polymer concentration itself affects saltiness perception, since concentration of polymer is about 10 times higher in dextran than in guar gum sample. This hypothesis has been tested in study C, see 3.3.3 for the results.

3.3.2 STUDY B: IS THE ZERO SHEAR VISCOSITY OR VISCOSITY MEASURED AT LOW SHEAR (10-50 s⁻¹) RELEVANT TO SALTINESS PERCEPTION?

Saltiness perception was compared using multiple paired comparisons in two subsets: samples A, B, C and samples C, D, E. The composition of the samples and their

flow behaviour were presented in Table 3.3 and Figure 3.2, respectively (see 3.2.3.2). The rank sum scores for saltiness are represented in line diagrams in Figure 3.4a) and b) and are graphically depicted in Figure 3.5. The Friedman's statistic T was equal to 80 and 95, respectively for the two sets of samples indicating that panellists were able to distinguish between the samples within each set ($p < 0.005$). Tabulated results can be found in Appendix 3.1.

Samples A, B and C exhibited similar viscosity for shear rates $\geq 50 \text{ s}^{-1}$, yet they differed in saltiness and saltiness perception was found to decrease with increasing viscosity at low shear rate ($< 10 \text{ s}^{-1}$). Similarly, samples D and E exhibited similar viscosity for shear rates $\geq 100 \text{ s}^{-1}$ but saltiness perception was found to decrease with increasing viscosity at low shear rate ($< 10 \text{ s}^{-1}$). In addition, D was found significantly saltier than C, despite the samples exhibiting similar viscosity at very low shear ($< 0.5 \text{ s}^{-1}$). Thus, viscosity governing saltiness perception should be measured at low shear rates (about $1\text{-}10 \text{ s}^{-1}$), see Figure 3.5.

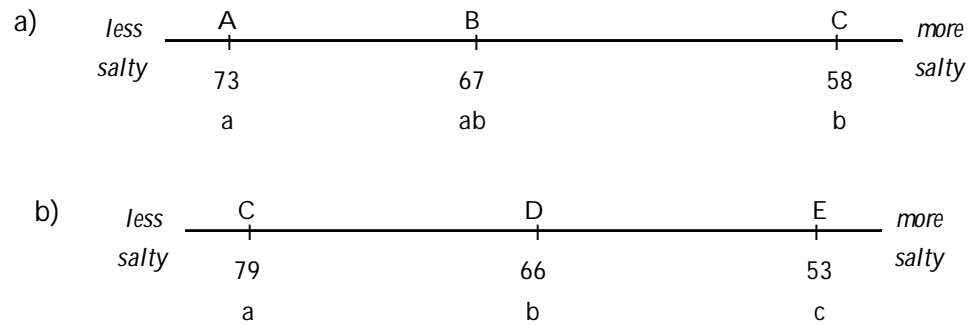


Figure 3.4: Line diagram representations of the rank sum scores for saltiness in the multiple paired comparisons of a) the samples A, B and C b) the samples C, D and E (22 panellists). Samples with the same letter code are not significantly different ($p < 0.05$).

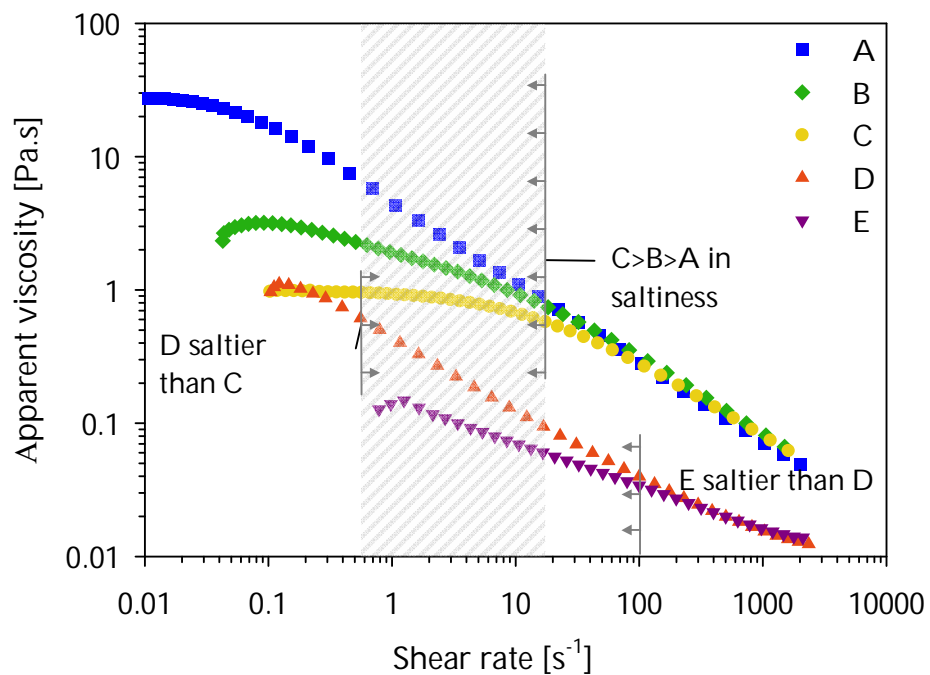


Figure 3.5: Flow behaviour and sensory perception of guar gum/xanthan gum mixtures. The viscosity in the shaded range of shear rates governs saltiness perception (result of this study).

With studies A and B it has been established that the decrease of saltiness perception with increasing shear viscosity was related to the viscosity measured at moderately

low shear rates (about 1-10 s⁻¹). Baines and Morris (1987) found that sweetness perception in random coil solutions correlates well with the zero shear viscosity, which is in agreement with the data reported here for saltiness in random coil solutions (Study A) but does not appear to stand for weak gel systems (study B). In addition, sweetness perception has previously been reported to correlate well to the Kokini oral shear stress (Kokini et al., 1977) (Cook et al., 2003a; Ferry et al., 2006a). Thus, the Kokini oral shear was calculated for the sake of comparison, though it requires the power-law behaviour of the viscosity-shear rate relationship and the fit of the power-law model to guar gum flow curves is poor. The Kokini oral shear stress was found to be highly correlated to the logarithm of the viscosity at 10 s⁻¹ (0.95 in study A and 0.96 in study B), which is surprising considering the poor power-law fit for guar gum solutions. The results of study A and B therefore indicate that saltiness perception is equally well correlated to the viscosity measured at 10 s⁻¹ and to the Kokini oral shear stress. Yet, since most food products do not display power-law behaviour, the viscosity at 10 s⁻¹ appears the best predictor of saltiness perception in thickened solutions as it can be obtained for any product and is not based on assumptions simplifying to the extremes the deformation in mouth (1.2.2).

To firm up the findings of study A, the effect of polymer concentration on saltiness perception was further investigated in study C and the results are presented subsequently.

3.3.3 STUDY C: TO WHICH EXTENT IS SALTINESS PERCEPTION AFFECTED BY POLYMER CONCENTRATION?

In study C, sensory evaluations were performed on dextran solutions of identical shear viscosity (30 mPa.s) but different polymer concentration by using different molecular weight. Sensory tests were presented in Table 3.4.

3.3.3.1 Test C1: perception in absence of tastant

To ensure the validity of the results, it was verified that the samples could not be distinguished on the basis of their intrinsic taste (due to the thickeners) or their mouthfeel (test C1, Table 3.4). It was found that in absence of tastant the samples could not be significantly distinguished (D_H vs. D_M , $p=0.266$; D_H vs. D_L , $p=0.411$ and D_M vs. D_L , $p=0.572$). Thus, any significant difference between the samples containing a tastant (NaCl or sugar) will be solely due to differences in taste perception.

3.3.3.2 Tests C2 and C3: effect of polymer concentration on saltiness perception

3.3.3.2.1 Tests C2: effect of polymer concentration on saltiness perception as a function of salt concentration type

As briefly discussed before (see study A), the polymer concentration affected the density of the samples and, therefore, changes in polymer concentration imparted differences between the salt concentration on a volume basis (w/v) and on a weight

basis (w/w). For the first time, the effect of the salt concentration type (w/w or w/v) on the saltiness of two samples D_L and D_H was investigated as part of this research.

Two sensory tests (tests C2a and C2b, see Table 3.4) were performed on dextran solutions of high and low molecular weight (D_H and D_L , respectively), adjusting salt solution concentration on a % w/w or a % v/w basis. The composition of the samples and sensory results are given in Table 3.7. In test C2b, the same amount of sodium chloride was delivered (12 mg), but the sample having the higher salt concentration in % w/v (0.68% w/v versus 0.63% w/v) was found to be saltier by 21 out of 26 assessors ($p=0.01$). In test C2a, both samples had the same concentration of salt in % w/v. The sample thickened with the low molecular weight dextran (higher polymer concentration) was by 27 panellists out of 40 found to be saltier, even though it had a lower salt concentration in % w/w. Thus, it appears that at constant salt concentration (regardless of the unit w/w or w/v), the sample containing the higher polymer concentration is significantly saltier, even if the amount of NaCl is actually lower. To validate these results, saltiness perception from dextran solutions of three different molecular weights was compared comprising test C3 (Table 3.4).

Table 3.7: Composition of samples for paired comparison test (Newtonian viscosity 0.03 Pa.s)

	Dextran		NaCl			Sensory
	type	Polymer % w/w	% w/w	% w/v	mg NaCl delivered	Number of times found saltier
test 2a	D _H	10.25	0.62	0.65	12.44	13
	D _L	29.00	0.58	0.65	11.52	27
test 2b	D _H	10.25	0.60	0.63	12	5
	D _L	29.00	0.60	0.68	12	21

3.3.3.2.2 Test C3: samples salted at 0.6% w/v

The dextran solutions of three different molecular weights (D_L, D_M and D_H) were salted at 0.6% w/v and panellists were instructed to compare them for saltiness using multiple paired comparisons (test C3, Table 3.4). The results are presented in Figure 3.6 and tabulated data can be found in Appendix 3.2. Panellists were able to distinguish the samples based on saltiness (Friedman's statistic $T=13.6$, $p=0.01$). D_H appeared significantly less salty than D_M ($p=0.1$), itself significantly less salty than D_L ($p=0.1$), the difference in saltiness between D_H and D_L being highly significant ($p=0.01$). This confirms that, for a given polymer type, saltiness perception increases with increasing polymer concentration, as the concentration required to match viscosity (at 30 mPa.s) increased with decreasing molecular weight. This finding was confirmed at a lower salt concentration (0.45% w/v NaCl, 40 panellists, $p<0.01$). To investigate whether the effect of polymer concentration was specific to saltiness perception, a

similar comparison was performed with the sweetness of dextran solutions containing sucrose (test C4).

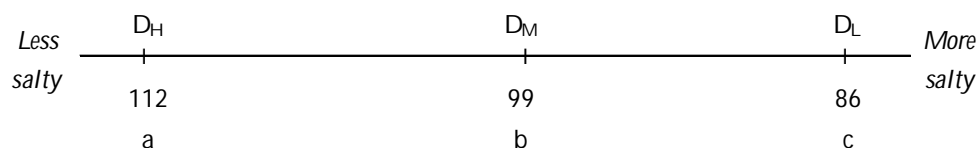


Figure 3.6: Line diagram representation of the rank sum scores for saltiness in the multiple paired comparisons of dextran samples D_H, D_M and D_L salted at 0.6% w/v (viscosity 30 mPa.s, 33 panellists). Samples with the same letter code are not significantly different ($p < 0.1$). D_H and D_L are significantly different at $p = 0.001$.

3.3.3.3 Test C4: effect of polymer concentration on sweetness perception

Is *sweetness* perception enhanced by a high polymer concentration in a similar way as found for *saltiness*? To investigate this effect, similar samples as used in Test C3 (dextran solutions of three different molecular weights of viscosity of 30 mPa.s) but containing 5% w/v sucrose instead of NaCl were compared for sweetness using multiple paired comparisons (test C4, Table 3.4). The results are presented in Figure 3.7 and tabulated data can be found in Appendix 3.3. Sweetened samples could not be distinguished by the panellists (Friedman's statistic $T = 3.8$, $p > 0.1$), which contrasts with the large differences in saltiness reported above (in 3.3.3.2.2). D_L appeared slightly sweeter but no significant differences were found. Thus, the effect of polymer concentration on taste perception is specific to saltiness perception.

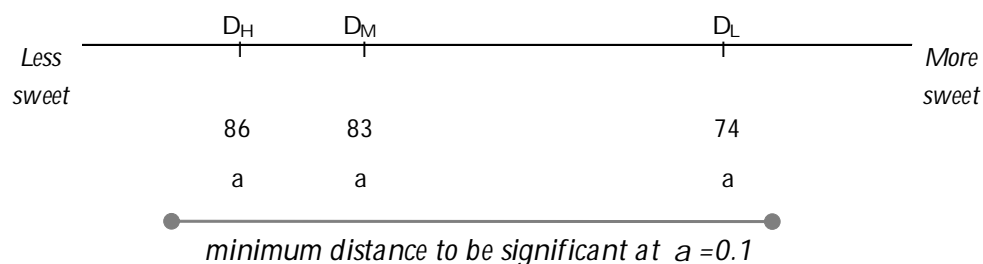


Figure 3.7: Line diagram representation of the rank sum scores for sweetness in the multiple paired comparisons of dextran samples D_H, D_M and D_L sweetened at 5% w/v sucrose (viscosity 30 mPa.s, 27 panellists). Samples with the same letter code are not significantly different ($p < 0.1$).

3.3.3.4 Discussion of study C

The results of this research demonstrate that a higher polymer concentration enhances saltiness perception, but not sweetness perception. This finding was verified at two concentrations of NaCl (0.6% and 0.45% w/v) and for salt concentration fixed on volume basis (w/v) or on weight basis (w/w). It is therefore very likely that the higher saltiness perceived in dextran solutions compared to guar gum solutions (in study A, 3.2.3.1) is related to the much higher polymer concentrations in the former samples. The effect of polymer concentration on saltiness perception has never been reported in literature which is not surprising as highly efficient thickeners are generally used in studies on saltiness perception (carboxymethylcellulose, xanthan gum, guar gum, carrageenan, HPMC, methycellulose... see Table 1.1) and therefore the range of polymer concentration studied is at the low end of the scale (max. 2 %). This narrow

concentration range may not have been sufficiently broad to observe an effect of polymer concentration.

The enhancement of saltiness perception with increasing polymer concentration could be related to the increase in salt concentration in grams per gram of water, in a similar fashion to the salt concentration expressed for a two-phase system. Indeed, the polymer concentration was on a weight basis in this study (w/w), so an increase in polymer concentration lead to a reduction in available water and therefore the salt concentration reported to a mass of water is higher. For a set concentration of 0.6% w/v of NaCl, a 10% dextran solution contains 0.64 g of NaCl for 100 g water whereas a 30% dextran solution contains 0.76 g NaCl for a 100 g of water. It may be hypothesized that the stimulus for taste perception is the tastant concentration per gram of water, rather than per gram (w/w basis) or per liter (w/v basis). However, if this was the case, an enhancement of both saltiness and sweetness would have been found with increasing polymer concentration. As the results of test C4 did not show an enhancement of sweetness, the effect of polymer concentration on the tastant concentration in grams per grams of water is unlikely to be the underlying mechanism of the saltiness enhancement.

As presented in Chapter 1 (1.2.1), it has been established at the cellular level that the nervous activity following NaCl stimulation is higher when the tastant solution is

hyperosmotic (also containing solutes such as urea or mannitol) than when it is only NaCl in water (Lyall et al., 1999). The osmolality being a measure of the number of solute particles per kg of solvent, polymer chains in solution are likely to affect sample's osmolality. Consequently, it is hypothesised that the enhanced saltiness perception reported in study C could be due to high osmolality of the samples, imparted by the high polymer concentration. This hypothesis was tested by measuring the osmolality of dextran solutions and the values are reported in Table 3.8.

Table 3.8: Osmolality of dextran samples of different molecular weight, matched at viscosity of 30 mPa.s. All results are significantly different ($p < 0.001$). Standard deviation < 3 mOsm.kg⁻¹.

Sample	Osmolality (mOsm.kg ⁻¹) of the dextran samples containing		
	0.6% w/v NaCl	0.45% w/v NaCl	5% sucrose
D _H	238	195	230
D _M	373	n/a	370
D _L	680	650	725

The effect of polymer concentration on solution osmolality is evident from the data presented in Table 3.8. The high osmolality could indeed be the origin of the enhancement of saltiness perception reported above. This hypothesis is supported by the in-vitro findings of Lyall et al. (1999). According to those authors, the osmolyte-induced increase in the rat chorda tympani response to NaCl involves the activation of apical Na⁺ channels (amiloride sensitive, see Figure 1.2) and results in a reduction in

the taste receptor cells (TRCs) volume. The tastant used for the study of saltiness (Tests C2 and C3), NaCl, activates these ion channels and the therefore high osmolality of the samples may have increased the nervous response. The sweetness perception study (C4) showed a non-significant effect of polymer concentration. As sweetness perception is not mediated by ion channels, this supports the hypothesis that the hyperosmolality of the salt solutions leads to increased saltiness perception in humans. The osmolality effect on taste perception depends on the taste modality studied and this could partially explain the taste-specific effect of thickeners on taste perception reported in literature (Moskowitz and Arabie, 1970; Pangborn and Trabue, 1973) (see 1.3). Lyall et al. (1999) demonstrated in-vitro using rodents that the effect of osmolality also involved amiloride sensitive ion channels. This pathway is, however, not predominant for saltiness perception in humans (Ossebaard and Smith, 1995) (see Chapter 1, 1.2.1). Therefore, if the effect of osmolality on saltiness perception in humans was validated, it would indicate that a modulation of the activity of the amiloride sensitive ion channel would enable control over saltiness perception. Alternatively, it may be hypothesised that in humans, osmolality also affects the submucosal pathway for saltiness transduction. For example, it is possible that the decrease in cell volume observed in hyperosmotic solutions facilitates the passage of salt ions through the tight junctions, thereby increasing the activity of the submucosal ion channels (see Figure 1.2). A study of taste perception in hyperosmotic solutions following amiloride treatment would enable to identify the mechanisms.

Osmolality of saliva and food products was measured to investigate whether the range of osmolality studied here 200-700 mOsm.kg⁻¹ with the dextran samples was relevant for possible food applications, that is to say if high osmolality could be used as a 'saltiness enhancer' in foods. The osmolality of saliva was found to be between 50 and 100 mOsm.kg⁻¹, the osmolality in soups and fruit juices ranged between 150 and 1000 mOsm.kg⁻¹ whereas sauces and condiments exhibited very high osmolality values of 1000-2000 mOsm.kg⁻¹ (because their water content is very low). Those values are in good agreement with the values published by Feldman and Barnett (1995). Thus, osmolality values as high as evaluated in the saltiness perception study are found in existing food products and therefore food products of high osmolality could be designed to enhance saltiness perception. A possible application would be to use high concentrations of low molecular weight polymers, rather than low concentrations of high molecular weight polymers to enhance saltiness perception. However, this option is likely not to be cost-effective.

3.3.4 MOUTHFEEL PERCEPTION

Evaluation of mouthfeel was not the focus of the sensory studies conducted during this PhD research, however, as the panel created mouthfeel attributes it was decided to use the opportunity of obtaining some mouthfeel data during study A and B (see Figure 3.1 and Figure 3.2 for flow behaviour) in addition to other saltiness perception

values. The shear rate relevant to thickness perception was reported in shear-thinning samples (study A) and samples exhibiting yield behaviour (study B). As reported in Table 3.2, the panel selected the four mouthfeel attributes *thickness*, *stickiness*, *lubrication* and *residues* but the scores for the different mouthfeel attributes were strongly correlated ($r^2 > 0.93$), which may have been due to the close similarity of the samples in molecular behaviour (not or only weakly elastic; non-starch, random coil polysaccharides). Only the attribute *thickness* will be considered in the following as it is the first key attribute to describe texture in the mouth (Kokini et al., 1977).

Correlation analysis (Malone, Appelqvist and Norton, 2003a) was performed to investigate the shear rate involved in the perception of thickness. For each shear rate ($1-10^5 \text{ s}^{-1}$), the correlation coefficient r^2 between the thickness scores and the viscosity was calculated. Thickness perception was best correlated to shear viscosities measured between $80-700 \text{ s}^{-1}$ as illustrated in Figure 3.8a ($r^2 > 0.90$) as panellists were able to perceive differences in thickness for samples that exhibited differences in shear viscosity only at shear rates above 100 s^{-1} (samples matched at zero shear). The range of shear rate $80-700 \text{ s}^{-1}$ is higher than $10-50 \text{ s}^{-1}$ often referred as typical in-mouth shear rate (Wood, 1968; Shama and Sherman, 1973).

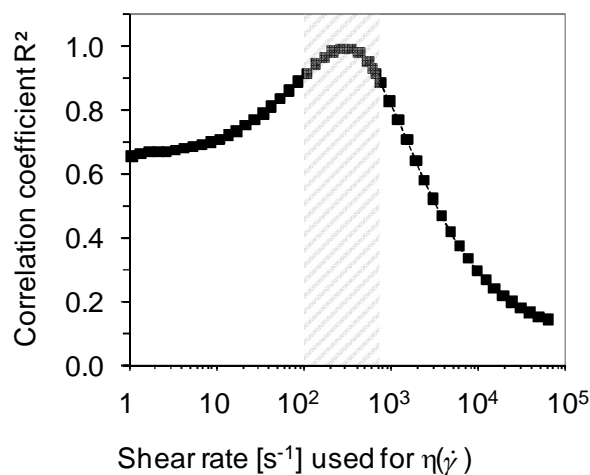


Figure 3.8: Correlation coefficient between the sensory scores for *thickness* and *viscosity* defined at a given shear rate $\eta(\dot{\gamma})$ for samples of study A. The range of shear giving a correlation coefficient > 0.9 is indicated by a shaded area.

The thickness perception of mixtures of guar gum and xanthan gum (showing yield behaviour) (study B) was evaluated using multiple paired comparisons in two subsets: samples A, B, C and samples C, D, E. The tabulated results and rank sum scores for thickness can be found in Appendix 3.4 and Appendix 3.5. The Friedman's statistic T was equal to 8 and 28, respectively ($p=0.05$ and $p=0.005$, respectively). Within each set, panellists found the samples of high viscosity at low shear significantly thicker, in spite of all the samples exhibiting identical viscosity for shear rates $> 50 s^{-1}$. This indicates that for samples exhibiting a yield stress, thickness perception is correlated to low shear viscosities.

Though the two sets of results may seem contradictory, we believe that a whole range of shear rate (low and high shear) is experienced in mouth, and panellists are focusing of the differences between samples to evaluate thickness. In guar gum or dextran solutions (study A), samples had identical low shear viscosity so panellists focussed on the differences in high shear (80-700 s⁻¹) viscosity. In contrast, in guar gum/xanthan gum mixtures (study B), samples had identical high shear viscosity and panellists focussed on differences in low shear (1-10 s⁻¹) viscosity.

Some authors discuss that the interaction between taste/aroma and mouthfeel occurs only at a cognitive level (see 1.3.2) (Weel et al., 2002). However in this research, mouthfeel and saltiness perception were correlated to the shear viscosity at different shear rates. In particular in study A, the viscosity at high shear rate had a significant impact on thickness perception but not on saltiness perception. This indicates that the reduction in saltiness perception is unlikely due to multimodal interactions but rather that the availability of tastant molecules to the taste buds is reduced in viscous solutions.

3.4 CONCLUSIONS

This chapter reports research on the effect of shear viscosity on saltiness perception. Using aqueous solutions thickened with random coil neutral polysaccharides (guar gum or dextran), it was found that the degree of shear-thinning and the viscosity at high shear rate had a significant impact on thickness perception but not on saltiness perception. Instead, saltiness perception was related to viscosity measured at low shear rate. In addition, it was identified from saltiness perception in mixtures of guar gum and xanthan gum that saltiness perception is related to *low* shear viscosity ($1-10\text{ s}^{-1}$), not to *zero* shear viscosity. This seems to indicate that the reduction of saltiness perception with increasing viscosity is most probably due to reduction of mixing efficiency with saliva rather than to reduction in diffusion or to a cognitive effect. By carefully choosing the flow behaviour of a liquid food, desirable mouthfeel (thickness) without apparent reduction in saltiness may be achieved. Finally, the enhancement of saltiness perception in hyperosmotic solutions was demonstrated and therefore the use of 'ineffective' thickeners at high levels could be an opportunity to reduce sodium intake without affecting saltiness perception. At present, this option is unlikely to be cost effective for food manufacturers, but other options to enhance osmolality should be investigated.

CHAPTER 4

FOOD GRADE BOGER FLUIDS

4.1 INTRODUCTION

The classical approach to investigate the effect of the rheological behaviour of liquid foods on saltiness perception is to consider viscosity measured at 50 s^{-1} (see 1.2.2). In this PhD research, see Chapter 3, the spectrum of rheological behaviour considered in its impact on saltiness has been broadened by investigating which shear rate is relevant for saltiness perception. It was found that the saltiness perception was correlated to the shear viscosity measured at about 10 s^{-1} . However, *viscosity* is not only defined in shear flow but also in extensional flow and this is why here, for the first time in published literature, work on the effect of extensional viscosity on saltiness and mouthfeel perception is reported. This work was based on the use of Boger fluids which represent a particular useful class of liquid material to separate the effect between viscous (shear) and elastic contribution in large deformation flow. Whereas elastic properties quantified in small deformation flows (oscillatory shear measurement) have previously been considered in correlation to mouthfeel perception (Chapter 1, 1.2.2), in-mouth flow fields ‘applied’ to foods can be assumed to typically not be within the small deformation limit. The correlation between elastic properties measured in large deformation and sensory properties has been investigated using Boger fluids.

Boger fluids were discovered by D.V. Boger (Boger, 1977/1978) and are elastic liquids of constant shear viscosity. Such fluids can be obtained by dissolving a high molecular weight polymer at low concentration, to minimise the degree of shear-thinning, in a high viscosity Newtonian solvent. The high solvent viscosity ensures elastic stress growth to be measurable (James, 2009). Concentrated glucose syrup, glycerol or polybutene solutions are often used as solvent and polyacrylamide, polyisobutylene, polystyrene or xanthan gum as the high molecular weight polymer imparting elasticity. The characteristic flow behaviour of Boger fluids becomes evident in large deformation shear flow where these fluids develop considerable normal stresses measured as the first normal stress difference N_1 (Lapasin and Prici, 1995). N_1 increases exponentially with shear rate and can be several orders of magnitude larger than the shear stress, which is proportional to shear rate. Boger fluids are also characterised by a high apparent extensional viscosity compared to the shear viscosity. The challenge in this research was to design food grade Boger fluids suitable for sensory evaluation. Therefore, out of the solvents mentioned above only glucose syrup and glycerol could potentially be used; and xanthan gum is the only food grade high molecular weight polymer previously used for the preparation of Boger fluids (Stokes et al., 2001a; 2001b). Albeit few, there are further food grade materials which develop a high Newtonian viscosity in solution or impart high elasticity. Most food grade materials forming high viscosity Newtonian solutions are small molecules also generating a sweet taste. This is incontestably a major issue for Boger fluids designed

to be used for taste perception studies, however, a sweetness inhibitor could be used to circumvent this issue. In addition, the shear viscosity of Boger fluids designed for sensory analysis should be kept as low as possible as it is difficult and unpleasant to taste and swallow salty Newtonian solutions with a viscosity greater than 0.1 Pa.s (results of preliminary sensory testing). This requirement was considered to possibly inhibit the successful formulation of suitable Boger fluids for this research as it is known from literature that at a shear viscosity of less than 1 Pa.s elastic effects are reduced and the rheological behaviour of the Boger fluid would not clearly differ from that of the inelastic Newtonian solvent (Stokes et al., 2001b; James, 2009). Nevertheless, two Boger fluids thought to be suitable to investigate the effect of elasticity on saltiness perception and mouthfeel were formulated. As mentioned in Chapter 1 (1.5), filament break-up (Anna and McKinley, 2001; Stokes et al., 2001b) and contractions flow experiments (Binding and Walters, 1988; Nigen and Walters, 2002) are two techniques used here to probe the extensional properties of Boger fluids. The elasticity of the fluids was also characterised in shear flow by measuring the first normal stress difference. Saltiness perception and mouthfeel of these two fluids were investigated in comparison to their respective solvent (referred to as inelastic reference).

4.2 MATERIALS AND METHODS

4.2.1 NEWTONIAN SOLVENTS

Glucose syrup and maltodextrin solutions were used as bases for Newtonian solvents. High viscosity glucose syrup of no particular specification was bought in a local shop specialising in bakery products. Maltodextrin are low molecular weight polymers of α -1 \rightarrow 4 glucose and in aqueous solution they appear less sweet than glucose syrup (Birch, Azudin and Grigor, 1991). Here, Maldex 150 from Tate & Lyle (UK) was used. Bottled water Evian (Danone, France) served as solvent instead of deionised water since the samples were also designated for human consumption.

4.2.2 ELASTICITY IMPARTING POLYMERS

As the only known suitable food grade polymer, xanthan gum was used. Xanthan gum of the type Keltrol®RD (CP Kelco) was dissolved in the various solvents and the elasticity of the solutions was evaluated. Polyacrylamide Praestol 2530 (Ashland, Germany) was also used with the intention to validate experimental protocol. Literature results were successfully reproduced (Stokes et al., 2001a; Stokes et al., 2001b); these have not been reported in this document.

4.2.3 ADDITIVES

Salt (sodium chloride) was bought in a local supermarket and added to both the inelastic reference samples (pure solvents) and the Boger fluids to a final concentration of 0.6 % w/w. The sodium salt of 2-(4-methoxyphenoxy)-propionic acid (NaPMP) also called lactisole (CAS number 13794-15-5) is a sweetness inhibitor recognized as safe for consumption by the Joint FAO/WHO Expert Committee on Food Additives (JECFA number 1029). It was added to reduce the sweetness imparted by maltodextrin and glucose syrup, which could affect saltiness perception, and it was chosen as it does not interfere with saltiness perception (Kinghorn and Compadre, 2001). Lactisole was provided by Endeavour Speciality Chemicals Ltd (Daventry, UK).

4.2.4 SAMPLE PREPARATION AND COMPOSITIONS

A stock solution of xanthan gum (0.5% w/w) was prepared by adding the appropriate amount of polymer into cold water and stirring the dispersion on a magnetic stirrer for 1 h at 80 °C followed by continued mixing on a roller bed at 4 °C until use. Maltodextrin and glucose syrup solutions were prepared by mixing the appropriate amount of powder or glucose syrup, respectively, into water followed by the addition of sodium chloride (0.6% w/w in the final sample) and sweetness inhibitor NaPMP (500 ppm in the final sample) and mixing for 3 h at 4 °C. The appropriate weight of xanthan gum stock solution was added to the solvents to obtain a concentration of 100 ppm (0.01% w/w) of xanthan gum in the final solution. Dispersing xanthan gum

powder directly into the solvent would have inhibited full dissolution and efficient dispersal of the polymer throughout the solvent which has been reported to be key for reproducible preparation of Boger fluids (Choplin, Carreau and Kadi, 1983; Binnington and Boger, 1986). Mixing at low shear over a long period of time is required (Binnington and Boger, 1986). Here, samples were mixed in lidded bottles using an end-over-end mixer (Reax2, Heidolph, Germany) at minimum setting for 24 h at 4 °C to avoid microbial spoilage. Boger fluids and inelastic references were left to rest for 24 h before use to degas.

The composition of the samples can be found in Table 4.1. The glucose syrup concentration was lower than usually reported in the literature (90 to 94%) to keep the samples' shear viscosity between 1 and 10 Pa.s as discussed in the introduction (and it also depends on the type of glucose syrup used). It should also be noted that the concentration of glucose syrup and maltodextrin in the Boger fluids was slightly lower than in the inelastic reference samples. This was necessary to ensure that shear viscosity was matched between 1 and 10 s⁻¹ which is the range of shear rates relevant to saltiness perception in mouth as discussed in Chapter 3.

Table 4.1: Composition of the Boger fluids and the corresponding inelastic reference samples. Concentrations are in %w/w, totalled to 100% with water.

	Maltodextrin-based		Glucose syrup-based	
	Boger fluid	Inelastic reference	Boger fluid	Inelastic reference
Maltodextrin / glucose syrup	63	63.48	88	88.5
Xanthan	0.01	0	0.01	0
NaCl	0.6	0.6	0.6	0.6
NaPMP	0.05	0.05	0.05	0.05

4.2.5 RHEOLOGICAL CHARACTERISATION

All rheological measurements were conducted at 20 °C corresponding to the temperature at which samples were presented during sensory analysis.

4.2.5.1 Rotational rheology

A shear stress controlled rotational rheometer (MCR301, Anton Paar, Austria) fitted with a cone and plate geometry (1° angle, 50 mm diameter) was used to measure the viscosity and the first normal stress difference (N1) at equilibrium at shear rates between 0.1 and 1000 s⁻¹. Low viscosity mineral oil was applied to the outer edge of the sample to avoid moisture loss.

4.2.5.2 Filament break-up

Filament break-up tests were carried out using a Haake CaBER 1 extensional rheometer (Thermo Haake GmbH, Karlsruhe, Germany) applying the experimental conditions reported in Chapter 2 (2.2.3). A suitable container filled with water was placed inside the sample chamber to minimise the loss of moisture from the fluid filament. Yet, changes in the appearance of the fluid filaments and time-dependence of the filament thinning were observed when the same loaded sample was used for several tests (highly concentrated glucose-based fluids often show free surface crystallisation phenomena) so each test was performed on a fresh sample. At least 7 replicate measurements were performed and a representative result was chosen for analysis. In addition to acquiring midpoint diameters using a laser as outlined in chapter 2, the filament self-thinning dynamics were recorded in one instance by a high-resolution digital video using a Phantom v5 high-speed digital video camera at around 2000 frames per second (in this case, tests were performed in a custom-made equipment identical to the commercial equipment).

The surface tension, σ , was not measured but the value for water, 72 mN.m⁻¹, was used in the analysis to calculate apparent extensional viscosity from filament break-up data. Surface tension measurement of the solvents used here is difficult due to their high viscosity and as absolute values for extensional viscosity were not required for this comparative study, the value for water was used. Presence of 100 ppm of xanthan

gum was also assumed to not significantly affect the surface tension. The apparent extensional viscosity was calculated with Equation 4.1 (Anna and McKinley, 2001). Extensional viscosity is often rendered dimensionless with the shear viscosity. This ratio is called the Trouton Ratio, see Equation 4.2 and Chapter 1 (1.5.1.2) (Tirtaatmadja and Sridhar, 1993), and $Tr = 3$ for an inelastic Newtonian fluid. Here, shear viscosity averaged over data measured between 0.1-1000 s^{-1} was used to calculate Tr as the shear viscosity behaviour was Newtonian (otherwise shear viscosity at the shear rate indicated in Equation 4.2 must be used).

$$\eta_e = -\frac{\sigma}{\frac{\partial D_{mid}}{\partial t}} \quad (4.1)$$

where η_e [Pa.s] is the extensional viscosity, σ [mN.m⁻¹] the surface tension, and $\partial D_{mid} / \partial t$ the rate at which the filament diameter decreases with time.

$$Tr = \frac{\eta_e(\dot{\epsilon})}{\eta_s(\dot{\gamma})} \text{ with } \dot{\gamma} = \sqrt{3} \dot{\epsilon} \quad (4.2)$$

where η_e [Pa.s] is the apparent extensional viscosity at a given strain rate $\dot{\epsilon}$ [s⁻¹], η_s [Pa.s] the apparent shear viscosity at a shear rate $\dot{\gamma}$ [s⁻¹] equal to $\sqrt{3} \dot{\epsilon}$.

4.2.5.3 Micro-contraction flow experiment

Boger fluids and their inelastic reference fluids were passed through a micro-contraction flow device (described in Chapter 2 in 2.2.4). For microfluidics experimentation very low flow rates (0.05 to 0.15 ml.hr⁻¹) were used due to the high shear viscosity of the samples (as otherwise, very high pressure (> 120 kPa) is

developed, which exceeds the linear working range of the pressure sensors and may lead to the rupture of the seal between the microscope slide and the channels) and the pressure drop between 3 mm upstream and 3 mm downstream of the contraction was recorded.

4.2.6 SENSORY METHODS

Three different tests were carried out on the glucose syrup-based and maltodextrin-based Boger fluids (containing xanthan gum) and the corresponding inelastic reference samples to investigate whether saltiness (tests 1, 2 and 3) and/or mouthfeel (test 2) differed across samples. For all tests, samples were evaluated under the conditions described in Chapter 2 (2.3) and samples were presented on spoons (about 2 ml).

4.2.6.1 Test 1

Paired comparisons between the Boger fluids and reference samples were performed using 12 untrained panellists with experience in saltiness detection. A Boger fluid sample and the corresponding reference sample were presented in pairs and the panellists were instructed to indicate which sample appeared the saltiest. Each pair was evaluated 9 times (over 3 days) by each panellist. This large number of repetitions allowed the calculation the value d' , which is an estimate of whether each panellist was able to distinguish between the two samples or whether the answer was provided

randomly. If d' is small, the two products will be similar; whereas if d' is large (generally $d' > 1$ is considered), the two products will be perceptibly different. The value of d' for a 2-alternative forced choice (pair comparison test) can be found in tables published by Ennis (1993). For this particular experiment, if a panellist found 6 out of 9 times the same sample saltier, d' equals to 0.6 (Ennis, 1993) which indicates that the panellist was barely able to differentiate between the two samples. If a panellist found the same sample 7 out of 9 times to be saltier, d' equals to 1.08 and the two samples were perceived as clearly different.

4.2.6.2 Test 2

As the untrained panellists participating to Test 1 reported difficulties in evaluation of saltiness due to the sweetness of the samples, six panellists from the panel specifically selected and trained for this research (Chapter 3, 3.2.3.1) were also asked to evaluate the samples using paired comparison tests. Samples were presented by pair in triplicate, each pair was composed of a Boger fluid and its inelastic reference sample.

In contrast to test 1, panellists were instructed to compare the samples not only for differences in saltiness but also in mouthfeel. The sensory attributes used had been defined by the same panel (see Chapter 3, Table 3.2): *initial saltiness, in-mouth saltiness, saltiness after swallowing, thickness, lubrication, stickiness and residues after swallowing*.

4.2.6.3 Test 3

The results of Test 2 indicated that Boger fluids and reference samples were not perceived as significantly different. However, trained panellists also reported difficulty to evaluate saltiness in these samples, and therefore differences in saltiness may exist, but may be difficult to perceive. Test 3 was designed to estimate whether saltiness sensitivity was indeed impaired in such samples, by including two levels of salt (0.6% and 0.7% w/w). In water, any difference in salt concentration larger than 0.058% is noticeable (Johansson et al., 1973). Multiple paired comparison based on four samples was used: Boger fluid (0.6% NaCl), Boger fluid (0.7% NaCl), inelastic reference (0.6% NaCl) and inelastic reference (0.7% NaCl). As in test 2, the samples were evaluated by seven of the panellists specifically selected and trained for this research. Friedman ranking's analysis was performed as described in Chapter 2 (2.3.2.2 and Appendix 3.6).

4.2.7 QUALITATIVE ANALYSIS OF SAMPLE MIXING WITH ORAL FLUIDS

It has been argued for some time that the efficiency at which liquid foods mix with saliva during oral processing has an impact on taste perception (Baines and Morris, 1987; Ferry et al., 2006a; Koliandris et al., 2007) (Chapter 1, 1.2.2). As Boger fluids are a new class of fluids considered in the context of taste perception, simple mixing experiments were conducted to obtain a qualitative measure of in-mouth mixing

efficiency. The following method developed by Ferry et al. (2006a) involving visual observation of the mixing behaviour of the samples with water was applied.

Five millilitres of sample, to which a blue food colouring (Dr Oetcker, bought in a local supermarket) had been added (100 μ l of colorant for 20 ml of sample), were carefully introduced with a plastic syringe into the bottom of a 50 ml glass beaker containing 20 ml of distilled water. The solutions were rapidly stirred by hand with a teaspoon for 2–3 s in a circular motion and photographed 1 min after stirring. The experiment was conducted isothermally at 20 °C and it was performed for maltodextrin-based and glucose syrup-based Boger fluids and their inelastic reference samples.

4.3 RESULTS AND DISCUSSION

4.3.1 SAMPLE RHEOLOGY

The rheological properties of maltodextrin- and glucose syrup-based Boger fluids and the respective inelastic reference samples were characterised in shear and extensional flow (filament break-up and micro-contraction flow). Initially, it is worth noting that it was verified that the addition of sodium chloride (NaCl) and sweetness inhibitor lactisole (NaPMP) did not affect the results, presented in the following section.

4.3.1.1 Shear rheology behaviour

The shear viscosity of the Boger fluids and reference samples is shown in Figure 4.1. As expected, the latter exhibited a constant shear viscosity, the glucose syrup-based fluid being more viscous than the maltodextrin sample (4.65 Pa.s vs. 3.02 Pa.s). The two Boger fluids were slightly shear-thinning in nature (power-law exponent of 0.94 for the shear stress over shear rate), which has previously been found (Stokes et al., 2001a; Stokes et al., 2001b). In this research, the solvent concentration was adjusted to obtain a Boger fluid and its inelastic reference fluid for a given solvent matched in viscosity at shear rates between 1 and 10 s^{-1} as this is the range of shear considered to be relevant for saltiness perception (Chapter 3). Therefore, the viscosity differences between a set of corresponding fluids were maximal at zero shear viscosity but the impact of this difference on mouthfeel or taste perception is unknown.

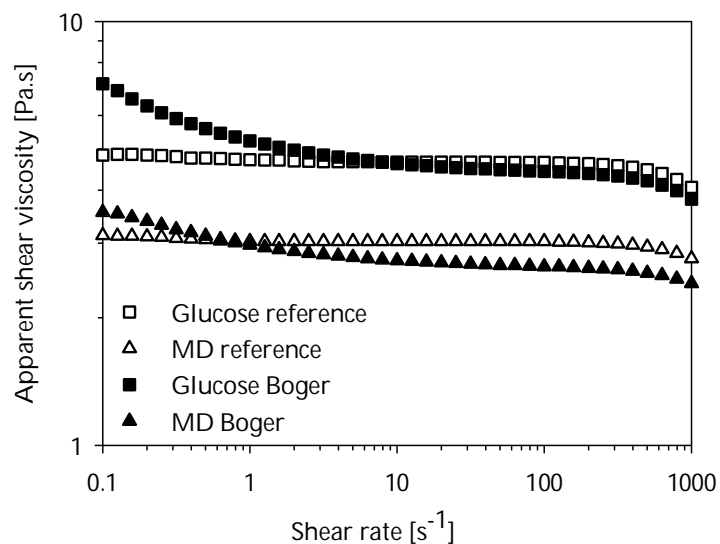


Figure 4.1: Shear viscosity of the Boger fluids and the inelastic reference samples maltodextrin-based (MD) and glucose syrup-based.

A plot of the shear stress and first normal stress difference for both Boger fluids is presented in Figure 4.2. The development of a first normal stress difference N_1 with shear indicates the viscoelastic behaviour of the Boger fluids, in contrast to the inelastic reference samples which did not exhibit normal stress growth. The slope of N_1 versus $\dot{\gamma}$ in the double logarithmic graph is 0.5 which is in agreement with literature data on xanthan gum-based Boger fluids (Stokes et al., 2001b) and close to the theoretical value of $2/3$ for dilute solutions of rigid rod-like molecules (Bird, Armstrong and Hassager, 1987). The first normal stress difference is approximately 100 Pa at 1000 s^{-1} for both Boger fluids. This is of the order of magnitude previously documented for a xanthan gum / glucose syrup-based Boger fluid (Stokes et al., 2001b) but at least an order of magnitude lower than the first normal stress difference developed by a dilute solution of a flexible polymer (polyacrylamide) in glucose syrup of similar shear viscosity. This illustrates the impact of the polymer conformation on the properties of the Boger fluid.

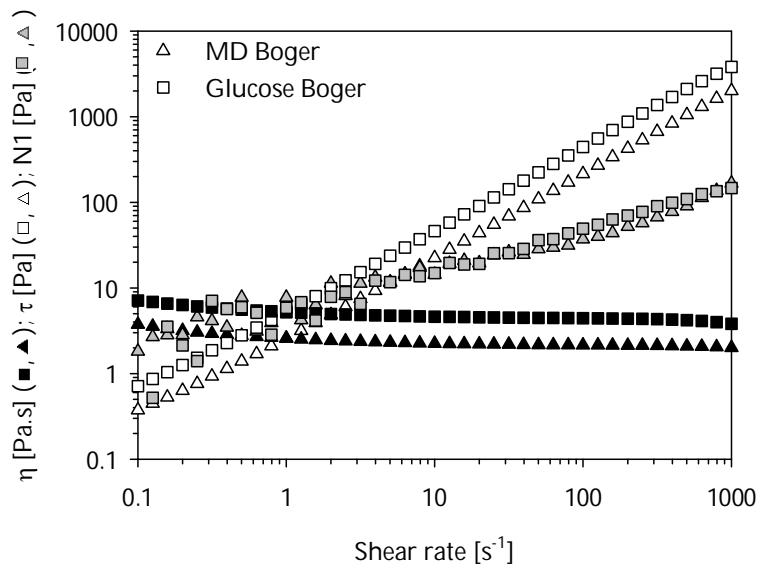


Figure 4.2: Shear viscosity (black symbols), shear stress (void symbols) and 1st normal stress difference (grey symbols) of the maltodextrin-based Boger fluid (MD) (triangles) and the glucose syrup-based Boger fluid (squares).

4.3.1.2 Filament break-up characteristics

The dynamics of the filament thinning is illustrated in Figure 4.3 and the decrease of the mid-point diameter as a function of time can be found in Figure 4.4. The addition of xanthan gum dramatically alters the properties of the fluids in extension. The time to filament break-up is 2 to 3 times longer for the Boger fluids compared to the inelastic reference fluids. In addition, the mid-point diameter decreases linearly with time for the inelastic samples whereas the decrease is exponential for the Boger fluids. This exponential decrease and the longer break-up time are both fingerprints of the elastic nature of the Boger fluids (Anna and McKinley, 2001) whereas linear decrease is characteristic for Newtonian fluids (McKinley, 2005) (see 1.4.3). The maltodextrin-

based fluids break up quicker than the glucose syrup-based fluids which is consistent with the lower shear viscosity (Figure 4.1).

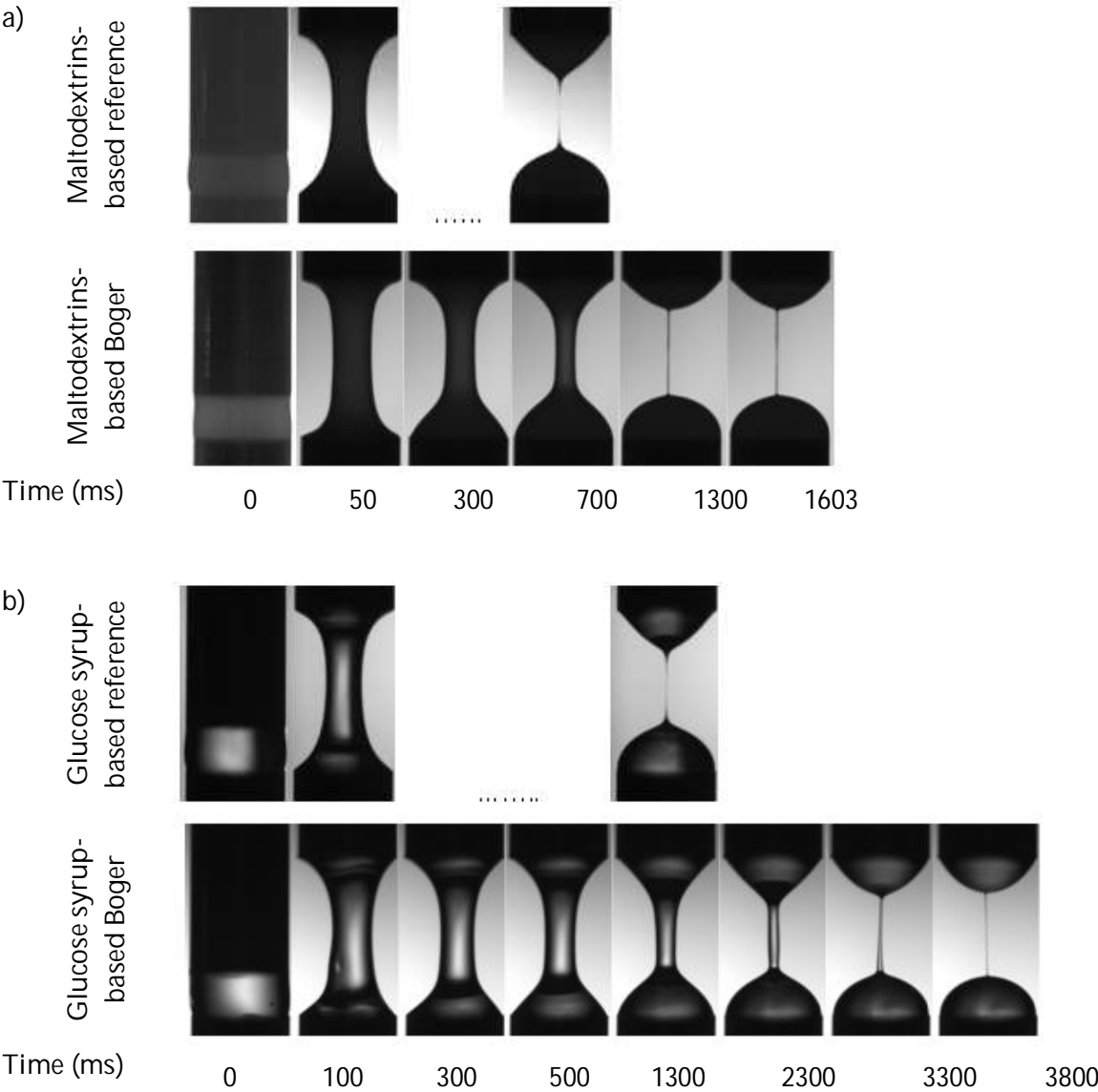


Figure 4.3: Filament thinning of the Boger fluids and inelastic reference samples a) maltodextrin-based and b) glucose syrup-based.

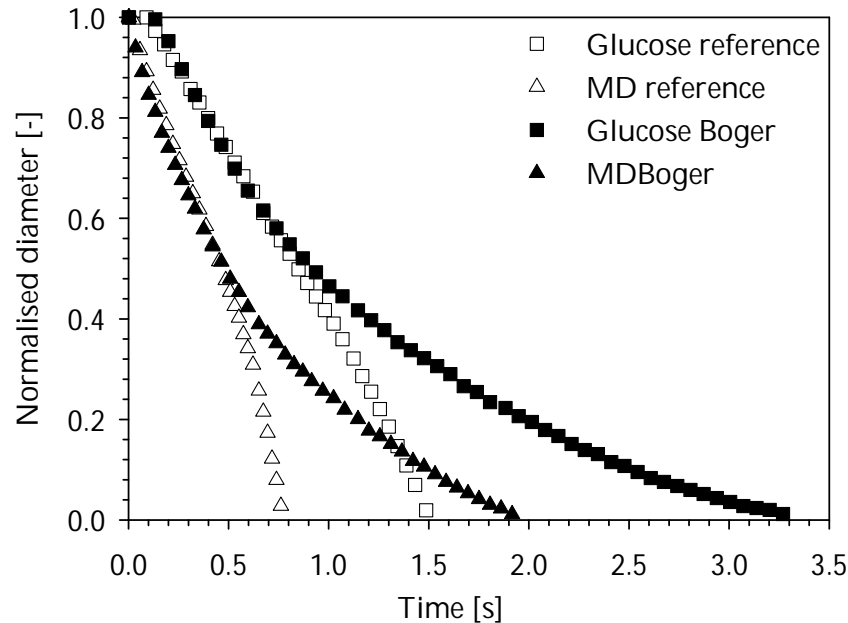


Figure 4.4: Evolution of the normalised filament mid-point diameter for the Boger fluids and the inelastic reference samples for maltodextrin-based (MD) and glucose syrup-based samples.

Values calculated for the Trouton ratio have been plotted as a function of strain in Figure 4.5. Data for both solvent types superimpose indicating that the two Boger fluids only differ in shear viscosity whilst exhibiting a similar degree of elasticity. The Trouton ratio of the inelastic reference samples is close to 3 as expected for Newtonian fluids. In case of the Boger fluids it increases steadily before assuming a plateau value of about 20 at roughly 8 strain units corresponding to an extension rate of 10 s^{-1} . This reflects the higher apparent extensional viscosity of the Boger fluids compared the inelastic reference samples. The Trouton ratio does not necessarily depend on strain or extension rate and this finding is largely a result of the experimental technique used. An alternative technique to characterise liquid flow behaviour in extension is the so-

called opposed jet technique (Macosko, 1994) in which Trouton ratios largely independent of extension rates have been found (Ng et al., 1996; Stokes et al., 2001b). These two techniques differ by the rate of stretching of the samples, which affects the strain-dependence of the Trouton ratio (Anna et al. (2001).

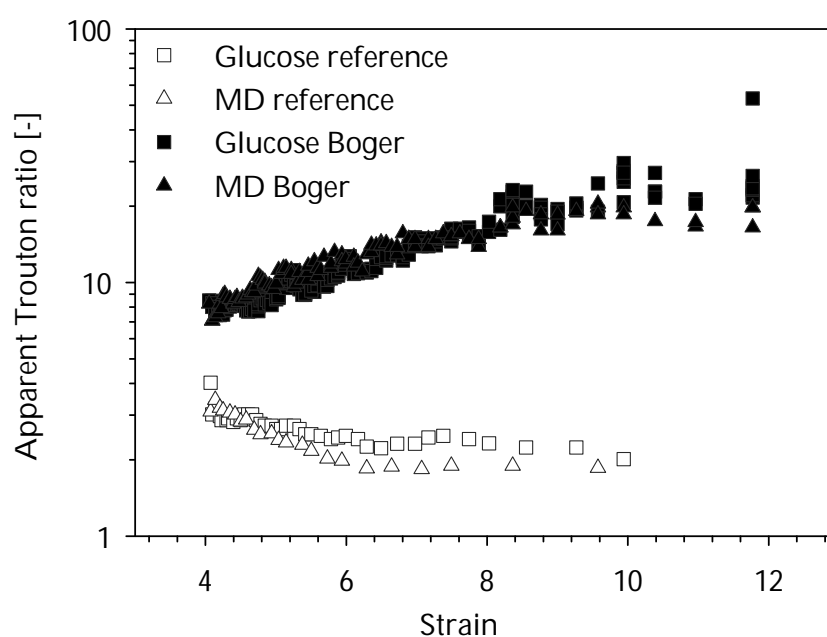


Figure 4.5: Trouton ratio for the Boger fluids and the reference samples (maltodextrin-based and glucose syrup-based) calculated from filament break-up data.

4.3.1.3 Elastic behaviour characterised in micro-contraction flow

The total pressure drop across the contraction of the micro-contraction flow device measured for the Boger fluids and the inelastic reference samples for the range of flow rates applied in the experiments is depicted in Figure 4.6. The pressure drop developed by the Boger fluids largely exceeds the pressure drop developed by the

inelastic reference samples. Such behaviour has been previously observed in macroscale cylindrical contraction flow, but there are no literature data indicating whether this behaviour is also characteristic for (macroscale) planar contractions (Binding and Walters, 1988; Nigen and Walters, 2002). In any case, here it was found that it holds for microscale planar contraction devices. It should be noted that microscale devices have a comparatively much higher surface-to-volume ratio and it has been reported that the flow tends to be three dimensional (Oliveira et al., 2008; Pipe and McKinley, 2009) whereas macroscale contraction flow is in first approximation two dimensional. The excess pressure drop developed by the Boger fluids in the experiments of this research is likely a result of alignment of the xanthan gum molecules in the contraction followed by relaxation downstream of the contraction. The higher pressure drop observed for glucose syrup-based samples compared to maltodextrin-based samples is due to the higher shear viscosity of the former (Figure 4.1).

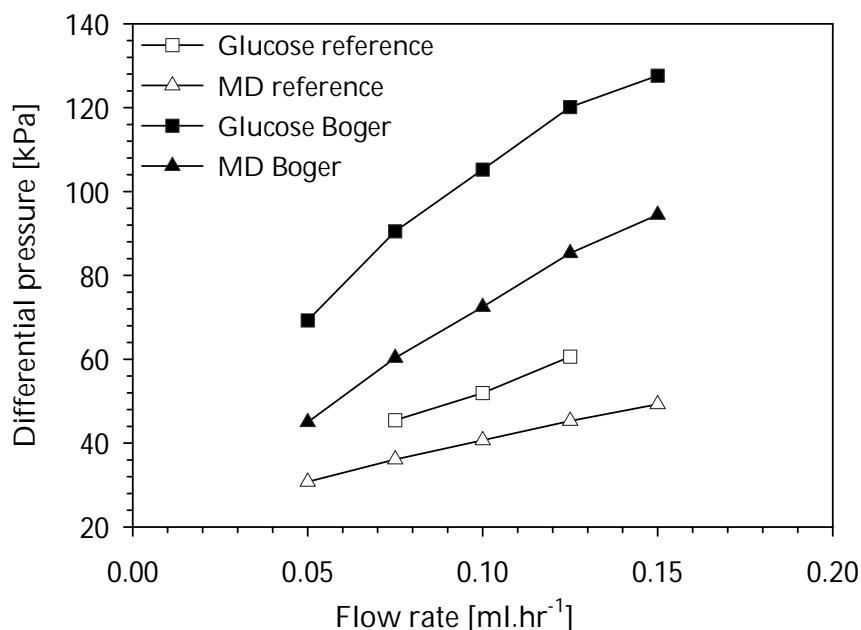


Figure 4.6: Total pressure drop vs. flow rate in the micro-contraction flow device for the Boger fluids and the inelastic reference samples, maltodextrin-based and glucose syrup-based.

4.3.1.4 Testing alternative compositions for Boger fluids

Alternative Newtonian solvents

Glucose syrup and maltodextrin solutions generate a sweet taste undesirable for taste perception studies necessitating use of a sweetness inhibitor. Alternative less sweet tasting Newtonian solvents were investigated. 100 ppm of xanthan gum was added to aqueous solutions of glycerol (technical grade, Fisher Scientific), bovine gelatin (type B, Sigma-Aldrich) and dextran (T40 and T500, Pharmacosmos, Denmark). The fluids were prepared and characterised as indicated above (see 4.2). The gelatin solution was an exception as gelatin is a gel at ambient temperature. Thus, gelatin solution was

prepared by dispersing the powder in hot water and followed by keeping the sample above 35°C (approximate gelation temperature; gelatin type, concentration and solution condition dependent) and rheological measurements were also carried out at 35 °C.

Gelatin solutions were tested as viscous solvents but were discarded for several reasons. Firstly, gelatin solutions' smell and taste were very strong, which is not desirable for sensory analysis. Secondly, gelatin solutions had to be prepared and kept above 35 °C to avoid gelation and this is impractical especially for the sensory analysis as the samples were served on a spoon and would therefore cool down very quickly. Finally, whereas dilute solutions of xanthan gum in gelatin showed elastic behaviour in the filament stretching experiment, first normal stress development was absent in shear rheology. This intriguing phenomenon has not previously been reported and is worthy of further study.

Glycerol was chosen as it was previously used as Boger fluid solvent (Stokes et al., 2001b; Stokes et al., 2001a), in association with polyacrylamide. Here, dilute solutions of xanthan gum in glycerol were tested. These did indeed exhibit Boger fluids properties comparable to those of the glucose syrup-based samples. However, it turned out that glycerol is unpalatable due to a strong characteristic taste for which

taste inhibitors could not be identified. Thus, glycerol-based samples were not suitable for sensory analysis.

As a further alternative to the sweet tasting solvent based Boger fluids, dilute solutions of xanthan gum in concentrated dextran solutions (two different molecular weights, 40 and 500 kDa) were prepared and characterised. The rheological behaviour was that of Boger fluids: constant shear viscosity, development of first normal stress and large extensional viscosity observed in filament break-up. A major advantage of dextran solutions is that they are far less sweet than glucose and maltodextrin solutions. However, despite GRAS status (generally recommended as safe), the European Union has restricted the use of dextran in foods and legally, no more than 12 g should be consumed per day. This limits the sample volume panellists would be able to evaluate within a sensory session which was not practical as the concentration of dextran was relatively high in the Boger fluid due to the high viscosity level required (dextran concentration used in this research in Chapter 3 was by 2-3 times lower).

Alternative high molecular weight polymer

For the sake of completeness, alternatives to xanthan gum as the elasticity imparting component in Boger fluids were tested. The choice is rather limited, but high molecular weight guar gum (Meyprodor 400, Danisco, Denmark) and high molecular

weight konjac mannan (Propal PA, Shimizu, Japan) were investigated. Samples were prepared and characterised as described above (in 4.2).

Maltodextrin-based as well as glucose syrup-based dilute solutions containing konjac mannan or guar gum (100 ppm) did not exhibit rheological properties significantly different from the solvents. In filament stretching experiments, the break-up was quick and the decrease of the diameter with time was linear, not exponential as expected for Boger fluids. This indicates that guar gum and konjac mannan were not able to impart sufficient elasticity in solution to obtain Boger fluids, which may be due to the semi-flexible solution conformation of these polymers. The xanthan gum molecule behaves as a rigid rod; a further discussion on the conformation of polysaccharides in solution can be found in Chapter 5.

The food grade Boger fluids that were successfully developed and their inelastic reference fluids were submitted to sensory tests for evaluation of saltiness and mouthfeel. The results are described in the following.

4.3.2 SALTINESS AND MOUTHFEEL PERCEPTION

Three different sensory tests were carried out on the glucose syrup- and maltodextrin-based Boger fluids (containing xanthan gum) and their respective inelastic reference samples to investigate whether the mouthfeel (test 2) and saltiness (tests 1, 2 and 3)

differed. The results of all three tests will be presented first and then discussed together.

4.3.2.1 Saltiness evaluated by an untrained panel (Test 1)

In the first test, samples were presented in pairs composed of a Boger fluid and its inelastic reference sample and panellists were asked to identify which sample was the saltiest. Each pair was presented 9 times to each panellist. If a panellist identified the same sample as saltier at least 7 times, it is considered that the panellist was able to differentiate between the samples ($d' > 1$). The results are presented in Figure 4.7. Considering the data from all panellists, Boger fluids and inelastic reference samples could not be distinguished (maltodextrin-based and glucose syrup-based inelastic reference samples were found 55.6% and 50.9% of the time saltier than the corresponding Boger fluids). However, some individual panellists were able to distinguish between the samples. Panellists 1 to 7 found the reference significantly saltier than the Boger fluid for at least one of the two pairs. Panellists 8 to 11 then found the Boger fluid saltier than the reference sample for one of the two pairs whereby it was not consistent for which pair this was the case. Panellist 12 showed extreme 'behaviour' with perceiving the reference sample as clearly saltier than the Boger fluid in case of the maltodextrin-based system and perceiving the opposite as clearly for the glucose syrup-based system.

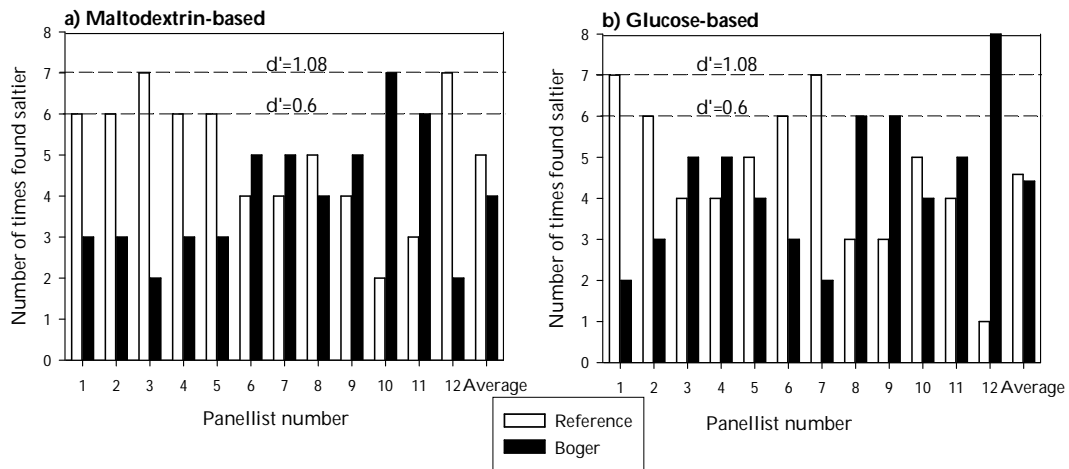


Figure 4.7: Attribute difference test: number of time the inelastic reference sample (in white) and the Boger fluids (in black) were found saltier a) for maltodextrin-based and b) for the glucose syrup-based. Each pair was presented 9 times and a d' analysis was performed (see 4.2.6.1): it is traditionally considered that panellists are able to distinguish between the samples when $d' > 1$ (same sample found saltier 7 out of 9 times).

Several hypotheses can be developed to explain this discrepancy across panellists. Some panellists mentioned that the temporal profile of saltiness in the samples was peculiar due to still detectable sweetness which was perceived at early and late stages of sample tasting. Panellists were instructed to compare saltiness at maximum intensity but this may have been difficult and the discrepancy across panellists may originate from evaluation of saltiness at different points in time. As a second hypothesis, panellists may have noticed a difference, such as in mouthfeel, sweetness and/or bitter taste, which they wrongly associated with a difference in saltiness. Indeed, all panellists pointed out difficulty in analysing saltiness as samples were also sweet, bitter and extremely viscous.

4.3.2.2 Saltiness and mouthfeel evaluated by a trained panel (Test 2)

Following the difficulties observed in Test 1, Boger fluids and inelastic reference samples were tested and compared by a trained panel for each of the attributes defined by the panel in Chapter 3 (Table 3.2). The results of this test are shown in Table 4.2. It is evident that the panel could not distinguish between the fluids of each pair for any of the saltiness and mouthfeel attributes, with the exception the glucose syrup-based Boger fluid which appeared significantly thicker than its inelastic reference sample. As in Test 1 (4.3.2.1), differences amongst panellists were observed, however, these differences will not be commented on as each panellist tested the samples only three times.

Table 4.2: Number of times (out of 18 comparisons) where the Boger fluid was found more intense for each of the attribute defined by the panel (6 panellists, 3 replicates).

		Maltodextrin- based	Glucose -based
Mouthfeel	Thickness	9	16 ($p < 0.01$)
	Lubrication	11	6
	Stickiness	9	9
	Residue	10	9
Saltiness	Initial saltiness	9	7
	In-mouth saltiness	8	8
	Saltiness after swallowing	8	12

4.3.2.3 Perception of different salt concentration (Test 3)

The initial saltiness of Boger fluids and inelastic reference samples at 0.6% and 0.7% w/w NaCl was compared using multiple paired comparison for both glucose syrup-based and maltodextrin-based samples and the results are given in Figure 4.8. The Friedman's T statistic for the glucose syrup-based samples is equal to 4.41, which indicates that the panellists were not able to distinguish the samples, not even for pairs of samples in which only the salt content was varied and not the type of fluid behaviour (elastic, inelastic). The two levels of salt would appear significantly different if samples were NaCl in water (Johansson et al., 1973). If panellists cannot distinguish between the two levels of salt, it therefore indicates that saltiness sensitivity was impaired in such samples, probably because of the thick and unpleasant mouthfeel and the sweet taste. It can therefore be concluded that the glucose syrup-based samples were not suitable for taste perception study.

The Friedman's T statistic for the maltodextrin-based samples is equal to 10.43 (significant at $p=0.05$). This indicates that panellists were able to distinguish between samples and as shown in Figure 3.4, samples containing 0.7% w/w NaCl were found saltier than samples with 0.6% w/w NaCl. However, no significant differences were found between the Boger fluid and inelastic reference for the same salt level, though, on a non-significant level, the panellists tended to find the inelastic samples saltier.

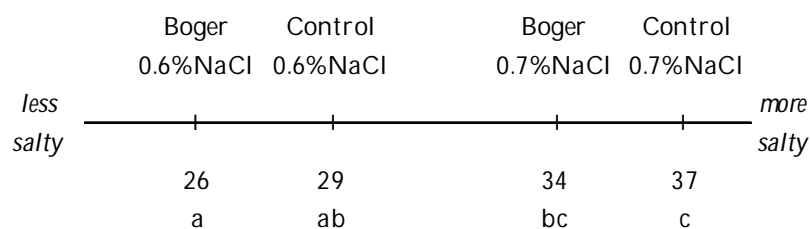


Figure 4.8: Line diagram representations of the rank sum scores for saltiness in the multiple paired comparison of maltodextrin-based samples. Samples with the same letter code are not significantly different ($p < 0.1$).

4.3.2.4 Discussion

Three different sensory tests were performed and no significant difference between Boger fluids and inelastic reference samples were found for saltiness perception and mouthfeel perception.

The lack of discrimination for mouthfeel attributes may seem surprising considering the large rheological differences between Boger fluids and their inelastic reference samples (4.3.1). Several hypotheses can be formulated to explain the lack of difference and can be grouped into two categories: either the Boger fluids and inelastic reference samples exhibit different flow behaviour in mouth but panellists were not able to identify it, or the rheological behaviour of the samples changed drastically in mouth, reducing the differences between Boger fluid and inelastic reference sample. Dilution with saliva and increase in temperature could have indeed modified the fluids' rheology. The Boger fluids' elasticity may be reduced as the shear viscosity decreases

upon dilution with saliva. Similarly, the temperature increase of the samples upon ingestion may have altered differently the rheology of the Boger fluid and the inelastic reference. Indeed, Binnington and Boger (1986) mentioned the extreme sensitivity of the shear viscosity to temperature for Boger fluids, which is not found for the glucose syrups alone. Alternatively, the panellists may not have been able to identify differences despite the very different rheological behaviour. Possibly, the attributes chosen for mouthfeel perception were not optimal to discriminate between samples as those attributes were established based on guar gum and dextran samples (Chapter 3, 3.2.3.1), that is to say on samples much less viscous and weakly elastic. In addition introducing tight protocols standardising sample handling in mouth may improve results. As a result, to be able to establish the mouthfeel perception of highly elastic fluids, it would be desirable to generate new attributes with a panel using Boger fluids and inelastic reference samples as references and use tight protocols to standardise samples handling in mouth. Finally, it is possible that the sweet taste of the samples affected mouthfeel perception, as has been suggested previously, albeit for rheologically less complex samples (Theunissen and Kroeze, 1995; Lethuaut et al., 2003; Tournier et al., 2009).

The three tests gave similar results regarding saltiness perception: Boger fluid and inelastic reference did not appear significantly different. The use of a trained panel (test 2, 3) and consideration of the temporal aspect of saltiness perception (test 2) did

not modify the results. However, the results as obtained in this research should be considered with care before concluding that elasticity has no impact on saltiness perception. Firstly, it should be ensured that the rheological behaviour of the samples differs *in mouth*, as discussed for the lack of mouthfeel differences. Secondly, the absence of significant differences between 0.6% w/w and 0.7% w/w NaCl for the glucose syrup-based sample (test 3) clearly indicates that the discrimination ability of the panellists was impaired by the complexity of the samples (presence of a second tastant and sample rheology, in particular high viscosity). Panellists were able to differentiate maltodextrin solutions containing 0.6% w/w and 0.7% w/w NaCl but yet, the smallest difference in concentration leading to significant differences in perception (just noticeable difference or *jnd*) is expected to be much higher in maltodextrin solutions than in water (not determined here). As a result, panellists may not be able to perceive saltiness differences imparted by the fluids' elasticity even if they do exist.

4.3.3 MIXING EXPERIMENT

In order to gain insight into the mixing behaviour of the samples of this study with saliva in mouth, the mixing experiment as introduced by Ferry et al. (2006a) was carried out, see 4.2.7. Though this technique does not mimic exactly oral conditions as respective volumes of sample and water, temperature, shear and other factors are clearly different in the test situation, it has been employed to infer the efficiency with which samples mix with saliva (Ferry et al., 2006a; Koliandris et al., 2007). Results are

presented in Figure 4.9. Pictures obtained for gelatin and locust bean gum by Koliandris et al. (2007) have been added as reference point. Gelatin exhibits good mixing behaviour even at high concentrations, whereas a marked decrease in mixing efficiency is observed for LBG at 0.6%. The efficient mixing was related to a higher salt release and the better flavour perception in gelatin solution (Koliandris et al., 2007) (see 1.3.1). Pictures taken one minute after mixing do not show differences between Boger fluid and inelastic reference as can be seen in Figure 4.9. Despite the high shear viscosity of these samples, blue colorant is clearly visible throughout the sample as was observed for gelatin with the red colorant. However, the dark region in the bottom of the beakers indicates that part of the samples remained unmixed, similarly to what is observed for locust bean gum. In agreement with the sensory results, this experiment did not demonstrate differences between elastic and inelastic samples but should probably not be over interpreted due to the simplistic set-up.

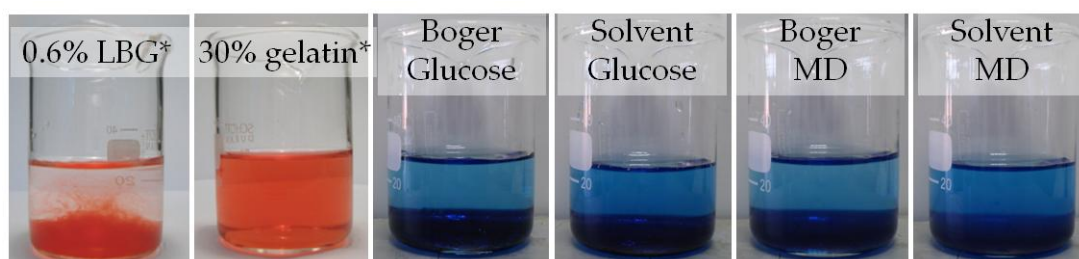


Figure 4.9: Appearance after mixing 5 ml of viscous solutions containing a blue dye with 20 ml of water. *: pictures where samples are coloured in red are taken from Koliandris et al. (2007) (taken with permission). LBG stands for locust bean gum.

4.4 CONCLUSIONS

Two food grade Boger fluids suitable for taste and mouthfeel perception studies have been successfully designed. They are based on glucose syrup or maltodextrin solution as solvent and xanthan gum as the high molecular weight polymer. Their shear viscosity was almost constant with variation being within the range reported in literature for 'technical' Boger fluids. The addition of xanthan gum to the viscous solvent imparted elastic properties as identified by development of a first normal stress difference in shear, values of the Trouton ratio of larger than three calculated from filament break-up experiments, and lastly a pressure drop fingerprint in the micro-contraction flow experiment characteristic for elastic fluids. Results of sensory experiments did not reveal any saltiness or mouthfeel differences between Boger fluids and inelastic reference fluids. However, this finding should be treated with caution as a number of difficulties were identified. It seems that the Boger fluids used here were too complex for taste perception studies, and alternative formulations could not be identified. The only reasonable way of assessing the effect of elasticity developed in high deformation flows on taste perception may be to use low shear viscosity polysaccharide solutions of varying elasticity. Such an approach goes along with the challenge of measuring the elastic contribution of low viscosity solutions in large deformation flow. Microfluidics offers a way forward and an initial assessment of a choice of polysaccharide solutions is presented in Chapter 5.

CHAPTER 5

SHEAR AND EXTENSIONAL RHEOLOGY OF POLYSACCHARIDE SOLUTIONS OF VARIOUS MOLECULAR STRUCTURES

5.1 INTRODUCTION

One of the aims of this PhD research was to investigate the effect of fluid elasticity as developed in large deformation flow on saltiness perception. The initial approach to study this relationship based on Boger fluids was not successful mainly, as reported in Chapter 4, because the fluids were too viscous for sensory analysis. Thus, the only real alternative approach is to use aqueous based polysaccharide solutions (shear viscosity less than ~ 1 Pa.s, see Chapter 4) and to vary the degree of elasticity through appropriate choice of the polysaccharide and its solution concentration. However, very little data are available on the elasticity of aqueous polysaccharide solutions and, therefore, as part of this thesis, considerable effort has gone into supplementing what little data are available. Work reported in this Chapter can therefore be regarded as foundation for the identification of food grade polymers of variable elasticity suitable for further saltiness perception studies.

As graphically depicted in Figure 5.1, the objective was to study polysaccharide solution elasticity in shear and extension, and to relate it to molecular structure and molecular flexibility. Polysaccharides are polymeric carbohydrate structures, formed of repeating saccharides units joined together by glycosidic bonds. The variety of saccharide units and glycosidic bonds available (α or β , between carbons 1 and 4, 1 and 6, 1 and 3 etc) generates the large variety of carbohydrate polymers found in

nature. Six out of the eight polysaccharides included in this study have been chosen for their common β -1 \rightarrow 4 linked backbone and the 'variables' were side-chain composition and degree of branching. Two polymers linked in α -1 \rightarrow 6 were also studied to observe the impact of backbone linkage. With the exception of xanthan gum, all the polymers selected in this research are non-ionic. The polysaccharides used in this research are introduced in section 5.2. Subsequently in 5.3, literature data regarding the flexibility/rigidity of the polymers will be presented and related to the polymer structure. Fundamentals of polymer solutions in extensional flows will be presented in 5.4, followed by the description of the materials and methods used in this particular chapter (5.5) and the presentation of the results (5.6).

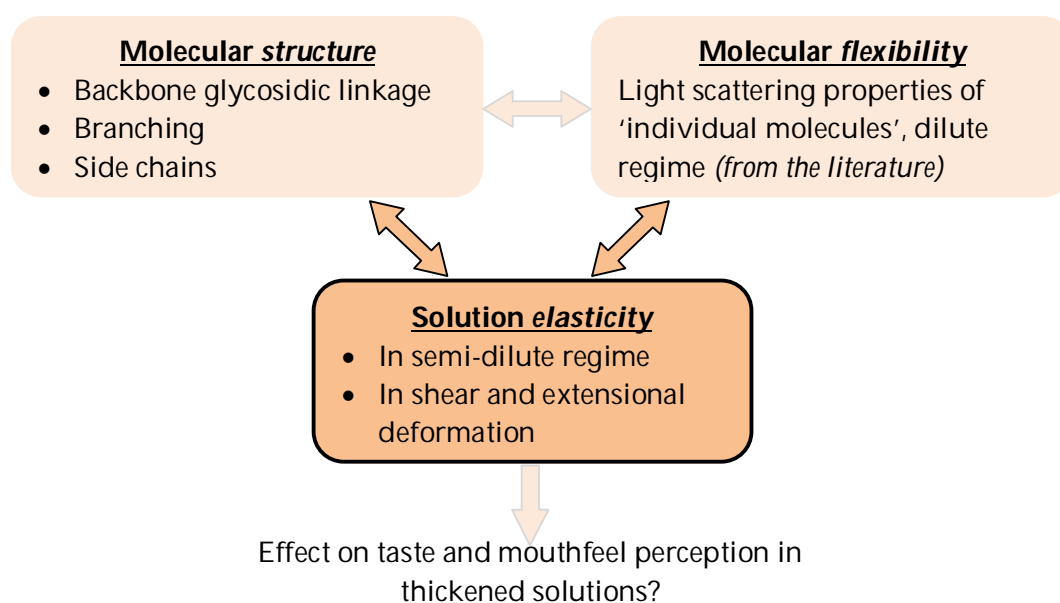


Figure 5.1: Schematic representation of the research questions tackled in Chapter 5.

5.2 POLYSACCHARIDES USED IN THIS RESEARCH

5.2.1 GALACTOMANNANS

Galactomannans are plant reserve carbohydrates present in a large amount in the seeds of plants from the Leguminosae family. Two galactomannans, guar gum, extracted from *Cyamopsis tetragonoloba*, and locust bean gum (LBG), extracted from *Ceratonia siliqua*, were studied. The galactomannan backbone consists of mannose units linked β -1 \rightarrow 4, partially substituted at α -1 \rightarrow 6 with galactose side-chains, imparting water solubility to the molecule (Figure 5.2). The mannose to galactose ratio and the degree of blockiness of the substituted residues vary depending on plant origin (McCleary et al., 1985) and these differences in fine structure have been shown to affect the rheology of the polymer solutions (Daas et al., 2002). Guar gum is more substituted than LBG, with mannose/galactose approximately equal to 1.5 and 3, respectively.

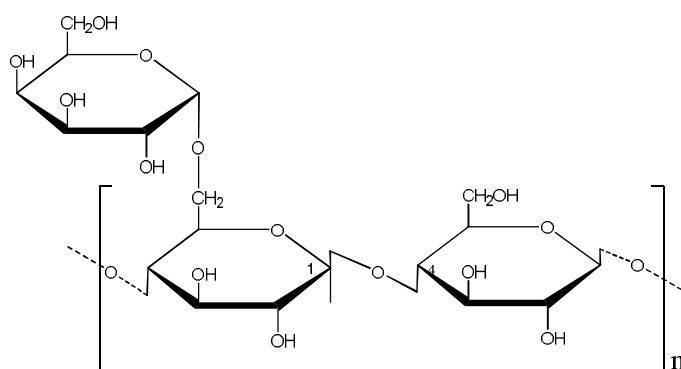


Figure 5.2: Molecular structure of galactomannan.

Galactomannans are extensively used in a variety of industries such as food, oil recovery and personal care due to their high thickening power. The very large viscosity is believed to originate from the high molecular weight of the polymers as well as the presence of intermolecular hydrogen bonds (Morris et al., 1981; Goycoolea, Morris and Gidley, 1995; Cheng et al., 2002; Doyle, Lyons and Morris, 2008).

5.2.2 XANTHAN GUM

Xanthan gum is a bacterial polysaccharide produced by fermentation of glucose or sucrose by *Xanthomonas campestris*. The backbone of the molecules is identical to cellulose (β -1 \rightarrow 4 linked glucose), to which is attached at every second glucose residue a charged trisaccharide side-chain imparting solubility (Jansson, Kenne and Lindberg, 1975) (Figure 5.3). Xanthan gum is the only polysaccharide in this research to carry a net charge (negative).

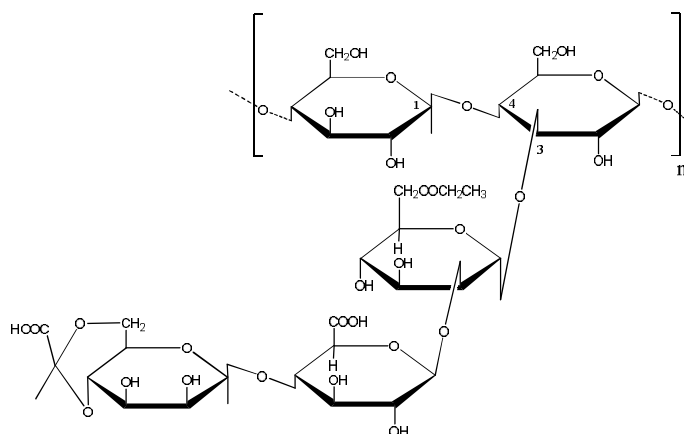


Figure 5.3: Molecular structure of xanthan gum.

Xanthan gum is widely used in foods, yet the market of non-food applications is at least as important and diverse (agrochemistry, oil drilling and recovery, personal care, pharmacy, paints,...). Xanthan gum became a major hydrocolloid due to its properties in solution as it develops a high viscosity at relatively low concentration and exhibits strong shear-thinning behaviour. Xanthan gum solutions are sometimes described as 'weak gels' (Lapasin and Prici, 1995). This particular solution behaviour is attributed to the 'rigid rod' conformation of xanthan gum molecules in solution as discussed in more detail below.

5.2.3 DEXTRAN

Dextran was the first industrially produced microbial polysaccharide and is based on fermentation of sucrose by *Leuconostoc mesenteroides*. Dextran is primarily composed of glucose residues linked α -1 \rightarrow 6 with approximately 5% of randomly distributed α -1 \rightarrow 3 or α -1 \rightarrow 4 branched linkages (Bovey, 1959) (Figure 5.4). Most of these branches are only one to three glucose units long, but there are also a few very long branches. The number of these long branches probably never exceeds 1% of the total number of glucose units. However, they have a great influence on the solution properties of dextran as it has been shown that dextran can be considered as a moderately strong branched polymer (Nordmeier, 1993).

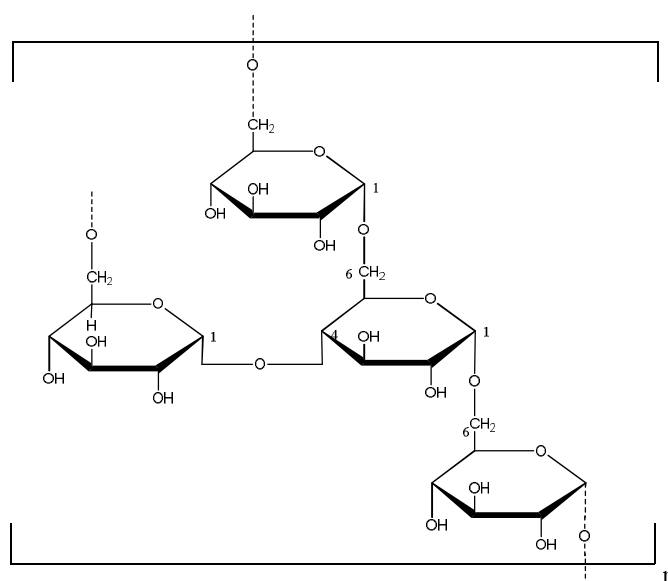


Figure 5.4: Molecular structure of dextran.

Dextran is of low to medium molecular weight (10-2000 kDa) and shows Newtonian behaviour in aqueous solution, developing a low viscosity compared to other polysaccharides (Sabatie et al., 1988). Because of its low thickening power and the inability to form a gel, food applications have been very limited in contrast to its extensive use in pharmacy and medicine (as a blood substitute for example).

5.2.4 PULLULAN

Pullulan is an exocellular microbial polysaccharide produced by the fungus *Aureobasidium pullulans*. Pullulan is a linear molecule with series of three glucose units (maltotriose) linked α -1 \rightarrow 4. Consecutive maltotriose units are linked in α -1 \rightarrow 6 (Figure 5.5).

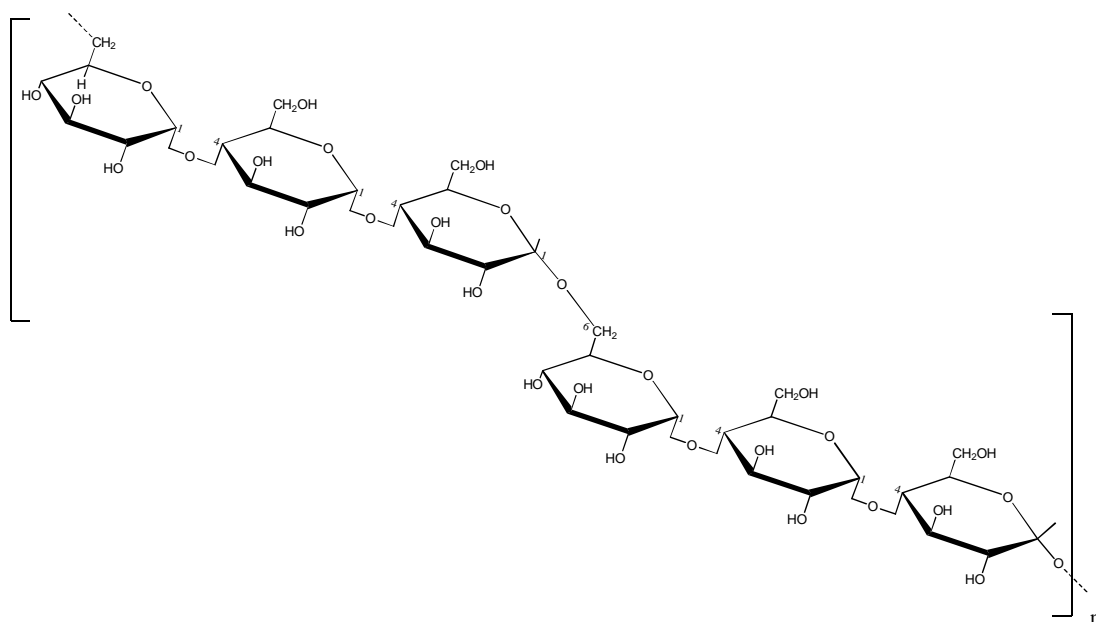


Figure 5.5: Molecular structure of pullulan.

Pullulan solutions exhibit much lower viscosity than guar gum and xanthan gum solutions at low comparable concentration. As a result, pullulan is used for low-viscosity applications in foods and cosmetics. It is also widely used for its film-forming and adhesive properties (Singh, Saini and Kennedy, 2008).

5.2.5 METHYLCELLULOSE

Methylcellulose is synthetically produced by reacting methylchloride with cellulose thus attaching a methyl residue onto the cellulose backbone, which is constituted of glucose residues linked by β -1 \rightarrow 4 glycosidic bonds (Figure 5.6). Different types of methylcellulose differ in molecular weight and degree of methylation. Methylcellulose is widely used in food and personal care products, as a thickener and emulsifier.

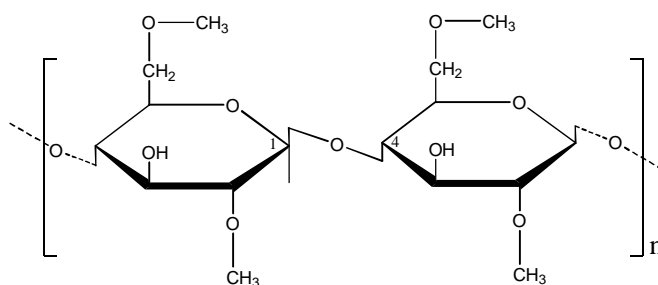


Figure 5.6: Molecular structure of methylcellulose.

5.2.6 XYLOGLUCANS

Xyloglucans are plant polysaccharides extracted from the cell walls of different species, for example from Tamarind-seed (Gidley et al., 1991), from Afzelia (Ren et al., 2004) and from Detarium (Wang et al., 1997; Picout et al., 2003). They have a common backbone of β -1 \rightarrow 4 glucan. Three out of four residues in the backbone are substituted in C6 by xylose residues, hence the name xyloglucan (Figure 5.6). The xylose residues can themselves be substituted in C2 by galactose residues, and therefore the side chain can be up to 3 residues long (Yamatoya and Shirakawa, 2003).

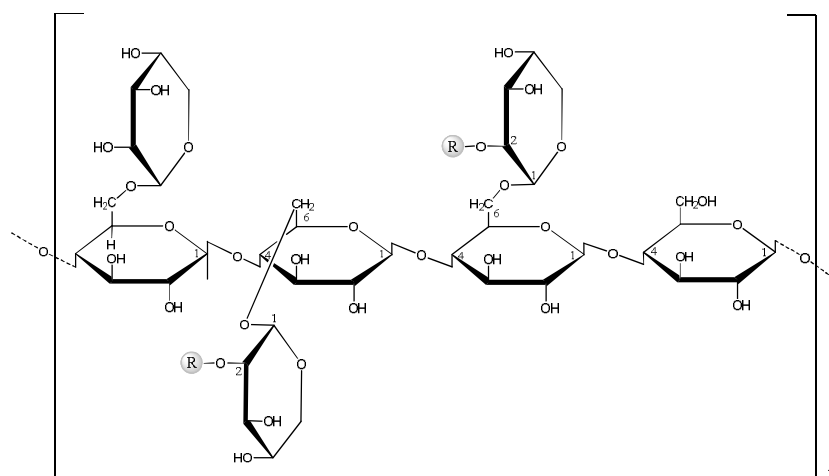


Figure 5.7: Molecular structure of xyloglucans. The residue R is either hydrogen or Galactose.

Xyloglucans have been reported to form gels in presence of high sugar concentration (50%) (Yamatoya and Shirakawa, 2003) and are mainly used in the food industry namely as thickener and gelling agent. The high viscosity in solution has been speculated to be due to some aggregation of the polymer strands (Lang, Kajiwara and Burchard, 1993; Doyle et al., 2008).

5.2.7 KONJAC MANNAN

Konjac mannans are plant polysaccharides extracted from the tubers of *Amorphophallus konjac*. They belong to the glucomannan family and consist of glucose (G) and mannose (M) in a proportion of 5:8 joined by β -1 \rightarrow 4 linkages but the repeating structural unit of the main chain is still uncertain (Kok et al., 2009) (Figure 5.8). The degree of branching is about 8% through β -(1 \rightarrow 6)-glucosyl linkages.

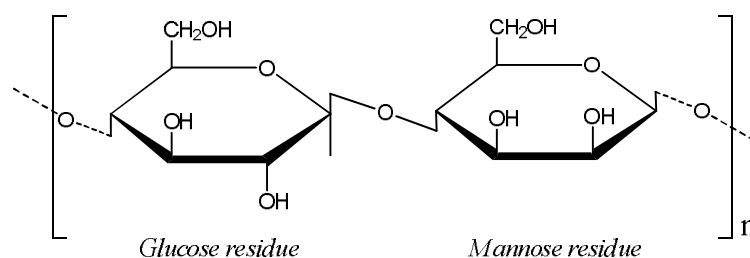


Figure 5.8: Molecular structure of konjac mannan.

Konjac mannan solutions have been reported to exhibit high viscosity at low concentration (Yaseen et al., 2005). In addition, konjac mannan can form a gel, alone or in synergy with xanthan gum and κ -carrageenan thus its use as a thickening and gelling agent in foods.

5.3 POLYMER CONFORMATION AND SOLUTION PROPERTIES

The molecular structure of polymers has an impact on conformation in solution which impacts on the viscoelastic solution properties. Here, after briefly describing different polymer conformations generally possible in solution, known structure-conformation relationships for the polymers used in this research are presented.

5.3.1 INTRODUCTION

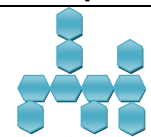
The molecular weight of a polymer defines the 'absolute size' of a polymer chain but the 'actual size' in solution depends on the stiffness of the polymer chain leading to compact or extended conformation in solution. Determination of the volume of a polymer in solution in relation to its molecular weight allows quantifying polymer stiffness, or flexibility. The two extremes of chain flexibility are a perfectly rigid body or 'rigid rod' (Doi and Edwards, 1986) and a highly flexible random coil (based on the Zimm and Rouse theory, reviewed by Ferry (Ferry, 1961)). More detailed information can be found elsewhere (Mitchell and Ledward, 1986; Lapasin and Prici, 1995).

The measure of the hydrodynamic volume occupied by the polymer in solution is called the intrinsic viscosity, $[\eta]$. It depends primarily on the molecular weight of the molecule, chain rigidity and also solvent quality. It is generally determined by measuring solution viscosity at a range of low solution concentrations followed by extrapolation to zero concentration in a combined Huggins and Kraemer regression plot (Morris et al., 1981). The relationship between intrinsic viscosity and molecular weight is then described by the Mark-Houwink-Sakurada equation (Equation 5.1). Although the coefficient K also reflects the local chain flexibility, the exponent a is most commonly used to describe the chain conformation as shown in Table 5.1.

$$[\eta] = KM_w^a \quad (5.1)$$

where $[\eta]$ is the intrinsic viscosity, K and a the Mark-Houwink constants and M_w the molecular weight.

Table 5.1: Theoretical values of the Mark-Houwink-Sakurada exponent a as a function of the polymer conformation in solution.

a	Polymer conformation in solution	Schematic representation
0.1-0.3	Very compact molecules (e.g. highly branched polymers)	
0.5	Fully flexible coil in an ideal solvent	
0.5-0.8	Random flight (semi flexible polymer with excluded volume)	
0.8-2	Rigid rods	

The relationship between intrinsic viscosity and molecular weight has also been used to obtain other polymer chain dimensions such as the characteristic chain ratio C_∞ . It is calculated from the intercept of the so-called Stockmayer-Fixman plot ($[\eta]/M_w^{1/2}$ versus $M_w^{1/2}$) and it is related to conformational freedom or intrinsic chain flexibility (Picout et al., 2001). The higher the characteristic ratio is, the stiffer is the molecule. For example, $C_\infty=4$ for amylose whereas $C_\infty=51$ for cellulose (Mezzasalma, Angioletti and Cesaro, 2004). The chain characteristic ratio can in turn be used to calculate the chain persistence length L_p (in nm) defined as maximum length of the uninterrupted polymer chain persisting in a particular direction. This is in theory nil for flexible

random coil and ∞ for rigid rod conformation. In practice, L_p is about 1 nm for flexible coil and 200 nm for rigid rods (Kok et al., 2009).

The type of backbone linkage, as well as the frequency of branching, has a direct impact on the flexibility or rigidity of the molecule. Indeed, different glycosidic bonds, as in the polymers used in this research, have different angles of freedom. For example, the angle of freedom of a 1 \rightarrow 6 bond is larger than that of a 1 \rightarrow 4 bond (Lapasin and Prici, 1995) which thus imparts more flexibility to the polymer chain.

5.3.2 POLYSACCHARIDE CHAIN FLEXIBILITY

Published data on chain flexibility of the polysaccharides used in this research can be found in Table 5.2. It is worth mentioning that the values for persistence length and the Mark-Houwink-Sakurada exponent are larger than typically found for synthetic polymers (Lapasin and Prici, 1995) which is indicative of partial stiffness of carbohydrate polymers. Dextran and pullulan, with α -1 \rightarrow 6 backbone linkage, are the two more flexible polymers among those used in this research. Yet, because of the relatively high degree of branching, dextran is fairly compact and has therefore also been classified as a soft sphere (Nordmeier, 1993). Methycellulose is classified as an extended coil (Patel et al., 2008). Guar gum and locust bean gum only differ by the extent of backbone substitution, which was shown to not affect persistence length (Picout et al., 2002). Xyloglucans exhibit a higher characteristic ratio and a higher

persistence length. This is probably due to longer side chains than in case of guar gum and LBG which leads to an increase in the excluded volume (Ren et al., 2004). Konjac mannan seems to appear even stiffer than galactomannans and xyloglucans, which may be due to its high degree of short chain branching. Finally, xanthan gum, with its long and charged side chains, is characterised by rigid rod solution behaviour. The xanthan gum molecule's persistence length is about 10 times higher than for the other polysaccharides and the Mark-Houwink exponent a is greater than 1.

Table 5.2: Mark-Houwink-Sakurada exponent a , characteristic ratio C_∞ and persistence length L_p (nm) of the polymers used in this work in relation to their structure. Side-chain frequency is indicated in % of backbone residues, and side-chain in number of saccharide residues.

Polymer	Structure				Chain flexibility		
	Backbone linkage	Bran- ching	Side-chain Freque ncy	Side-chain Length	a	C_∞	L_p
Synthetic polymers					0.5		1
Dextran	α 1 \rightarrow 6	~5%	None		0.3- 0.5		
Pullulan	α 1 \rightarrow 6		None		0.65	4.3	
Methylcellulose	β 1 \rightarrow 4		None		0.55-0.7		12-17
LBG	β 1 \rightarrow 4		~33%	1	0.75	12	3-7
Guar	β 1 \rightarrow 4		~50%	1	0.7	9-16	3-5
Xyloglucans	β 1 \rightarrow 4		75%	1-3	0.67	19-25 (110)	5-8
Konjac mannan	β 1 \rightarrow 4	~8%	None	0	0.754		13-27
Xanthan	β 1 \rightarrow 4		50%	3	0.93-1.3		120
Dextrans	(Lapasin & Pricl, 1995) (Granath, 1958; Tirtaatmadja et al., 2001)						
Pullulan	(Launay et al., 1986; Nishinari et al., 1991; Kasai, 2006)						
Methylcellulose	(Lapasin & Pricl, 1995; Keary, 2001; Patel et al., 2008)						
LBG	(Lapasin & Pricl, 1995) (Launay et al., 1986; Picout et al., 2002; Morris et al., 2008)						
Guar	(Robinson et al., 1982; Picout et al., 2001; Laguna et al., 2003; Morris et al., 2008)						
Xyloglucans	(Picout et al., 2003; Ren et al., 2004) (Gidley et al., 1991)						
Konjac Mannan	(Ratcliffe et al., 2005; Li et al., 2006; Kok et al., 2009)						
Xanthan	(Lapasin & Pricl, 1995)						

For synthetic polymers it is well known that chain flexibility increases with increasing molecular weight (Bur and Roberts, 1969; Jennings and Brown, 1971). This effect was

considered in this research by including guar gums of various molecular weights in the list of materials tested.

5.3.3 CONCENTRATION DEPENDENCE OF POLYMER SOLUTION BEHAVIOUR

Very dilute solution characteristics are not always the most appropriate as in practice, particularly in foods, solutions are at most semi-dilute but mostly concentrated. The conformation of the polymer depending on concentration is typically quantified by measuring solution viscosity and followed by analysis as a function of concentration. Such analysis also highlights the intermolecular interactions in concentrated solutions, as initially described by the theories of Graessley and Ferry (Porter and Johnson, 1966; Ferry, 1980; Graessley, 1980; Graessley and Edwards, 1981). A review of the theory for rigid rods and flexible coils for the different concentration regimes can be found elsewhere (Nwammuo and Maitland, 1991)

5.3.3.1 Classical work on carbohydrate polymers by Morris et al. (1981)

Morris et al. (1981) plotted the specific viscosity, see Equation 5.2 for definition, for various carbohydrate polymers versus solution concentration, see Figure 5.9, and found a characteristic concentration c^*_M separating dilute from concentrated solution behaviour (the subscript M is used here in reference to this original work). Morris et

al. (1981) also observed that data for different carbohydrate polymers fall onto a master curve when the specific viscosity is plotted versus the degree of coil occupancy, $c \cdot [\eta]$. In the dilute regime, $c < c^*_{\text{M}}$ or $c \cdot [\eta] < 4$, the slope of $\log(\eta_{\text{SP}})$ vs. $\log(c \cdot [\eta])$ is about 1.4 and the polymer chains are considered to not interact with each other, i.e., they are isolated in solution. For $c > c^*_{\text{M}}$ (or $c \cdot [\eta] > 4$) the slope of $\log(\eta_{\text{SP}})$ vs. $\log(c \cdot [\eta])$ is about 3.3. In this domain, the total volume occupancy of the carbohydrate chains considering their hydrodynamic volume exceeds the volume of the solution and the chains are considered to be entangled.

$$\eta_{\text{SP}} = \frac{\eta - \eta_{\text{S}}}{\eta_{\text{S}}} \quad (5.2)$$

where η_{SP} is the specific viscosity, η the zero shear viscosity of the solution and η_{S} the solvent viscosity.

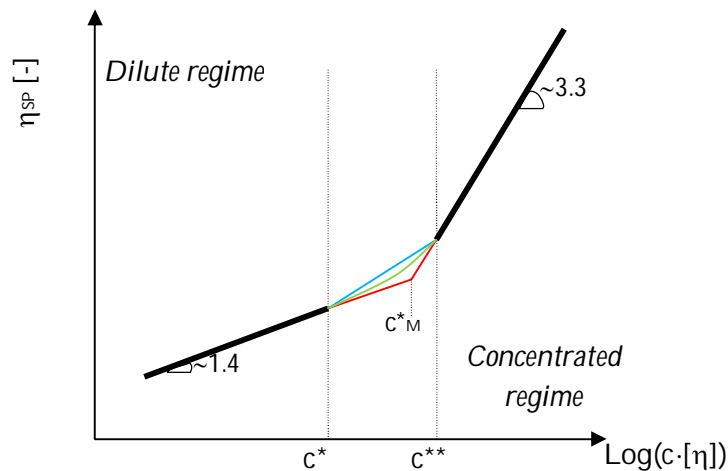


Figure 5.9: Schematic representation of the $\log(\eta_{\text{SP}})$ vs. $\log(c \cdot [\eta])$. The transition between the dilute and concentrated regimes could be linear (blue line), continuous (green curve) or marked by a single transition c^*_{M} (Morris et al. 1981) (red lines).

Since the paper by Morris et al. (1981), a large number of publications on the concentration dependence of the zero shear viscosity for polysaccharide solutions have appeared discussing the existence of the second critical concentration c^{**} and the slope of $\log(\eta_{SP})$ vs. $\log(c \cdot [\eta])$ above c^{**} . Some of the debate crucial to this research is outlined in the following.

5.3.3.2 Specific viscosity behaviour of carbohydrate polymers debated in literature since Morris' classical paper

The existence of two critical concentrations c^* and c^{**} to mark a transition region rather than a single critical point between the dilute and concentrated regime has been reported for most polysaccharides, except for Konjac Mannan (Castelain, Doublier and Lefebvre, 1987; Sabatie et al., 1988; Milas et al., 1990; Launay, Cuvelier and Martinez-Reyes, 1997; Ren et al., 2004; Hemar and Pinder, 2006). Some researchers fit the region between c^* and c^{**} with a third log-log linear regression of slope 2 (Castelain et al., 1987; Sabatie et al., 1988; McCurdy et al., 1994; Launay et al., 1997; Hemar and Pinder, 2006), whereas others suggest to regard the c^* - c^{**} region as a continuous transition as polysaccharides generally show a wide distribution of molecular weight (Wang et al., 1997).

The interpretation of why two critical concentrations should exist ranges from changes in coil size to the type of intermolecular interactions. A reduction of coil volume of up to 30% in the concentrated regime compared to the dilute regime has been reported (Simha and Zakin, 1960). Thus, the c^* - c^{**} region is interpreted as the region where the coil size gradually decreases reaching its minimum size at c^{**} (Castelain et al., 1987; Launay et al., 1997). The intermolecular interaction interpretation is based on the argument that intermolecular interactions are weak in the transition region, and this is as these may be intermolecular hydrogen bonds, compared to strong interactions based on real physical entanglement of the polymer chains above c^* (Guo et al., 2003; Ren et al., 2004). In that case, c^{**} is sometimes called the entanglement concentration, c_e . The type of intermolecular interactions is also believed to control the slope of $\log(\eta_{sp})$ vs. $\log(c \cdot [\eta])$ in the concentrated regime which is briefly discussed in the following.

Morris et al. (1981) were the first to report that the galactomannans guar gum and LBG depart from the generalised behaviour by showing a greater concentration dependence above c^*_M (slope ~ 4.5). This was attributed to be due to presence of specific attractive forces or hyperentanglements in addition to physical entanglements. The nature of the hyperentanglements was later shown to be alkali labile and non covalent interactions (Goycoolea et al., 1995) and recent work indicates that such hyperentanglements could exist in konjac mannan and xyloglucans solutions (Doyle

et al., 2008). Subsequently, similarly large slopes have been reported for dextran (4; (McCurdy et al., 1994)), Konjac Mannan (4.3; (Ratcliffe et al., 2005)), Xyloglucans (4.7 ; (Gidley et al., 1991)) and Hydroxyethylcellulose (5; (Castelain et al., 1987)).

The concentration dependence of the specific viscosity in carbohydrate solutions can be argued in terms of entanglements and intermolecular hydrodynamic interaction and can also be related to the stiffness of the molecules (Sato, Ohshima and Teramoto, 1998; Sato, Hamada and Teramoto, 2003). The type of intermolecular interactions in concentrated solutions will affect the behaviour in shear and extensional flows.

5.3.3.3 Modelling concentration dependence of specific viscosity

The concentration dependence of the specific viscosity can also be modelled over a large range of $c \cdot [\eta]$ using the Martin Equation (Martin, 1951) (Equation 5.3)

$$\eta_{sp} = c[\eta] \exp(K_H c[\eta]) \quad (5.3)$$

where η_{sp} is the specific viscosity, c the polymer concentration, $[\eta]$ the intrinsic viscosity and K_H a constant and a measure of polymer-polymer and polymer-solvent interactions

This equation can also be expressed in the form of an infinite series shown in Equation 5.4.

$$\eta_{sp} \approx c[\eta] \times \left[1 + K_H c[\eta] + \frac{1}{2!} (K_H c[\eta])^2 + \frac{1}{3!} (K_H c[\eta])^3 + \frac{1}{4!} (K_H c[\eta])^4 + \frac{1}{5!} (K_H c[\eta])^5 + \dots \right] \quad (5.4)$$

Each term in Equation 5.4 can be interpreted as resulting from the overlap of the associated volumes for one, two, three, etc, molecules (Matsuoka and Cowman, 2002). For very dilute systems where polymer-polymer interactions are reduced, the right hand side of Equation 5.4 can be truncated after the first 2 components and in this form Equation 5.4 is known as the Huggins Equation 5.5 (Ma and Pawlik, 2007).

$$\frac{\eta_{SP}}{c} = [\eta] + [\eta]^2 K_H c \quad (5.5)$$

where η_{SP} is the specific viscosity, c the polymer concentration, $[\eta]$ the intrinsic viscosity and K_H the Huggins constant.

For higher values of $c \cdot [\eta]$, i.e., in the semi-dilute and concentrated regime, specific viscosity data calculated with Equation 5.3 are known to deviate from experimental data largely overestimating the solution viscosity. Considering interactions between up to 5 neighbouring molecules has been shown to successfully model rigid molecules (Kwei et al., 2000) as well as semi-flexible (Ohshima et al., 1999) and flexible (Matsuoka and Cowman, 2002) polymer chains up to $c \cdot [\eta] = 100$ (Matsuoka and Cowman, 2002).

5.4 EXTENSIONAL FLOW BEHAVIOUR OF POLYMER SOLUTIONS

The fundamentals of shear and extensional flow have been briefly presented in Chapter 1 (1.4). Whereas molecules essentially align in flow direction and may

partially disentangle in shear flow, stretching of molecules is induced in extensional flow. Therefore, the concentration dependence of parameters obtained in extensional flows will be affected not only by the type of intermolecular interactions, but also by the chain flexibility and 'stretchability', giving an interesting insight into the polymer's characteristics. As described in Chapter 1, the filament break-up technique (Capillary Break-up Extensional Rheometer) consists of quickly separating two plates and following the self-thinning of a fluid filament contained between the plates. In this project, the technique was successfully applied to characterising solutions of synthetic polymers and Boger fluids (see Chapter 4), however the break-up times for the solutions of carbohydrate polymers were extremely small (often <100 ms) due to the inherent low elasticity of the solutions. This renders measurements difficult as previously reported in literature (Rodd et al., 2005b). Recently, microfluidics rheometry has been demonstrated as a successful tool to quantify the viscoelastic behaviour of low viscosity polymer solutions (Rodd et al., 2005a). In this research, a filament break-up device was used to obtain a characteristic relaxation time in elongational flow as it is an essential parameter to analyse microfluidics data. Microfluidics data were used to characterise the elasticity of polysaccharide solutions.

5.4.1 CHARACTERISATION OF SOLUTION VISCOELASTICITY USING A FILAMENT BREAK-UP DEVICE

The filament breaking device was presented in Chapter 1 and in Chapter 4 its use to demonstrate the large differences in extensional flow behaviour exhibited by Boger fluids and inelastic solvents was discussed. The objective here is to describe how filament break-up data can be analysed to obtain quantitative extensional flow properties of polymer solutions.

As mentioned in Chapter 1 (1.4), the decay of the filament diameter with time is not linear and, for polymer solutions, generally an exponential region and a linear region can be found. Initially, an exponential decay of the fluids filament is observed (Stelter and Brenn, 2000; McKinley, 2005; Rodd et al., 2005b). As shown in Equation 5.6, the exponent is a function of the relaxation time, λ , more rigorously called 'characteristic time scale for viscoelastic stress growth in uniaxial elongational flow'. This elastic stress growth is due to the uncoiling and stretching of the molecules in direction of flow for flexible polymers or, for rigid molecules, to the orientation in flow direction.

$$d(t) = d_0 \exp\left(-\frac{t}{3\lambda}\right) \quad (5.6)$$

where $d(t)$ [mm] is the mid-point diameter of the filament, d_0 [mm] the mid-point diameter of the filament at the end of the stretching (t_0), t [s] the time and λ [s] the relaxation time.

At longer time, the decay of the diameter of the aged filament has been shown to be linear with time, following Equation 5.7 (Stelter and Brenn, 2000). This has been

interpreted as a quasi Newtonian state: the molecules are viewed to be either completed oriented in the flow or stretched to the maximum. The filament decay is then proportional to the ratio of the surface tension, σ , and inversely proportional to the steady state extensional viscosity, η_e . The transition between exponential and linear decay may not be sudden but rather cover a domain of time, especially for polydisperse samples.

$$d(t) = d_0 - \frac{\sigma}{\eta_e} t \quad (5.7)$$

where $d(t)$ [mm] is the mid-point diameter of the filament, d_0 [mm] the mid-point diameter of the filament at the end of the stretching (t_0), σ [mN.m⁻¹] the surface tension, η_e [Pa.s] the steady state extensional viscosity and t [s] the time.

Various models predict the decrease of the filament diameter with time for the different fluids (yield stress fluids, power law fluids, etc). They will not be described here but can be found elsewhere (McKinley, 2005).

It is well known that the relaxation time and the extensional viscosity of a polymer solution increases with polymer concentration. This increase scales with c/c^* and the slope of the power-law regression relates to the nature of chain-chain interactions, which very likely depend on the polymer conformation. For example, the relaxation time was reported to depend on the ratio c/c^* to the power of 1.5 for semi-flexible hydroxypropyl ether guar (Duxenneuner et al., 2008) whereas theory predicts a dependence to the power $7/3$ for true random coils (Liu, Jun and Steinberg, 2009). In

addition, the extensional viscosity exhibits a log-linear dependence to relaxation time and data for different polymers were shown to collapse on two mastercurves depending on the molecular extensibility (flexible versus rigid rod polymers) (Stelter et al., 2002).

5.4.2 CHARACTERISATION OF SOLUTION VISCOELASTICITY USING MICRO-CONTRACTION FLOW

In this work, visualisation of flow patterns and pressure drop measurements in microscale contractions devices (presented in Chapter 1) were used to study the extensional behaviour of low viscosity polymer solutions. These two techniques will be briefly reviewed following the definition of relevant dimensionless numbers.

5.4.2.1 Dimensionless numbers

Just as no rotational shear viscosity data would be presented without stating the shear rate/stress applied, microfluidics data are associated with dimensionless numbers such as the Reynolds number, Re , and the Weissenberg number, Wi , to characterise the flow in the channel. Before defining these numbers, conventions to describe channel geometry will be introduced.

As can be seen in Figure 5.10, the width of the channel upstream and downstream of the contraction is denoted as w_u , and w_c is the channel within the contraction. The

height of the channel is kept constant throughout the device and denoted as h . Finally, the length of the contraction is denoted as L_c . The contraction ratio is defined by the ratio of w_u/w_c and the hydraulic diameter, D_h , is defined according to Equation 5.8.

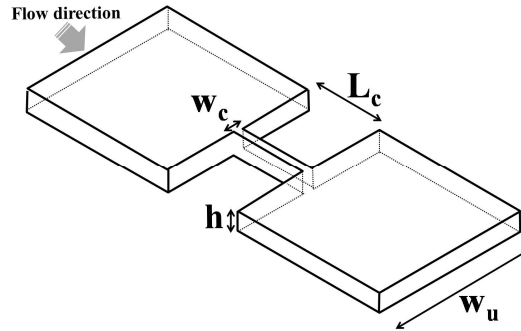


Figure 5.10: Planar microfluidics contraction.

$$D_h = \frac{2w_c h}{w_c + h} \quad (5.8)$$

where D_h is the hydraulic diameter, w_c the contraction width and h the contraction height.

The Reynolds number quantifies the relative importance of inertial forces to viscous forces. It includes density and shear viscosity of the fluid properties, the average velocity V and a characteristic length L of the flow situation. For a microfluidics device, the characteristic length is typically taken as the hydraulic diameter defined by Equation 5.8 and the average velocity is a function of the flow rate and given by Equation 5.9 . Thus, the Reynolds number for planar micro contraction flow is given by Equation 5.10.

$$V = \frac{Q}{w_c h} \quad (5.9)$$

where V is the average velocity in the channel, Q the volumetric flow rate, w_c the contraction width and h the contraction height.

$$\text{Re} = \frac{\rho VL}{\eta} = \frac{2\rho Q}{(w_c + h)\eta} \quad (5.10)$$

where Re is the Reynolds number, ρ the fluid density, η the shear viscosity, V the average velocity, L the characteristic length scale, Q the volumetric flow rate, w_c the contraction width and h the contraction height.

The Weissenberg number compares the relaxation time of the fluid to the characteristic residence time in the contraction region. The latter is approximated by the inverse of the shear rate in the channel. The definition of the Weissenberg number for a planar micro contraction flow can be found in Equation 5.11.

$$\text{Wi} = \frac{\lambda}{t_{\text{flow}}} = \lambda \dot{\gamma}_c = \frac{\lambda Q}{hw_c^2/2} \quad (5.11)$$

where Wi is the Weissenberg number, λ the fluid relaxation time, t_{flow} the characteristic residence time in the contraction, $\dot{\gamma}_c$ the average shear rate in the contraction throat, Q the volumetric flow rate, w_c the contraction width and h the contraction height.

The relative importance of elastic stresses to inertial stresses is given by the Elasticity number defined as the ratio of Wi to Re as shown in Equation 5.12. The interest of microfluidics is to be able to probe the viscoelastic behaviour of fluids at high Elasticity number since flow in microfluidics devices occurs at low Reynolds number and high Weissenberg number. As a result, the elastic response to a high Weissenberg number is not masked by inertial effects (low Reynolds number).

$$El = \frac{Wi}{Re} = \frac{2\lambda\eta}{\rho w_c D_h} = \frac{\lambda\eta(w_c + h)}{\rho w_c h} \quad (5.12)$$

where El is the Elasticity number, Wi the Weissenberg number, Re the Reynolds number, λ the fluid relaxation time, ρ the fluid density, η the shear viscosity, D_h is the hydraulic diameter, w_c the contraction width and h the contraction height.

5.4.2.2 Pressure drop

For any flow in a tube or a channel of some kind, a pressure drop is observed as a result of frictional forces caused by the resistance of the fluid to flow (see the example of a Newtonian fluid in Figure 5.11). For elastic fluids in a contraction flow device, the pressure drop shows a second component due to entrance and exit effects in the contraction region (Oliveira et al., 2008). The presence of recirculating regions (see below in 5.4.2.3) upstream of the contraction, the elongation of molecules in the contraction and the rearrangement of the velocity profile downstream of the contraction dissipate energy and cause a pressure drop greater than in case of a purely viscous Newtonian fluid. This is called excess pressure drop (Macosko, 1994). Pressure drop measurements therefore give information on the elasticity of a sample as depicted in Figure 5.11. Elastic flexible polymers such as PEO exhibit a sigmoidal shape: at very low flow rates, the pressure drop increases linearly with the flow rate, corresponding to Newtonian-like flow, followed by a large increase of the pressure drop with increasing flow rates, associated to viscoelastic flow (Rodd et al., 2005a; Rodd et al., 2007). The pressure drop levels off at very high flow rate, as molecules are stretched to the maximum. For guar gum solutions, however, no linear increase of the

pressure drop at low shear was observed (Koliandris et al., manuscript in preparation). This was attributed to the fact that molecules are likely to be stretched in the contraction even at very low flow rates due to the partially extended conformation of guar gum molecules. In addition, the flow of guar gum solutions through a micro-contraction resulted in only a moderate increase of pressure drop with flow rate, very likely due to both the weak elasticity of the solutions and the shear-thinning behaviour. Indeed for shear-thinning solutions, the rate of increase of the Newtonian component of the pressure drop with increasing flow rate is less pronounced since the shear viscosity decreases (Figure 5.11). Finally, a number of publications report on quantifying apparent extensional viscosity based on pressure drop measurements (Binding and Walters, 1988; Padmanabhan and Macosko, 1997; Sarkar and Gupta, 2001). However, this is not straightforward as the strain rate in the contraction is not uniform rendering the flow problem three dimensional (Rodd 2005).

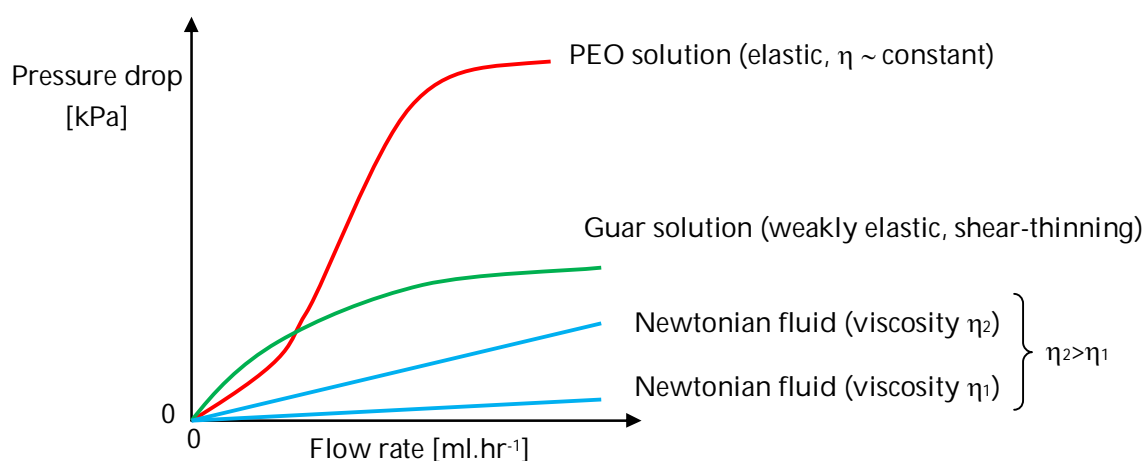


Figure 5.11: Diagrammatic representation of the pressure drop vs. flow rate during flows of various solutions through a micro-contraction device.

5.4.2.3 Flow visualisation

Streak lines can be visualised by adding small fluorescent particles as shown in the literature for macroscale axisymmetric contractions (circular section) (Cable and Boger, 1978b; Cable and Boger, 1978a; Cable and Boger, 1979; Boger, 1987) and as well as macroscale planar contraction (Evans and Walters, 1986; Evans and Walters, 1989; Chiba, Sakatani and Nakamura, 1990; Chiba, Tanaka and Nakamura, 1992) and microfluidics planar contractions (Rodd et al., 2005a; Rodd et al., 2007). It was demonstrated that Newtonian fluids do not exhibit vortex formation upstream of the contraction, but in high inertia flows (high Re) lip vortices develop downstream of the contraction. For highly elastic fluids, Newtonian-like behaviour is observed at very low Re and Wi numbers. With increasing value of these numbers, lip vortices appear which develop into full corner vortices and the vortices grow in size (characterised by the dimensionless vortex length, see Equation 5.13). For even higher Re and Wi numbers, the flow becomes instable (diverging flow, asymmetric vortex growth) for highly elastic solutions. In contrast, for solutions of rigid rods, such as xanthan gum or fibres, the vortex length was almost independent of the flow rate (Zirnsak and Boger, 1998). It was found that guar gum also exhibited vortex recirculations but vortex length was dependent on the flow rate (contrary to rigid rod polymer solutions) and appeared symmetric and steady for all conditions investigated (contrary to fully flexible polymers at equivalent Elasticity number) (Koliandris et al., manuscript in preparation).

$$\chi_L = \frac{L_V}{w_u} \quad (5.13)$$

where χ_L is the dimensionless vortex length, L_V the vortex length and w_u the width of the channel upstream the contraction.

Recently, interesting entry flow phenomena in a micro contraction device were reported for solutions of polyethylene oxide (PEO) in absence (Rodd et al., 2007) or in presence of sodium dodecyl sulphate (SDS) (Miller and Cooper-White, 2009). PEO is a true random coil in solution in absence of SDS but its rigidity increases in presence of SDS. Differences in flow pattern and pressure drop were observed with the change of conformation of PEO. This illustrates the potential of microfabricated devices to study conformation effect of weakly viscoelastic polysaccharide solutions.

5.5 MATERIALS AND METHODS

5.5.1 MATERIALS

The carbohydrate polymers used in this work can be found in Table 5.3. The different types of guar gum mainly differ by their molecular weight as the samples have about the same mannose/galactose ratio (1.75, indicated by Danisco). The two xyloglucans PXYlo and glyloid 3S (denoted as Gly3S) can be considered as identical except that the PXYlo sample was reported to be of higher purity. The third xyloglucan considered, GlyEight showed a lower degree of substitution than Gly3S and PXYlo. The

polyacrylamides were used as reference samples to validate filament break-up data with literature data and silicon oil was used as Newtonian reference fluid.

Table 5.3: Origin of the polymers used in this work.

	Material	Origin
<i>Galactomannans</i>	Guar L	Meyprodor 30, Danisco, Denmark
	Guar M	Meyprodor 100, Danisco, Denmark
	Guar H	Meyprodor 400, Danisco, Denmark
	LBG	Sigma Aldrich
<i>Xyloglucans</i>	Gly3S	
	PXylo	Dainippon Sumitomo Pharma, Japan
	GlyEight	
<i>Konjac mannan</i>	KM LM	Rheolex LM, Shimizu, Japan
	KM PRS	Propal RS, Shimizu, Japan
	KM PA	Propal A, Shimizu, Japan
<i>Dextran</i>	40	T40, Pharmacosmos, Denmark
	500	T500, Pharmacosmos, Denmark
<i>Reference samples</i>	Pullulan	TCI-Europe, Belgium
	Methylcellulose	Methocel A40M, Dow, USA
	Xanthan	Keltrol RD, CP Kelco, USA
	Praestol 2500	
	Praestol 2530	Ashland, Germany
	Praestol 2540	
	Silicon oil 100 cSt	Dow Corning, USA

5.5.2 SAMPLE PREPARATION

Stock solutions of each polysaccharide at the highest concentration (weight basis) applied in this research were prepared by dispersing the dry powder in cold water

using a magnetic stirrer. Dextran and pullulan samples were fully dissolved after stirring for 3 h at room temperature. For all the other polymers, the dispersions were stirred at 80 °C for 1 h followed by continued mixing overnight on a roller mixer at 4 °C. Preliminary experiments showed that all but solutions of dextrans, pullulan, xanthan gum, PXYlo and Praestrol contained a small amount of insoluble impurities (8-15%), probably cell debris and insoluble proteins. These were removed by centrifugation for 45 min at 5000 g after which the samples appeared less cloudy. To obtain desired viscosity or polymer concentration, the samples were diluted with water and placed for a further 2 h onto the roller mixer. Concentrations are reported based on the purified samples.

Two sets of samples were prepared. For the first set, the polymer concentration was fixed to 0.5% w/w for all samples, with the exception of the dextrans and pullulan exhibiting too low viscosity at 0.5% w/w. In the second set, the polymer concentration was adjusted so that the zero shear viscosity was equivalent to 0.1 Pa.s for all samples. The concentrations required for viscosity matching were: 1.5% for guar L, 0.35% for guar H, 0.45% for LBG, 0.82% for Gly3S, 0.85% for PXYlo, 2.11% for GlyEight, 0.13% for konjac mannan PA, 0.21% for konjac mannan PRS, 28% for dextran 40, 15% for dextran 500, 9.33% for pullulan, 0.72% for methylcellulose and 0.08% for xanthan gum (approximation as xanthan gum solutions do not exhibit a zero shear plateau). The

konjac mannan LM was excluded from the study as it did not display a zero shear plateau for semi-dilute solutions.

5.5.3 ROTATIONAL RHEOLOGY

Viscosity data were acquired for shear rates of up to the order of 10^6 s^{-1} using thin film rheology and all necessary data corrections (gap error (Kramer, Uhl and Prudhomme, 1987) and non-Newtonian behaviour (Shaw and Liu, 2006)) as described in Chapter 2 (2.2.1). Small deformation oscillatory shear (SAOS) data were acquired as indicated in Chapter 2 applying the direct strain option of the rheometer used here (MCR 301, Anton Paar, Austria). The linear viscoelastic region was very extended ($> 10\%$ strain) and the frequency sweep was performed at 5% strain. 0.1% SDS solution was placed at the rim of the geometry to avoid surface tension effect. Solutions were compared based on the values for the moduli, G' and G'' , at 5% strain and $10 \text{ rad}\cdot\text{s}^{-1}$, obtained from both strain sweep and frequency sweep as the type of test did not have a significant effect ($p=0.657$ and $p=0.712$ for loss modulus, G'' , and storage modulus, G' , respectively).

The intrinsic viscosity, $[\eta]$, of the polymers was determined following a well established method (Morris et al., 1981). Flow curves were acquired using a shear stress controlled rotational rheometer (MCR301, Anton Paar, Austria) fitted with a cone and plate geometry or a double concentric cylinder geometry for the less viscous

samples. Flow curves were fitted to the Cross equation using the rheometer's software to obtain the zero shear viscosity η_0 . These data were used to calculate the intrinsic viscosity, $[\eta]$, of each hydrocolloid from the y-axis intercept of a Huggins and Kraemer plot (Morris et al., 1981).

5.5.4 FILAMENT BREAK-UP

The filament mid-point diameter as a function of time was obtained as indicated in Chapter 2 (2.2.3). A very high rate of data point acquisition ('high speed' option, 6000 to 12000 points per second) was chosen to be able to capture the very quick break-up of the polysaccharide solutions filaments. As indicated above (5.4.1), the decrease of the diameter function of time was fitted with two equations. At early times, Equation 5.6 was fitted to obtain the relaxation time, λ . Equation 5.7 was fitted to the aged filament to obtain the apparent extensional viscosity of the samples. The filament diameter at the instant t is often normalised with the diameter d_0 at the beginning of the self-thinning process (see Chapter 2, 2.2.3).

5.5.5 MICRO-CONTRACTION FLOW

The microchannels were built and the pressure drop measured as indicated in Chapter 2 (2.2.4). In addition, the flow was visualised by the addition of small fluorescent particles (Fluospheres® 1.0 μm , Invitrogen, Oregon, USA). The solutions were seeded at a concentration of 0.01% w/v. Streak images were acquired at 20x

magnification at the centre plane of the microchannels (Rodd et al., 2005a). A constant illumination mercury lamp provided excitation through a filter cube (Nikon G-2A). Exposures were taken from the second frame of a double-pulsed camera system (PCO Sencicam) using an exposure time of 20 ms to provide significant streaking.

5.5.6 MOLECULAR WEIGHT

Dilute samples (0.1% w/w) were analysed using size exclusion chromatography coupled to multi-angle laser light scattering and differential pressure viscometry (SEC-MALLS-DPV). Analytical fractionation was carried out using TSK G6000PW_{XL} and TSK G4000PW_{XL} size exclusion columns protected by a similarly packed guard column (Tosoh Bioscience, Tokyo, Japan) with an on-line MALLS (Dawn HELEOS II), differential pressure viscometer (Viscostar II) and refractive index (Optilab rEX) detectors (Wyatt Technology, Santa Barbara, U.S.A.). The eluent (distilled water) was pumped at 0.8 ml.min⁻¹ (PU-2080, Jasco Corporation, Great Dunmow, U.K.) and the injected volume was 100 µl for each sample. Absolute weight-average molar masses (M_w), polydispersity indices (M_w/M_n) and weight-average intrinsic viscosities ($[\eta]_w$) were calculated from the Debye and Huggins models incorporated in the ASTRA® (Version 5.3.2.17) software (Wyatt Technology, Santa Barbara, U.S.A.), using the refractive index increment, $dn/dc = 0.150 \text{ ml.g}^{-1}$ (Theisen et al., 2000). These measurements were done as a service in the labs of the National Centre for Macromolecular Hydrodynamics.

5.5.7 DENSITY

The density of the samples was measured in triplicate using the density meter described in Chapter 2 (2.4) and values can be found in Appendix 5.1. The density can be fitted using a linear regression function of the concentration, irrespectively of the polymer type (density= 0.4249 concentration + 1.0006, $R^2 = 0.996$). On close examination, the guar samples exhibited a slightly higher density than the other samples, probably due to the presence of remaining impurities despite the centrifugation step designed to remove insoluble impurities.

5.5.8 SURFACE TENSION

Surface tension measurements were performed at the air/water interface via the pendant drop profile analysis tensiometer (PAT1, Sinterface technologies, Berlin, Germany). Surface tension was recorded with a constant drop volume of 25 mm³, 20 °C for 30 minutes (which was also when equilibrium was reached). Surface tension was determined by fitting the coordinated of a drop to the Gauss-Laplace equation, for all data presented this was done using the built in fitting software provided with the tensiometer. The values are reported in Appendix 5.2.

5.6 RESULTS AND DISCUSSIONS

This section is organised into three main parts. In the first part, the molecular characteristics of the polymers as determined using SEC-MALLS and viscometry methods are presented and discussed. The large deformation flow behaviour is presented in a second part. In the third and final section, viscoelastic solution behaviour, as evaluated in small amplitude oscillatory shear, filament break-up experiments and micro planar contraction flow, is presented and discussed.

5.6.1 MOLECULAR BEHAVIOUR

5.6.1.1 Molecular weight and intrinsic viscosity

The molecular weight of the different carbohydrate polymers as determined by SEC-MALLS can be found in Table 5.4. The comparison with the nominal molecular weight as provided by each supplier has been included as well. For some polymers such as pullulan and dextran 40, the two values were in excellent agreement. For other polymers (in particular guar M, guar H and konjac mannan PRS), the molecular weight obtained by SEC-MALLS data was lower than the nominal molecular weight. This may be due to experimental error arising, for example, from polymer association with the chromatography column, and real differences between the molecular weight of the batch under study and the general molecular weight given by the supplier.

Table 5.4: Molecular weight indicated by the supplier and obtained by light scattering results and intrinsic viscosity of the polymers as determined by the combined Kraemer and Huggins regression and comparison with the values obtained by light scattering.

		Molecular weight [kDa]		[η] [dl.g ⁻¹]	
		Supplier indication	Light Scattering results	Rheology results	Light scattering results
<i>Galactomannans</i>	Guar H	2640	1509	18.0	13.4
	Guar M	1640	1135	9.0	
	Guar L	426	323	3.6	4.2
	LBG	na	699	12.5	9.5
<i>Xyloglucans</i>	Gly3S	500	299	6.1	3.8
	PXylo	400	226	6.1	2.9
	GlyEight	100	377	2.6	1.7
<i>Konjac mannan</i>	KM PA	2000 to 5000	2307	22.5	15.8
	KM PRS	1400 to 2000	982	12.7	17.0
	KM LM	10	93		1.1
<i>Dextran</i>	500	496	400	0.45	0.55
	40	37	33	0.18	0.24
	Pullulan	270	272	0.57	0.94
	MCellulose	na	187	5.8	6.7
	Xanthan	na	8667	20(with salt) 66.5(no salt)	12.17

Table 5.4 also shows the intrinsic viscosity values determined by SEC-MALLS and by the combined Huggins and Kraemer regressions. Graphical representations of the Huggins and Kraemer regressions for the different polymers can be found in Appendix 5.3. The two methods (light scattering and rheology) gave slightly different

intrinsic viscosity values yet the order of magnitude is similar. The intrinsic viscosity obtained by the combined Huggins and Kraemer regression is in excellent agreement with the data available in the literature for the exact same polymers. Values of 8.6-9.5 dl.g⁻¹ and 3.3-3.6 dl.g⁻¹ were found for guar M and guar L, respectively (Wientjes et al., 2000; Picout et al., 2001), of 6 dl.g⁻¹ for glyloid 3S (Gidley et al., 1992), of 0.22 dl.g⁻¹ and 0.55 dl.g⁻¹ for Dextran 40 and Dextran 500, respectively (Tirtaatmadja, Dunstan and Roger, 2001). The excellent agreement with literature data led to the decision to use these intrinsic viscosity values (obtained by the combined Huggins and Kraemer regressions) in this project if required for data analysis.

The data presented in Table 5.4 provide an indication of molecular flexibility, as described above (Chapter 5.3). For example, the two polymers pullulan and Gly3S are of similar molecular weight but the flexible chain polymer pullulan (α -1 \rightarrow 4 linkages) was found to have an intrinsic viscosity of about 10 times lower than the semi-flexible chain polymer Gly3S (β -1 \rightarrow 4 linkages). The effect of branching can also be observed as dextran 500 exhibited a smaller intrinsic viscosity than pullulan despite its higher molecular weight (both polymers are highly flexible). Finally, methylcellulose seemed to be quite rigid as it exhibited a relatively high intrinsic viscosity (5.8 dl.g⁻¹) for a small molecular weight polymer (187 kDa), in agreement with the 'extended coil' conformation reported by Patel et al. (2008).

5.6.1.2 Concentration dependence of the zero shear viscosity

The plot $\log(\eta_{SP})$ vs. $\log(c \cdot [\eta])$ for the different polymers and the corresponding values of the critical concentrations, c^* and c^{**} , as well as the slopes of the different domains can be found in Figure 5.12 and Table 5.5, respectively. The individual plots for each polymer can be found in Appendix 5.4 ($\log(\eta_{SP})$ vs. $\log(c)$). The data for the different polymers fell onto a single curve below c^* , and on average the viscosity of the solutions depends on the concentration to the power 1.49, which is in agreement with the literature. All polymers exhibited a c^* - c^{**} transition region, which can be fitted with a linear regression of slope 2-2.4. This has been previously observed for CMC and HEC (Castelain et al., 1987), Gly3S (Gidley et al., 1991), PXYlo (Wang et al., 1997; Ren et al., 2004), pullulan (Hemar and Pinder, 2006), galactomannans (Launay et al., 1997) and dextran (Sabatie et al., 1988; McCurdy et al., 1994). The existence of a transition region was confirmed here for these polymers, and was also found for methylcellulose. Only Konjac mannan exhibits a sudden transition from the dilute to the concentrated regime, which has been reported before (Jacon et al., 1993; Ratcliffe et al., 2005). Above c^{**} , the concentration dependence of the viscosity is fairly similar for all polymers investigated here ($\eta_{SP} \propto c^{4.4}$). As mentioned in the introduction (5.3.3), this value is substantially higher than initially reported by Morris et al. (1981), but in excellent agreement with data published later for a range of polymers (Castelain et al., 1987; Gidley et al., 1992; Ratcliffe et al., 2005).

Table 5.5: Critical concentrations, reduced critical concentrations $c \cdot [\eta]$ and slopes of the regression lines $\log \eta_{SP}$ versus $\log c \cdot [\eta]$ in the three flow regimes for the different polymers studied.

		Critical concentration [% w/w]		Reduced critical concentration $c \cdot [\eta]$ [-]		Slopes of the linear regressions		
		c^*	c^{**}	at c^*	at c^{**}	$c < c^*$	$c^* - c^{**}$	$c > c^{**}$
<i>Galactomannans</i>	Guar H	0.08	0.24	1.48	4.34	1.61	2.88	4.66
	Guar M	0.12	0.36	1.08	3.22	1.40	2.26	4.14
	Guar L	0.21	0.82	0.75	2.91	1.22	1.87	3.84
	LBG	0.12	0.33	1.47	4.19	1.60	2.55	4.03
<i>Xyloglucans</i>	3S	0.16	0.62	0.96	3.79	1.30	2.12	4.10
	PXylo	0.30	0.83	1.81	5.04	1.53	2.71	4.03
	GlyEight	0.73	1.57	1.88	4.10	1.49	2.26	3.46
<i>Konjac mannan</i>	KM PA	0.08	/	1.73	/	1.66	/	4.15
	KM PRS	0.10	/	1.30	/	1.99	/	4.50
<i>Dextran</i>	500	4.90	19.29	2.21	8.68	1.41	2.24	5.73
	40	10.60	25.50	1.91	4.59	1.40	2.62	5.35
	Pullulan	2.22	9.54	1.27	5.45	1.30	2.20	5.40
	MC	0.25	1.09	1.46	6.27	1.45	2.74	4.06
	Xanthan	0.04	0.10	2.41	6.79	1.54	2.09	4.16
	<i>average</i>			1.55	4.80	1.49	2.44	4.40
	<i>Standard deviation</i>			0.47	1.66	0.19	0.38	0.66

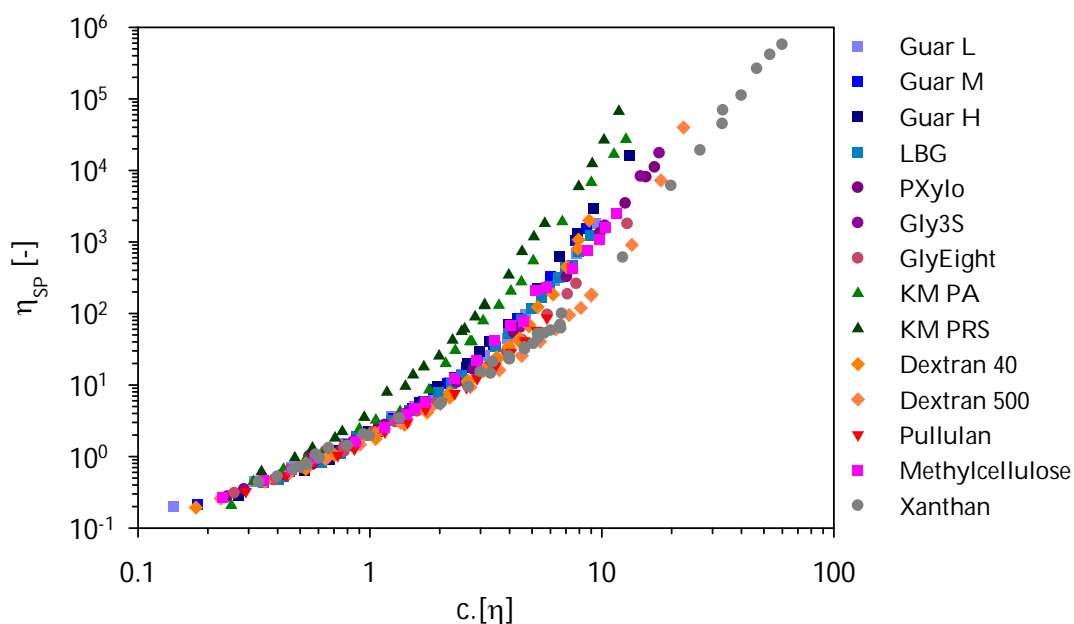


Figure 5.12: $\log(\eta_{SP})$ vs. $\log(c \cdot [\eta])$ for the different polymers studied.

The concentration dependence of the zero shear viscosity (plot $\log(\eta_{SP})$ vs. $\log(c \cdot [\eta])$) was fitted for each polymer with two conditions of the Martin Equation (see above in 5.3.3.3), either considering an infinity of neighbours (Equation 5.3) or 5 neighbours for each molecule (modified Martin Equation, Equation 5.14). The graphs for each individual polymer can be found in Appendix 5.5. Based on the good fitting of Equations 5.3 and 5.14, three subgroups of polymers were established:

- (1) Pullulan, dextran 500 and dextran 40;
- (2) Guar M, guar L, LBG and GlyEight;
- (3) Guar H, PXYlo, Gly3S, methylcellulose, xanthan gum, konjac mannan PA and konjac mannan PRS.

Characteristic results for each subgroup are presented in Figure 5.13.

$$\eta_{SP} = c[\eta] \times \left[1 + K_H c[\eta] + \frac{1}{2!} (K_H c[\eta])^2 + \frac{1}{3!} (K_H c[\eta])^3 + \frac{1}{4!} (K_H c[\eta])^4 \right] \quad (5.14)$$

where η_{SP} is the specific viscosity, c the polymer concentration, $[\eta]$ the intrinsic viscosity and K_H a constant and a measure of polymer-polymer and polymer-solvent interactions.

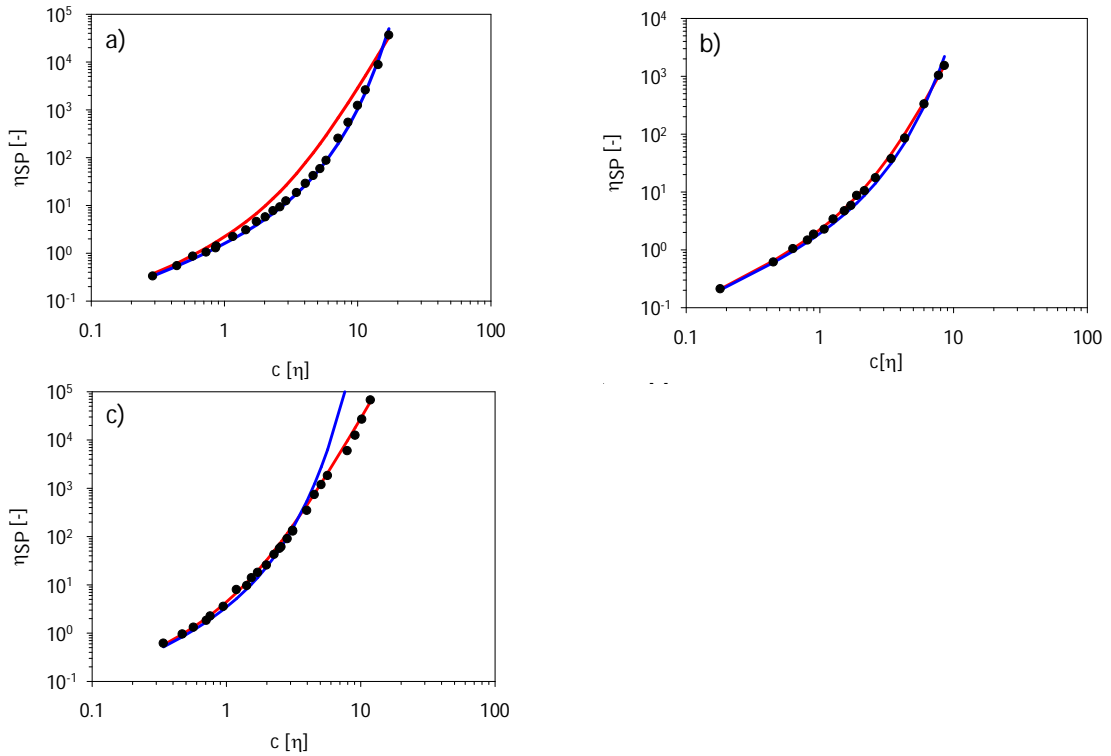


Figure 5.13: Fit of the Martin equation (in blue, considering infinite neighbours, Equation 5.3) and the modified Martin Equation (in red, considering 5 neighbours, equation 5.14) to experimental data (●) from a) pullulan, b) guar M and c) konjac mannan PRS.

The first subgroup (Figure 5.13a) was established based on the excellent fit of the Martin equation over the whole range of $c \cdot [\eta]$ ($R^2 > 0.99$) whereas the fit of the modified Martin equation was poor in the $c^* - c^{**}$ domain (overall $R^2 < 0.96$). For polymers of the second subgroup (Figure 5.13b), both equations fitted equally well over the range of $c \cdot [\eta]$ studied ($R > 0.98$). Finally, the third subgroup (Figure 5.13c) was characterised by a

good fit of the Martin equation only at low $c \cdot [\eta]$ (< 2), whereas the fit of the modified Martin equation was excellent over the whole range of $c \cdot [\eta]$ studied here ($R^2=0.99$ on average).

The observation of different fit quality for the different polymers analysed here can be related to the flexibility and size of the polymers and to the intermolecular associations of polymer in solution. For the polymers included in the first subgroup, the full Martin Equation offered a better fit, indicating that each polymer chain interacts with more than 5 neighbours. Pullulan and dextrans are the most flexible polymers studied here and data therefore suggest that flexible polymers interact with a large number of neighbouring chains (Matsuoka and Cowman, 2002). On the other hand, for the third subgroup, the fit of the Martin equation was good only at low $c \cdot [\eta]$ whereas the model at 5 neighbours provided a good fit even at high degree of coil occupancy. The lower number of interacting chains at high concentrations can be related to the more rigid conformation, as the third subgroup gathers large polymer with semi-rigid behaviour (Kwei et al., 2000). Finally, data for polymers of second subgroup could be equally well fitted by the model at 5 neighbours and infinite neighbours, indicating that chain-chain interactions were more important than for rigid high molecular weight polymers of the third subgroup but less important than for the highly flexible polymers of the first subgroup. This can be related to the semi-flexible conformation of the polymers of the second subgroup. To conclude, the plot

$\log(\eta_{sp})$ vs. $\log(c \cdot [\eta])$ was fitted over the whole range of $c \cdot [\eta]$ values using the Martin equation (infinite neighbours) and the modified Martin equation (5 neighbours) and this provided insight into intermolecular interaction in polysaccharides solutions as the number of chain-chain interactions in solutions and polymer conformation were related. It was found that the more rigid and the longer the molecules are, the lower the number of interacting chains was.

5.6.2 LARGE DEFORMATION SHEAR BEHAVIOUR

The viscosity of polymer solutions was measured up to high shear rates (10^6 s^{-1}) using thin film rheology. The samples were either prepared at a constant polymer concentration (0.5% w/w) or at the polymer concentration required to match at zero shear viscosity of 0.1 Pa.s. The flow curves of the samples at 0.5% w/w polymer concentration can be found in Figure 5.14, showing large differences in zero shear viscosity (ranging from 0.001 Pa.s for KM-LM to 23 Pa.s for KM-PA). A positive log-log correlation of $r^2=0.89$ was found between the zero shear viscosity and the intrinsic viscosity, since the degree of polymer coil occupancy in solution, $c \cdot [\eta]$, relates to the zero shear viscosity (as discussed above in 5.6.1.2). At high shear, however, the viscosity seemed to asymptotically approach a value of about 6 mPa.s irrespectively of the polymer type (with the exception of KM-LM). In contrast to low shear, the molecules are totally oriented in the flow field at very high shear ($> 10^6 \text{ s}^{-1}$) and the

effect of polymer conformation on the shear viscosity is reduced. Cross-model parameters can be found in Appendix 5.6.

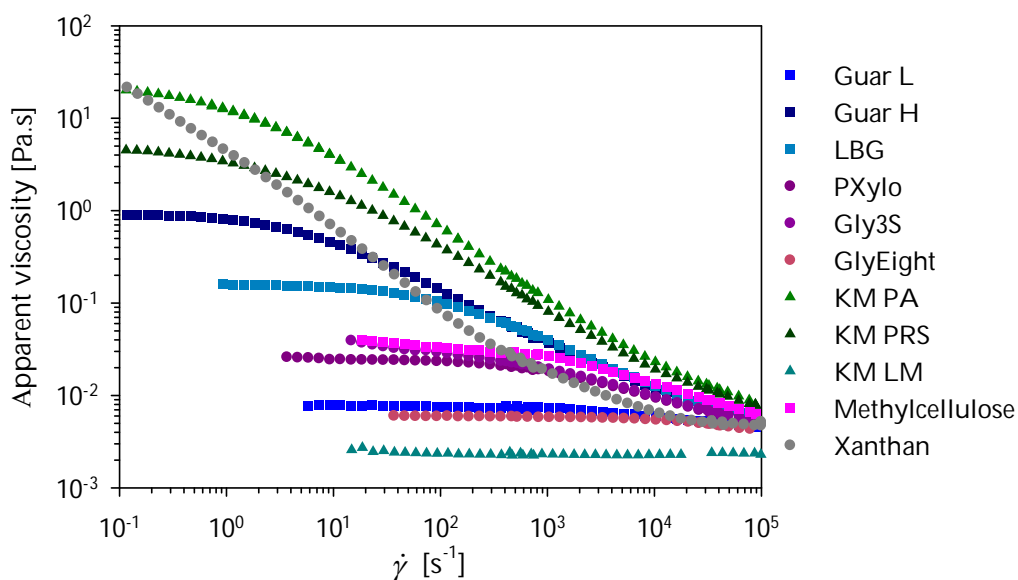


Figure 5.14: Flow curves of all the samples with a polymer concentration of 0.5% w/w.

The data shown in Figure 5.15 illustrate the flow behaviour of the samples matched at zero shear viscosity of 0.1 Pa.s and Cross model parameters can be found in Appendix 5.6. Here, polymer concentration and intrinsic viscosity, $[\eta]$ are inversely proportional (log-log correlation of -0.99). Indeed, samples of matched zero shear viscosity exhibit identical specific viscosity values, η_{sp} , and since the curves $\log(\eta_{sp})$ vs. $\log(c \cdot [\eta])$ largely superimpose for the different polymers (Figure 5.12), the degree of coil occupancy, $c \cdot [\eta]$, is almost constant (5 ± 1). Therefore, the higher the intrinsic viscosity of the polymer, the lower the concentration required to reach a zero shear viscosity of 0.1 Pa.s. When samples were matched at zero shear, differences of almost two decades

were observed in high shear viscosity. The shear viscosity measured at $35,000 \text{ s}^{-1}$ was found to be strongly correlated to the concentration ($r^2=0.97$) and inversely correlated to the intrinsic viscosity ($r^2=-0.97$). This confirms the general thinking that molecules with a large hydrodynamic volume tend to align in flow direction, which results in a decrease of the entanglement density.

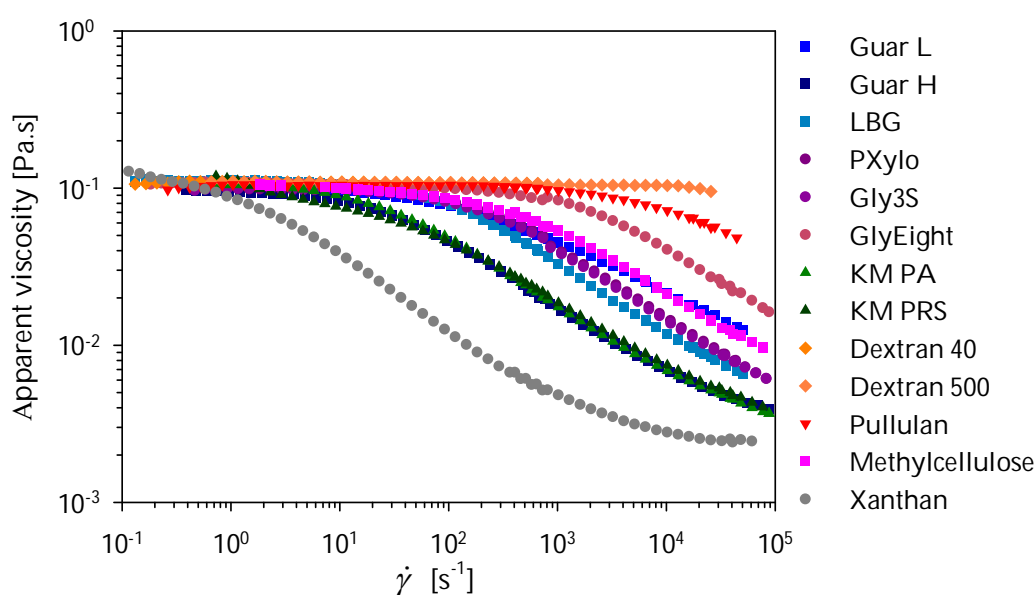


Figure 5.15: Flow curves of all the samples matched at zero shear viscosity of 0.1 Pa.s (polymer concentrations: guar L 1.5%, guar H 0.35%, LBG 0.45%, Gly3S 0.82%, PXYlo 0.85%, GlyEight 2.11%, konjac mannan PA 0.13%, konjac mannan PRS 0.21%, dextran 40 28%, dextran 500 15%, pullulan 9.33%, methylcellulose 0.72%, xanthan gum 0.08%).

To compare the extent of shear-thinning between the different polymers, it is useful to present the fractional decrease of the viscosity (η/η_0) versus the dimensionless shear rate as presented in Figure 5.16 (Robinson, Ross-Murphy and Morris, 1982). The dimensionless shear rate is obtained by multiplying the shear rate by the relaxation

time of the solution, obtained from filament break-up data (as described later). The data for different polymers do not superimpose, indicating that self-similar shear-thinning does not occur. Solutions of polymers of large intrinsic viscosity at zero shear exhibit a higher degree of shear-thinning. These polymers were also characterised by an excellent fit of the modified Martin Equation (Equation 5.14, see 5.6.1.2), whereas the less shear thinning polymers (pullulan and dextrans) were characterised by an excellent fit of the Martin Equation (Equation 5.3), which highlights the relationship between polymer type, dynamics of entanglements in solution and shear-thinning behaviour. In addition, data for a given polymer at different polymer concentration do not always superimpose, despite the fact that the relaxation time acts as a normalisation toward concentration. This has been noticed also for guar gum H at a wider range of concentrations, where data in the range of 0.5-1% superimposed, but differed from lower concentrations (0.22% and 0.35%) (Koliandris et al., manuscript in preparation). The absence of self-similar shear-thinning therefore demonstrates that type and dynamics of intermolecular interactions can vary with concentration as well as polymer type/ molecular weight.

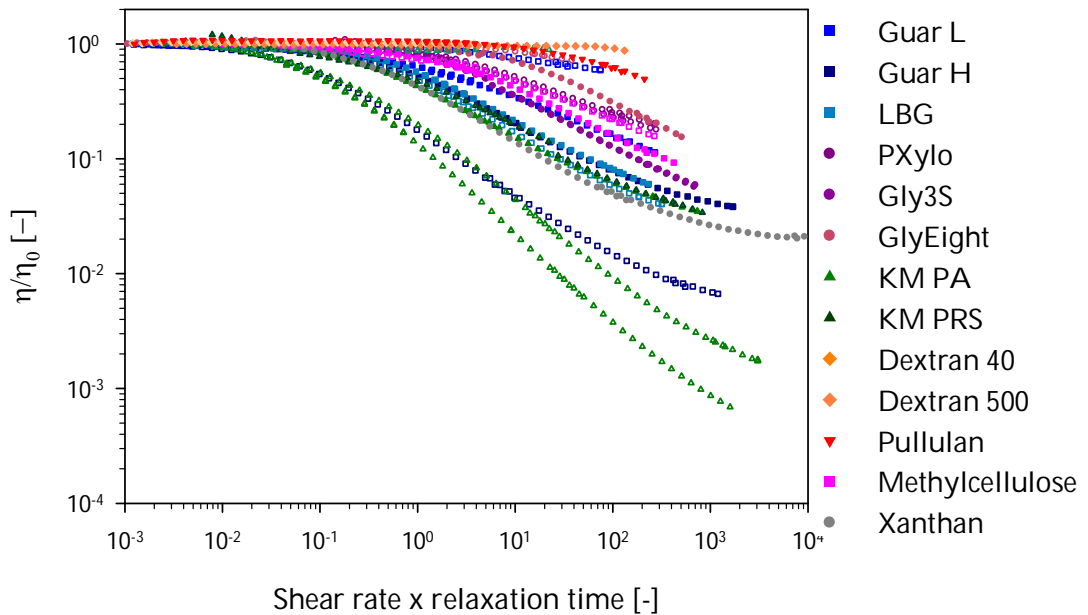


Figure 5.16: Fractional decrease of the viscosity with increasing generalised shear rate for polysaccharide solutions matched in zero shear viscosity (filled symbol) and at 0.5% w/w (void symbols).

5.6.3 VISCOELASTIC BEHAVIOUR OF POLYSACCHARIDE SOLUTIONS

With the exception of Boger fluids described in Chapter 4, shear-thinning and elasticity are two non-Newtonian effects difficult to dissociate. Because of the large differences in shear viscosity across the samples analysed here, it is difficult to analyse the effect of the molecular properties on the elastic component of the flow behaviour measured in Small Angle Oscillatory Shear (5.6.3.1), filament break-up (5.6.3.2) and micro-contraction flow (5.6.3.3) (Boger, 1977/1978). Therefore, the sample set was divided into five groups. Within each group, molecular characteristics of the samples

differed but the shear viscosity behaviour was nearly identical over the full range of shear rates:

- 1) Konjac mannan PA 0.13%, guar H 0.35% and konjac mannan PRS 0.21% (high to low molecular weight). Konjac mannan is more rigid according to literature data (see 5.3.2);
- 2) LBG 0.45%, PurXylo 0.85% and Gly3S 0.82%. LBG is of higher molecular weight and intrinsic viscosity than the xyloglucans but the latter are more rigid according to literature data (see 5.3.2);
- 3) Methylcellulose 0.5%, PXylo 0.5% and Gly3S 0.5%. Methylcellulose is linear and rigid whereas the xyloglucans have small side chains. Limiting analysis to high shear rates data which is relevant for microfluidics, Guar H 0.5% and LBG 0.5% also form part of this group;
- 4) Guar L 1.5% and methylcellulose 0.72%. The molecular weight of methylcellulose was lower than guar L (187 vs. 323 kDa) but its intrinsic viscosity was higher (5.8 vs. 3.6 dl.g⁻¹) which indicates the higher rigidity of methylcellulose;
- 5) Guar L 0.5% and Gly8 at 0.5%. Both polymers have similar molecular weight (323 and 377 kDa, respectively) but Gly8 has a higher degree of branching.

5.6.3.1 Behaviour in Small Angle Oscillatory Shear (SAOS)

SAOS strain sweep (at 10 rad.s⁻¹) and frequency sweep (5% strain) data were acquired for the polysaccharides solutions for the sake of complete solution characterisation. As

this type of deformation (SAOS) is far from an in-mouth situation, and this research was concerned with large deformation elastic phenomena, the results are presented but not discussed in great detail. Strain sweeps showed the typical behaviour of polymer solution with an extended linear viscoelastic domain followed by a rapid decrease of the storage modulus, G' , and a less rapid decrease of the loss modulus, G'' . Moduli values from the linear viscoelastic elastic domain acquired for the polymer solutions matched at zero shear viscosity of 0.1 Pa.s are shown in Figure 5.17 as a function of intrinsic viscosity, $[\eta]$. G'' values are higher than G' values and decrease with increasing $[\eta]$, whereas G' values initially increase steeply followed by an asymptotic approach of a 'maximum' G' (about 0.1 Pa). Increasing $[\eta]$ values correspond to larger and stiffer molecules. It appears that there is a maximum storage modulus than can be obtained for polymer solutions of a given zero shear viscosity. Thus, conformational behaviour of polymers in solution as induced by polymer size and stiffness is a means of 'controlling' sample elasticity measured in SAOS. This conclusion is based on one set of data only and therefore further experimental work is required to generalise this finding.

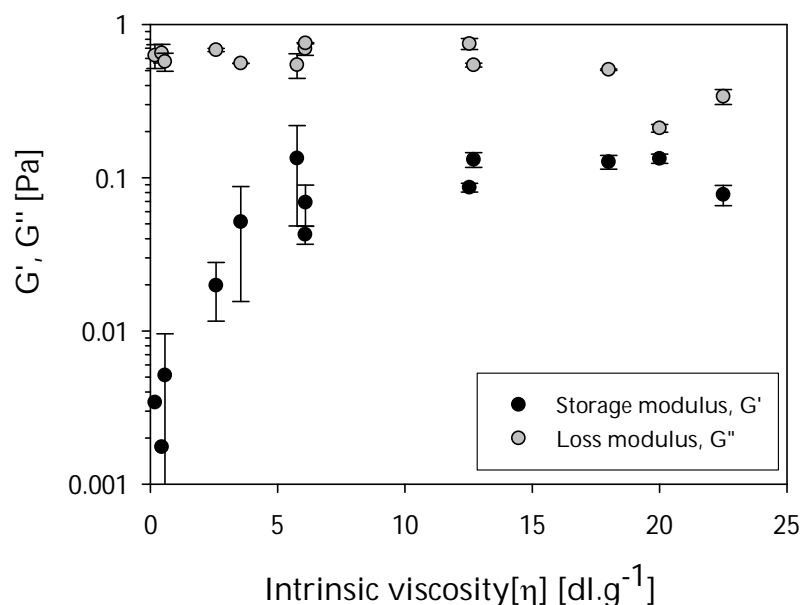


Figure 5.17: Storage modulus G' (●) and loss modulus G'' (○) of the samples matched at zero shear viscosity of 0.1 Pa.s as a function of the intrinsic viscosity of the polymer (5% strain, 10 rad.s⁻¹).

Typical frequency sweep plots obtained are presented in Figure 5.18. The slope of $\log(G'')=f(\log(\omega))$ was about 1, as expected. Whereas the theory predicts G' to be proportional to ω^2 , the slope found for most of the polymers was close to 1.2. In addition, for dextrans, pullulan (see Figure 5.18), GlyEight, and Methylcellulose, G' was essentially independent of the frequency.

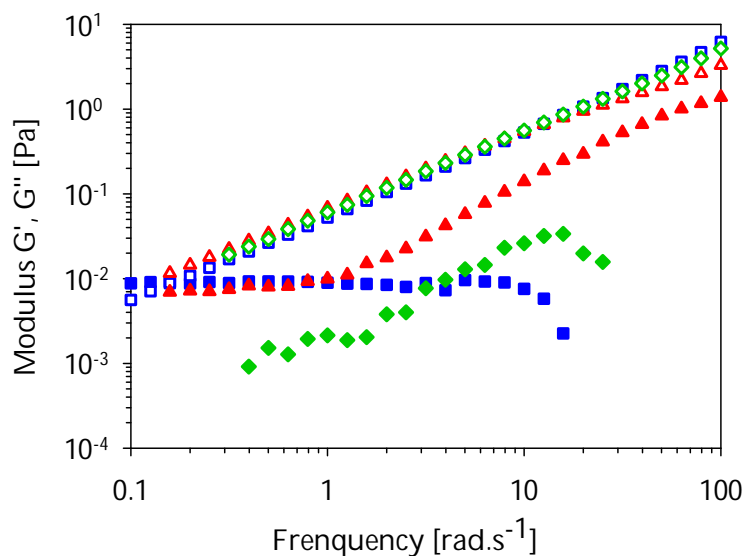


Figure 5.18: Storage modulus, G' , (full symbols) and loss modulus, G'' , (void symbols) for pullulan (■), konjac mannan PRS (▲) and Guar L (◆) matched at zero shear viscosity of 0.1 Pa.s in a frequency sweep at 5% strain.

Table 5.6: Storage and loss modulus at 5% strain and 10 rad.s⁻¹ for the different polymer solutions.

		All matched at zero shear viscosity		All polymers at 0.5%		
		G' [Pa]	G'' [Pa]	G' [Pa]	G'' [Pa]	
Galactomannans	Guar L	1.50%	0.052±0.036	0.558±0.001	0.002 ± 0.003	0.057 ± 0.005
	Guar M	0.45%	0.086±0.006	0.748±0.062	0.157 ± 0.045	1.047 ± 0.087
	Guar H	0.35%	0.127±0.013	0.507±0.005	0.979 ± 0.044	1.940 ± 0.057
	LBG	1.50%	0.052±0.036	0.558±0.001	0.002 ± 0.003	0.057 ± 0.005
Xyloglucans	3S	0.82%	0.069±0.021	0.754±0.006	0.003 ± 0.004	0.183 ± 0.002
	PXylo	0.85%	0.043±0.006	0.694±0.065	0.030 ± 0.002	0.139 ± 0.012
	GlyEight	2.11%	0.020±0.008	0.682±0.017	0.000 ± 0.000	0.049 ± 0.005
Konjac mannan	KM PA	0.13%	0.077±0.012	0.338±0.038	18.09 ± 0.275	16.450 ± 0.252
	KM PRS	0.21%	0.131±0.014	0.543±0.016	5.315 ± 0.105	7.458 ± 0.159
	KM LM		n/a		0.001 ± 0.002	0.026 ± 0.003
Dextrans	40	28.00%	0.003±0.006	0.628±0.112		n/a
	500	15.50%	0.002±0.004	0.651±0.091		n/a
	Pullulan	9.33%	0.005±0.004	0.572±0.077		n/a
	MCellulose	0.72%	0.134±0.085	0.544±0.099	n/a	0.197 ± 0.031
	Xanthan	0.08%	0.133±0.009	0.211±0.012	8.284 ± 0.226	3.284 ± 0.079

Table 5.6 gives the values for G'' and G' at 5% strain and 10 rad.s⁻¹ averaged from strain sweep and frequency sweep data. As described in the introduction of this section (5.6.3), some polymer solutions exhibited identical shear viscosity and can therefore directly be compared for elastic behaviour.

Comparison n°1: Konjac Mannan PA, PRS and guar H matched at zero shear viscosity

G' of Guar H and KM-PRS solutions were not significantly different (0.127 and 0.131 Pa, respectively), but were higher than G' of KM-PA solution (0.077 Pa).

Comparison n°2: LBG, PXylo and Gly3S matched at zero shear viscosity

G' of PXylo and Gly3S were not significantly different (0.043 and 0.069 Pa, respectively), but the G' of LBG was significantly higher (0.086 Pa).

Comparison n°3: Methylcellulose, PXylo, Gly3S, Guar H and LBG at 0.5% w/w

These three samples were characterised by a frequency-independent storage modulus, which were near the sensitivity limit of the rheometer and of the lowest measured across the sample set. Differences were found (PXylo had a higher G'), however these should be interpreted with caution.

Comparison n°4: guar L and methylcellulose matched at zero shear viscosity

G' of methylcellulose was found to be significantly higher than G' of guar L (0.134 Pa and 0.052 Pa, respectively).

Comparison n°5: guar L and GlyEight at 0.5% w/w

The storage modulus of GlyEight was very low (10^{-3} Pa) and could only be measured at low frequency. Guar L exhibited higher elastic behaviour in SAOS.

5.6.3.2 Behaviour in filament break-up

Reports on filament break-up work with polysaccharides solutions are seldom found in literature and to be confident that robust data were obtained in this research, experimental procedure and data analysis were validated using polyacrylamide solutions and literature data was successfully reproduced (Stelter and Brenn, 2000; Stelter et al., 2002). Polyacrylamide is known to mechanically degrade during filament break-up experiments, thus repeated analysis of the same loaded sample is not possible (Stelter and Brenn, 2000). In contrast, it was found here that the polysaccharide solutions did not show mechanical degradation. Thus, several tests could be performed on the same loaded sample. In addition, the dynamics of the filament diameter with time did not indicate that bead-on-string phenomena occurred (Rodd et al., 2005b), though this should be confirmed in further experimental work by visualising the break-up with a high speed camera.

5.6.3.2.1 Comparison of polysaccharides of different molecular structure

The decay of the normalised filament diameter ($d(t)/d_0$) is illustrated in Figure 5.19 and the values of break-up time, relaxation time, λ , and steady state apparent extensional viscosity, η_E , (short referred to as extensional viscosity in the following) obtained from the filament break-up experiments are displayed in Table 5.7. As hypothesised, a clear concentration effect is visible: for a given polymer, break-up time, relaxation time and extensional viscosity increased with increasing concentration. Very large differences exist between the different polysaccharides. The break-up time ranged between 12.1 ms and 67.1 ms for the samples matched at zero shear viscosity and between 1.8 ms and 359 ms for all samples at 0.5% w/w polymer concentration. The solutions exhibiting very short break-up time (<20 ms) are samples of very low viscosity as well as elasticity and data for these samples must be interpreted with caution as they are known to be difficult to characterise with the filament break-up device (see Chapter 1, 1.4.3., (Rodd et al., 2005b)) . A quicker stretch or a smaller final gap between the plates may have led to better data for these samples, however, it was preferred to apply the same protocol across all samples.

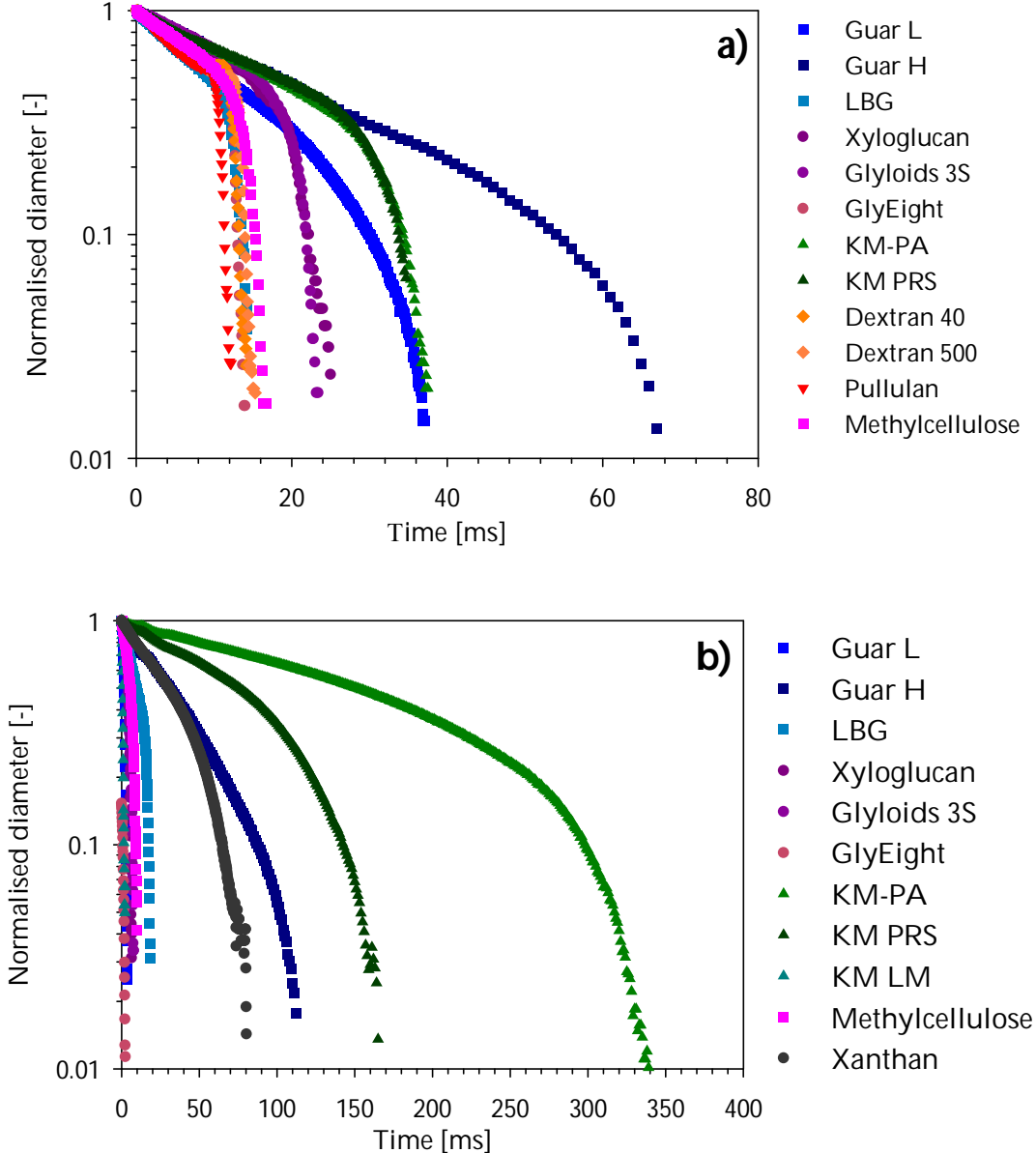


Figure 5.19: Decay of the fluids filament mid-point diameter for a) polysaccharide solutions matched at zero shear and b) polymer solutions at 0.5% w/w.

Table 5.7: Break-up time [ms], relaxation time λ [ms] and extensional viscosity η_e [mPa.s] obtained from the filament break-up experiments.

		All matched at zero shear viscosity				All polymers at 0.5% w/w			
		c/c*	break up time	λ	η_e	c/c*	break up time	λ	η_e
<i>Galactomannans</i>	Guar L	2.4	30.9 ± 2.8	5.3	2.9	0.8	3.4 ± 0.4	0.8	0.2
	Guar H	2.3	67.1 ± 2.5	8.7	7.4	3.3	109.7 ± 5.0	13.4	10.7
	LBG	2.3	15.5 ± 1.2	4.6	0.5	2.5	19.8 ± 1.5	4.5	0.7
<i>Xyloglucans</i>	3S	1.7	23.4 ± 2.1	6.8	0.78	1.1	9.7 ± 0.9	3.1	0.6
	Pxylo	1.7	24.6 ± 3.4	6.7	1.1	1.0	7.4 ± 1.4	3.0	0.2
	GlyEight	2.1	12.4 ± 1.4	5.8	0.2	0.5	2.5 ± 0.3	0.5	0.2
<i>Konjac mannan</i>	KM PA	1.7	36.4 ± 3.1	8.4	2.2	6.5	359.1 ± 48.2	62.2	9.1
	KM PRS	1.3	32.2 ± 3.2	10.1	2.0	3.2	175.4 ± 22.8	34.2	6.3
	KM LM		n/a			n/a	1.8 ± 0.4	0.2	n/a
<i>Dextrans mannan</i>	40	2.0	14.6 ± 1.3	5.7	0.2			n/a	
	500	2.4	13.9 ± 1.0	5.1	0.3			n/a	
	Pullulan	2.6	12.1 ± 0.6	4.8	0.272			n/a	
	MCellulose	2.9	15.8 ± 2.5	5.5	0.484	2.0	11.1 ± 2.2	3.0	0.589
	Xanthan		n/a			17.2	72.9 ± 4.1	14.4	10.806

It was found that dilute samples ($c < c^*$) showed short break-up times and behaviour characteristic for inelastic samples (linear decrease of the diameter with time. Such samples were 0.5% w/w GlyEight, 0.5% w/w guar L, 0.5% w/w PXYlo and 0.5% w/w Gly3S. Samples at polymer concentration above c^* showed either inelastic or elastic behaviour. Inelastic behaviour was observed for dextran 500, dextran 40, pullulan and GlyEight matched at zero shear viscosity of 0.1 Pa.s. Indeed, the normalised diameter shows an almost linear behaviour as a function of time which is characteristic for Newtonian (thus inelastic) solutions. These polymers are very compact ($[\eta] < 2.6 \text{ dl.g}^{-1}$, Table 5.4) and were shown to also exhibit largely Newtonian-like behaviour in large shear deformation (5.6.2) and small angle oscillatory shear (5.6.3.1) despite the

concentration being about $2c^*$. In addition, the concentration-dependence of the zero-shear viscosity were characterised by the excellent fit of the Martin Equation (Equation 5.3, 5.6.1.2). The other polysaccharides, of intrinsic viscosity values higher than 3.6 dl.g^{-1} behaved elastically. In the introduction of this section (5.6.3), five subgroups of polymer solutions of identical shear behaviour were described in order to directly compare their elastic behaviour.

Comparison n°1: Konjac Mannan PA, PRS and guar H matched at zero shear viscosity

The relaxation time of the three solutions was similar (8.7 ms, 8.4 ms and 10.1 ms, respectively for of guar gum H, konjac mannan PA and PRS), hence the superposition of the curves in Figure 5.19a) until about 30 ms. The exponential decay, therefore the relaxation process, was identical for the three solutions. The Newtonian-like steady state, however, was reached earlier for konjac mannan solutions (about 25 ms) than for guar H solution (about 40 ms) and the extensional viscosity was several folds higher for guar H. The break-up of guar H thus occurred almost 30 ms later than the konjac mannan solution and indicates the higher elasticity of guar H.

Comparison n°2: LBG, PXylo and Gly3S matched at zero shear viscosity

The break-up of the LBG solution matched at zero shear was quicker than for PXylo and Gly3S solutions. This is surprising since LBG solutions are at about $2c^*$ and LBG is fairly extended in solution (699 kDa, $[\eta]=12.5 \text{ dl.g}^{-1}$, Table 5.4). Aggregation of LBG in

solution has been reported (Picout et al., 2002), resulting in a drop in viscosity. Such aggregation may have occurred in the solutions used for filament break-up.

Comparison n°3: Methylcellulose, PXYlo, Gly3S, Guar H and LBG at 0.5% w/w

The break-up time of methylcellulose (11.1 ms) was slightly longer than PXYlo and Gly3S (7.4 ms and 9.7 ms, respectively), however this should be interpreted with caution as the solutions are only weakly elastic.

Comparison n°4: guar L and methylcellulose matched at zero shear viscosity

The relaxation time of guar L (5.3 ms) was close to that of methylcellulose 0.72% (5.5 ms) and the filaments of the two solutions decayed exponentially identically until approximately 15 ms. As previously observed for guar H in comparison n°1, the Newtonian-like steady state is reached later by guar L 1.5% (25 ms vs. 15 ms for methylcellulose), which also exhibits higher extensional viscosity (2.88 Pa.s vs. 0.48 Pa.s for methylcellulose). The comparisons n°1 and 3 demonstrate that guar gum molecules seem to take longer to uncoil and stretch and the extensional viscosity seems to be higher than for the other polysaccharides studied in this research. However, the other galactomannan, LBG, did not exhibit similar behaviour as guar gum and breaks-up extremely quickly (< 20 ms) and further experimental work would be required to investigate the effect of the degree of galactose substitution on behaviour in filament break-up.

Comparison n°5: guar L and GlyEight at 0.5%

No statement can be made about the fifth group as the polymer solutions were not suited for filament break-up analysis (extremely quick break-up).

5.6.3.2.2 *Overall behaviour of polysaccharide solution behaviour in filament break-up*

To further analyse the behaviour of polymer solutions in filament break-up, the relationship between the relaxation time and the dimensionless polymer concentration c/c^* has been plotted in Figure 5.20. The data obtained for the different polysaccharide solutions fall onto a single curve despite the range of concentration (0.13-28%) and the variety of polymer structures. The curve exhibits the well-known universal power law scaling behaviour (Bazilevskii et al., 1997; Stelter and Brenn, 2000; Duxenneuner et al., 2008) with an exponent of 1.63. The value of the exponent is slightly higher than previously reported for hydrophobically modified guar exhibiting a more rigid structure (1.5 (Duxenneuner et al., 2008)) but lower than predicted by the theory for random coil polymers ($7/3$, (Liu et al., 2009)). The value of the exponent suggests that the interactions between semi-flexible polysaccharides chains are weak and possibly only based on hydrogen-hydrogen bonding rather than real physical entanglements. Such type of interaction has previously been described for galactomannans and was termed 'hyperentanglements' (Goycoolea et al. (1995), Cheng et al. (2002) and Doyle et al. (2008)). The present research demonstrates more universal occurrence of

hyperentanglements in solutions of semi-flexible polysaccharides, possibly existing for all 1→4 diequatorially linked polysaccharides. The xanthan gum molecule, despite having the same linkage, behaves as a rigid rod and therefore does not follow the same power law.

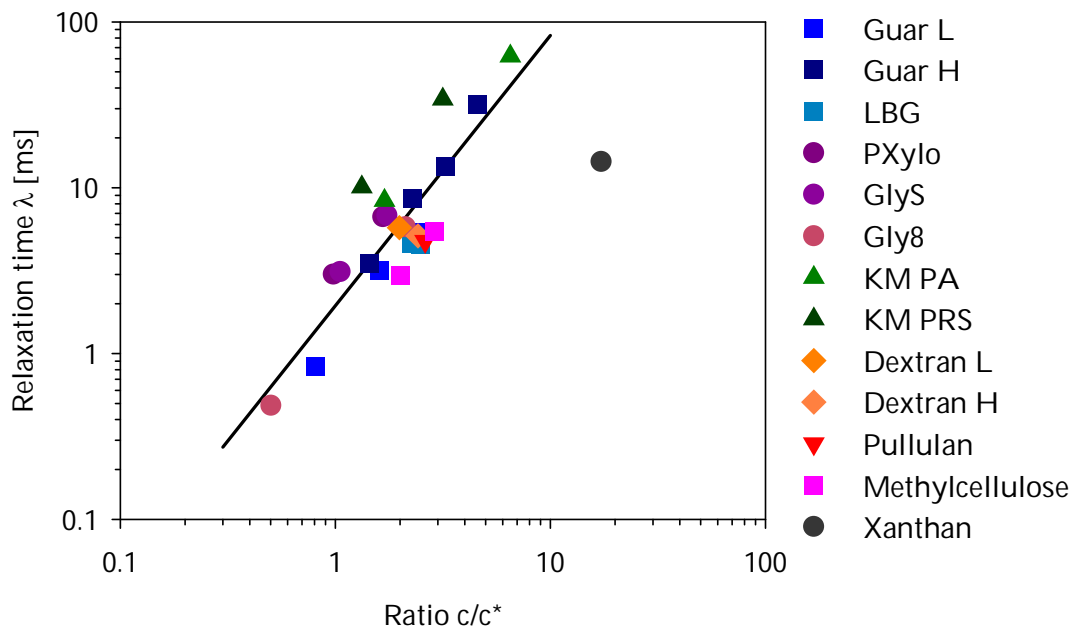


Figure 5.20: Relaxation time determined by filament break-up experiment as a function of the ratio c/c^* . The log-linear regression (xanthan gum excluded) is indicated by a black line ($R^2=0.74$).

The dependence of the extensional viscosity on the relaxation time is depicted in Figure 5.21. In contrary to what might have been expected, data for the semi-flexible polysaccharides did not lie in between the regressions for flexible polymers and rigid polymers reported by Stelter et al. (2002) but at a lower level overall. This may be related to the low elasticity of carbohydrate polymer solutions. Thus, it appears that

literature knowledge on filament break-up behaviour of polymer solutions gained on work with synthetic polymers is not transferable to polysaccharide solutions due to differences in molecular extensibility. Figure 5.20 shows nicely what has been discussed before (5.6.3.2.1) that guar gum has the highest observed extensional viscosity while exhibiting similar relaxation times to the other polysaccharide solutions.

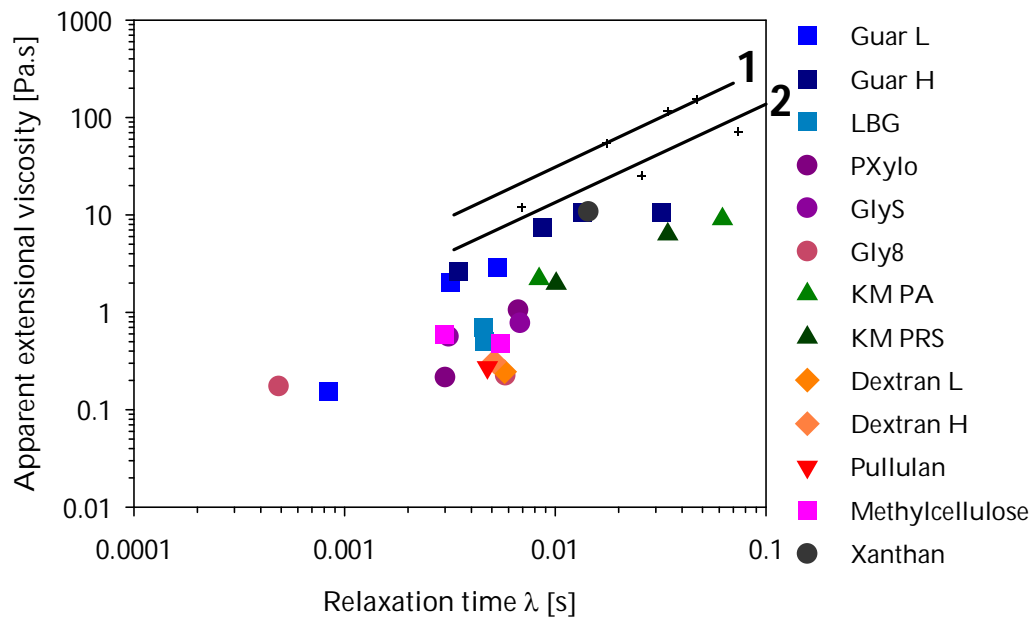


Figure 5.21: Extensional viscosity as a function of the relaxation time for different polysaccharide solutions. The black lines indicate the regression obtained by Stelter et al. (2002): line 1 corresponds to flexible behaviour and line 2 to rigid-like behaviour. The black cross are experimental data points verifying the results of Stelter et al. (2002).

5.6.3.3 Behaviour in micro-contraction flow

5.6.3.3.1 Comparison of polysaccharides of different molecular structure

Micro-contraction flow experiment was applied in addition to filament break-up to probe elastic behaviour since low viscosity / low elastic fluids are not applicable to filament break-up analysis. Initially, a range of solutions of the different guar gums used in this project were analysed to gain some understanding of polysaccharide solution behaviour in microfluidics contraction flow. The results were introduced above (5.4.2) and are not detailed here (Koliandris et al., manuscript in preparation). The polysaccharide solutions discussed in this thesis chapter exhibited overall similar behaviour to guar gum, which is why the focus in the following is on the differences in elastic behaviour between polysaccharides rather on the differences between polysaccharides and synthetic polymers.

Initially, streak images of the different polysaccharide solutions will be discussed. Figure 5.21 shows the recirculation patterns upstream of the contraction for 0.5% w/w polymer solutions and in Figure 5.23 images are presented for polymer solutions matched at zero shear viscosity of 0.1 Pa.s. The flow rate of the experiments was 4 ml.hr⁻¹ corresponding to an approximate shear rate of 18,000 s⁻¹ in the contraction. Despite the shear thinning nature of the solutions, as a result of which the shear viscosity, denoted for this condition $\eta_{Q=4}$, differed across the samples, solution behaviour at 4 ml.hr⁻¹ was characteristic for the whole flow rate range investigated.

Pressure drop values as function of the Reynolds number are reported in Figure 5.24. Solution behaviour can be grouped into inelastic, weakly elastic and most elastic amongst the samples investigated. In the following, the inelastic case and most elastic case will be discussed separately followed by a comparison between all samples grouped as introduced in 5.6.3 (5 groups). Finally, the specific behaviour of xanthan gum solutions is described in a separate paragraph as its rigid rod conformation and iconicity are unique in sample set.

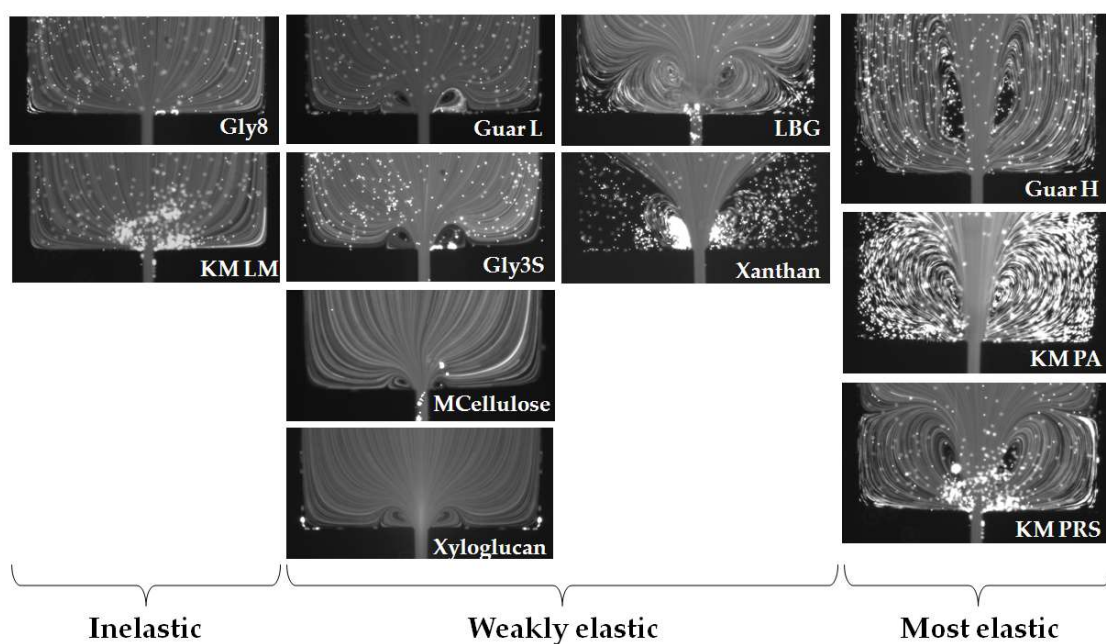


Figure 5.22: Flow pattern streak images at $4\text{ml}\cdot\text{hr}^{-1}$. All samples at 0.5% w/w.

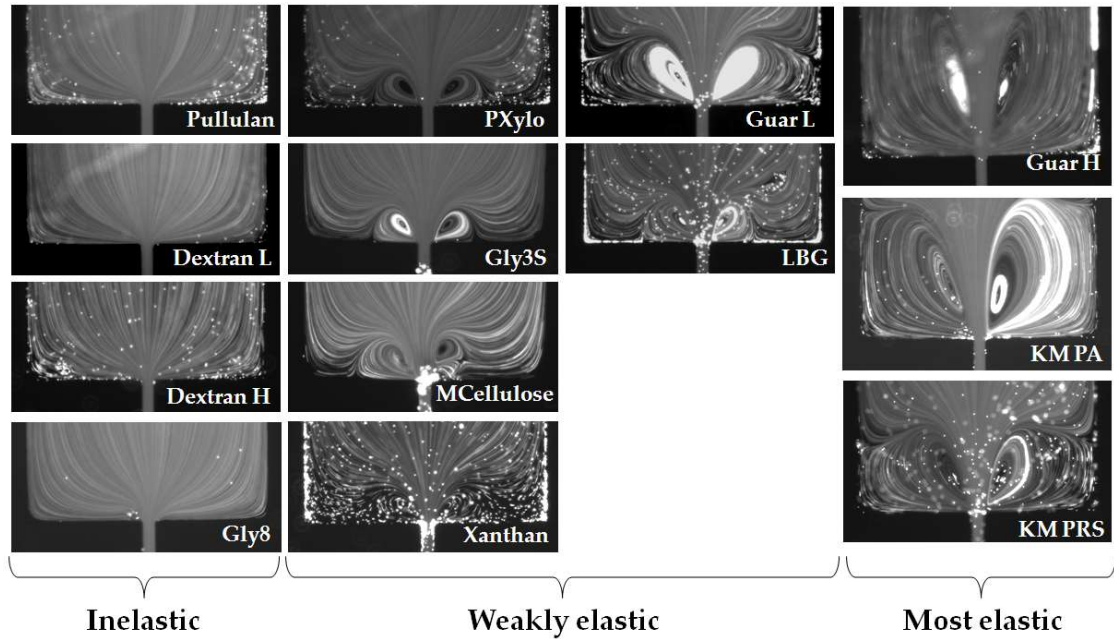


Figure 5.23: Flow pattern streak images at $4\text{ ml}\cdot\text{hr}^{-1}$. All samples matched at zero shear viscosity.

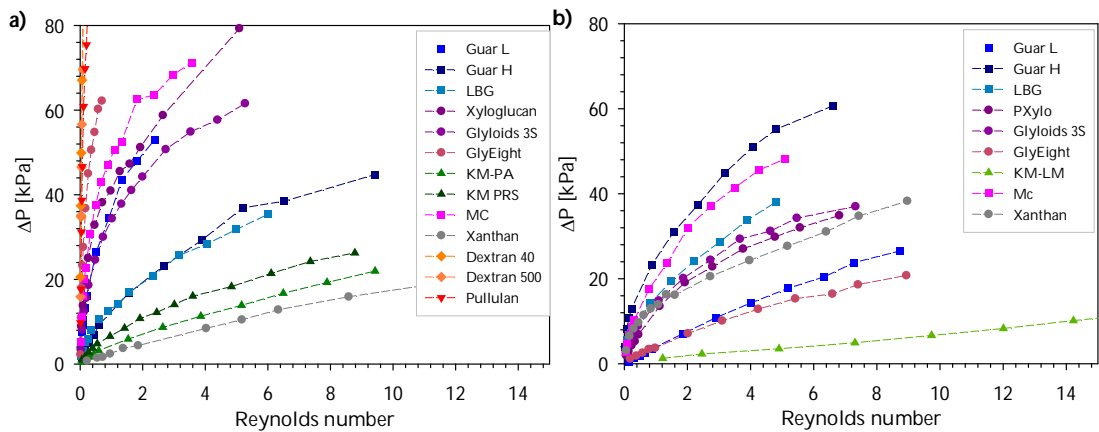


Figure 5.24: Dimensional pressure drop as a function of Reynolds number for polysaccharide solutions a) matched at zero shear viscosity of $0.1\text{ Pa}\cdot\text{s}$. b) at 0.5% w/w. NB: data for KM PA and KM PRS at 0.5% not available.

Inelastic samples

The flow patterns of GlyEight (0.5% w/w) and KM LM (0.5% w/w) (Figure 5.22) as well as the flow patterns of Pullulan, Dextran L and H and GlyEight matched at zero shear viscosity of 0.1 Pa.s (Figure 5.23) did not exhibit any characteristics of non-Newtonian behaviour. Pressure drop data lead to the same conclusion. Indeed, the pressure drop developed by the solutions of constant shear viscosity (KM LM 0.5%, dextran 500 and dextran 40 matched at zero shear viscosity, see Figure 5.14 and Figure 5.15) was identical to the pressure drop developed by a Newtonian fluid, increasing linearly with flow rate ($R^2=0.99, 0.96$ and 0.98 , respectively). For GlyEight and pullulan solutions matched at zero shear viscosity of 0.1 Pa.s, the pressure drop functions are curved which is a result of the slight shear-thinning nature of these solutions (Figure 5.15). The micro-contraction flows therefore enable to conclude unequivocally to the absence of elasticity for dextrans, pullulans and GlyEight samples in the conditions of the experiment, whereas such conclusion could only be hypothesised from filament break-up and SAOS results. As reported in 5.6.3.2.1, these polymers are very compact, either because they are highly branched and/or very flexible and it seems they do not to align, rotate or stretch with either shear or extension flows, hence a Newtonian-like behaviour even for solutions of $c > c^*$.

Most elastic samples

In both sample sets (at 0.5% w/w and matched at zero shear viscosity of 0.1 Pa.s), guar H, konjac mannan PA and konjac mannan PRS solutions exhibited the biggest vortices. These solutions exhibited *low* values of $\eta_{\Omega=4}$ in the design matched at zero shear viscosity but *high* values of $\eta_{\Omega=4}$ across the samples prepared at 0.5% w/w. Thus, the observations in terms of vortices are not due to shear viscosity. It can be hypothesised that the high molecular weight of these polysaccharides, which controls the density of molecule interactions, is the origin of the elastic behaviour observed. These samples, solutions of guar H, konjac mannan PA and konjac mannan PRS, were also the most shear-thinning (Figure 5.15), those of the highest intrinsic viscosity (Table 5.4), those of higher storage modulus (Table 5.6) and those exhibiting the highest relaxation times and extensional viscosity in filament break-up (Table 5.7) across all samples investigated here. However, it was difficult to identify the elastic behaviour from the pressure drop data (Figure 5.24) as the elastic component of the pressure drop was largely hidden by the Newtonian component, decreasing with flow rate because of the shear-thinning behaviour (see 5.4.2.2 and Figure 5.11 for further explanation). In order to be able to separate out the elastic component, it would be necessary to numerically calculate the Newtonian component for each flow rate, which was outside the scope of this PhD research.

Comparison n°1: Konjac Mannan PA, PRS and guar H matched at zero shear

As discussed above, these samples were among the most elastic. Whereas they exhibited identical flow curves (Figure 5.15), guar H exhibited bigger vortex recirculation (Figure 5.23) and larger pressure drop (Figure 5.24) compared to the other two samples. Therefore, micro-contraction flow, in agreement with filament break-up data (5.6.3.2.1) indicated a higher elasticity of guar gum H sample. According to light scattering data, konjac mannan molecules are stiffer than guar gum (Table 5.2). A possible explanation is that konjac mannan molecules are too rigid to develop high elasticity based on polymer chain uncoiling/stretching (as fully flexible polymers such as PEO, or guar to a lesser extent), but not rigid enough to develop elasticity like rigid-rod like solutions.

Comparison n°2: LBG, PXYlo and Gly3S matched at zero shear

Despite the large differences in molecular weight and intrinsic viscosity (Table 5.4), the behaviour of LBG, PXYlo and Gly3S in micro-contraction flow was similar (vortex patterns and pressure drop) as was previously found for large deformation shear flow and filament break-up. These results indicate that a given flow behaviour can be obtained with polymers of different molecular weight and different polymer conformation in solution. Based on comparisons n°1 and n°2, an identical shear flow behaviour *may or may not* be associated with a different behaviour in extensional flow.

This reinforces the necessity of characterisation for polysaccharides solutions in extension.

Comparison n°3: Methylcellulose, PXYlo, Gly3S, Guar H and LBG at 0.5%

The polymers in this group showed differences in pressure drop and recirculation patterns (Figure 5.23 and Figure 5.24) whereas their shear viscosity behaviour was comparable. Guar H solution developed the highest pressure drop and the biggest vortex, once again suggesting the comparatively high elasticity of guar H solutions. Methylcellulose also developed a relatively high pressure drop, but did not develop large vortex recirculations. This may be due to the fairly rigid conformation of methylcellulose (Table 5.2 in 5.3.2), leading to a behaviour in micro-contraction flow similar to xanthan gum. As will be even more clear in the discussion of the xanthan gum data, solutions of rigid rod or stiff molecules only develop small vortices, independent of flow rate (whereas it is flow rate dependent for other molecular behaviour). Finally, the xyloglucans PXYlo and Gly3S as well as LBG exhibited similar pressure drop, lower than guar H or methylcellulose, which is indicative of lower elasticity. The vortex growth of LBG was slightly more pronounced than the vortex growth of PXYlo or Gly3S solutions, which may be related to the stiffer conformation of the xyloglucans as indicated by persistence length data (Table 5.2). Methylcellulose, PXYlo and Gly3S at 0.5% had a relatively low shear viscosity (~30 mPa.s). SAOS and

filament break-up data were therefore associated to a large experimental errors whereas microfluidics data were much more reliable to establish the comparison.

Comparison n°4: guar L and methylcellulose matched at zero shear viscosity of 0.1 Pa.s

Methylcellulose developed a higher pressure drop (Figure 5.24) which can be associated with a higher elastic component as the shear viscosity behaviour of both samples was identical (Figure 5.15) and this is in agreement with the higher storage modulus found for methylcellulose (Table 5.6). Guar L, however, exhibited larger vortices than methylcellulose and, in filament break-up, a longer exponential decay and a higher extensional viscosity. Molecular weight and intrinsic viscosity data confirm the rigidity of methylcellulose molecules (Table 5.4). The comparative viscoelastic behaviour of guar L and methylcellulose therefore demonstrates that elasticity can arise from either a rather flexible conformation (like guar L) or a rather rigid conformation (like methylcellulose). The elasticity of methylcellulose arises from rotation with flow and alignment of molecules whereas the more flexible guar L will be uncoiled and stretched in extensional flows, exhibiting a higher steady state extensional viscosity.

Comparison n°5: guar L and GlyEight at 0.5%

In micro-contraction flow device, guar L exhibited elastic behaviour whereas GlyEight did not: Guar L developed a higher pressure drop and significant vortex growth

whereas the flow appeared to be Newtonian-like for GlyEight over the range of flow rate under investigation. Guar L 0.5% and GlyEight 0.5% are both dilute solutions ($c < c^*$) with very low shear viscosity (~ 7 mPa.s) for which it was impossible to establish elastic behaviour in SAOS or filament break-up. This comparison therefore illustrates the interest of microfluidics to investigate viscoelastic behaviour, displayed by some polymers even in dilute solutions. Both molecules have similar molecular weight (~ 350 kDa), but GlyEight is more branched and stiffer (not a rigid rod), which may explain the absence of elastic behaviour. This also confirms that guar gum molecules of both small and large molecular weight are more elastic than the other polysaccharides investigated here.

A rigid rod molecule, xanthan gum

Xanthan gum exhibited vortex recirculation from low flow rates. In contrast to other polymers, the fluid appeared to be stagnant in the corners as exposed fluorescent particles are visible as dots and not as streamlines (Figure 5.22). This is very likely related to the yield stress behaviour of the solution. In addition, the dimensionless vortex length was much less dependent on the flow rate than observed for other polymers, which had been attributed to the rigid-rod conformation of xanthan gum (Zirnsak and Boger, 1998; Mongruel and Cloitre, 2003).

5.6.3.3.2 Overall behaviour of polysaccharide solution behaviour in filament break-up

In the microfluidics literature, it is common to plot the dimensionless vortex length and the pressure drop as a function of the Weissenberg number as this scales the solutions behaviour with relaxation time, hence with concentration (see relationship between λ and ratio c/c^* in Figure 5.20).

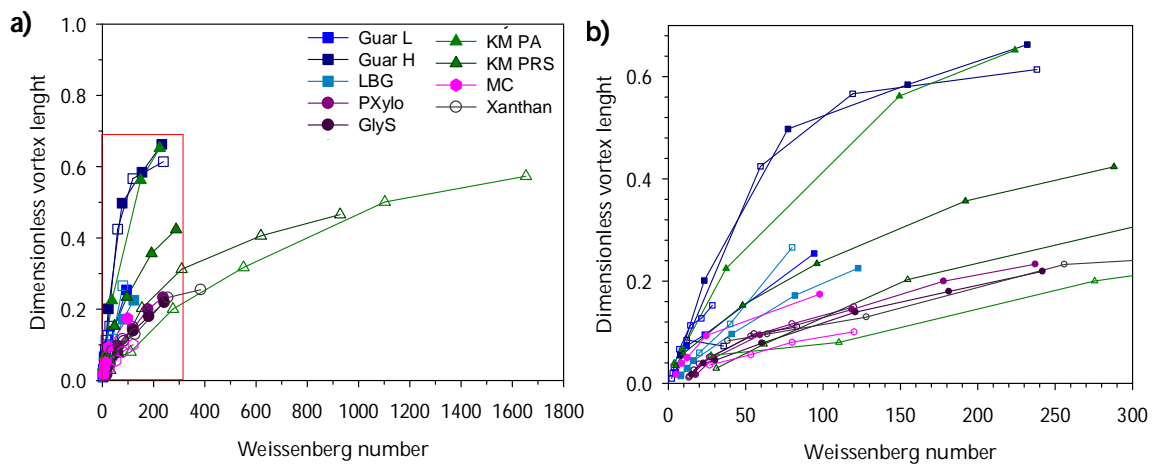


Figure 5.25: Dimensionless vortex length as a function of Weissenberg number for flow through a 16:1 planar contraction for polysaccharide solutions matched in zero shear viscosity (filled symbol) and at 0.5% (void symbols). a) all data, b) at low Weissenberg number.

Figure 5.24 shows the dimensionless vortex length as a function of the Weissenberg number. Data for guar H at two concentrations fall onto a single curve as observed before (Koliandris et al., manuscript in preparation). Data for PXYlo and Gly3S at different concentration also fall onto a single curve, but not the same as guar gum H. For guar L, LBG, MC and Xanthan gum, data at different concentrations do not superpose perfectly, which is likely to be due to the high uncertainty in determining the relaxation time from filament break-up (very short break-up times, see 5.6.3.2.1).

Data for different polymers do not superimpose, which indicates that the dimensionless vortex length is also affected by a parameter independent of concentration, for example, molecular extensibility or molecular flexibility, as discussed about for the extensional viscosity data (Figure 5.21). This demonstrates the variability in elastic behaviour among polysaccharide solutions of comparable shear viscosity behaviour. This important conclusion is also evident from the plot of the pressure drop versus the Weissenberg number, see Figure 5.26. Data for the same polysaccharide albeit at different concentrations overall superimpose. However, data are separated by variation in molecular characteristics including ‘simply’ molecular weight.

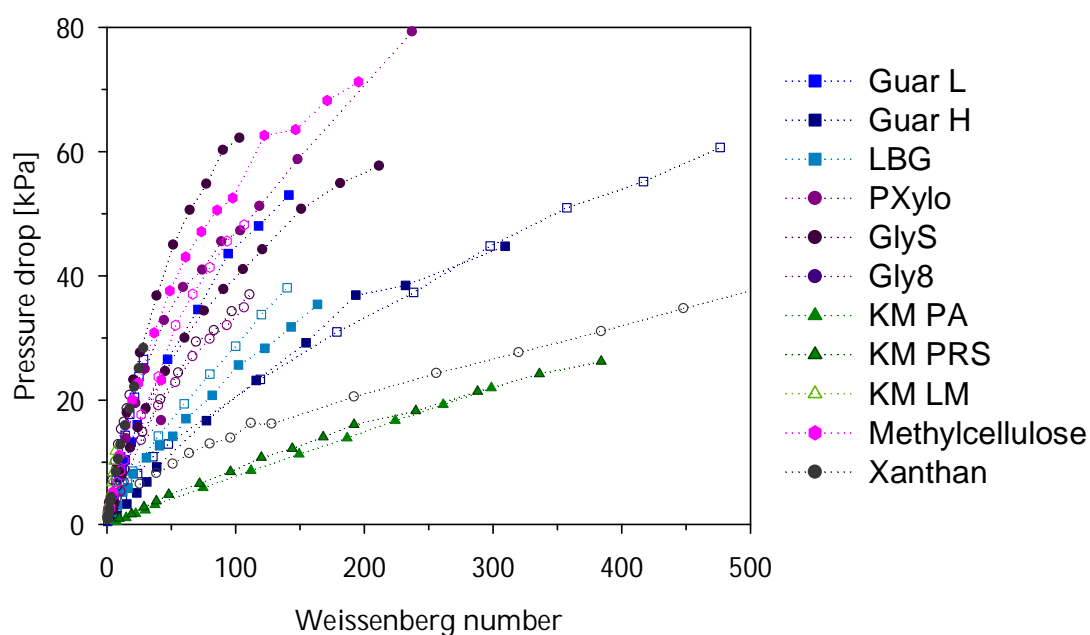


Figure 5.26: Dimensional pressure drop (kPa) as a function of Weissenberg number for polysaccharide solutions matched in zero shear viscosity (filled symbol) and at 0.5% (void symbols). NB: data for KM PA and KM PRS at 0.5% not available.

5.7 CONCLUSIONS

The objective of the work reported in this Chapter was to study the viscoelastic behaviour of polysaccharide solutions, in shear and extension, and to relate it to the molecular structure and molecular flexibility. Data from small angle oscillatory shear, filament break-up and micro-contraction flow delivered congruent results but micro-contraction flow experiments were more sensitive and were better able to highlight the elastic behaviour of low shear viscosity solutions.

Based on the current evidence, a model is suggested to summarise the effect of molecular structure on viscoelasticity. Three main factors have been identified:

1) Type of backbone linkage: the three polymers with α -1 \rightarrow 6 and α -1 \rightarrow 4 backbone linkage did not exhibit elastic behaviour in extensional flow and behaviour in shear flow was mainly Newtonian. Polymers with α linkages are much more compact polymers than polymers linked in β as the molecules are more flexible. The highly compact structure is less easily deformed in flow, hence the apparent inelasticity. The six other polymers studied here all had a β -1 \rightarrow 4 linkage. Since large differences in viscoelastic behaviour were observed among them, other factors were included in the model.

2) Molecular weight: solutions of high molecular weight polymer are more elastic. Irrespectively of the concentration, solutions of guar H and konjac mannans PA and PRS were the most elastic ($M_w > 1.10^6$ Da). Xanthan gum was of very high

molecular weight (8.10^6 Da), yet the elastic behaviour of xanthan gum solutions was directly affected by the chain rigidity of the molecule.

3) Chain rigidity: in addition to the type of backbone linkage, chain rigidity can arise from the frequency and length of side chain, the type of sugar and the presence of a net charge or hydrophobic residues. Xanthan gum and methylcellulose were the most rigid molecules included in this research and their elastic behaviour clearly differed from the elastic behaviour of more flexible polymers such as guar gum (high storage modulus, small vortices). According to light scattering data from literature (see Table 5.2), xyloglucans and konjac mannans are more rigid than guar gum but far less rigid than xanthan gum molecules, and these (xyloglucans and konjac mannans) were here found to be less elastic than both the more rigid and the more flexible molecules. It can be hypothesised that solutions of semi-rigid polymer do not develop high elasticity as molecules are not rigid enough to rotate but too rigid to uncoil and stretch in flow direction.

Further experiments are required to validate the model. In particular, a study of different galactomannans could reveal if the degree of mannose substitution and/or the blockiness of galactose can explain the fact that LBG solutions are far less elastic as guar gum solution despite the similarity in structure.

Filament break-up and microfluidics data also highlighted the specificities of polysaccharide solutions compared to solutions of synthetic polymers. Extensional viscosity was shown to scale linearly with the relaxation time and all polysaccharides data superimposed. However, they did not superimpose with literature data for fully

flexible or rigid-rod synthetic polymers. In addition, the relaxation time of all polymers showed a weak power-law dependence with the ratio c/c^* , indicating that chain-chain interactions in the semi-dilute regime were rather weak, and they were very likely based on hydrodynamic interactions or hydrogen bondings rather than real physical entanglements. This illustrates the necessity to characterise polysaccharides flow in extension.

In addition to the fundamental interest, this research is preliminary work to understand the effect of elasticity on taste and mouthfeel perception, as no definitive conclusions could be drawn from the sensory study based on Boger fluids as reported in Chapter 4. It was demonstrated here that, by characterising solution elasticity of polysaccharides, high and low elasticity polysaccharides can be identified. For instance, guar H and konjac mannan, or guar L and methylcellulose, or guar L and GlyEight have identical shear flow behaviour but different behaviour in extensional flows and sensory studies could be carried out to investigate whether solution elasticity has an impact on taste and mouthfeel perception.

CHAPTER 6

EMULSION INTERFACE STABILISATION BY CHEMICAL CROSS-LINKING OF ADSORBED PROTEIN

6.1 INTRODUCTION

Up until this point, the current study concerned one phase aqueous systems. However, few food products are one phase aqueous systems and most of them are emulsions, that is to say, a dispersion of small spherical droplets of one liquid in another liquid, both being immiscible (Murphy and Howell, 1991; Frieberg, Larsson and Sjöblom, 2004). The work described in Chapters 3 to 5 can be applied to the water-continuous phase of oil-in-water emulsions, such as soups and sauces. The focus of this chapter is the oil-water interface itself. As mentioned in Chapter 1 (Introduction), the global project this PhD research was embedded in aims at designing complex microstructures such as duplex emulsions to reduce salt content in foods. It is believed that only the salt contained in the outer water phase of the duplex emulsions will be perceived, hence a careful design of the properties of duplex emulsions may enable a controlled salt delivery. Stability is a major issue for duplex emulsions and chemical cross-linking of adsorbed Bovine Serum Albumin (BSA) was studied here as a possible approach to stabilise duplex emulsions. The research was initially carried out on single oil-in-water emulsions and subsequently applied to the duplex emulsions of the type (water-in-oil)-in-water.

6.1.1 BOVINE SERUM ALBUMIN AS EMULSIFIER

Bovine serum albumin (BSA) is the most abundant protein in plasma (5 g for 100 ml) and therefore readily available as a by-product from animal slaughter. It is composed of a single polypeptide chain of 67 kDa (about 583 amino acid residues and no carbohydrates). The secondary structure contains 17 intrachain disulfide bridges and 1 sulfhydryl group (at pH 5-7), organising the chain predominantly in α -helices (65 to 70%) with a minority of β -sheets (8-10%) (Murphy and Howell, 1991; Jorgensen et al., 2004).

Proteins have been extensively used to stabilise emulsions as they are natural, non-toxic, cheap and widely available (Wilde et al., 2004). The mechanism of emulsion stabilisation is similar for all proteins. They adsorb at the oil-water interface, thereby lower the surface tension which allows the dispersion of the oil phase into small droplets (Frieberg et al., 2004). The adsorbed proteins form a protective membrane around the oil droplets, imparting strong viscoelastic properties to the interfacial film. The properties of the adsorbed layer determine the colloidal interaction between droplets which itself governs the rheology and long term stability of the emulsions (Dickinson, 1999).

The efficiency of proteins to stabilise an emulsion strongly depends on their secondary structures. Heat denaturation for example has been shown to affect coalescence stability (Das and Kinsella, 1990). The structure of the proteins is affected by the electrical charge carried by the amino acid residues, itself a function of the pH. The isoelectric point of a protein (IEP) is defined as the pH at which the protein is overall neutrally charged, about pH 4.7 for BSA. Around the IEP, the intramolecular and intermolecular electrostatic repulsions are weak, leading to a fairly compact structure and dense packing of the molecules adsorbed at the oil-water interface (Das and Chattoraj, 1980). At pH below the IEP, the proteins are positively charged and at pH above the IEP, negatively charged. The charges carried by the different amino acids residues induce intramolecular repulsion leading to a more expanded and less globular molecule. The ionic strength of the solvent also affects the structure of the proteins and therefore their emulsifying properties.

The emulsifying properties of proteins originate from their amphipathic character, imparting the ability to adsorb at the oil-water interface. Residues such as Alanine and Leucine are apolar, shielded in the core of the protein when dissolved in water. However, during emulsification, the proteins undergo conformational rearrangements to expose the hydrophobic residues at the oil interface. The secondary structure of BSA has been reported to change by 12% after emulsification (Jorgensen et al., 2004).

Besides the unfolding and rearrangement of the individual molecules, it is believed that intermolecular interactions slowly occur between neighbouring molecules, such as disulfide bond formation (Dickinson, Rolfe and Dalgleish, 1990; Kim, Decker and McClements, 2002). The dynamics of the protein adsorption layer has been reviewed by Yampolskaya and Platikanov (2006).

Charge and protein conformation are two attributes determinant of protein emulsification properties. They can be modified through chemical modification (Kinsella and Whitehead, 1988) or cross-linking to modify protein functionality as detailed below.

6.1.2 CROSS-LINKING OF PROTEINS

6.1.2.1 Cross-linking methods

The formation of inter- and intramolecular associations has been studied as a possibility to improve emulsion stability. Heat denaturation can lead to formation of intermolecular β -sheet structures (Wetzel et al., 1980; Monahan, McClements and German, 1996; Cai and Arntfield, 1997). Enzymatic cross-linking has also been investigated to generate a protein network (Arai and Watanabe, 1988; Faergemand, Murray and Dickinson, 1997; Faergemand and Murray, 1998; Faergemand, Otte and

Qvist, 1998b; Faergemand, Otte and Qvist, 1998a; Faergemand et al., 1999). Enzymes are very specific and the reaction generally occurs between two given amino acids. For example, the enzyme transglutaminase catalyses the transfer reaction between glutamine and lysine residues, inter- or intramolecularly. Apart from enzymes, chemical products can be used to cross-link proteins. Kato et al. (1986) studied the effect of intramolecular cross-linking using iodine or diphenyl sulfone reagent on foaming and emulsifying properties of proteins. Another major type of cross-linking is the carbodiimide-mediated condensation, first described more than 50 years ago (Sheehan and Hess, 1955). It is widely used in biochemistry and polymer sciences but has not yet been applied to protein-stabilised emulsions and this is the object of the present research.

6.1.2.2 Cross-linking with EDC (Carbodiimide-mediated condensation)

EDC (1-(3-Dimethylaminopropyl)-3-ethylcarbodiimide hydrochloride) is a water-soluble cross-linker used to couple carboxyl groups to amines. The cross-linking reaction is depicted in Figure 6.1. EDC does not introduce an atom into the cross-linked molecules, hence the denomination of 'zero-length cross-linker'. The optimal pH for the reaction has been described to be between pH 4.7 and pH 6 (Wong, 1993).

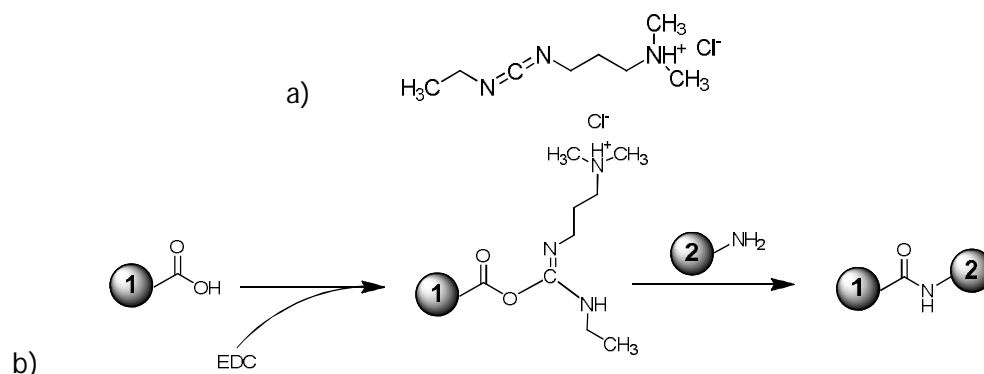


Figure 6.1: Carbodiimide-mediated condensation (Cross-linking with EDC) a) structure of EDC b) reaction scheme. The group 1 represents the protein or polysaccharide molecule carrying the carboxyl group and the group 2 the protein molecule carrying the amine group.

The carboxyl groups, quite sensitive to light and heat, are engaged in the reaction and therefore this reaction has been used in the industry to improve the stability of polymers (Murphy and Howell, 1991). It is also used in the dye industry. In biochemistry, it is frequently used to couple haptens to carrier proteins, to label DNA, or to attach protein to carboxyl coated surfaces (PierceProtein, 2010).

The consequences of the carbodiimide-mediated condensation on the BSA molecule in aqueous systems have been studied by Murphy and Howell (1991). As the carboxyl groups are blocked by the reaction, an increase in hydrophobicity and in positive charge is observed. The IEP of BSA was reported to increase by more than two pH units after cross-linking to about 6.5 (Murphy and Howell, 1991). These modifications alter the electrostatic and hydrophobic interactions within the protein leading to

dramatic changes in the secondary structure of the protein. A sharp decrease of the proportion of α -helices and an increase in β -sheets and in random coil conformation is observed. The conformational changes affect the functional properties of the proteins as reviewed below.

6.1.2.3 Functional properties of cross-linked proteins

Cross-linking (not only with EDC) modifies the net charge carried by the protein (Kinsella and Whitehead, 1988), thereby modifying the electrostatic interaction within the protein, leading to changes in secondary structure and interaction between proteins. In addition, cross-linking in general increases the amphiphilic behaviour and decreases molecular flexibility (Kinsella and Whitehead, 1988). The effect of cross-linking on gelling, foaming and emulsification has been studied in different conditions.

The strength of physical gels (upon heat treatment) has been shown to decrease after protein cross-linking in some conditions (Kato et al., 1986; Murphy and Howell, 1991). This was attributed to the decrease of the proportion of α -helices required for gelation. On the contrary, the formation of very strong chemical gels ($G' > 10^4$ Pa) has been reported following the addition of EDC to high concentrations of BSA (16% HSA and

HSA:EDC ratio 1:60) (Dong et al., 2008). In this case, EDC generates sufficient intermolecular cross-linking to form a dense protein network.

The emulsification properties of proteins cross-linked prior to emulsification either by Maillard reaction (Kim et al., 2003), by transglutaminase (Faergemand et al., 1997; Faergemand et al., 1998b) or by chemical treatment (Kato et al., 1986; Murphy and Howell, 1991) have been studied. The different types of cross-linking probably result in varying levels of intra- and intermolecular cross-linking and yet, the data coherently indicate a reduction in the emulsifying properties. This was attributed to a reduction in protein flexibility and an increase in protein size leading to a decrease interfacial adsorption level and hence to a lower surface coverage. To circumvent this issue, the proteins can be cross-linked after they have been adsorbed at the interface, which has been studied based on enzymatic cross-linking (Faergemand et al., 1998b; Faergemand et al., 1999). In this case, emulsion storage stability was improved as less creaming and better stability toward coalescence was observed (Faergemand et al., 1998b). This was explained by the large increase of surface viscosity and dilatational elasticity (Faergemand et al., 1999). It seems therefore that the cross-linking after emulsification presents a real potential to improve emulsion stability.

One of the advantages of chemical cross-linking versus enzymatic cross-linking is that, being much less specific, it offers the possibility of mixed cross-linking, for example between proteins and polysaccharides as discussed below.

6.1.3 EDC MEDIATED CROSS-LINKING OF PROTEIN-POLYSACCHARIDES

As discussed in the previous chapters, polysaccharides are widely used in food products as thickening, gelling and suspending agents. However, the low surface activity of polysaccharides limits their utilisation as sole emulsifying agents in a formulation. Thus many researchers have tried to combine proteins and polysaccharides to improve the emulsion stability (Dickinson and Euston, 1991) and the interactions between proteins and polysaccharides have been extensively studied (Doublier et al., 2000).

Two types of protein-polysaccharide mixtures have been studied based on covalent or non-covalent bonds between the two entities. Non-covalent associations are based on electrostatic attraction between anionic polysaccharides and cationic proteins (for $\text{pH} < \text{IEP}$). This principle has been used to generate multilayered interfacial membranes (Moreau et al., 2003; Guzey, Kim and McClements, 2004; Surh, Decker and McClements, 2006). Emulsions are prepared in two steps: initially, cationic proteins are adsorbed to the interface and in a second step, the droplets are coated with pectin,

an anionic polymer. These emulsions were shown to have enhanced stability, especially at intermediate pHs where proteins alone normally fail to function (Guzey et al., 2004). A BSA-pectin solution can also form a gelled network by inducing thermal gelation of the protein (Cai and Arntfield, 1997). Electrostatic interactions are non-specific and non-covalent. They are sensitive to solution conditions which is why some authors have investigated covalent bondage of proteins to polysaccharides as reviewed below.

The formation of covalent protein-polysaccharide bonds is by conjugation (Oliver, Melton and Stanley, 2006), which is based on the Maillard reaction and mainly occurs at low water activity (<0.7). Hence conjugates have to be prepared initially in the adequate conditions followed by emulsification. Emulsifying properties of proteins were improved by conjugation with polysaccharides under certain conditions (see the review by Oliver et al. (2006)). For example, it was found that a BSA-galactomannan conjugate improved the emulsion stability compared to BSA alone and to a BSA-galactomannan mixture (Kim et al., 2003). It was suggested that the polysaccharides reinforce adsorption at the oil-water interface and stabilize the oil droplets by forming a viscoelastic layer in the aqueous phase, leading to improved emulsion stability (Khan et al., 1999). The strict conditions to obtain conjugates remain a major drawback of the technique, by opposition to the ease of use of EDC.

Any polysaccharide containing carboxyl groups could be covalently cross-linked to proteins in solutions by the carbodiimide-mediated condensation detailed above. In this research, pectin was chosen due to previous work on mixed gelation of BSA and pectin with EDC (Dong et al., 2008). Pectin is one of the most common polysaccharides containing carboxylic function. It is a food grade additive (E440) extracted from plant cell walls (mainly citrus and apples). Pectins have a galacturonic acid backbone and can be methylated to different extends. Pectin could be used to design the interfacial properties of cross-linked emulsions and EDC-mediated cross-linking would present the advantages of covalent bonds but created *in-situ* at the oil-water interface.

6.1.4 COMPETITION PROTEIN/SURFACTANT AT THE INTERFACE AS A TOOL TO INVESTIGATE INTERFACIAL CROSS-LINKING OF BSA

In most food emulsions, different types of surface-active molecules compete for the oil-water interface. Comparing the resistance of native and cross-linked BSA to competition with other molecules can be used to estimate the success of cross-linking. The main class of emulsifiers competing with proteins are low molecular weight surfactants (below referred to as surfactants). Surfactants (or small emulsifiers) and proteins have very different ways of action (Wilde et al., 2004). Surfactants do not form a viscoelastic interface as they, being small molecules, diffuse freely at the

interface and do not impart mechanical strength to the interface. They tend to have a higher surface activity than proteins and stabilise the interface through reduction of surface tension and the Gibbs-Marangoni mechanism. As a result of the different mechanism to stabilise emulsions, it was observed that proteins tend to be displaced from the interface by small surfactants.

Original work studying the competition between proteins and water soluble surfactants was carried out with caseins and lactoglobulin (Dickinson, Rolfe and Dalgleish, 1989; Courthaudon, Dickinson and Dalgleish, 1991a; Courthaudon et al., 1991b; Courthaudon et al., 1991c; Dickinson and Tanai, 1992). More recently, such studies have been extended to BSA (Rampon et al., 2003a; Rampon et al., 2003b). All studies indicate that small molecular weight surfactants displace adsorbed proteins from the interface. The surfactant adsorbs at the interface initially in small domains which then expand until the interfacial protein network fails and the protein is displaced from the interface (Wilde et al., 2004). Extent and kinetics of displacement depend on several factors including the order of exposure at the interface (Dickinson et al., 1989), the age of the adsorbed layer (Courthaudon et al., 1991c) and the extent of thermal denaturation (Das and Kinsella, 1990). The addition of oil-soluble surfactants prior to emulsification has been shown to lead to a reduction in droplet size (Courthaudon et al., 1991a; Dickinson and Tanai, 1992; Dickinson et al., 1993), in some

conditions associated with a reduction in protein surface concentration (Dickinson and Tanai, 1992). The extent to which protein is displaced by a small surfactant can be used as a measure of the strength of the adsorbed protein layer (Kim et al., 2002).

6.1.5 DUPLEX EMULSIONS

In this research, duplex emulsions of (water-in-oil)-in-water or W/O/W (see Figure 6.2 for schematic of such a duplex emulsion microstructure) were of interest as discussed in the introduction of Chapter 1. The difference with simple oil-in-water emulsions is that water droplets (w1) are dispersed within the oil droplets.

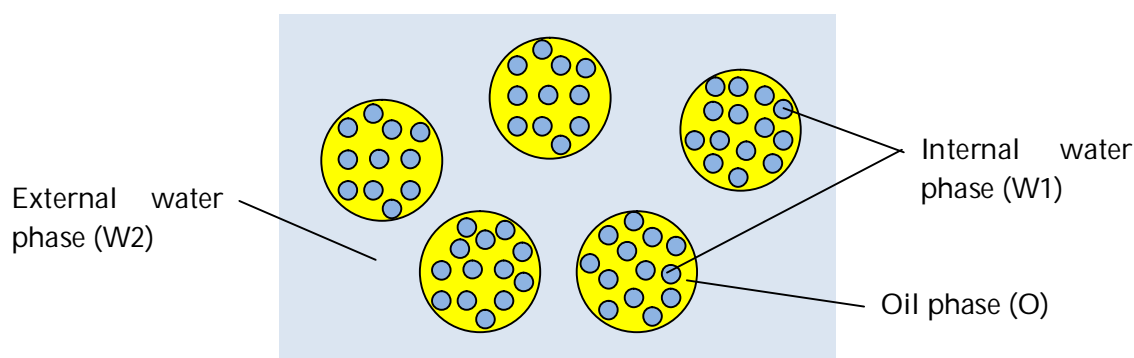


Figure 6.2: Schematic representation of duplex emulsions (W1/O/W2).

Duplex emulsions are traditionally prepared in two steps and contain two emulsifiers: one predominantly hydrophobic to stabilise the W1/O interface and one predominantly hydrophilic to stabilise the O/W2 interface (Garti, Aserin and Cohen,

1994). The W1/O emulsion is prepared in high shear conditions. This primary emulsion is then mixed with the external water phase W2 at moderate shear to avoid disruption of the internal water droplets. The drawback of this method is lack of precision over droplet size and internal water content of individual oil droplets. Recent researches have focussed on microfluidic devices or membrane emulsification to increase duplex emulsion quality.

Coalescence of the internal water droplets and emptying of the internal water phase into the external water phase have been reported (Garti et al., 1994). The presence of BSA in the external water phase has been shown to improve the stability (Garti and Aserin, 1996), as well as gelation of the internal water phase (Surh et al., 2007).

In this research, it was investigated whether interfacially adsorbed proteins can be chemically cross-linked with EDC. If successful, it was then investigated whether the interfacial strength can be modified by including pectin in the cross-linked interface. Finally, the interest of chemically cross-linking BSA to enhance the stability of duplex emulsion is reported.

6.2 MATERIALS AND METHODS

6.2.1 MATERIALS

Bovine serum albumin (BSA) lyophilized powder (pH 6.5-7.5, 1% in 0.15M sodium chloride, purity $\geq 96\%$) was of bio-reagent grade and purchased from Sigma-Aldrich Co. (UK). BSA was cross-linked through addition of an aqueous solution of 1-(3-Dimethylaminopropyl)-3-ethylcarbodiimide hydrochloride (EDC, CAS number 25952-53-8) of technical grade, purchased from Sigma-Aldrich (UK). Polyethylene glycol sorbitan monolaurate (trademark Tween® 20, CAS number 9005-64-5) is a water-soluble surfactant which was used to compete with BSA for the interface and was bought from Sigma-Aldrich (UK). High methoxyl pectin in form of citrus pectin with a claimed DE $>60\%$ and no added sugar (classic CU 401 USP standard) was kindly provided by Herbstreith & Fox (Neuenbürg, Germany). Polyglycerol Polyricinoleate (PGPR, CAS number 29894-35-7) is a food grade oil-soluble surfactant (E476) and provided by AAK Baker Services (Oldham, Lancashire). Hexadecane (CAS number 544-76-3, purity $\geq 99\%$) was used as the dispersed phase of oil-in-water emulsions and purchased from Sigma-Aldrich (UK). Corn oil (Mazola Pure Corn Oil) was used as the oil phase for duplex emulsions and was purchased from a local supermarket.

Deionised water was used for the preparation of the aqueous phase of the emulsions, to which 0.02% of sodium azide (NaN_3) was added as a preservative.

Solutions of 1M hydrochloric acid (HCl) and sodium hydroxide (NaOH) were employed to adjust the pH. In one experiment, citric acid and disodium hydrogenophosphate ($\text{Na}_2\text{HPO}_4, 2\text{H}_2\text{O}$), both reagent grade and obtained from Sigma-Aldrich (UK), were used to prepare a pH 5 buffer.

6.2.2 METHOD TO DEMONSTRATE SUCCESSFUL CROSS-LINKING

Figure 6.3 provides an overview of the experimental design conducted with single emulsions to investigate the possibility of interfacial chemical cross-linking of proteins. The success of interfacial cross-linking was evaluated by the strength of the BSA adsorbed layer against displacement by Tween® 20. Tween® 20 was added to the cross-linked and non cross-linked samples, whereas an equivalent amount of water was added to the control samples. The concentration of BSA adsorbed at the interface was then inferred from the concentration of BSA in the serum (see 6.2.5). As all phenomena of interest occur at the oil-water interface, the emulsion preparation protocol was designed to provide a maximal possible total interfacial area to improve the sensitivity of the experiment. This was achieved by preparing emulsions with high oil content and by homogenising at high pressure to obtain small droplets. A low density oil (hexadecane, $\rho \sim 0.7$) was chosen to maximise the density difference between

the dispersed phase and continuous phase to facilitate bulk phase separation to analyse the protein content in the serum as lipids interfere with the protein assay. Preliminary tests showed that small droplets of high density oil such as corn oil ($\rho \sim 0.92$) could not be successfully separated from the serum phase. The experimental design presented in Figure 6.3 was repeated for several composition of the 'initial emulsion': with BSA only (denoted below as 'reference experiment'), with BSA and pectin and, with oil phase containing PGPR, as PGPR is required for duplex emulsion (see 6.2.11).

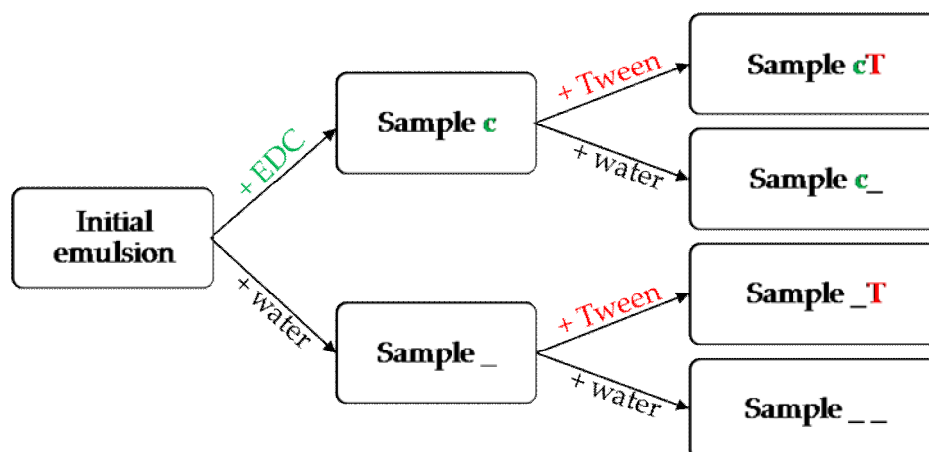


Figure 6.3: Schematic representation of the experimental design.

6.2.3 SINGLE EMULSION PREPARATION

The aqueous phase of the emulsions was prepared by dispersing 0.5% w/w of BSA in deionised water containing 0.02% NaN₃. The solution was stirred for 2 h at room temperature to ensure complete dissolution of the protein. For the emulsions

containing pectin, a stock solution of 0.25% w/w of pectin was prepared by dispersing the powder in cold water followed by stirring for 1 h at 80 °C. The solution was then stirred at 4 °C overnight to ensure complete dissolution. BSA and pectin stock solutions were combined at room temperature to obtain a mixture containing 0.5% w/w BSA and 0.025% w/w pectin. These concentrations were chosen based on unpublished data on EDC cross-linked bulk gel. Time constraints did not allow a systematic study varying BSA and pectin concentration to be conducted.

The oil-in-water emulsion, referred to as 'initial emulsion' in Figure 6.3, was prepared by homogenising hexadecane and aqueous phase to obtain an emulsion with 30% w/w oil content. For emulsions containing PGPR, 2.85% w/w of the oil phase was replaced with PGPR, leading to emulsions containing in total 0.85% PGPR, 29.15% w/w hexadecane and 70% w/w aqueous phase. Initially, a coarse emulsion was prepared by blending the two phases for 30 s using a high-shear mixer set at 7000 rpm (small screen, Silverson L5M, Chesham, UK). The emulsion was then passed three times through a bench scale high pressure homogeniser (Emulsiflex C5, Avestin, Ontario, Canada). The first pass was performed with no added pressure to ensure a homogeneous sample for the later stages of homogenisation: one pass at 35 MPa and one at 75 MPa. It has been shown that BSA in solution was not denatured by high pressure (Hayakawa et al., 1992; Rampon et al., 2003c). Cross-linking with EDC can be

performed on heat denatured protein (10 min at 80 °C, data not shown), although here it was ensured that the temperature of the samples did not exceed 35 °C during homogenisation.

Freshly prepared emulsions were divided into several aliquots, to each the appropriate amount of EDC stock solution (0.3997% w/w) or an equivalent amount of water (control samples) was added. 'Cross-linked samples' have been denoted with a letter *c* and the control samples with a lower dash (┘) (Figure 6.3). Next, the emulsions were mixed overnight on a roller bed. A molar ratio EDC:BSA of 80:1 was chosen as this corresponds theoretically to the cross-linking of all sites available. The emulsions' composition was then: 25% w/w hexadecane with 0.25% w/w BSA and 0-0.089% w/w EDC in the aqueous phase.

On the morning following the addition of EDC or water, an appropriate amount of Tween® 20 stock solution (3.736% w/w) or an equivalent amount of water (control samples) was added to the aliquots. The solutions were mixed on a roller bed for 2 h before quantification of protein displacement following literature protocol (see 6.1.4) (Dickinson and Tanai, 1992). The samples containing Tween® 20 have been denoted with *T* and the control samples with a lower dash (┘) (Figure 6.3). A molar ratio Tween® 20:BSA of 60:1 was chosen as it has been shown that for such high surfactant

concentration, the majority of BSA is displaced from the droplet surfaces (Rampon et al., 2003b). The final composition of the emulsions and sample names are given in Table 6.1. All emulsions were prepared at room temperature.

Table 6.1: Composition of single emulsions and sample codes cT (cross-linked, Tween® 20 added), c_ (cross-linked, no Tween® 20), _T (non cross-linked, Tween® 20 added), _ _ (non cross-linked, no Tween® 20).

Sample code	Hexa decane [% w/w]	BSA [% w/w]	EDC [% w/w]	EDC:BSA Molar ratio	Tween®20 [% w/w]	Tween:BSA Molar ratio
c_	23.1	0.35	0.089	80:1	0	0
cT	23.1	0.35	0.089	80:1	0.374	60:1
_ _	23.1	0.35	0	0	0	0
_T	23.1	0.35	0	0	0.374	60:1

6.2.4 DUPLEX EMULSIONS PREPARATION

The W1 phase of the duplex emulsions was prepared by dispersing 0.5% w/w of BSA in deionised water (0.02% NaN₃) by stirring for 2 h at room temperature. For the cross-linked samples, the appropriate amount of EDC stock solution (to obtain a molar ratio EDC:BSA of 80:1) was added immediately prior to emulsification. An equivalent amount of water was added to the non cross-linked samples so that the final BSA concentration was equal to 0.49% w/w. 2.85% of PGPR was added to corn oil to form the oil phase. The primary emulsion was obtained by adding 10 g of W1 aqueous phase to 90 g of the oil phase while mixing at 2000 rpm using the same overhead high

shear mixer as for preparation of single emulsion. Once the water had been added, the emulsion was sheared for 2 min at 4000 rpm. A small drop of hydrophilic black food colorant (Supercolor) was added to a few drops of the primary emulsion to verify that oil constituted the continuous phase.

To obtain duplex emulsions, external aqueous phase (W2) was added to the primary emulsion followed by emulsification for 5 minutes at 4000 rpm. The composition of W2 was identical to the internal aqueous phase, W1. The composition of the W1/O/W2 emulsions was 5/45/50 or 3/27/70. During the second step of emulsification, the samples were cooled down by placing the sample container into a cool water jacket. A small drop of hydrophilic black colorant was added to a few drops of duplex emulsion to verify that the continuous phase was now water.

6.2.5 QUANTIFICATION OF BSA IN THE SERUM

The concentration of BSA adsorbed at the interface was deducted from the BSA concentration in the serum and based on the assumption that the proteins not detected in the serum are adsorbed at the oil-water interface. This method is valid provided that the separation of the serum from the droplet does not lead to partial droplet break-up and that there are no reverse micelles within the oil droplets.

The samples were centrifuged to separate the serum from the cream. 2 ml of emulsion was placed in Eppendorf tubes and centrifuged for 10 min at 13,000 g using a microcentrifuge (Heraeus Fresco 21, Thermo-Fisher, Waltham, USA). The serum (~ 1 ml) was then extracted with a pipette and placed in a new Eppendorf tube to be centrifuged again for 10 min at 13,000g. This two-step procedure reduced the risk of contamination of the serum with oil droplets.

In the literature, the Lowry method is often used to determine the free protein concentration in the serum of emulsions (Das and Kinsella, 1990; Rampon et al., 2003b). However, it has been shown that the cross-linker used in this study (Kumar et al., 2005) as well as pectin (Alkorta, Llama and Serra, 1994) interfere with the Lowry method. Therefore, the protein concentration was determined using biocinchoninic acid (BCA) Protein Assay Kit (Pierce Protein, Thermo Scientific, Rockford, USA). This method is based on the Biuret reaction (reduction of Cu^{2+} into Cu^+ by proteins), with a colorimetric detection of the Cu^+ ions by a reaction involving biocinchoninic acid (Smith, 1985). It was verified that cross-linking of BSA with EDC or the presence of Tween® 20 does not interfere with the BCA assay. BCA assay has been used previously to quantify proteins in presence of pectin (Girard, Turgeon and Gauthier, 2002).

The quantification of BSA using BCA assay was performed following the instructions in the kit. A higher BSA concentration in the serum was expected for the samples containing Tween® 20 (as a result of competition for the interface with BSA) thus those samples were diluted 1:1 with distilled water prior to the assay to be in the linear working range of the assay (0.002-0.2% BSA). For the samples not containing Tween® 20, the serum was used without dilution. The reagents A and B were mixed as indicated in the kit (50:1). 2 ml of the reagent mixture was added to 100 µl of serum in a transparent cuvette and let to incubate for 2 h at room temperature. The absorbance at 562 nm was then measured within 10 min of the end of incubation using a spectrophotometer (PU8720, Phillips, Eindhoven Netherland). A series of dilutions of known concentrations of BSA (0.01-0.17%) were prepared and assayed alongside the unknowns samples. The BSA concentration in the serum of the samples was determined based on the standard curve and 2-4 replicates were performed for each sample.

6.2.6 MEASUREMENT OF EMULSION DROPLET SIZE

The droplet size distribution of the emulsions was measured using a laser diffraction instrument (Beckman-Coulter LS13 320, Brea, USA). Each sample was measured four times: two replicates in two different loadings of the sample. The emulsions were stirred continuously throughout the measurement to ensure the samples were

homogenous. Between each sample, the system was thoroughly rinsed and the background noise was measured. To avoid multiple scattering effect, the emulsions prepared at pH 5 or 8 were diluted with distilled water of a pH matching the pH of the samples.

Results of droplet size measurements are reported as droplet size distributions (DSDs). Characteristic droplet size is expressed as the volume-surface mean diameter, d_{32} , also called Sauter Mean Diameter.

The interest in using d_{32} is that it is related to the oil-water interface area (McClements, 2007) using Equation 6.1. Knowing the concentration of emulsifier adsorbed at the interface, the surface load Γ_s can be obtained using Equation 6.2. The surface load, or surface coverage, corresponds to the mass of emulsifier covering a unit area of droplet surface. It is generally of the order of a few $\text{mg}\cdot\text{m}^{-2}$ (1 to 3 $\text{mg}\cdot\text{m}^{-2}$). A higher surface coverage suggests a multilayer adsorption of emulsifier at the interface (Das and Kinsella, 1990). As the samples were prepared using mass fraction, the calculation of the oil *volume* fraction based on the oil *mass* fraction can be found in Equation 6.3.

$$S = \frac{6\phi V_e}{d_{32}} \quad (6.1)$$

where S [m^2] is the specific surface area, ϕ [-] the volume fraction of dispersed phase, V_e [ml] the volume of emulsion and d_{32} [μm] the Sauter diameter.

$$\Gamma_s = \frac{C_a V_e}{S} = \frac{C_a d_{32}}{6\phi} \quad (6.2)$$

where Γ_s [mg.m⁻²] is the surface load, C_a [mg.ml⁻¹] is the concentration of adsorbed emulsifier, V_e the volume of emulsion [ml], S [m²] is the specific surface area, ϕ [-] the volume fraction of dispersed phase and d_{32} [μm] the Sauter diameter.

$$\phi = \phi_m \left(\phi_m + (1 - \phi_m) \frac{\rho_2}{\rho_1} \right)^{-1} \quad (6.3)$$

where ϕ [-] is the dispersed phase volume fraction, ρ_1 and ρ_2 [g.cm⁻³] the densities of continuous and dispersed phase respectively, and ϕ_m the dispersed phase mass fraction.

6.2.7 OPTICAL LIGHT MICROSCOPY

Emulsions were placed on a standard glass microscope slide and covered with coverlid. The samples were observed under a Leitz Diaplan (Leica Microsystems, Wetzlar, Germany) and the images were recorded with a Pixelink megapixel Camera (model PL-A662) and captured with the software PL-A6xx (Pixelink, Ottawa, Canada).

6.2.8 RHEOLOGY

All rheological measurements were conducted at 20 °C using a rotational rheometer (MCR301, Anton Paar, Austria). Steady state viscosity data were acquired using a double concentric cylinder geometry. Shear rate was stepwise increased from 1 to 1000 s⁻¹ immediately followed by decreasing shear rate from 1000 to 1 s⁻¹. Small angle oscillatory shear measurements were performed with a cone-plate geometry (50 mm,

2 °angle), at 1 Hz and 1% strain (the MCR was fitted with the Direct Strain Oscillation option for better accuracy (Lauger, Wollny and Huck, 2001)).

6.2.9 PH ADJUSTMENT

The pH was measured with a pHmeter (Inolab, pH 720, wtw, Weilheim, Germany). In most of the experiments, the pH was adjusted by addition of 1M solutions of NaOH and HCl, as the use of a buffer modifies dramatically the ionic strength of the solution. For one experiment, a pH 5 buffer was prepared by mixing 447 ml of citric acid stock solution at 21.014 g.l⁻¹ and 553 ml of Na₂HPO₄·2H₂O stock solution at 35.60 g.l⁻¹.

6.2.10 STATISTICAL ANALYSIS

Data were subjected to analyses of variance, ANOVA, using the software package SPSS (SPSS Inc, Chicago, USA). Where appropriate, Tukey's HSD test was used to identify which samples were significantly different to others ($\alpha=0.05$).

6.2.11 EXPERIMENTAL PLAN

As shown in Figure 6.3, each emulsion was divided into 4 aliquots followed by the addition of cross-linker and Tween® 20 (or water for the control samples). Different experimental conditions were tested:

- *Reference conditions.* The original emulsions contained BSA only and the pH was not adjusted. Three replicates were performed.
- *Effect of pH (1).* The original emulsions contained BSA only and the pH was adjusted to 5, 7 or 9 after emulsification followed by correction for any changes after addition of cross-linker or Tween® 20. Tests at pH 7 and 9 were performed in one replicate*. Test at pH 5 was performed in duplicate: one in buffer and one with HCl addition.
- *Effect of pH (2).* The objective was to investigate if the pH during the cross-linking step is determinant. The pH was adjusted to pH 5 or pH 8 immediately after emulsification and corrected for any changes after the addition of cross-linker. After the addition of Tween® 20 to all samples (molar ratio Tween® 20:BSA of 70:1), the pH was then either readjusted to its initial value (5 or 8) or modified (increased to pH 8 for the samples initially at pH 5 or decreased to pH 5 for the samples initially at pH 8). One replicate* was performed.
- *Presence of pectin.* The aqueous phase contained 0.025% w/w of pectin added prior to emulsification. The pH was adjusted at pH 7.5. Two replicates were performed.
- *Presence of PGPR.* The emulsion contained 0.85% PGPR added into the oil phase prior to emulsification. The pH was adjusted at pH 7.5. Two replicates were performed.

* Results of one replicate in *Effect of pH(2)* confirmed findings in *Effect of pH(1)* and in *Reference conditions* and therefore repeats were omitted.

In addition to the work carried out on single emulsions, four duplex emulsions of composition 5/45/50 or 3/27/70 in presence or absence of EDC in both aqueous phases were prepared.

6.3 RESULTS AND DISCUSSION

6.3.1 REFERENCE CONDITIONS: DISPLACEMENT OF BSA FROM THE INTERFACE BY TWEEN® 20 WITHOUT pH ADJUSTMENT

The results reported in this section are from experiments in which the pH was not adjusted but it was monitored and the values are reported in Table 6.2. The factor *sample* was found significant in the ANOVA ($p < 0.001$). The addition of EDC (sample c_) induces a significant increase in pH (from 7.09 to 8.87). On the contrary, the addition of Tween® 20 induced a decrease in pH in both cross-linked and non cross-linked samples. As hypothesised, the pH of the original emulsion is close to neutral and the addition of water (sample __) did not modify the pH.

Table 6.2: pH in reference conditions of the samples cT (cross-linked, Tween® 20 added), c_ (cross-linked, no Tween® 20), _T (non cross-linked, Tween® 20 added) and __ (non cross-linked, no Tween® 20). Samples with the same letter code are not significantly different (p<0.05).

Sample	pH	
Initial emulsion	7.09 ±0.19	a
__	7.10 ±0.14	a
_T	6.18 ±0.7	a
c_	8.87 ±0.15	b
cT	7.12 ±1.31	a

The BSA concentration in the serum was measured and the results can be seen in Figure 6.4. The factors *sample* and *replicate* were both significant to explain the concentration of free BSA (p<0.001). The addition of water or cross-linker did not affect the concentration of BSA in the serum significantly (compare samples __, ___, c and c_). This indicates that the addition of EDC did not lead to desorption of BSA from the interface. The free BSA concentration for the cross-linked samples c and c_ appears lower than the controls _ and ___, though not significantly. Hence, this indicates that cross-linking between adsorbed and bulk proteins, which would lead to a decrease in Free BSA concentration, did not occur predominantly. After addition of Tween® 20 about half of the BSA adsorbed was displaced from the interface for non cross-linked samples. This was previously observed by Rampon et al. (2003), though they observed almost complete displacement of the protein for a similar molar ratio of Tween® 20 to BSA (Rampon et al., 2003b). When BSA had been cross-linked at the interface prior to the addition of surfactant (sample cT), the displacement of protein by Tween® 20

occurred to a significantly smaller extent. It can be concluded that the resistance of the interfacial layer of BSA to displacement has been increased by cross-linking with EDC.

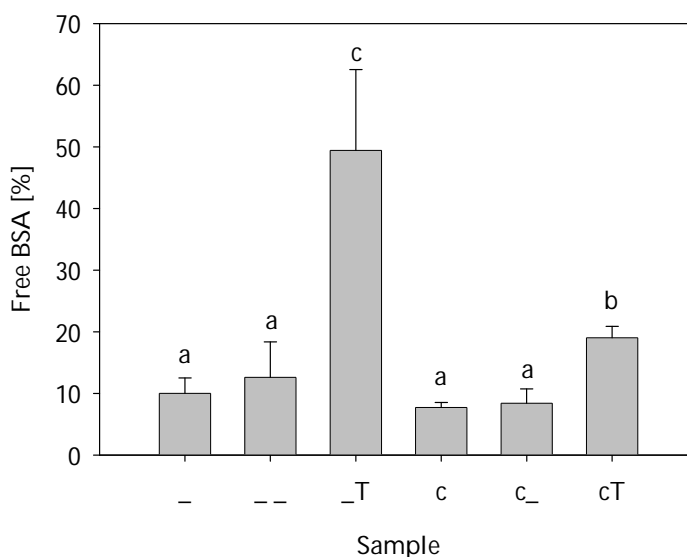


Figure 6.4: Free BSA concentration of emulsions in reference conditions for samples cT (cross-linked, Tween® 20 added), c_ (cross-linked, no Tween® 20), _T (non cross-linked, Tween® 20 added), __ (non cross-linked, no Tween® 20). The samples _ and c are taken after the cross-linking step (_: non cross-linked, c: cross-linked). Samples with the same letter code are not significantly different ($p < 0.05$).

Droplet size distributions of the emulsions discussed so far are shown in Figure 6.5. Samples __ and _T exhibit a very similar droplet size distribution, indicating that the displacement of BSA by Tween® 20 was not associated with a change in droplet size as reported elsewhere (Courthaudon et al., 1991c; Dickinson and Tanai, 1992; Rampon et al., 2003b). Cross-linked samples had larger droplets than non cross-linked samples. As micrographs did not reveal this difference in drop sizes, the light scattering results

are very likely a result of bridging flocculation following cross-linking between BSA adsorbed at the interface of different droplets. An increase of d_{32} following enzymatic cross-linking of adsorbed caseins has been reported previously (Faergemand et al., 1999). In addition, it has been shown that disulfide bonds form after protein adsorption at the interface induced flocculation (Kim et al., 2002). In that work, the flocs were disrupted by the addition of surfactant and the authors postulate that the disulfide bond formation was not extensive enough to prevent the protein from being desorbed by surfactant. The data presented in Figure 6.5 show only a small reduction in d_{32} following the addition of Tween® 20 on cross-linked samples as $d_{32}(c_-)=1.53 \mu\text{m}$ and $d_{32}(cT)=1.27 \mu\text{m}$. The flocculation is only weakly disrupted by the addition of Tween® 20 and this indicates that a strong network was created with the addition of cross-linker. After two months of storage, the droplet size distribution of the cross-linked samples had not changed. On the contrary, non cross-linked samples exhibit multimodal droplet size distributions after two months with size up to $4 \mu\text{m}$, sometimes $200 \mu\text{m}$. This seems to indicate better storage stability of the cross-linked samples however, these findings need to be confirmed by thorough storage trials

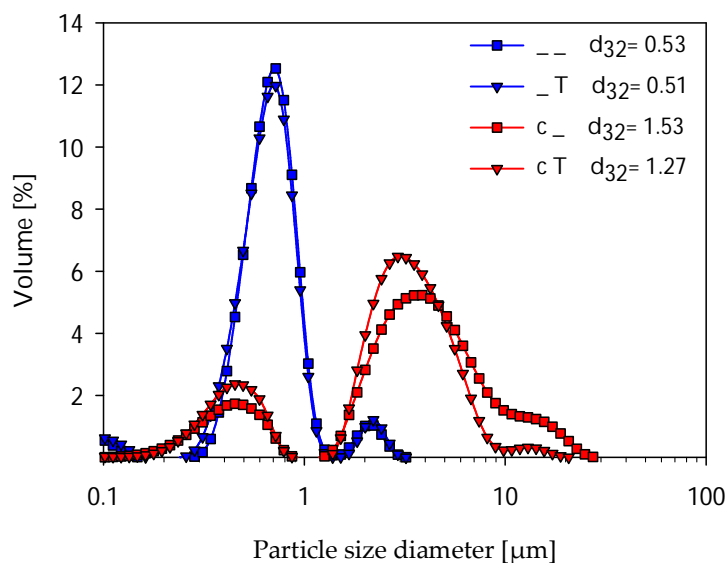


Figure 6.5: Droplet size distribution in the reference conditions for sample cT (cross-linked, Tween® 20 added), c_ (cross-linked, no Tween® 20), _T (non cross-linked, Tween® 20 added) and __ (non cross-linked, no Tween® 20) from replicate 3. The volume-surface mean diameters in the graph are given in μm .

The effect of the addition of EDC on the viscosity of the continuous phase (0.5% BSA) was evaluated. Oscillation test was chosen as shearing may affect the cross-linking. Tests were started immediately after addition of EDC to a 0.5% BSA solution and changes in viscous and elastic modulus were recorded as shown in Figure 6.6. The storage modulus remains very low ($<1\text{ Pa}$) whereas it exceeds 10^4 Pa when the BSA concentration is 16% (Dong et al., 2008). The shear viscosity was lower than $2\text{ mPa}\cdot\text{s}$ 12 h after cross-linking. This indicates that the addition of EDC does not affect the bulk viscosity of the emulsions. The local concentration of BSA at the interface, however, can be as high as 50% (Frieberg et al., 2004) and efficient cross-linking can lead to a

gelled interface. A more detailed rheological study of the cross-linking reaction can be found elsewhere (Dong et al., 2008).

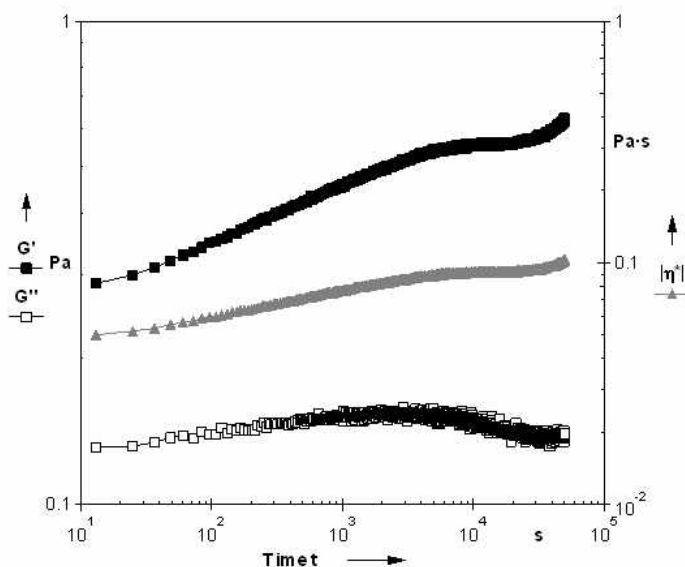


Figure 6.6: G' (■), G'' (□) and $|\eta^*|$ (▲) recorded from the addition of EDC to 0.5% BSA at pH 7 (1 Hz, 1% strain).

In summary, cross-linking of BSA adsorbed at the oil-water interface was followed by a pH increase as well as an increase in droplet size, very likely due to bridging flocculation. The addition of Tween® 20 to non cross-linked samples displaced the protein from the interface without change in the DSD. For cross-linked samples, the protein displacement from the interface was less, and only a small decrease in droplet size was observed. This indicates that cross-linking at the interface has been extensive and that the resistance of BSA to displacement by a surfactant was significantly improved by cross-linking.

6.3.2 EFFECT OF pH ON THE DISPLACEMENT OF BSA FROM THE INTERFACE BY TWEEN® 20

The optimum pH for cross-linking of protein with EDC in aqueous solutions has been described to be between 4.6 and 6 (Wong, 1993). Higher pH conditions (up to 7.2) are compatible with the reaction chemistry albeit with lower efficiency (source: Pierce Protein web site). Here, the proteins were adsorbed at the oil-water interface prior to cross-linking. This will affect protein conformation and possibly also the pH dependency of the cross-linking reaction, which is why the results presented in 6.3.1 have been repeated at different pH. Different pH conditions will be applied during cross-linking and during addition of Tween® 20 to identify the pH sensitivity of each stage of the experiment (6.3.2.2). The results are discussed in section 6.3.2.3.

6.3.2.1 Effect of pH (1): pH constant throughout the experiment

When pH was set to 5, two methods have been used to adjust the pH: using a buffer solution or by HCl addition. Droplet size data and free BSA concentration showed no significant difference between the two methods ($p=0.825$ and $p=0.420$, respectively). The two sets of data will be treated as one in the following. As previously observed, an increase in pH was observed for samples cross-linked at pH 7 (+1.5 pH point on average, $p<0.01$). For samples cross-linked at pH 5, the pH seemed to decrease slightly

whereas for samples cross-linked at pH 9, the pH remained about constant (not enough data for statistical analysis).

The free BSA concentration data are presented in Figure 6.7. They were subjected to an ANOVA with three factors *cross-linked*, *Tween* and *pH*. All factors were significant ($p < 0.01$) as well as the interaction *Tween* \times *pH* ($p < 0.05$). At pH 7 and pH 9, the BSA concentration in the serum was not significantly different for samples c_{-} and $_{-}$. The addition of Tween® 20 induced a significant increase in the BSA concentration for cross-linked samples (cT , $p < 0.05$), yet less important than for the non cross-linked samples ($_{-}T$, $p < 0.05$). These results confirm those of reference conditions presented above in 6.3.1. At pH 5, however, the displacement of BSA from the interface by Tween® 20 was identical for cross-linked and non cross-linked samples, and more extensive than at pH 7 or 9.

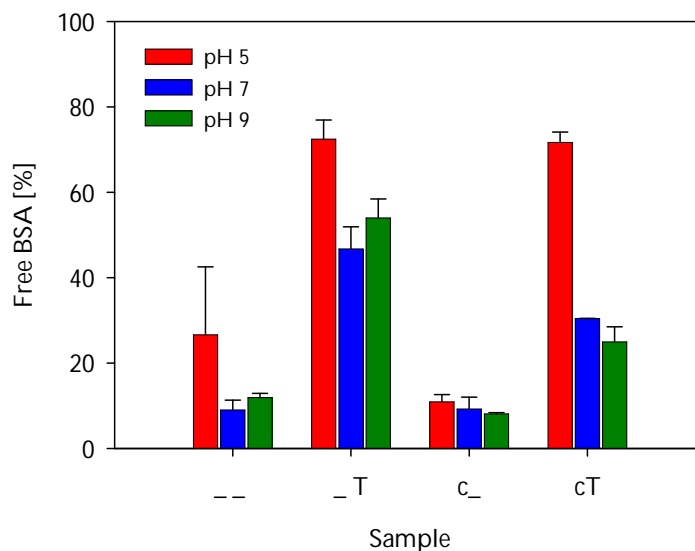


Figure 6.7: Free BSA concentration for pH adjusted as indicated in the legend for cT (cross-linked, Tween® 20 added), c_ (cross-linked, no Tween® 20), _T (non cross-linked, Tween® 20 added) and __ (non cross-linked, no Tween® 20).

The droplet size distribution for samples prepared at pH 5 was also very different compared to the pH 7 samples (compare Figure 6.8 and Figure 6.5). At pH 5, in absence of Tween® 20, both cross-linked and non cross-linked samples appear to be flocculated ($d_{32}(_ _) = 6.23 \mu\text{m}$ and $d_{32}(c _) = 5.29 \mu\text{m}$), presumably due to the fact that pH 5 is very close to the IEP of BSA. Hence, protein charge is not large enough to generate electrostatic repulsion between droplets (Rampon et al., 2003a). Addition of Tween® 20 disrupts the flocs as the mean diameter is reduced to about $1.6 \mu\text{m}$, regardless of the addition of EDC. This has been reported previously for non cross-linked samples (Rampon et al., 2003a).

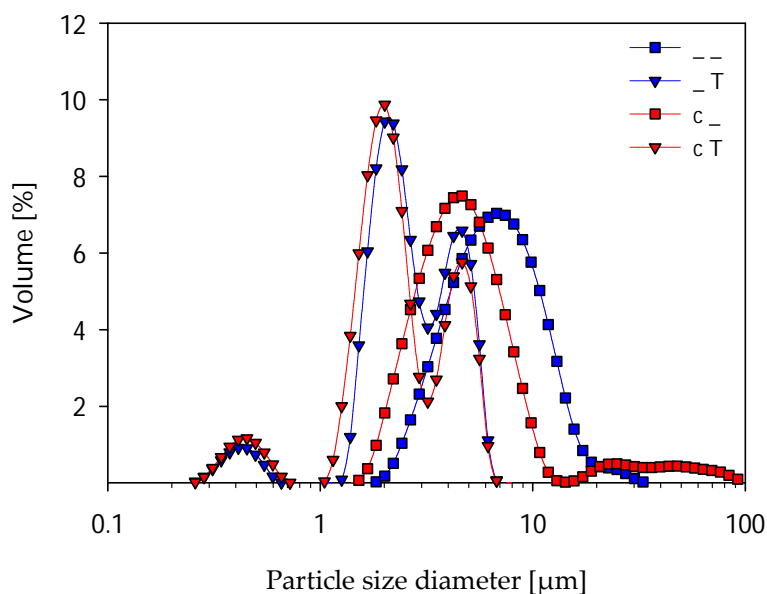


Figure 6.8: Droplet size distribution for samples at pH 5 for samples cT (cross-linked, Tween® 20 added), c_ (cross-linked, no Tween® 20), _T (non cross-linked, Tween® 20 added) and __ (non cross-linked, no Tween® 20).

The results presented in this chapter section demonstrate that the addition of cross-linker successfully improved the mechanical strength of the interfacial adsorbed layer of BSA when the pH of sample was 7 or 9 whereas it seemed not affect the properties of the samples when the pH was 5 prior to addition of chemical cross-linker. However, this experiment did not examine whether the pH during the cross-linking stage or during the competition with Tween® 20 is critical. This is discussed in the next section.

6.3.2.2 Effect of pH (2): pH modified after the cross-linking stage

In this section, results of an experiment designed to identify the pH sensitivity of each stage of the experiment are presented. During the cross-linking stage, the pH was adjusted to 5 or 8. After the addition of Tween® 20, the pH was then either re-adjusted to its initial value (5 or 8) or modified (increased to pH 8 for the samples initially at pH 5 or decreased to pH 5 for the samples initially at pH 8). All samples contained Tween® 20.

Free BSA concentration and droplet size distribution measured 2 h after addition of Tween® 20 are presented in Figure 6.9 and Figure 6.10, respectively. The two variables were subjected to an ANOVA with three factors: *pH during cross-linking stage*, *pH during Tween®20 addition* and *addition of cross-linker*. All factors were significant at $p < 0.001$ except *pH during Tween® 20 addition* which was significant only at $p = 0.05$. Cross-linked and non cross-linked samples 5-5 can be compared to samples cT and _T at pH 5, respectively. Similarly, cross-linked and non cross-linked samples 8-8 can be compared to the samples cT and _T at pH 7 or 9. The present results confirm the conclusions drawn in 6.3.2.1. The specific interest of this experiment was when the pH was different at the cross-linking stage and at the addition of Tween® 20 (samples 5-8 and 8-5). Data for samples 5-8 and 5-5 are very similar, and so are data for samples 8-5

and 8-8 for cross-linked samples. When the pH was adjusted at 5 during the cross-linking stage, droplet size and free BSA concentration were identical for cross-linked and non cross-linked samples. On the contrary, samples cross-linked at pH 8 exhibited flocculation despite the presence of Tween® 20 (higher d_{32} , Figure 6.10) and a significantly lower displacement of BSA from the interface (Figure 6.9). This was observed independent of the pH during the addition of Tween® 20. It can be concluded that a pH in the range of 7-9 during the cross-linking stage is critical to ensure improved resistance of the BSA layer, but that the pH can be altered after the reaction without altering the properties of cross-linked BSA. This property of cross-linked systems greatly enhances the possible products applications as many food products are acidic.

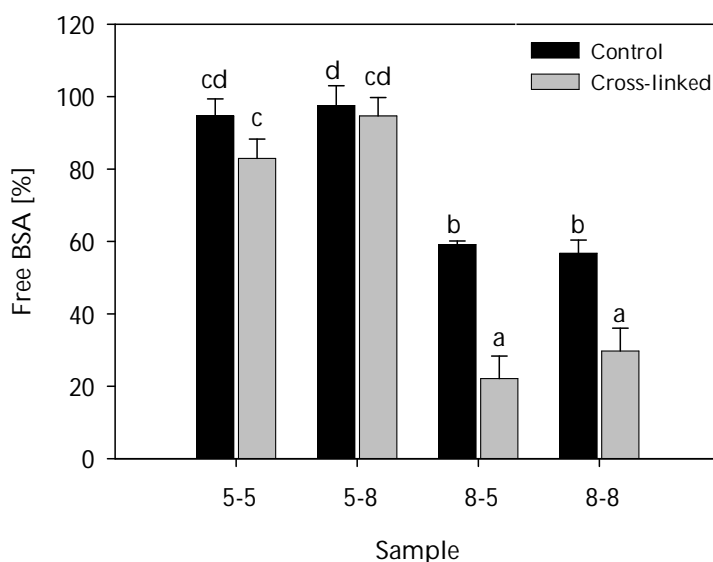


Figure 6.9: Free BSA concentration in different pH conditions for samples containing Tween® 20. In samples name, the first figure indicates the pH during the cross-linking stage and the second figure the pH during

the addition of Tween® 20. Samples with the same letter code are not significantly different ($p < 0.05$).

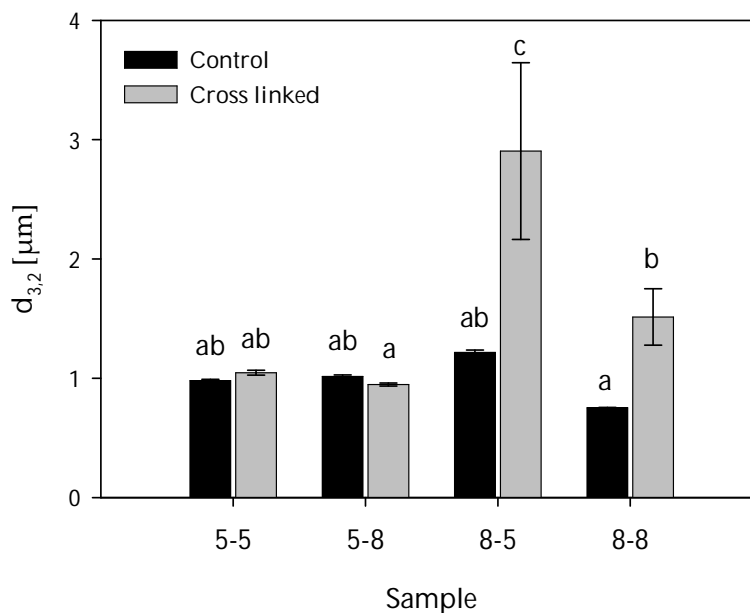


Figure 6.10: Particle size of samples containing Tween® 20 submitted to different pH conditions. In samples name, the first figure indicates the pH during the cross-linking stage and the second figure the pH during the addition of Tween® 20. Samples with the same letter code are not significantly different ($p < 0.05$).

Shear viscosity measurement were performed on those samples and data are presented in Figure 6.11. For sake of clarity, only the data acquired during shear rate increase have been plotted as very little hysteresis had been observed. The samples cross-linked at pH 8 exhibit a higher shear viscosity regardless of the pH of the emulsion during the measurement. The data are in agreement with the droplet size data and indicate flocculation. The flocs were not disrupted by shear.

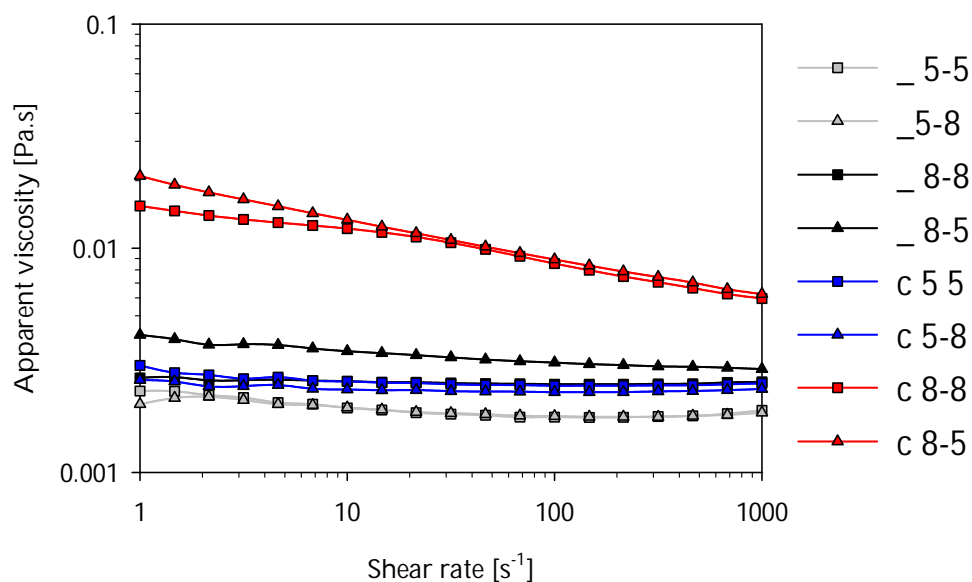


Figure 6.11: Viscosity of samples containing Tween® 20 submitted to different pH conditions. In samples name, the first figure indicates the pH during the cross-linking stage and the second figure the pH during the addition of Tween® 20. Cross-linked samples are indicated by the letter c and non cross-linked samples by a lower dash. Samples with the same letter code are not significantly different ($p < 0.05$).

6.3.2.3 Effect of pH: discussion

The results of experiments 1 and 2 indicated that the pH during the cross-linking stage needs to be relatively high (7-9) to ensure improved resistance of the BSA layer. These data do not indicate that cross-linking did not take place when pH was set at 5 during the cross-linking reaction: it is indeed likely that cross-linking occurred at pH 5 as pH 4-6 is optimal for the cross-linking reaction, but lead to different characteristics of the BSA adsorbed layer than at pH 7 or above. One hypothesis could be that at pH 5

intramolecular cross-linking was predominant over intermolecular cross-linking. Indeed pH 5 is very close to the IEP of BSA and the protein packing at the interface has been reported to be very dense at pH close to IEP due to the absence of net charge in the proteins (Das and Chattoraj, 1980; Kim and Kinsella, 1985). Intramolecular cross-linking would not cause bridging flocculation and is very likely to increase the mechanical strength of the interface to a lesser extent than intermolecular cross-linking, therefore not increasing the resistance to Tween® 20. On the contrary at pH 7-9 the molecules have a net negative charge and are much more expanded at the interface. This may have favoured intermolecular cross-linking and molecular weight data would be required to confirm this hypothesis. It would be interesting to study the cross-linking at pH below the IEP (pH 3-4 for example). In this range of pH, the proteins carry a positive net charge but, as at pH 7, they are more deployed at the interface than at pH 5. An alternative hypothesis explaining the results at pH 5 could be that droplet flocculation reduced the accessibility to certain reaction sites.

6.3.3 EFFECT OF THE PRESENCE OF PECTIN ON THE DISPLACEMENT OF BSA FROM THE INTERFACE BY TWEEN® 20

The free BSA concentration for the samples prepared in presence of pectin is reported in Figure 6.12. The addition of pectin had a significant effect on the concentration of BSA in the serum ($p < 0.001$). The addition of Tween® 20 displaced BSA more

extensively for the samples containing pectin, but the displacement for cross-linked samples was significantly lower than for the non-cross linked samples. The mixed cross-linking with pectin did not increase the strength of the adsorbed layer compared to the cross-linking of BSA only.

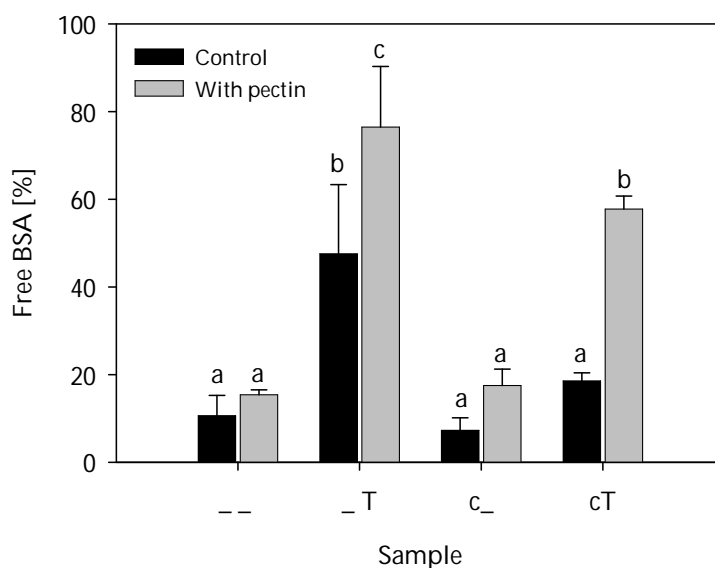


Figure 6.12: Free BSA concentration for the samples with or without added pectin. cT (cross-linked, Tween® 20 added), c_ (cross-linked, no Tween® 20), _T (non cross-linked, Tween® 20 added) and __ (non cross-linked, no Tween® 20). Samples with the same letter code are not significantly different ($p < 0.05$).

The droplet size data are presented in Figure 6.13. The samples not containing Tween® 20 are not significantly different ($d_{32}(_) = d_{32}(c_) = 2.26 \mu\text{m}$). The relatively large volume-surface mean diameter indicates that flocculation occurred when pectin was added to the system. At pH 7 the protein and the pectin are both negatively

charged, it is thus very likely that pectin did not adsorb at the droplets interface and the flocculation observed may be due to depletion attraction as reported elsewhere (Dickinson and Galazka, 1991).

The size measured for non cross-linked samples is smaller when Tween® 20 has been added ($d_{32}(T)=1.20 \mu\text{m}$, $d_{32}(C)=2.26 \mu\text{m}$) probably due to the disruption of the flocs as observed in systems not containing pectin (6.3.1). For the cross-linked samples the addition of Tween® 20 modified the droplet size distribution (increased proportion of droplets of $\sim 1 \mu\text{m}$) but did not significantly affect the volume-surface mean diameter ($d_{32}(CT)=1.76 \mu\text{m}$). This indicates that the flocs were only partially disrupted by the addition of Tween® 20 and, in agreement with the free BSA concentration, that the cross-linking in presence of pectin did increase the resistance of the BSA adsorbed layer to the displacement by Tween® 20 compared to the non cross-linked samples containing pectin.

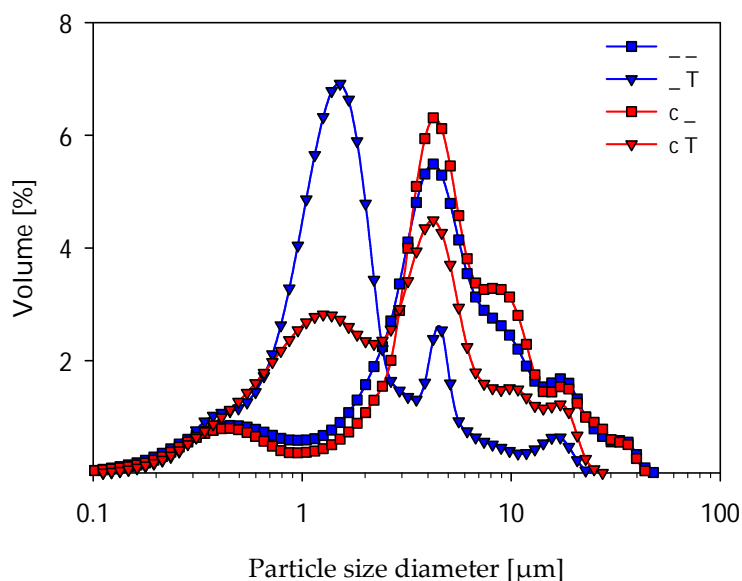


Figure 6.13: Droplet size distribution of the samples containing pectin cT (cross-linked, Tween® 20 added), c_ (cross-linked, no Tween® 20), _T (non cross-linked, Tween® 20 added) and -- (non cross-linked, no Tween® 20).

It can be concluded that the addition of pectin did not increase the strength of the adsorbed layer compared to the cross-linked BSA only. However, it cannot be assumed that mixed cross-linking occurred as depletion-attraction due to the non-adsorbed pectin may have been present. The work was carried out at pH 7 as it was judged optimal in 6.3.2, but this pH may not be optimal to obtain mixed cross-linking. It would be interesting to conduct a detailed study on the effect of the pH, in particular below the IEP of BSA where pectin and BSA are oppositely charged. In addition, pectin was added before homogenisation whereas in most studies pectin has been added after homogenisation (Moreau et al., 2003; Guzey et al., 2004; Surh et al.,

2006) and this may have affected the results. In summary, too few experiments were carried out at this stage to be conclusive on the interest of pectin addition for mixed cross-linking.

6.3.4 EFFECT OF THE PRESENCE OF PGPR ON THE DISPLACEMENT OF BSA FROM THE INTERFACE BY TWEEN® 20

In this experiment, PGPR was added to the oil prior to emulsification to investigate the effect of cross-linking when BSA competes for the interface with an oil-soluble surfactant. The interest in introducing PGPR in the system arises from the fact that cross-linking is studied to improve the stability of duplex emulsions, which requires the use of an oil-soluble surfactant (see 6.1.5).

The free BSA concentration and the droplet size distribution measured for the samples prepared where PGPR was present in the oil phase can be found in Figure 6.14 and Figure 6.15 respectively. The addition of PGPR increased the BSA concentration in the serum significantly ($p < 0.001$) (from 10.6% to 32.8% with the addition of PGPR for sample __). The presence of PGPR also lead to smaller droplets (sample __: $d_{32} = 0.55 \mu\text{m}$ in presence of PGPR versus $0.92 \mu\text{m}$ in the reference conditions, in absence of PGPR). The BSA surface load was thus lower when PGPR was present in the system: $\Gamma_s = 0.96 \text{ mg.m}^{-2}$ in absence of PGPR and $\Gamma_s = 0.77 \text{ mg.m}^{-2}$ in presence of

PGPR. The reduction in droplet size has previously been observed for proteins other than BSA in presence of oil-soluble surfactant (Courthaudon et al., 1991a; Dickinson and Tanai, 1992; Dickinson et al., 1993) and was associated to a reduction in protein surface coverage (Dickinson and Tanai, 1992). It was inferred that the oil-soluble surfactant reduces the concentration of BSA that can be accommodated in the adsorbed layer.

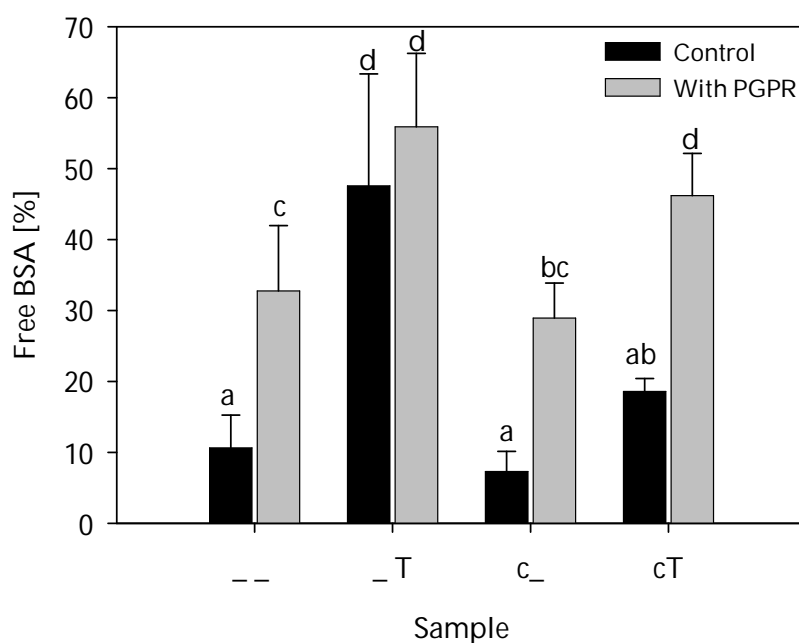


Figure 6.14: Free BSA concentration in presence of PGPR for samples cT (cross-linked, Tween® 20 added), c_ (cross-linked, no Tween® 20), _T (non cross-linked, Tween® 20 added) and -- (non cross-linked, no Tween® 20). Samples with the same letter code are not significantly different ($p < 0.05$).

The addition of cross-linker imparts a significant increase in droplet size ($d_{32}(_ _) = 0.54 \mu\text{m}$ and $d_{32}(c_) = 2.32 \mu\text{m}$, Figure 6.15), as observed in the reference

conditions. Droplet size of the cross-linked samples remains significantly higher than the non cross-linked samples after addition of Tween® 20 ($d_{32}(T)=0.56 \mu\text{m}$ and $d_{32}(CT)=1.79 \mu\text{m}$, Figure 6.15). Supposing that the higher droplet size of cross-linked samples was due to flocculation, this indicates that Tween® 20 was not able to disrupt the flocs, as observed in the reference conditions and therefore, from the particle size data, cross-linked samples appear different from non cross-linked samples. This contrasts with the data of free BSA concentration (Figure 6.14): the displacement of BSA from the interface by Tween® 20 is not significantly different for cross-linked and non cross-linked samples (though it may be slightly less pronounced for cross-linked samples). It is therefore difficult at this stage to conclude whether or not the addition of EDC improved the resistance of the adsorbed layer in presence of an oil-soluble surfactant, PGPR.

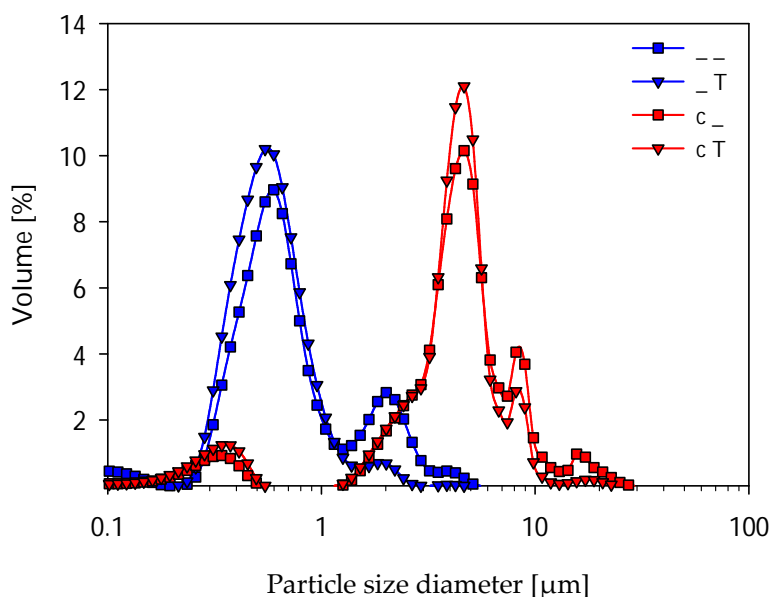


Figure 6.15: Droplet size distribution of the samples containing PGPR for samples cT (cross-linked, Tween® 20 added), c_ (cross-linked, no Tween® 20), _T (non cross-linked, Tween® 20 added) and __ (non cross-linked, no Tween® 20).

In presence of oil-soluble surfactant, BSA very likely covers the interface by domains, separated by domains where PGPR occupies the interface. Therefore the intermolecular cross-linking exists between neighbouring droplets (hence the flocculation) but, within individual droplets, is restricted to small domains. The competition with Tween® 20 is very likely to depend on the size of the domains. Some BSA domains on individual droplets may be sufficiently small to be displaced by Tween® 20, despite being cross-linked, which would explain the free BSA concentration results. On the contrary, large cross-linked BSA regions, such as inter-droplets cross-linking, are hypothesised to resist better the attack by Tween® 20 which

would explain the flocculated state of the emulsion cT. The size of the BSA domains at the cross-linker addition could therefore be a critical factor in the resistance to Tween® 20, but it is not controlled at present and this may be the origin of the large variability in the free BSA concentration data. Also, the addition of PGPR was studied here as it is required to stabilise w/o/w emulsions. However, in duplex emulsions, oil is the continuous phase of the internal interface, not the dispersed phase as studied here and therefore the present results may not be directly applicable.

6.3.5 DUPLEX EMULSIONS

Duplex emulsions of the W/O/W type were prepared by addition of PGPR to the oil phase to stabilise the primary water-in-oil emulsion. Internal and external aqueous phase both contained BSA and EDC which were mixed immediately prior to emulsification. Micrographs of the emulsions on the day of the preparation and at 4 days old are displayed in Figure 6.16 and Figure 6.17. At day 0 duplex emulsion droplets appear quite dark for both cross-linked and non cross-linked samples because of the presence of many small water droplets inside the oil droplets. At day 4 the appearance of the cross-linked samples has not changed, the oil droplets still appear dark. On the other hand, the non cross-linked emulsion droplets seem to have lost some optical density and appear much lighter. At a higher magnification (Figure 6.17)

a few large inner water droplets can clearly be seen. These observations were made for both emulsion compositions (3/27/70 and 5/45/50).

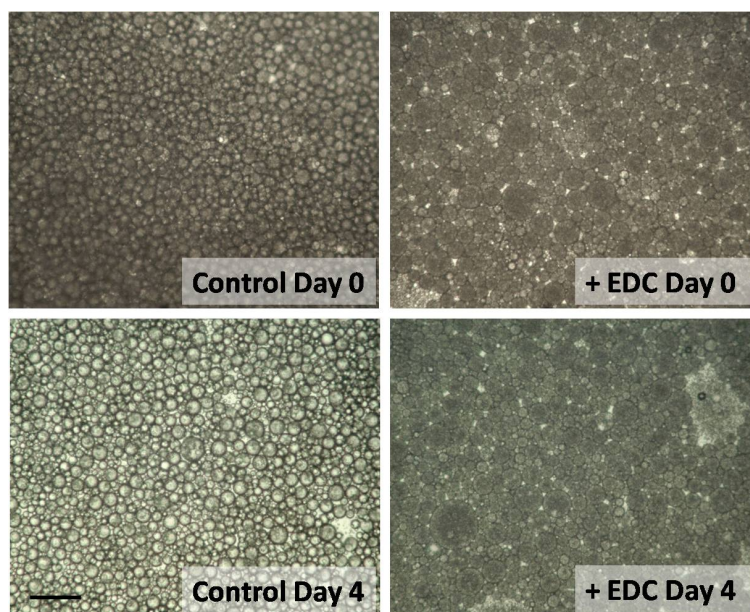


Figure 6.16: Micrograph of the duplex emulsion (5/45/50) cross-linked (+ EDC) or not (Control) at day 0 and day 4. Scale: bar: 50 μm .

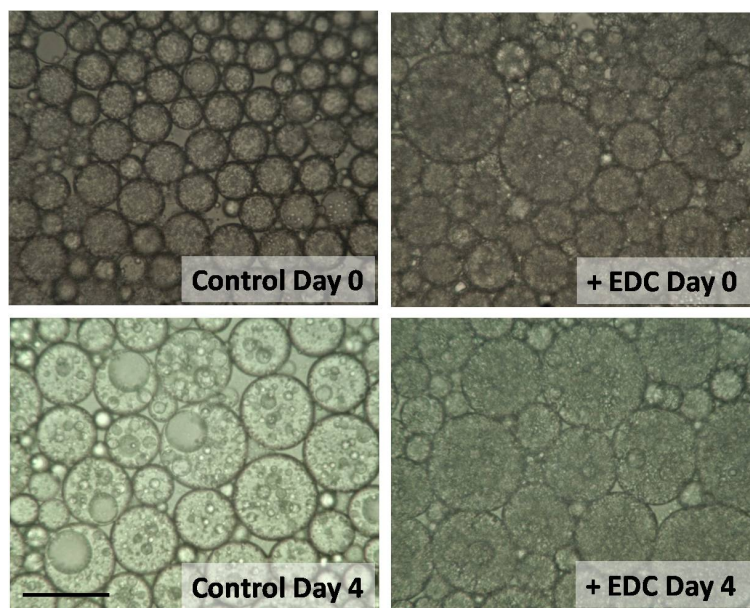


Figure 6.17: Micrograph of the duplex emulsion (5/45/50) cross-linked (+ EDC) or not (Control) at day 0 and day 4. Scale bar: 20 μm .

After two months (Figure 6.18), the enhanced stability of the cross-linked samples was still noticeable compared to the non cross-linked samples which exhibited very few but large inner water droplets. However, it should be noted that after two months, the stability of the cross-linked emulsion with lower primary emulsion content (3/27/70) seemed better than the cross-linked emulsion with high primary emulsion content (5/45/50) which exhibited signs of coalescence of the inner water droplets (Figure 6.18). Those data seem to indicate that the addition of cross-linker prevents the emptying out and/or the coalescence of the inner water droplets to a certain extent.

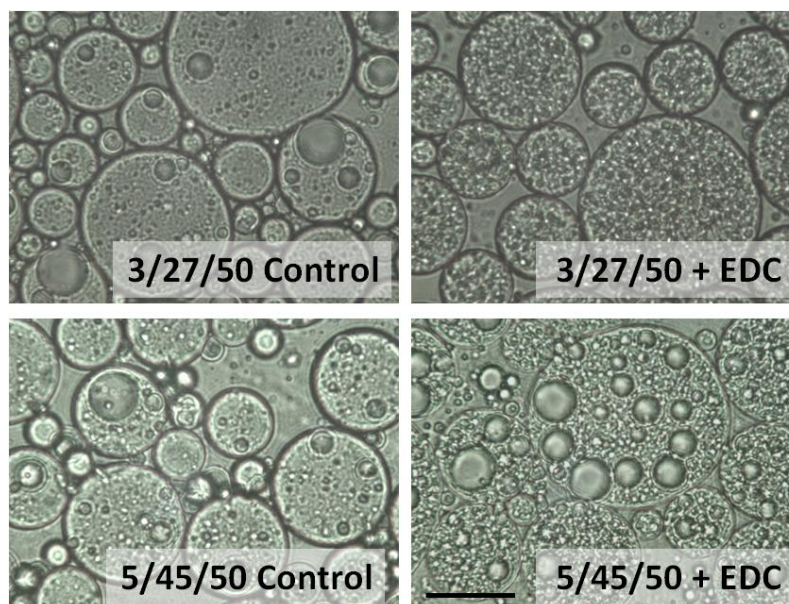


Figure 6.18: Micrograph of the duplex emulsions W1/O/W2 containing different proportion of primary emulsions, cross-linked (+ EDC) or not (Control) after 2 months. Scale bar: 20 μm .

Droplet size data are shown in Figure 6.19. Immediately after preparation, the droplet size distribution of the cross-linked and non cross-linked samples is identical (data not shown). After three days, however, a reduction in droplet size is observed for the non cross-linked samples with an increase in the proportion of droplets of about 15 μm . The droplet size distribution of the cross-linked samples did not change and no further change was observed after two months. The results support the microscopic evidence since release of inner water phase into the outer water phase results in droplet size reduction of the (W/O) droplets.

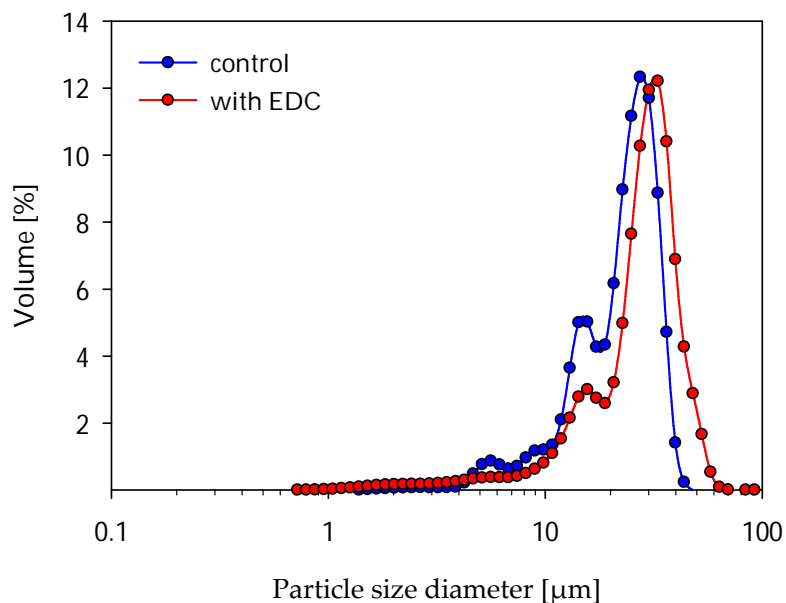


Figure 6.19: Droplet size distribution of the duplex emulsions in absence (control sample) or presence of cross-linker EDC or not 3 days after preparation.

It can be concluded that the addition of cross-linker to both, inner and outer, aqueous phase improved the stability of duplex emulsions. This is very likely due to strengthening of the interfacial layer rather than a viscosifying effect of the continuous phase (see 6.3.1). More experiments are to be carried out to obtain more quantitative data (quantification of the rate of emptying out by the addition of a tracer) and to determine whether cross-linking at both interfaces is required or not to achieve the level of interfacial stability preventing release of the internal water phase.

6.4 CONCLUSIONS

In this chapter, research on the cross-linking of interfacially adsorbed Bovine Serum Albumin with EDC as a possibility to improve emulsion stability and particularly duplex emulsion stability has been reported.

The addition of EDC to oil-in-water emulsions containing BSA was found to generate weak flocculation which is very likely due to bridging flocculation. The strength of the interfacial layer was then tested by its resistance to competition with Tween® 20. After Tween® 20 addition, cross-linked samples showed little displacement of BSA from the interface compared to the extensive displacement for non cross-linked samples. In addition, the flocculated state of the cross-linked samples was maintained. The data suggest that the cross-linking of adsorbed BSA at the interface had been quite extensive and had significantly improved the strength of the adsorbed layer. However, the improved strength was only observed when the pH during the cross-linking stage was slightly basic (7-9). It was hypothesised that intramolecular cross-linkage may have been predominant when the pH was close to the IEP of BSA during the addition of EDC and intramolecular cross-linking is likely not to significantly improve resistance of BSA to displacement by Tween® 20.

Cross-linking of BSA with EDC was also studied in presence of pectin. In the literature, polysaccharides such as pectin have been added to improve the stability of protein-stabilised emulsions. As pectin contains carboxylic function, mixed cross-linking of pectin-BSA with EDC is possible. The cross-linked samples exhibited more resistance to the addition of Tween® 20 compared to non cross-linked samples, as observed in absence of pectin. However, the presence of pectin and possible mixed cross-linking pectin-BSA did not seem to improve emulsion stability compared to cross-linked samples containing BSA only. More research is required to determine whether the addition of pectin could be of interest in cross-linked systems under certain conditions.

PGPR is an oil-soluble surfactant often applied in the preparation of duplex emulsions to stabilise the internal water-in-oil interface. Cross-linking of BSA with EDC in oil-in-water emulsions containing PGPR was studied as a preliminary to work on duplex emulsions. The addition of EDC generated weak flocculation not disrupted by the addition of Tween® 20 as observed in absence of PGPR. However, BSA was displaced to a greater extent from the interface by Tween® 20 when PGPR was present in the system. The data suggest that cross-linking at the interface occurred in presence of PGPR but less extensively than in absence of PGPR. This is probably due to discontinuity of the BSA network at the interface.

Finally, cross-linking with EDC was applied to duplex emulsions (w/o/w). The cross-linker was added to both, inner and outer, aqueous phases, which also contained BSA. The addition of EDC seemed to improve the stability of duplex emulsions by reducing the rate of coalescence and emptying out of the internal water droplets. This was hypothesised to be due to strengthening of the interfacial layer rather than increased viscosity of the aqueous phase, but the data remain qualitative and quantitative work is required.

As mentioned above, some parts of this work can be viewed as preliminary as it is the first time that chemical cross-linking of adsorbed proteins has been considered to stabilise emulsions. The system could be characterised in different conditions using different techniques. Possible directions for future work are reviewed below.

Improving the understanding of the system by using other characterisation techniques

- Molecular weight measurement of BSA (maybe SDS-PAGE gels) to estimate the proportion of intramolecular (no change in molecular weight) versus intermolecular cross-linking (increase in molecular weight).
- Investigation of the interfacial rheology of the systems or surface shear viscometry.
- Investigation of the zeta potential. As cross-linking affects the positive net charge on the BSA molecules, measure of zeta potential should provide a direct way to estimate if cross-linking occurred.
- As the flocculation is not really desirable in a food product, investigation of the flocculation type (flocs size, shape etc) could be interesting.

- Visualisation of the structure of the interface using cryo SEM or confocal microscope

Probing the stability of the system

- Storage stability. For enzymatic cross-linking, the storage stability of cross-linked droplets was better than the non cross-linked samples despite the larger droplet size (Faergemand et al., 1998b).
- Compare the resistance of cross-linked and non cross-linked samples
 - to thermal shocks
 - to pH changes
 - to proteases
 - to other water soluble surfactants

Investigating the reference system (BSA only) in different conditions

- Investigate different BSA:EDC molar ratios. There may be an optimum in the extent of cross-linking (too extensive cross-linking may induce a brittle interface).
- Investigate the effect of the age of the protein interfacial layer.
 - Effect of adding EDC when the BSA interface is aged (24h after emulsification for example) instead of immediately after emulsification
 - Effect of adding Tween® 20 at different times after the addition of EDC (+5 h, +10 h, +15 h or +30 h for example)
- Investigate different initial BSA concentrations: this would modify the initial BSA surface load which may affect the extent of intra- and inter- molecular cross-linking.

Investigating the system containing pectin

- Investigate the effect of adding pectin after emulsification.
- Investigate the optimal pH for mixed cross-linking.
- Investigate the optimal BSA:pectin ratio (to avoid depletion flocculation)

Investigating the duplex emulsions

- Addition of EDC inner or outer water phase only.
- Addition of tracer molecules (one initially in W1 and one in W2) to follow the transfer of aqueous phase during secondary emulsification and during storage.
- Compare the storage stability of systems of different proportion of primary emulsion.
- Investigate the interest of including a rest period (10h for example) between the primary and secondary emulsification process to ensure cross-linking occurred in the internal phase before preparing the duplex emulsion.

CHAPTER 7

OVERALL GENERAL CONCLUSIONS

7.1 IMPLICATIONS OF THIS THESIS

As described in the very beginning of the introduction (Chapter 1), this work was embedded in a project aiming to develop advanced technologies that allow significant salt reduction in processed foods, in order to meet the governmental guidelines without detriment to saltiness perception. The project dealt with products that exist in semi-liquid form, such as marinades, salad dressings, various sauces, soups etc. and most of those products are either aqueous systems or oil-in-water emulsions. As a result of the wide product spectrum of interest, this PhD research covered two aspects: a large part of the work was carried out on thickened aqueous systems (water-based products or continuous phase of emulsion products) whereas the second part of this work was concerned with emulsions systems.

7.1.1 WORK ON THICKENED AQUEOUS SOLUTIONS

The main research questions framing this work were established in Chapter 1 of this thesis: which shear viscosity affects saltiness perception? Does elasticity affect saltiness perception? The saltiness perception in thickened products was studied in relation to shear flow parameters (Chapter 3) and extensional flow parameters (Chapter 4 and 5). The results not only contribute to a better fundamental understanding of the mechanisms of saltiness perception, they also carry an applied aspect in view to low-salt product formulation.

7.1.1.1 Contribution to fundamental understanding

The results presented in this thesis contribute to a better understanding of saltiness perception in thickened solutions. The saltiness perception was found to be related to shear viscosity measured at 10 s^{-1} . This is the first time such a result has been reported in literature for saltiness and it is in agreement with findings for sweetness perception by Baines and Morris (1987) and Cook et al. (2003). Yet the results reported in this thesis are more universal as Baines and Morris worked only with random coil solutions and not samples exhibiting yield behaviour (Chapter 3) and the calculation of the Kokini oral shear stress is restricted to fluids exhibiting power-law behaviour. Here, the relevance of shear viscosity measured at 10 s^{-1} for taste perception was validated for the range of flow behaviours typically encountered in liquid and semi-liquid foods.

The different mechanisms suggested to underlie the decrease of taste perception in viscous solutions were reviewed in Chapter 1 (1.3.2). The data presented in this thesis tend to contradict the hypothesis of a sole cognitive effect of texture on taste perception as mouthfeel and saltiness data were correlated to shear viscosity measured at different shear rates (Chapter 3). The results of this thesis also do not support the hypotheses of restricted diffusion of salt ions or binding to polymer molecules. These theories would predict a greater reduction in saltiness perception with increase in polymer concentration whereas the opposite trend was found

(Chapter 3). The hypothesis of a decreased area of taste bud stimulation in viscous solutions was not tested in this thesis, however, it is very likely that this mechanism contributes to the reduction in taste perception. Unfortunately, no definitive conclusions were obtained with regard to the effect of extensional viscosity on taste perception (Chapter 4, Boger fluids) and, the link between extensional viscosity, efficiency of mixing with saliva and taste perception (Baines and Morris, 1987; Ferry et al., 2006; Koliandris et al., 2007) remains to be further investigated. A basis of future work was provided in Chapter 5 by identifying polysaccharides of identical shear behaviour exhibiting different behaviour in extensional flow fields. Finally, a positive effect of osmolality (or high polymer concentration) on taste perception was reported, a first in published literature. A taste-specific effect of viscosity has been reported previously (1.3) but in Chapter 3, differences between saltiness and sweetness perception were clearly demonstrated and satisfactorily explained to be an osmolality effect.

Finally, during this project it was attempted to adapt rheological techniques that are currently mainly used for synthetic polymers to polysaccharides. Though food grade Boger fluids could not successfully be used for saltiness perception studies (Chapter 4), further studies could be carried using Boger fluids to investigate the effect of elasticity/extensional viscosity on sweetness and mouthfeel. Though many processes involve extensional flows, very little attention has been paid so far to the

characterisation of polysaccharide solution behaviour in extensional flows. In this work, filament break-up and micro-contraction flow, two techniques commonly used for synthetic polymers, were employed to characterise polysaccharide solution behaviour (Chapter 5). Insights into chain-chain interactions and effect of molecular flexibility on behaviour in extensional flow were reported. In particular, the application of microfluidics to polysaccharide solutions has never been reported before. Yet fundamental understanding of the flow behaviour of polysaccharides in microfluidic devices is essential as the generation of food grade microstructures using microfluidics has become the focus of research (Rondeau and Cooper-White, 2008; Wong et al., 2009).

7.1.1.2 Industrial relevance

The improved knowledge of the interaction between taste perception and viscosity is important not only for reformulating products at low salt content but also for replacing key thickeners without experiencing inferior quality in terms of texture and flavour. Based on the conclusions of Chapter 3, the following recommendations can be made for product formulation. It is important to quantify the viscosity at 10 s^{-1} as it correlates to saltiness perception, but a range of flow behaviours (shear-thinning, yielding) can be obtained using polysaccharides alone or in mixture so that desired thickness perception can be obtained. As a result, careful design of flow behaviour enables us to formulate a low-salt product which appears both thick and salty to the

consumer. Finally, the use of low molecular weight thickeners at high concentrations or other solutes increasing the osmolality of the product will significantly enhance saltiness perception, though this option is unlikely to be cost effective for food manufacturers.

7.1.2 EMULSIONS

The second part of this research was concerned with duplex emulsion systems as complex microstructures offering the possibility of increased local concentration and controlled release of NaCl, which may enhance saltiness perception. However, coalescence of the internal water droplets and emptying out of the internal water phase into the external water phase is an often encountered instability and hinders application of duplex emulsions in liquid foods. In Chapter 6 of this thesis research on chemical cross-linking of interfacially adsorbed proteins to improve stability of duplex emulsions has been reported. This work was the first to report on the use of a chemical cross-linker on adsorbed proteins but echoes studies carried on enzymatic cross-linking of adsorbed proteins (Faergemand et al., 1999). A cross-linked interface showed improved resistance to competitive adsorption of low molecular weight surfactants subsequently added to the aqueous emulsion phase. This may have several applications as proteins and surfactants are often concurrently present in food products. In addition, the possibility of mixed cross-linking between protein and pectin was reported. By carefully choosing the type of pectin, the molar ratio of pectin

to protein and the extent of cross-linking, specific interfacial properties could be designed, influencing both the overall stability and the rheology of the product. Finally, the stability of duplex emulsions stabilised through interfacially adsorbed proteins improved as a result of cross-linking these proteins (reduction in the rate of coalescence and emptying out of the internal water phase droplets). The extent of cross-linking very likely affects the release of active substances from the internal droplets to the oil phase to the water phase. Therefore interfacial cross-linking is not only a way of stabilising duplex emulsions but it also presents itself as a tool for controlled release of small molecules such as NaCl as well as of flavour compounds or drug molecules.

7.2 FUTURE DIRECTIONS

In this work saltiness perception was analysed based on simple model systems and validation of the findings in more complex systems, including aroma compounds, other tastants (e.g. monosodium glutamate) or solids (e.g. large vegetable fibres), would be essential to ensure applicability to the more complex formulations of 'real' foods. In addition, this work was solely based on true solutions but it would be interesting to investigate if the findings can be extended to particulate systems (suspensions). This has great industrial relevance as modified starches display suspension behaviour in solution. Finally, since most food products are emulsions

based, the present findings should be validated for polysaccharide solutions in the presence of emulsion droplets (relevant only for oil-in-water emulsions).

As indicated above, restricted mixing of liquid foods with saliva and the possibility that viscous foods lead to stimulation of a smaller area of the tongue appear to be the origin of the reduction in taste perception in viscous solutions. However, parameters controlling in-mouth phenomena are yet to be understood, in particular the role played by the viscoelastic properties of saliva. In addition, in this PhD, all samples were tested at room temperature. Most real food products, however, undergo a change in temperature upon ingestion (e.g. decrease in temperature for hot soups or sauces, increase in temperature for mayonnaises). This directly affects the viscosity of the product and therefore one must wonder at which temperature viscosity should be measured at 10 s^{-1} to give a good correlation with saltiness perception.

Finally, possible directions for future work on cross-linking of adsorbed proteins were given in Chapter 6. As in this thesis chemical cross-linking of interfacially adsorbed proteins to stabilise emulsions has been considered for the first time, there is plenty of further research required to fully understand these systems.

7.3 SUMMARY OF THE FINDINGS

The work presented in this thesis has resulted in a number of key findings. These are:

- The viscosity measured at low shear ($1-10\text{ s}^{-1}$) significantly impacts saltiness perception in solutions exhibiting shear-thinning or yield behaviour, and not the viscosity at zero or high shear.
- A high polymer concentration leading to hyperosmotic solutions enhances saltiness perception, but not sweetness perception.
- For the first time in the literature, highly elastic constant-viscosity food grade fluids (Boger fluids) were formulated but sensitivity for saltiness perception was altered in these fluids so that it remained open whether extensional viscosity affects saltiness perception.
- Polysaccharides of different molecular structures exhibited different behaviour in large deformation extensional flows, and the behaviour of polysaccharide solutions was different to that of synthetic polymers, which was concluded to be most likely due to the lower molecular flexibility of polysaccharide molecules.
- Chemical cross-linking of interfacially adsorbed proteins improved the resistance of single emulsions to protein displacement by Tween® 20 and chemical cross-linking improved the stability of duplex emulsions toward coalescence and emptying out of the internal water phase.

BIBLIOGRAPHIC REFERENCES

- ALKORTA, I., LLAMA, M. J. and SERRA, J. L. (1994) Interference by pectin in protein determination. *Food Science and Technology-Lebensmittel-Wissenschaft & Technologie* 27 (1), 39-41
- ANDERSSON, A. P. and OSTE, R. E. (1994) Diffusivity data of an artificial food system. *Journal of Food Engineering* 23 (4), 631-639
- ANNA, S. L. and MCKINLEY, G. H. (2001) Elasto-capillary thinning and breakup of model elastic liquids. *Journal of Rheology* 45 (1), 115-138
- ARAI, S. and WATANABE, M. (1988) Emulsifying and foaming properties of enzymatically modified proteins. In: *Advances in food emulsions and foams*. (E. Dickinson and G. Stainsby, eds). Elsevier applied science, Barking
- BAINES, Z. V. and MORRIS, E. R. (1987) Flavour/taste perception in thickened systems: The effect of guar gum above and below c^* . *Food Hydrocolloids* 3 197-205
- BAYRAKTAR, T. and PIDUGU, S. B. (2006) Characterization of liquid flows in microfluidic systems. *International Journal of Heat and Mass Transfer* 49 (5-6), 815-824
- BAZILEVSKII, A. V., ENTOV, V. M., LERNER, M. M. and ROZHKOVA, A. N. (1997) Degradation of polymer solution filaments. *Vysokomolekulyarnye Soedineniya Seriya a & Seriya B* 39 (3), 474-482
- BEAUCHAMP, G. K., BERTINO, M., BURKE, D. and ENGELMAN, K. (1990) Experimental sodium depletion and salt taste in normal human volunteers. *American Journal of Clinical Nutrition* 51 (5), 881-889
- BEAUCHAMP, G. K., BERTINO, M. and MORAN, M. (1982) Sodium-regulation - sensory aspects. *Journal of the American Dietetic Association* 80 (1), 40-45
- BERTINO, M., BEAUCHAMP, G. K. and ENGELMAN, K. (1982) Long-term reduction in dietary-sodium alters the taste of salt. *American Journal of Clinical Nutrition* 36 (6), 1134-1144

- BHATTERCHARJEE, P. K., OBERHAUSER, J. P., MCKINLEY, G. H., LEAL, L. G. and SRIDHAR, T. (2002) Extensional rheometry of entangled solutions. *Macromolecules* 35 (27), 10131-10148
- BINDING, D. M. and WALTERS, K. (1988) On the use of flow through a contraction in estimating the extensional viscosity of mobile polymer solutions. *Journal of Non-Newtonian Fluid Mechanics* 30 (2-3), 233-250
- BINNINGTON, R. J. and BOGER, D. V. (1986) Remarks on non-shear thinning elastic fluids. *Polymer Engineering and Science* 26 (2), 133-138
- BIRCH, G. G., AZUDIN, M. N. and GRIGOR, J. M. (1991) Solution properties and composition of dextrans. In: *Biotechnology of amylopectin oligosaccharides* (R. B. Friedman, ed). American Chemical Society, Washington, p. 261-272
- BIRD, R. B., ARMSTRONG, R. C. and HASSAGER, O. (1987) Dynamics of polymeric liquids. Volume 1: Fluid mechanics.
- BOGER, D. V. (1977/1978) A highly elastic constant-viscosity fluid. *Journal of Non-Newtonian Fluid Mechanics* 3 87-91
- (1987) Viscoelastic flows through contractions. *Annual Review of Fluid Mechanics* 19 157-182
- BOVEY, F. A. (1959) Enzymatic polymerization .1. Molecular weight and branching during the formation of dextran. *Journal of Polymer Science* 35 (128), 167-182
- BRESLIN, P. A. S. and SPECTOR, A. C. (2008) Mammalian taste perception. *Current Biology* 18 (4), R148-R155
- BULT, J. H. F., DE WIJK, R. A. and HUMMEL, T. (2007) Investigations on multimodal sensory integration: Texture, taste, and ortho- and retronasal olfactory stimuli in concert. *Neuroscience Letters* 411 (1), 6-10
- BUR, A. J. and ROBERTS, D. E. (1969) Rodlike and random-coil behavior of poly(n-butyl isocyanate) in dilute solution. *Journal of Chemical Physics* 51 (1), 406-&
- CABER. (2003). Haake instruction manual. Version 1.2

- CABLE, P. J. and BOGER, D. V. (1978a) Comprehensive experimental investigation of tubular entry flow of viscoelastic fluids. 1. Vortex characteristics in stable flow. *Aiche Journal* 24 (5), 869-879
- (1978b) Comprehensive experimental investigation of tubular entry flow of viscoelastic fluids. 2. Velocity-field in stable flow. *Aiche Journal* 24 (6), 992-999
- (1979) Comprehensive experimental investigation of tubular entry flow of viscoelastic fluids. 3. Unstable flow. *Aiche Journal* 25 (1), 152-159
- CAI, R. and ARNTFIELD, S. D. (1997) Thermal gelation in relation to binding of bovine serum albumin polysaccharide systems. *Journal of Food Science* 62 (6), 1129-1134
- CASAS, J. A., MOHEDANO, A. F. and GARCIA-OCHOA, F. (2000) Viscosity of guar gum and xanthan/guar gum mixture solutions. *Journal of the Science of Food and Agriculture* 80 (12), 1722-1727
- CASTELAIN, C., DOUBLIER, J. L. and LEFEBVRE, J. (1987) A study of the viscosity of cellulose derivatives in aqueous solutions. *Carbohydrate polymers* 7 (1), 1-16
- CHAN, P. S. K., CHEN, J. S., ETTALAIE, R., ALEVISOPOULOS, S., DAY, E. and SMITH, S. (2008) Filament stretchability of biopolymer fluids and controlling factors. *9th International Hydrocolloids Conference, Singapore*
- CHAN, P. S. K., CHEN, J. S., ETTALAIE, R., LAW, Z., ALEVISOPOULOS, S., DAY, E. and SMITH, S. (2007) Study of the shear and extensional rheology of casein, waxy maize starch and their mixtures. *Food Hydrocolloids* 21 (5-6), 716-725
- CHANDRASHEKAR, J., HOON, M. A., RYBA, N. J. P. and ZUKER, C. S. (2006) The receptors and cells for mammalian taste. *Nature* 444 (7117), 288-294
- CHENG, Y., PRUD'HOMME, R. K., CHIK, J. and RAU, D. C. (2002) Measurement of forces between galactomannan polymer chains: Effect of hydrogen bonding. *Macromolecules* 35 (27), 10155-10161
- CHIBA, K., SAKATANI, T. and NAKAMURA, K. (1990) Anomalous flow patterns in viscoelastic entry flow through a planar contraction. *Journal of Non-Newtonian Fluid Mechanics* 36 193-203
- CHIBA, K., TANAKA, S. and NAKAMURA, K. (1992) The structure of anomalous entry flow patterns through a planar contraction. *Journal of Non-Newtonian Fluid Mechanics* 42 (3), 315-322
-

- CHOPLIN, L., CARREAU, P. J. and KADI, A. A. (1983) Highly elastic-constant viscosity fluids. *Polymer Engineering and Science* 23 (8), 459-464
- CHRISTENSEN, C. M. (1980) Effects of solution viscosity on perceived saltiness and sweetness. *Perception & Psychophysics* 28 (4), 347-353
- CLASEN, C., PLOG, J. P., KULICKE, W. M., OWENS, M., MACOSKO, C., SCRIVEN, L. E., VERANI, M. and MCKINLEY, G. H. (2006) How dilute are dilute solutions in extensional flows? *Journal of Rheology* 50 (6), 849-881
- CONNELLY, R. K. and KOKINI, J. L. (2004) The effect of shear thinning and differential viscoelasticity on mixing in a model 2d mixer as determined using fem with particle tracking. *Journal of Non-Newtonian Fluid Mechanics* 123 (1), 1-17
- COOK, D. J., HOLLOWOOD, T. A., LINFORTH, R. S. T. and TAYLOR, A. J. (2002) Perception of taste intensity in solutions of random-coil polysaccharides above and below c^* . *Food Quality and Preference* 13 (7-8), 473-480
- (2003a) Oral shear stress predicts flavour perception in viscous solutions. *Chemical Senses* 28 (1), 11-23
- COOK, D. J., LINFORTH, R. S. T. and TAYLOR, A. J. (2003b) Effects of hydrocolloid thickeners on the perception of savory flavors. *Journal of Agricultural and Food Chemistry* 51 (10), 3067-3072
- COURTHAUDON, J. L., DICKINSON, E. and DALGLEISH, D. G. (1991a) Competitive adsorption of beta-casein and nonionic surfactants in oil-in-water emulsions. *Journal of Colloid and Interface Science* 145 (2), 390-395
- COURTHAUDON, J. L., DICKINSON, E., MATSUMURA, Y. and CLARK, D. C. (1991b) Competitive adsorption of beta-lactoglobulin + tween 20 at the oil-water interface. *Colloids and Surfaces* 56 293-300
- COURTHAUDON, J. L., DICKINSON, E., MATSUMURA, Y. and WILLIAMS, A. (1991c) Influence of emulsifier on the competitive adsorption of whey proteins in emulsions. *Food Structure* 10 (2), 109-115
- CUTLER, A. N., MORRIS, E. R. and TAYLOR, L. J. (1983) Oral perception of viscosity in fluid foods and model systems. *Journal of Texture Studies* 14 (4), 377-395

- DAAS, P. J. H., GROUPE, K., VAN VLIET, T., SCHOLS, H. A. and DE JONGH, H. H. J. (2002) Toward the recognition of structure-function relationships in galactomannans. *Journal of Agricultural and Food Chemistry* 50 (15), 4282-4289
- DAS, K. P. and CHATTORAJ, D. K. (1980) Adsorption of proteins at the polar oil-water interface. *Journal of Colloid and Interface Science* 78 (2), 422-429
- DAS, K. P. and KINSELLA, J. E. (1990) Effect of heat denaturation on the adsorption of [beta]-lactoglobulin at the oil/water interface and on coalescence stability of emulsions. *Journal of Colloid and Interface Science* 139 (2), 551-560
- DAVIES, G. A. and STOKES, J. R. (2008) Thin film and high shear rheology of multiphase complex fluids. *Journal of Non-Newtonian Fluid Mechanics* 148 73-87
- DAVIES, G. A., WANTLING, E. and STOKES, J. R. (2009) The influence of beverages on the stimulation and viscoelasticity of saliva: Relationship to mouthfeel? *Food Hydrocolloids* 23 (8), 2261-2269
- DE VICENTE, J., STOKES, J. R. and SPIKES, H. A. (2006) Soft lubrication of model hydrocolloids. *Food Hydrocolloids* 20 (4), 483-491
- DELWICHE, J. and OMAHONY, M. (1996) Changes in secreted salivary sodium are sufficient to alter salt taste sensitivity: Use of signal detection measures with continuous monitoring of the oral environment. *Physiology & Behavior* 59 (4-5), 605-611
- DELWICHE, J. F., HALPERN, B. P. and DESIMONE, J. A. (1999) Anion size of sodium salts and simple taste reaction times. *Physiology & Behavior* 66 (1), 27-32
- DESSE, M., MITCHELL, J. R., WOLF, B. and BUDTOVA, T. (2010) Droplet deformation and break-up under shear: Hydrocolloid solution versus suspension of starch granules. *Accepted for publication in Food Hydrocolloids*
- DICKINSON, E. (1999) Adsorbed protein layers at fluid interfaces: Interactions, structure and surface rheology. *Colloids and Surfaces, B* 15 161-176
- DICKINSON, E. and EUSTON, S. R. (1991) Stability of food emulsions containing both protein and polysaccharide. In: Food polymers, gels and colloids (E. Dickinson, ed). Royal society of Chemistry, Cambridge, p. 132-146
- DICKINSON, E. and GALAZKA, V. B. (1991) Bridging flocculation in emulsions made with a mixture of protein and polysaccharide. In: Food polymers, gels

and colloids (E. Dickinson, ed). Royal Society of Chemistry, Cambridge, p. 494-497

DICKINSON, E., OWUSU, R. K., TAN, S. and WILLIAMS, A. (1993) Oil-soluble surfactants have little effect on competitive adsorption of alpha-lactalbumin and beta-lactoglobulin in emulsions. *Journal of Food Science* 58 (2), 295-298

DICKINSON, E., ROLFE, S. E. and DALGLEISH, D. G. (1989) Competitive adsorption in oil-in-water emulsions containing alpha lactalbumin and beta lactoglobulin. *Food Hydrocolloids* 3 (3), 193-204

— (1990) Surface shear viscometry as a probe of protein-protein interactions in mixed milk protein films adsorbed at the oil-water interface. *International Journal of Biological Macromolecules* 12 (3), 189-194

DICKINSON, E. and TANAI, S. (1992) Protein displacement from the emulsion droplet surface by oil-soluble and water-soluble surfactants. *Journal of Agricultural and Food Chemistry* 40 (2), 179-183

DJORDJEVIC, J., ZATORRE, R. J. and JONES-GOTMAN, M. (2004) Effects of perceived and imagined odors on taste detection. *Chemical Senses* 29 (3), 199-208

DOI, M. and EDWARDS, S. F. (1986) The theory of polymer dynamics. Oxford Press, New York

DONG, Y., FOSTER, T. J., MITCHELL, J. and WOLF, B. (2008) A rheological study to analyse the mixed gelation of a protein with a polysaccharide with the use of a cross-linker. *Annual transactions of the nordic rheology society* 16 (83-89),

DOTSCH, M., BUSCH, J., BATENBURG, M., LIEM, G., TAREILUS, E., MUELLER, R. and MEIJER, G. (2009) Strategies to reduce sodium consumption: A food industry perspective. *Critical Reviews in Food Science and Nutrition* 49 (10), 841-851

DOUBLIER, J. L., GARNIER, C., RENARD, D. and SANCHEZ, C. (2000) Protein-polysaccharide interactions. *Current Opinion in Colloid & Interface Science* 5 (3-4), 202-214

DOYLE, J. P., LYONS, G. and MORRIS, E. R. (2008) New proposals on "Hyperentanglement" Of galactomannans: Solution viscosity of fenugreek gum under neutral and alkaline conditions. *9th International Hydrocolloids Conference, Singapore*

- DUXENNEUNER, M. R., FISCHER, P., WINDHAB, E. J. and COOPER-WHITE, J. J. (2008) Extensional properties of hydroxypropyl ether guar gum solutions. *Biomacromolecules* 9 (11), 2989-2996
- ENGELLEN, L., DE WIJK, R. A., PRINZ, J. F., JANSSEN, A. M., WEENEN, H. and BOSMAN, F. (2003) The effect of oral and product temperature on the perception of flavor and texture.
- ENNIS, D. M. (1993) The power of sensory discrimination methods. *Journal of Sensory Studies* 8 353-370
- ENTOV, V. M. and HINCH, E. J. (1997) Effect of a spectrum of relaxation times on the capillary thinning of a filament of elastic liquid. *Journal of Non-Newtonian Fluid Mechanics* 72 (1), 31-53
- EVANS, R. E. and WALTERS, K. (1986) Flow characteristics associated with abrupt changes in geometry in the case of highly elastic liquids. *Journal of Non-Newtonian Fluid Mechanics* 20 11-29
- (1989) Further remarks on the lip-vortex mechanism of vortex enhancement in planar contraction flows. *Journal of Non-Newtonian Fluid Mechanics* 32 (1), 95-105
- FAERGEMAND, M. and MURRAY, B. S. (1998) Interfacial dilatational properties of milk proteins cross-linked by transglutaminase. *Journal of Agricultural and Food Chemistry* 46 (3), 884-890
- FAERGEMAND, M., MURRAY, B. S. and DICKINSON, E. (1997) Cross-linking of milk proteins with transglutaminase at the oil-water interface. *Journal of Agricultural and Food Chemistry* 45 (7), 2514-2519
- FAERGEMAND, M., MURRAY, B. S., DICKINSON, E. and QVIST, K. B. (1999) Cross-linking of adsorbed casein films with transglutaminase. *International Dairy Journal* 9 343-346
- FAERGEMAND, M., OTTE, J. and QVIST, K. B. (1998a) Cross-linking of whey proteins by enzymatic oxidation. *Journal of Agricultural and Food Chemistry* 46 (4), 1326-1333
- (1998b) Emulsifying properties of milk proteins crosslinked with microbial transglutaminase. *International Dairy Journal* 8 (8), 715-723

- FELDMAN, M. and BARNETT, C. (1995) Relationships between the acidity and osmolality of popular beverages and reported postprandial heartburn. *Gastroenterology* 108 (1), 125-131
- FERRY, A. L., HORT, J., MITCHELL, J. R., COOK, D. J., LAGARRIGUE, S. and PAMIES, B. V. (2006a) Viscosity and flavour perception: Why is starch different from hydrocolloids? *Food Hydrocolloids* 20 (6), 855-862
- FERRY, A. L. S., MITCHELL, J. R., HORT, J., HILL, S. E., TAYLOR, A. J., LAGARRIGUE, S. and VALLES-PAMIES, B. (2006b) In-mouth amylase activity can reduce perception of saltiness in starch-thickened foods. *Journal of Agricultural and Food Chemistry* 54 (23), 8869-8873
- FERRY, J. D. (1961) *Viscoelastic properties of polymers*. Wiley, New York
- (1980) *Viscoelastic properties of polymers*. John Wiley, New York
- FRIEBERG, S. E., LARSSON, K. and SJÖBLOM, J. (2004) *Food emulsions*. Marcel Dekker, New York
- FULLER, G. G., CATHEY, C. A., HUBBARD, B. and ZEBROWSKI, B. E. (1987) Extensional viscosity measurements for low-viscosity fluids. *Journal of Rheology* 31 (3), 235-249
- GANS, R. F., WATSON, G. E. and TABAK, L. A. (1990) A new assessment invitro of human salivary lubrication using a compliant substrate. *Archives of Oral Biology* 35 (7), 487-492
- GARTI, N. and ASERIN, A. (1996) Double emulsions stabilized by macromolecular surfactants. *Advances in Colloid and Interface Science* 65 37-69
- GARTI, N., ASERIN, A. and COHEN, Y. (1994) Mechanistic considerations on the release of electrolytes from multiple emulsions stabilized by bsa and nonionic surfactants. *Journal of Controlled Release* 29 (1-2), 41-51
- GIDLEY, M. J., LILLFORD, P. J., ROWLANDS, D. W., LANG, P., DENTINI, M., CRESCENZI, V., EDWARDS, M., FANUTTI, C. and REID, J. S. G. (1991) Structure and solution properties of tamarind-seed polysaccharide. *Carbohydrate Research* 214 (2), 299-314
- (1992) Structure and solution properties of tamarind-seed polysaccharide. *Carbohydrate Research* 214 (2), 299-314

- GIRARD, M., TURGEON, S. L. and GAUTHIER, S. F. (2002) Interbiopolymer complexing between beta-lactoglobulin and low- and high-methylated pectin measured by potentiometric titration and ultrafiltration. *Food Hydrocolloids* 16 (6), 585-591
- GOYCOOLEA, F. M., MORRIS, E. R. and GIDLEY, M. J. (1995) Viscosity of galactomannans at alkaline and neutral pH - evidence of hyperentanglement in solution. *Carbohydrate polymers* 27 (1), 69-71
- GRAESSLEY, W. W. (1980) Polymer-chain dimensions and the dependence of viscoelastic properties on concentration, molecular-weight and solvent power. *Polymer* 21 (3), 258-262
- GRAESSLEY, W. W. and EDWARDS, S. F. (1981) Entanglement interactions in polymers and the chain contour concentration. *Polymer* 22 (10), 1329-1334
- GREEN, B. G. and FRANKMANN, S. P. (1987) The effect of cooling the tongue on the perceived intensity of taste. *Chemical Senses* 12 (4), 609-619
- GULATI, S., MULLER, S. J. and LIEPMANN, D. (2008) Direct measurements of viscoelastic flows of DNA in a 2:1 abrupt planar micro-contraction. *Journal of Non-Newtonian Fluid Mechanics* 155 (1-2), 51-66
- GUO, L., COLBY, R. H., LUSIGNAN, C. P. and HOWE, A. M. (2003) Physical gelation of gelatin studied with rheo-optics. *Macromolecules* 36 (26), 10009-10020
- GUZEY, D., KIM, H. J. and McCLEMENTS, D. J. (2004) Factors influencing the production of o/w emulsions stabilized by beta-lactoglobulin-pectin membranes. *Food Hydrocolloids* 18 (6), 967-975
- HAYAKAWA, I., KAJIHARA, J., MORIKAWA, K., ODA, M. and FUJIO, Y. (1992) Denaturation of bovine serum-albumin (bsa) and ovalbumin by high-pressure, heat and chemicals. *Journal of Food Science* 57 (2), 288-292
- HE, F. J. and MACGREGOR, G. A. (2010) Reducing population salt intake worldwide: From evidence to implementation. *Progress in Cardiovascular Diseases* 52 (5), 363-382
- HEMAR, Y. and PINDER, D. N. (2006) Dws microrheology of a linear polysaccharide. *Biomacromolecules* 7 (3), 674-676
- HOLLOWOOD, T. A., LINFORTH, R. S. T. and TAYLOR, A. J. (2002) The effect of viscosity on the perception of flavour. *Chemical Senses* 27 (7), 583-591

- HUMPHREY, S. P. and WILLIAMSON, R. T. (2001) A review of saliva: Normal composition, flow, and function. *Journal of Prosthetic Dentistry* 85 (2), 162-169
- HUTTON, T. (2000) Technological functions of salt in the manufacturing of food and drink products. In: Food & Drink Federation, p. 1-16
- ISHII, R., CHANG, H. K. and O'MAHONY, M. (2007) A comparison of serial monadic and attribute-by-attribute protocols for simple descriptive analysis with untrained judges. *Food Quality and Preference* 18 (2), 440-449
- ISHIMARU, Y. (2009) Molecular mechanisms of taste transduction in vertebrates. *Odontology* 97 (1), 1-7
- JACOBSON, M. F. (2005) Salt: The forgotten killer. Center for the Science in the public interest, Washington, DC
- JACON, S. A., RAO, M. A., COOLEY, H. J. and WALTER, R. H. (1993) The isolation and characterization of a water extract of konjac flour gum. *Carbohydrate polymers* 20 (1), 35-41
- JAMES, D. F. (2009) Boger fluids. *Annu. Rev. Fluid Mech.* 41 129-142
- JAMES, D. F. and YOGACHANDRAN, N. (2006) Filament-breaking length - a measure of elasticity in extension. *Rheologica Acta* 46 (2), 161-170
- JANSSON, P. E., KENNE, L. and LINDBERG, B. (1975) Structure of extracellular polysaccharide from xanthomonas-campestris. *Carbohydrate Research* 45 (DEC), 275-282
- JENNINGS, B. R. and BROWN, B. L. (1971) Physical properties of polyisocyanates in solution. *European Polymer Journal* 7 (7), 805-826
- JOHANSSON, B., DRAKE, B., PANGBORN, R. M., BARYLKOP, N and KOSTER, E. (1973) Difference taste thresholds for sodium-chloride among young adults - interlaboratory study. *Journal of Food Science* 38 (3), 524-527
- JORGENSEN, L., VAN DE WEERT, M., VERMEHREN, C., BJERREGAARD, S. and FROKJAER, S. (2004) Probing structural changes of proteins incorporated into water-in-oil emulsions. *Journal of Pharmaceutical Sciences* 93 (7), 1847-1859
- KANG, K., LEE, L. J. and KOELLING, K. W. (2005) High shear microfluidics and its application in rheological measurement. *Experiments in Fluids* 38 (2), 222-232

- KATO, A., YAMAOKA, H., MATSUDOMI, N. and KOBAYASHI, K. (1986) Functional-properties of cross-linked lysozyme and serum-albumin. *Journal of Agricultural and Food Chemistry* 34 (2), 370-372
- KEAST, S. J. R. and BRESLIN, P. A. S. (2003) An overview of binary taste-taste interactions. *Food Quality and Preference* 14 (2), 111-124
- KELLING, S. T. and HALPERN, B. P. (1988) Taste judgements and gustatory stimulus-duration - taste quality, taste intensity, and reaction-time. *Chemical Senses* 13 (4), 559-586
- KHAN, M. A. S., BABIKER, E. F. E., AZAKAMI, H. and KATO, A. (1999) Molecular mechanism of the excellent emulsifying properties of phosvitin-galactomannan conjugate. *Journal of Agricultural and Food Chemistry* 47 (6), 2262-2266
- KHOURYIEH, H. A., HERALD, T. J., ARAMOUNI, F. and ALAVI, S. (2007) Intrinsic viscosity and viscoelastic properties of xanthan/guar mixtures in dilute solutions: Effect of salt concentration on the polymer interactions. *Food Research International* 40 (7), 883-893
- KILCAST, D. and ANGUS, F. (2007) Reducing salt in food. Practical strategies. CRC Press
- KIM, H. J., CHOI, S. J., SHIN, W. S. and MOON, T. W. (2003) Emulsifying properties of bovine serum albumin-galactomannan conjugates. *Journal of Agricultural and Food Chemistry* 51 (4), 1049-1056
- KIM, H. J., DECKER, E. A. and McCLEMENTS, D. J. (2002) Impact of protein surface denaturation on droplet flocculation in hexadecane oil-in-water emulsions stabilized by beta-lactoglobulin. *Journal of Agricultural and Food Chemistry* 50 (24), 7131-7137
- KIM, S. H. and KINSELLA, J. E. (1985) Surface-activity of food proteins - relationships between surface pressure development, viscoelasticity of interfacial films and foam stability of bovine serum-albumin. *Journal of Food Science* 50 (6), 1526-1530
- KINGHORN, A. and COMPADRE, C. (2001) Less common high-potency sweeteners. In: *Alternative sweeteners* (L. O. B. Nabors, ed). CRC Press, New York, p. 209-233

- KINSELLA, J. E. and WHITEHEAD, D. M. (1988) Emulsifying and foaming properties of chemically modified proteins. In: *Advances in food emulsions and foams*. (E. Dickinson and G. Stainsby, eds). Elsevier Applied Science, Barking
- KOK, M. S., ABDELHAMEED, A. S., ANG, S., MORRIS, G. A. and HARDING, S. E. (2009) A novel global hydrodynamic analysis of the molecular flexibility of the dietary fibre polysaccharide konjac glucomannan. *Food Hydrocolloids* 23 (7), 1910-1917
- KOKINI, J. L. (1985) Fluid and semi-solid food texture and texture taste interactions. *Food Technology* 39 (11), 86-93
- KOKINI, J. L., BISTANY, K., POOLE, M. and STIER, E. (1982) Use of mass-transfer theory to predict viscosity-sweetness interactions of fructose and sucrose solutions containing tomato solids. *Journal of Texture Studies* 13 (2), 187-200
- KOKINI, J. L. and CUSSLER, E. L. (1983) Predicting the texture of liquid and melting semi-solid foods. *Journal of Food Science* 48 (4), 1221-1225
- KOKINI, J. L., KADANE, J. B. and CUSSLER, E. L. (1977) Liquid texture perceived in mouth. *Journal of Texture Studies* 8 (2), 195-218
- KOLIANDRIS, A., LEE, A., FERRY, A. L., HILL, S. E. and MITCHELL, J. R. (2007) Relationship between structure of hydrocolloid gels and solutions and flavour release. *Food Hydrocolloids* 22 (4), 624-630
- KOSTYRA, E. and BARYLKO-PIKIELNA, N. (2007) The effect of fat levels and guar gum addition in mayonnaise-type emulsions on the sensory perception of smoke-curing flavour and salty taste. *Food Quality and Preference* 18 (6), 872-879
- KRAMER, J., UHL, J. T. and PRUDHOMME, R. K. (1987) Measurement of the viscosity of guar gum solutions to 50,000 s⁻¹ using a parallel plate rheometer. *Polymer Engineering and Science* 27 (8), 598-602
- KREMER, S., MOJET, J. and KROEZE, J. H. A. (2005) Perception of texture and flavor in soups by elderly and young subjects. *Journal of Texture Studies* 36 (3), 255-272
- KUMAR, R., SHUKLA, A. K., BAGGA, E., KUMARI, S., BAJPAI, R. P. and BHARADWAJ, L. M. (2005) 1-ethyl-3-(3-dimethylaminopropyl) carbodilimide interference with lowry method. *Analytical Biochemistry* 336 (1), 132-134

- KWEI, T. K., NAKAZAWA, M., MATSUOKA, S., COWMAN, M. K. and OKAMOTO, Y. (2000) Concentration dependence of solution viscosities of rigid rod polymers. *Macromolecules* 33 (2), 235-236
- LANG, P., KAJIWARA, K. and BURCHARD, W. (1993) Investigations on the solution architecture of carboxylated tamarind seed polysaccharide by static and dynamic light-scattering. *Macromolecules* 26 (15), 3992-3998
- LAPASIN, R. and PRICL, S. (1995) Rheology of industrial polysaccharides. Blackie Academic and professional, New York
- LAPLAIZE, B. (2007) To salt or not to salt ? . In: Vital news
- LAUGER, J., WOLLNY, K. and HUCK, S. (2001) Direct strain oscillation: A new oscillatory method enabling measurements at very small shear stresses and strains. *Golden Jubilee Meeting of the German-Society-of-Rheology (DRG), Berlin, Germany*
- LAUNAY, B., CUVELIER, G. and MARTINEZ-REYES, S. (1997) Viscosity of locust bean, guar and xanthan gum solutions in the newtonian domain: A critical examination of the $\log(\eta(\dot{\gamma}))(\dot{\gamma}) - \log[\eta](\dot{\gamma})$ master curves. *Carbohydrate polymers* 34 (4), 385-395
- LAWLESS, H. T. and HEYMANN, H. (1997) Sensory evaluation of food. Principles and practices. Chapman & Hall, New York
- LAWRENCE, G., SALLES, C., SEPTIER, C., BUSCH, J. and THOMAS-DANGUIN, T. (2009) Odour-taste interactions: A way to enhance saltiness in low-salt content solutions. *Food Quality and Preference* 20 (3), 241-248
- LESHEM, M., ABUTBUL, A. and EILON, R. (1999) Exercise increases the preference for salt in humans. *Appetite* 32 (2), 251-260
- LETHUAUT, L., BROSSARD, C., ROUSSEAU, F., BOUSSEAU, B. and GENOT, C. (2003) Sweetness-texture interactions in model dairy desserts: Effect of sucrose concentration and the carrageenan type. *International Dairy Journal* 13 (8), 631-641
- LIANG, R. F. and MACKLEY, M. R. (1994) Rheological characterization of the time and strain dependence for polyisobutylene solutions. *Journal of Non-Newtonian Fluid Mechanics* 52 (3), 387-405

LIU, Y. G., JUN, Y. G. and STEINBERG, V. (2009) Concentration dependence of the longest relaxation times of dilute and semi-dilute polymer solutions. *Journal of Rheology* 53 (5), 1069-1085

LYALL, V., HECK, G. L., DESIMONE, J. A. and FELDMAN, G. M. (1999) Effects of osmolarity on taste receptor cell size and function. *American Journal of Physiology-Cell Physiology* 277 (4), C800-C813

LYNCH, J., LIU, Y. H., MELA, D. J. and MACFIE, H. J. H. (1993) A time intensity study of the effect of oil mouthcoatings on taste perception. *Chemical Senses* 18 (2), 121-129

MA, X. D. and PAWLIK, M. (2007) Intrinsic viscosities and huggins constants of guar gum in alkali metal chloride solutions. *Carbohydrate polymers* 70 (1), 15-24

MACKAY, M. E. and BOGER, D. V. (1987) An explanation of the rheological properties of boger fluids. *Journal of Non-Newtonian Fluid Mechanics* 22 (2), 235-243

MACKEY, A. (1958) Discernment of taste substance as affected by solvent medium. *Food res.* 23 580-583

MACOSKO, C. W. (1994) Rheology principles, measurements and applications. Wiley-VCH, New York

MALKIN, A. Y. (2002) The meaning and methods of determination of a relaxation spectrum. *Polymer Science Series B* 44 (9-10), 247-253

MALONE, M. E., APPELQVIST, I. A. M. and NORTON, I. T. (2003a) Oral behaviour of food hydrocolloids and emulsions. Part 1. Lubrication and deposition considerations. *Food Hydrocolloids* 17 763-773

— (2003b) Oral behaviour of food hydrocolloids and emulsions. Part 2. Taste and aroma release. *Food Hydrocolloids* 17 (6), 775-784

MARTIN, A. F. (1951) Toward a referee viscosity method for cellulose. *Tappi* 34 (8), 363-366

MATSUOKA, S. and COWMAN, M. K. (2002) Equation of state for polymer solution. *Polymer* 43 (12), 3447-3453

MCBURNEY, D. H. (1969) A note on relation between area and intensity in taste. *Perception & Psychophysics* 6 (4), 250

- MCCLEARY, B. V., CLARK, A. H., DEA, I. C. M. and REES, D. A. (1985) The fine-structures of carob and guar galactomannans. *Carbohydrate Research* 139 (JUN), 237-260
- MCCLEMENTS, D. J. (2007) Critical review of techniques and methodologies for characterization of emulsion stability. *Critical Reviews in Food Science and Nutrition* 47 (7), 611-649
- MCCURDY, R. D., GOFF, H. D., STANLEY, D. W. and STONE, A. P. (1994) Rheological properties of dextran related to food applications. *Food Hydrocolloids* 8 (6), 609-623
- MCKINLEY, G. H. (2005) Visco-elasto-capillary thinning and break-up of complex fluids. *Rheology reviews* 1-49
- MCKINLEY, G. H., ANNA, S. L., TRIPATHY, A. and YAO, M. (1999) Extensional rheometry of polymeric fluids and the uniaxial elongation of viscoelastic filaments. *15th Annual Meeting of the International Polymer Processing Society*
- MEILGAARD, M. C., CIVILLE, G. V. and CARR, B. T. (2006) Sensory evaluation techniques.
- MEZZASALMA, S. A., ANGIOLETTI, C. and CESARO, A. (2004) Conformational polymer statistics from the geometrical scaling of monomeric units and the characteristic ratio from circle maps. Application to carbohydrate macromolecules. *Macromolecular Theory and Simulations* 13 (1), 44-53
- MICHLIG, S., DAMAK, S. and LE COUTRE, J. (2007) Claudin-based permeability barriers in taste buds. *Journal of Comparative Neurology* 502 (6), 1003-1011
- MILAS, M., RINAUDO, M., KNIPPER, M. and SCHUPPISER, J. L. (1990) Flow and viscoelastic properties of xanthan gum solutions. *Macromolecules* 23 (9), 2506-2511
- MILLER, E., CLASEN, C. and ROTHSTEIN, J. P. (2009) The effect of step-stretch parameters on capillary breakup extensional rheology (caber) measurements. *Rheologica Acta* 48 (6), 625-639
- MILLER, E. and COOPER-WHITE, J. (2009) The effects of chain conformation in the microfluidic entry flow of polymer-surfactant systems. *Journal of Non-Newtonian Fluid Mechanics* 160 (1), 22-30

- MITCHELL, J. R. and LEDWARD, D. A. (1986) Functional properties of food macromolecules. Elsevier, Barking, UK
- MOHAN, S. and CAMPBELL, N. R. C. (2009) Salt and high blood pressure. *Clinical Science* 117 (1-2), 1-11
- MONAHAN, F. J., MCCLEMENTS, D. J. and GERMAN, J. B. (1996) Disulfide-mediated polymerization reactions and physical properties of heated wpi-stabilized emulsions. *Journal of Food Science* 61 (3), 504-509
- MONGRUEL, A. and CLOITRE, M. (2003) Axisymmetric orifice flow for measuring the elongational viscosity of semi-rigid polymer solutions. *Journal of Non-Newtonian Fluid Mechanics* 110 (1), 27-43
- MOREAU, L., KIM, H. J., DECKER, E. A. and MCCLEMENTS, D. J. (2003) Production and characterization of oil-in-water emulsions containing droplets stabilized by beta-lactoglobulin-pectin membranes. *Journal of Agricultural and Food Chemistry* 51 (22), 6612-6617
- MORRIS, C., KOLIANDRIS, A. L., WOLF, B., HORT, J. and TAYLOR, A. (2009) Effect of pulsed or continuous delivery of salt on sensory perception over short time intervals. *Chemosensory Perception* 2 (1), 1-8
- MORRIS, C., LABARRE, C., KOLIANDRIS, A. L., HEWSON, L., WOLF, B., TAYLOR, A. J. and HORT, J. (2010) Effect of pulsed delivery and bouillon base on saltiness and bitterness perceptions of salt delivery profiles partially substituted with kcl. *Food Quality and Preference* 21 (5), 489-494
- MORRIS, E. R., CUTLER, A. N., ROSS-MURPHY, S. B. and REES, D. A. (1981) Concentration and shear rate dependence of viscosity in random coil polysaccharide solutions. *Carbohydrate polymers* 1 5-21
- MORRIS, M. J., NA, E. S. and JOHNSON, A. K. (2007) Salt craving: The psychobiology of pathogenic sodium intake. *Annual Meeting of the Society-for-the-Study-of-Ingestive-Behavior, Steamboat Springs, CO*
- MOSKOWITZ, H. R. and ARABIE, P. (1970) Taste intensity as a function of stimulus concentration and solvent viscosity. *Journal of Texture Studies* 1 502-510
- MURPHY, M. C. and HOWELL, N. K. (1991) Effects of the attachment of small molecules by carbodiimide-mediated condensation on the physicochemical

and functional-properties of bovine serum-albumin. *Journal of the Science of Food and Agriculture* 55 (1), 117-140

NG, S. L., MUN, R. P., BOGER, D. V. and JAMES, D. F. (1996) Extensional viscosity measurements of dilute solutions of various polymers. *Journal of Non-Newtonian Fluid Mechanics* 65 (2-3), 291-298

NICOSIA, M. A. and ROBBINS, J. (2001) The fluid mechanics of bolus ejection from the oral cavity. *Journal of Biomechanics* 34 (12), 1537-1544

NIGEN, S. and WALTERS, K. (2002) Viscoelastic contraction flows: Comparison of axisymmetric and planar configurations. *Journal of Non-Newtonian Fluid Mechanics* 102 (2), 343-359

NOBLE, A. C. (1996) Taste-aroma interactions. *Trends in Food Science & Technology* 7 (12), 439-444

NORDMEIER, E. (1993) Static and dynamic light-scattering solution behavior of pullulan and dextran in comparison. *Journal of Physical Chemistry* 97 (21), 5770-5785

NWAMMUO, O. P. and MAITLAND, G. C. (1991) Effects of chain flexibility on polymer-solution dynamics. *Symp on the Conformations of Flexible Molecules in Fluid Phases, Southampton, England*

OHSHIMA, A., YAMAGATA, A., SATO, T. and TERAMOTO, A. (1999) Entanglement effects in semiflexible polymer solutions. 3. Zero-shear viscosity and mutual diffusion coefficient of poly(n-hexyl isocyanate) solutions. *Macromolecules* 32 (25), 8645-8654

OLIVEIRA, M. S. N., RODD, L. E., MCKINLEY, G. H. and ALVES, M. A. (2008) Simulations of extensional flow in microrheometric devices. *Microfluidics and Nanofluidics* 5 (6), 809-826

OLIVER, C. M., MELTON, L. D. and STANLEY, R. A. (2006) Creating proteins with novel functionality via the maillard reaction: A review. *Critical Reviews in Food Science and Nutrition* 46 (4), 337-350

OMAHONY, M., KLAPMAN, K., WONG, J. and ATASSI, S. (1982) Salt taste sensitivity and stimulus volume - effect of stimulus residuals. *Perception* 11 (3), 347-357

- OSSEBAARD, C. A. and SMITH, D. V. (1995) Effect of amiloride on the taste of nacl, na-gluconate and kcl in humans - implications for na⁺ receptor mechanisms. *Chemical Senses* 20 (1), 37-46
- PADMANABHAN, M. and MACOSKO, C. W. (1997) Extensional viscosity from entrance pressure drop measurements. *Rheologica Acta* 36 (2), 144-151
- PANGBORN, R. M., GIBBS, Z. M. and TASSAN, C. (1978) Effect of hydrocolloids on apparent viscosity and sensory properties of selected beverages. *Journal of Texture Studies* 9 (4), 415-436
- PANGBORN, R. M. and SZCZESNIAK, A. S. (1974) Effect of hydrocolloids and viscosity on flavor and odor intensities of aromatic flavor compounds. *Journal of Texture Studies* 4 (4), 467-482
- PANGBORN, R. M. and TRABUE, I. M. (1973) Effect of hydrocolloids on oral viscosity and basic taste intensities. *Journal of Texture Studies* 4 (32), 224-241
- PAPAGEORGIU, D. T. (1995) On the breakup of viscous-liquid threads. *Physics of Fluids* 7 (7), 1529-1544
- PARK, M. S., CHUNG, J. W., KIM, Y. K., CHUNG, S. C. and KHO, H. S. (2007) Viscosity and wettability of animal mucin solutions and human saliva. *Oral Diseases* 13 (2), 181-186
- PARKINSON, C. and SHERMAN, P. (1971) The influence of turbulent flow on the sensory assesment of viscosity in the mouth. *Journal of Texture Studies* 2 451-459
- PATEL, T. R., MORRIS, G. A., DE LA TORRE, J. G., ORTEGA, A., MISCHNICK, P. and HARDING, S. E. (2008) Molecular flexibility of methylcelluloses of differing degree of substitution by combined sedimentation and viscosity analysis. *Macromolecular Bioscience* 8 (12), 1108-1115
- PAULUS, K. and HAAS, E. M. (1980) The influence of solvent viscosity on the threshold values of primary tastes. *Chemical Senses* 5 (1), 23-32
- PETRIE, C. J. S. (2006a) Extensional viscosity: A critical discussion. *Journal of Non-Newtonian Fluid Mechanics* 137 (1-3), 15-23
- (2006b) One hundred years of extensional flow. *Journal of Non-Newtonian Fluid Mechanics* 137 (1-3), 1-14

PICOUT, D. R., ROSS-MURPHY, S. B., ERRINGTON, N. and HARDING, S. E. (2001) Pressure cell assisted solution characterization of polysaccharides. 1. Guar gum. *Biomacromolecules* 2 (4), 1301-1309

— (2003) Pressure cell assisted solubilization of xyloglucans: Tamarind seed polysaccharide and detarium gum. *Biomacromolecules* 4 (3), 799-807

PICOUT, D. R., ROSS-MURPHY, S. B., JUMEL, K. and HARDING, S. E. (2002) Pressure cell assisted solution characterization of polysaccharides. 2. Locust bean gum and tara gum. *Biomacromolecules* 3 (4), 761-767

PIERCEPROTEIN (2010) Edc a water-soluble carbodiimide for rapid preparation of peptides conjugates. www.piercenet.com

PIPE, C. J. and MCKINLEY, G. H. (2009) Microfluidic rheometry. *Mechanics Research Communications* 36 (1), 110-120

PORTER, R. S. and JOHNSON, J. F. (1966) The entanglement concept in polymer systems. *Chemical Reviews* 66 (1), 1-27

RAMPON, V., GENOT, C., RIAUBLANC, A., ANTON, A., AXELOS, M. A. V. and MCCLEMENTS, D. J. (2003a) Front-face fluorescence spectroscopy study of globular proteins in emulsions: Influence of droplet flocculation. *Journal of Agricultural and Food Chemistry* 51 (9), 2490-2495

RAMPON, V., GENOT, C., RIAUBLANC, A., ANTON, M., AXELOS, M. A. V. and MCCLEMENTS, D. J. (2003b) Front-face fluorescence spectroscopy study of globular proteins in emulsions: Displacement of bsa by a nonionic surfactant. *Journal of Agricultural and Food Chemistry* 51 (9), 2482-2489

RAMPON, V., RIAUBLANC, A., ANTON, M., GENOT, C. and MCCLEMENTS, D. J. (2003c) Evidence that homogenization of bsa-stabilized hexadecane-in-water emulsions induces structure modification of the nonadsorbed protein. *Journal of Agricultural and Food Chemistry* 51 (20), 5900-5905

RATCLIFFE, I., WILLIAMS, P. A., VIEBKE, C. and MEADOWS, J. (2005) Physicochemical characterization of konjac glucomannan. *Biomacromolecules* 6 (4), 1977-1986

REN, Y. L., PICOUT, D. R., ELLIS, P. R. and ROSS-MURPHY, S. B. (2004) Solution properties of the xyloglucan polymer from *afzelia africana*. *Biomacromolecules* 5 (6), 2384-2391

- RICHARDSON, R. K., MORRIS, E. R., ROSS-MURPHY, S. B., TAYLOR, L. J. and DEA, C. M. (1989) Characterization of the perceived texture of thickened systems by dynamic viscosity measurements. *Food Hydrocolloids* 3 175-191
- ROBINSON, G., ROSS-MURPHY, S. B. and MORRIS, E. R. (1982) Viscosity molecular-weight relationships, intrinsic chain flexibility, and dynamic solution properties of guar galactomannan. *Carbohydrate Research* 107 (1), 17-32
- RODD, L. E., COOPER-WHITE, J. J., BOGER, D. V. and MCKINLEY, G. H. (2007) Role of the elasticity number in the entry flow of dilute polymer solutions in micro-fabricated contraction geometries. *Journal of Non-Newtonian Fluid Mechanics* 143 (2-3), 170-191
- RODD, L. E., SCOTT, T. P., BOGER, D. V., COOPER-WHITE, J. J. and MCKINLEY, G. H. (2005a) The inertio-elastic planar entry flow of low-viscosity elastic fluids in micro-fabricated geometries. *Journal of Non-Newtonian Fluid Mechanics* 129 (1), 1-22
- RODD, L. E., SCOTT, T. P., COOPER-WHITE, J. J. and MCKINLEY, G. H. (2005b) Capillary break-up rheometry of low-viscosity elastic fluids. *Applied Rheology* 15 12-27
- ROININEN, K., LAHTEENMAKI, L. and TUORILA, H. (1996) Effect of umami taste on pleasantness of low-salt soups during repeated testing. *Physiology & Behavior* 60 (3), 953-958
- RONDEAU, E. and COOPER-WHITE, J. J. (2008) Biopolymer microparticle and nanoparticle formation within a microfluidic device. *Langmuir* 24 (13), 6937-6945
- ROSETT, T. R., HAMILL, T., MORRIS, K. and KLEIN, B. P. (1997) Taste qualities of reduced-sodium soups as affected by serving temperature. *Journal of Food Science* 62 (2), 421-424
- ROSETT, T. R., KENDREGAN, S. L., GAO, Y., SCHMIDT, S. J. and KLEIN, B. P. (1996) Thickening agents effects on sodium binding and other taste qualities of soup systems. *Journal of Food Science* 61 (5), 1099-1104
- ROSETT, T. R., SHIRLEY, L., SCHMIDT, S. J. and KLEIN, B. P. (1994) Na⁺ binding as measured by na-23 nuclear-magnetic-resonance spectroscopy influences the perception of saltiness in gum solutions. *Journal of Food Science* 59 (1), 206-210

ROSETT, T. R., WU, Z. H., SCHMIDT, S. J., ENNIS, D. M. and KLEIN, B. P. (1995) KCl, CaCl₂, Na⁺ binding, and salt taste of gum systems. *Journal of Food Science* 60 (4), 849-853

SABATIE, J., CHOPLIN, L., DOUBLIER, J. L., ARUL, J., PAUL, F. and MONSAN, P. (1988) Rheology of native dextrans in relation to their primary structure. *Carbohydrate polymers* 9 (4), 287-299

SAINT-EVE, A., MARTIN, N., GUILLEMIN, H., SEMON, E., GUICHARD, E. and SOUCHON, I. (2006) Flavored yogurt complex viscosity influences real-time aroma release in the mouth and sensory properties. *Journal of Agricultural and Food Chemistry* 54 (20), 7794-7803

SARKAR, D. and GUPTA, M. (2001) Further investigation of the effect of elongational viscosity on entrance flow. *Journal of Reinforced Plastics and Composites* 20 (17), 1473-1484

SATO, T., HAMADA, M. and TERAMOTO, A. (2003) Solution viscosity of a moderately stiff polymer: Cellulose tris(phenyl carbamate). *Macromolecules* 36 (18), 6840-6843

SATO, T., OHSHIMA, A. and TERAMOTO, A. (1998) Entanglement effects in semiflexible polymer solutions. 2. Huggins coefficient and inclusion of intermolecular hydrodynamic interactions. *Macromolecules* 31 (9), 3094-3098

SCHIFFMAN, S. S., MCELROY, A. E. and ERICKSON, R. P. (1980) Range of taste quality of sodium-salts. *Physiology & Behavior* 24 (2), 217-224

SCHMIDT, S. J. and AYYA, N. (1989) Characterization of sodium binding in polysaccharides using sodium 23 nmr. In: *Frontiers in carbohydrate research 1: Food application*. Elsevier Applied Science Co., New York.

SCHORSCH, C., GARNIER, C. and DOUBLIER, J. L. (1997) Viscoelastic properties of xanthan/galactomannan mixtures: Comparison of guar gum with locust bean gum. *Carbohydrate polymers* 34 (3), 165-175

SHAMA, F. and SHERMAN, P. (1973) Identification of stimuli controlling the sensory evaluation of viscosity ii oral methods. *Journal of Texture Studies* 4 111-118

SHATWELL, K. P., SUTHERLAND, I. W., ROSS-MURPHY, S. B. and DEA, I. C. M. (1991) Influence of the acetyl substituent on the interaction of xanthan with

plant polysaccharides ii. Xanthan guar gum systems. *Carbohydrate polymers* 14 (2), 115-130

SHAW, M. T. and LIU, Z. H. Z. (2006) Single-point determination of nonlinear rheological data from parallel-plate torsional flow. *Applied Rheology* 16 (2), 70-79

SHEEHAN, J. C. and HESS, G. P. (1955) A new method of forming peptide bonds. *Journal of the American Chemical Society* 77 (4), 1067-1068

SIMHA, R. and ZAKIN, J. L. (1960) Compression of flexible chain molecules in solution. *Journal of Chemical Physics* 33 (6), 1791-1793

SINGH, R. S., SAINI, G. K. and KENNEDY, J. F. (2008) Pullulan: Microbial sources, production and applications. *Carbohydrate polymers* 73 (4), 515-531

SLOTNICK, B. M., WITTICH, A. R. and HENKIN, R. I. (1988) Effect of stimulus volume on taste detection threshold for NaCl. *Chemical Senses* 13 (3), 345-353

SMITH, D. V. (1971) Taste intensity as a function of area and concentration - differentiation between compounds. *Journal of Experimental Psychology* 87 (2), 163-171

SMITH, P. K. (1985) Measurement of protein concn. in fluid - using colour formation due to complex with bicinchoninic acid of copper(s). In: Pierce Chem Co (Piec)

SQUIRES, T. M. and QUAKE, S. R. (2005) Microfluidics: Fluid physics at the nanoliter scale. *Reviews of Modern Physics* 77 (3), 977-1026

SRIDHAR, T., TIRTAATMADJA, V., NGUYEN, D. A. and GUPTA, R. K. (1991) Measurement of extensional viscosity of polymer-solutions. *Journal of Non-Newtonian Fluid Mechanics* 40 (3), 271-280

STAHLER, F., RIEDEL, K., DEMGENSKY, S., NEUMANN, K., DUNKEL, A., TAUBERT, A., RAAB, B., BEHRENS, M., RAGUSE, J. D., HOFMANN, T. and MEYERHOF, W. (2008) A role of the epithelial sodium channel in human salt taste transduction? *Chemosensory Perception* 1 (1), 78-90

STELTER, M. and BRENN, G. (2000) Validation and application of a novel elongational device for polymer solutions. *Journal of Rheology* 44 (3), 595-616

- STELTER, M., BRENN, G., YARIN, A. L., SINGH, R. P. and DURST, F. (2002) Investigation of the elongational behavior of polymer solutions by means of an elongational rheometer. *Journal of Rheology* 46 (2), 507-527
- STEVENS, S. S. (1969) Sensory scales of taste intensity. *Perception & Psychophysics* 6 (5), 302-308
- STEVENSON, R. J. and TOMICZEK, C. (2007) Olfactory-induced synesthesias: A review and model. *Psychological Bulletin* 133 (2), 294-309
- STEWART, R. E., DESIMONE, J. A. and HILL, D. L. (1997) New perspectives in gustatory physiology: Transduction, development, and plasticity. *American Journal of Physiology-Cell Physiology* 272 (1), C1-C26
- STOKES, J. R., DAVIES, G. A., MACAKOVA, L., YAKUBOV, G., BONGAERTS, J. and ROSSETTI, D. (2008) From rheology to tribology: Multiscale dynamics of biofluids, food emulsions and soft matter. *15th International Congress on Rheology/80th Annual Meeting of the Society-of-Rheology, Monterey, CA*
- STOKES, J. R., GRAHAM, L. J. W., LAWSON, N. J. and BOGER, D. V. (2001a) Swirling flow of viscoelastic fluids. Part 1. Interaction between inertia and elasticity. *Journal of Fluid Mechanics* 429 67-115
- (2001b) Swirling flow of viscoelastic fluids. Part 2. Elastic effects. *Journal of Fluid Mechanics* 429 117-153
- STONE, H. and OLIVER, S. (1966) Effect of viscosity on detection of relative sweetness intensity of sucrose solutions. *Journal of Food Science* 31 (1), 129-133
- SURH, J., DECKER, E. A. and MCCLEMENTS, D. J. (2006) Influence of pH and pectin type on properties and stability of sodium-caseinate stabilized oil-in-water emulsions. *Food Hydrocolloids* 20 (5), 607-618
- SURH, J., VLADISAVLJEVIC, G. T., MUN, S. and MCCLEMENTS, D. J. (2007) Preparation and characterization of water/oil and water/oil/water emulsions containing biopolymer-gelled water droplets. *Journal of Agricultural and Food Chemistry* 55 (1), 175-184
- TAKAHASHI, J. and NAKAZAWA, F. (1991) Effects of viscosity of liquid foods on palatal pressure. *Journal of Texture Studies* 22 (1), 13-24
- TAKO, M. and NAKAMURA, S. (1985) Synergistic interaction between xanthan and guar gum. *Carbohydrate Research* 138 (2), 207-213

- TATHAM, J. P., CARRINGTON, S., ODELL, J. A., GAMBOA, A. C., MULLER, A. J. and SAEZ, A. E. (1995) Extensional behavior of hydroxypropyl guar solutions - optical rheometry in opposed jets and flow-through porous-media. *Journal of Rheology* 39 (5), 961-986
- THEISEN, A., JOHANN, C., DEACON, M. P. and HARDING, S. E. (2000) Refractive increment data-book. Nottingham University Press, Nottingham, U.K.
- THEUNISSEN, M. J. M. and KROEZE, J. H. A. (1995) The effect of sweeteners on perceived viscosity. *Chemical Senses* 20 (4), 441-450
- TIRTAATMADJA, V., DUNSTAN, D. E. and ROGER, D. V. (2001) Rheology of dextran solutions. *Journal of Non-Newtonian Fluid Mechanics* 97 (2-3), 295-301
- TIRTAATMADJA, V., MCKINLEY, G. H. and COOPER-WHITE, J. J. (2006) Drop formation and breakup of low viscosity elastic fluids: Effects of molecular weight and concentration. *Physics of Fluids* 18 (4),
- TIRTAATMADJA, V. and SRIDHAR, T. (1993) A filament stretching device for measurement of extensional viscosity *Journal of Rheology* 37 (6), 1081-1102
- TOURNIER, C., SULMONT-ROSSE, C., SEMON, E., VIGNON, A., ISSANCHOU, S. and GUICHARD, E. (2009) A study on texture-taste-aroma interactions: Physico-chemical and cognitive mechanisms. *International Dairy Journal* 19 (8), 450-458
- VAISEY, M., BRUNON, R. and COOPER, J. (1969) Some sensory effects of hydrocolloid sols on sweetness. *Journal of Food Science* 34 (5), 397-400
- VAN AKEN, G. A., VINGERHOEDS, M. H. and DE HOOG, E. H. A. (2007) Food colloids under oral conditions. *Current Opinion in Colloid & Interface Science* 12 (4-5), 251-262
- VAN VLIET, T. (2002) On the relation between texture perception and fundamental mechanical parameters for liquids and time dependent solids. *Food Quality and Preference* 13 227-236
- WANG, Q., ELLIS, P. R., ROSS-MURPHY, S. B. and BURCHARD, W. (1997) Solution characteristics of the xyloglucan extracted from detarium senegalense gmelin. *Carbohydrate polymers* 33 (2-3), 115-124
- WEEL, K. G. C., BOELRIJK, A. E. M., ALTING, A. C., VAN MIL, P., BURGER, J. J., GRUPPEN, H., VORAGEN, A. G. J. and SMIT, G. (2002) Flavor release and

perception of flavored whey protein gels: Perception is determined by texture rather than by release. *Journal of Agricultural and Food Chemistry* 50 (18), 5149-5155

WETZEL, R., BECKER, M., BEHLKE, J., BILLWITZ, H., BOHM, S., EBERT, B., HAMANN, H., KRUMBIEGEL, J. and LASSMANN, G. (1980) Temperature behavior of human serum albumin. *European Journal of Biochemistry* 104 (2), 469-478

WHITESIDES, G. M. (2006) The origins and the future of microfluidics. *Nature* 442 368-373

WIJNTJES, R. H. W., DUIJS, M. H. G., JONGSCHAAP, R. J. J. and MELLEMA, J. (2000) Linear rheology of guar gum solutions. *Macromolecules* 33 (26), 9594-9605

WILDE, P., MACKIE, A., HUSBAND, F., GUNNING, P. and MORRIS, V. (2004) Proteins and emulsifiers at liquid interfaces. *Advances in Colloid and Interface Science* 108 63-71

WONG, E. H. M., RONDEAU, E., SCHUETZ, P. and COOPER-WHITE, J. (2009) A microfluidic-based method for the transfer of biopolymer particles from an oil phase to an aqueous phase. *Lab on a Chip* 9 (17), 2582-2590

WONG, S. S. (1993) Chemistry of protein conjugation and cross-linking. CRC Press, Boca Raton, London

WOOD, F. W. (1968) Psychophysical studies on the consistency of liquid foods. In: Rheology and texture of foodstuffs, SCI monograph No 27

WUNDERLICH, T., STELTER, M., TRIPATHY, T., NAYAK, B. R., BRENN, G., YARIN, A. L., SINGH, R. P., BRUNN, P. O. and DURST, F. (2000) Shear and extensional rheological investigations in solutions of grafted and ungrafted polysaccharides. *Journal of Applied Polymer Science* 77 (14), 3200-3209

YAMATOYA, K. and SHIRAKAWA, M. (2003) Xyloglucan: Structure, rheological properties, biological functions and enzymatic modification. *Current Trends in Polymer Science* 8 27-72

YAMPOLSKAYA, G. and PLATIKANOV, D. (2006) Proteins at fluid interfaces: Adsorption layers and thin liquid films. *Advances in Colloid and Interface Science* 128 159-183

YASEEN, E. I., HERALD, T. J., ARAMOUNI, F. M. and ALAVI, S. (2005) Rheological properties of selected gum solutions. *Food Research International* 38 (2), 111-119

YE, Q., HECK, G. L. and DESIMONE, J. A. (1991) The anion paradox in sodium taste reception - resolution by voltage-clamp studies. *Science* 254 (5032), 724-726

YOSHIDA, R. and NINOMIYA, Y. (2010) New insights into the signal transmission from taste cells to gustatory nerve fibers. *International Review of Cell and Molecular Biology, Vol 279* 279 101-134

ZIRNSAK, M. A. and BOGER, D. V. (1998) Axisymmetric entry flow of semi-dilute xanthan gum solutions: Prediction and experiment. *Journal of Non-Newtonian Fluid Mechanics* 79 (2-3), 105-136

APPENDICES TO CHAPTER 2

Appendix 2.1: Origin of the Kramer equation for determination of the gap error (Kramer et al., 1987).

In parallel plate geometry, the constitutive equation defining the shear rate is:

$$\dot{\gamma}_R = \frac{R\omega}{h}$$

where $\dot{\gamma}_R$ the shear rate at the rim of the geometry, R the radius of the plate, ω the angular velocity and h the gap height.

This equation can be written for both values of the shear rate: the shear rate commanded to the software ($\dot{\gamma}_{R\ com}$), function of the commanded gap height (h_{com}), and the actual value of the shear rate ($\dot{\gamma}_{R\ real}$), function of the actual gap height (h_{real}):

$$\dot{\gamma}_{R\ com} = \frac{R\omega}{h_{com}} \text{ and } \dot{\gamma}_{R\ real} = \frac{R\omega}{h_{real}}$$

Combining the two previous equations, the actual shear rate at the rim $\dot{\gamma}_{R\ real}$ can be expressed as a function of the commanded shear rate $\dot{\gamma}_{R\ com}$:

$$\dot{\gamma}_{R\ real} = \frac{h_{com}\dot{\gamma}_{R\ com}}{h_{real}}$$

In addition, the actual gap height (h_{real}) can be expressed as the commanded gap height (h_{com}) plus the gap error ε :

$$h_{real} = h_{com} + \varepsilon$$

The two previous equations are combined to obtain:

$$\dot{\gamma}_{R\ real} = \frac{h_{com} \dot{\gamma}_{R\ com}}{h_{com} + \varepsilon}$$

The actual shear rate can also be expressed as function of the shear stress τ and the fluid viscosity η :

$$\dot{\gamma}_{R\ real} = \frac{\tau}{\eta}$$

Combining the two previous equations, we obtain:

$$\tau = \eta \frac{h_{com} \dot{\gamma}_{R\ com}}{h_{com} + \varepsilon}$$

After rearrangement, Equation 2.1 is finally obtained. Based on Equation 2.1, the plot

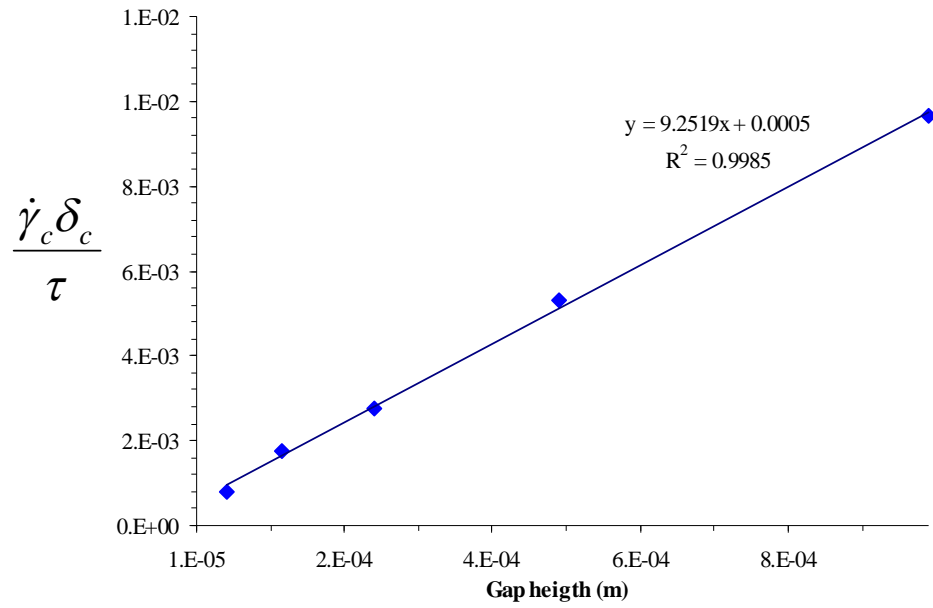
$\frac{h_{com} \dot{\gamma}_{R\ com}}{\tau}$ in function of h_{com} should be a straight line of slope $\frac{1}{\eta}$ and of intercept $\frac{\varepsilon}{\eta}$.

A direct numerical estimation of the gap error is obtained from the regression. Such a plot is depicted in Appendix 2.2.

$$\frac{h_{com} \dot{\gamma}_{R\ com}}{\tau} = \frac{1}{\eta} h_{com} + \frac{\varepsilon}{\eta}$$

Where h_{com} is the commanded gap height, h_{real} the actual gap height, $\dot{\gamma}_{R\ com}$ the commanded shear rate, τ the shear stress, η the apparent viscosity at the edge for $\dot{\gamma}$ and ε the gap error.

Appendix 2.2: Example of Kramer regression based on the data at 200 s⁻¹ and different gap heights for silicon oil 100 cS.



Appendix 2.3: Derivation of the equations to correct thin film data for non-Newtonian behaviour and gap error.

As shown in Appendix 2.1, the actual shear rate as the rim accounting for gap error is given by:

$$\dot{\gamma}_{R \text{ real}} = \frac{h_{com} \dot{\gamma}_{R \text{ com}}}{h_{com} + \varepsilon}$$

This can be rearranged:

$$\dot{\gamma}_{R \text{ real}} = \frac{\dot{\gamma}_{R \text{ com}}}{1 + \frac{\varepsilon}{h_{com}}}$$

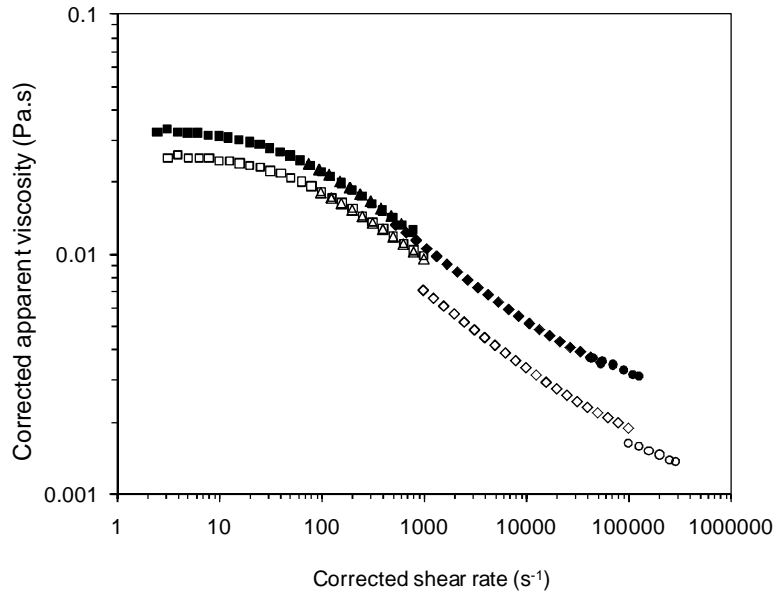
To account for non-Newtonian behaviour, the 4/5 single point correction is applied:

$$\dot{\gamma}_{\text{average real}} = \frac{4}{5} \dot{\gamma}_{R \text{ real}}$$

Hence combining the two equations above, the corrected shear rate is given by:

$$\dot{\gamma}_{\text{corrected}} = \frac{4}{5} \times \frac{\dot{\gamma}_{R \text{ com}}}{1 + \frac{\varepsilon}{h_{com}}}$$

Appendix 2.4: Viscosity data for a guar solution at 0.5% acquired using thin film rheology at gap 1000 μm (■), 500 μm (▲), 50 μm (◆) and 30 μm (●) before corrections (full symbols) and after corrections (void symbols).



Appendix 2.5: Example of scoresheet/computer screen for paired comparison.

Difference in saltiness: Test 1

You have two coded samples in front on you. Taste them from left to right and circle the sample that appears the MORE SALTY.

239 573

Even if you do not perceive any difference, you have to make a choice.

Appendix 2.6: Example of data pooling and Friedman analysis for multiple paired comparison of three samples A, B and C by 30 panellists.

Comparing **A to B**, A was found saltier 22 times (B was found saltier 8 times)

Comparing **B to C**, C was found saltier 25 times (B was found saltier 5 times)

Comparing **A to C**, C was found saltier 18 times (A was found saltier 12 times)

Those results are pooled and tabulated as follow:

Row sample (saltier)	Column sample (less salty)		
	A	B	C
A		22	12
B	8		5
C	18	25	
Rank sums:	86	107	77

The rank sums are obtained by adding the sum of the row frequencies to twice the sum of the column frequency, e.g. for sample A, $(22+12) + 2 \times (8+18) = 86$.

The test statistic, Friedman's T, is computed as followed:

$$T = \frac{4}{pt} \left(\sum_{i=1}^t R_i^2 \right) - 9p(t-1)^2$$

where p is the number of judges, t the number of samples, R_i the rank sum for the i^{th} sample.

In this case, $T=21.07$, which is significant at 0.05% (value of T compared to the critical value of χ^2 with (t-1) degree of freedom).

The HSD for comparing two rank sums is given by $HSD = q_{\alpha,t,\infty} \sqrt{pt/4}$ ($q_{\alpha,t,\infty}$ can be found in the tables). In this case, $q_{\alpha,t,\infty} = 3.31$ for $\alpha=0.05$, so $HSD=15.7$. Since the difference between the rank sum of A and B is larger than 15.7, samples A and B appeared significantly different, as were B and C. However, the difference between the rank sum of A and C is only 9, A and C are not significantly different.

Appendix 2.7: Example of a scoresheet/computer screen for triangle test.

Triangle test		
<p>You have three coded samples in front on you. Two are identical and one is different. Please taste them from left to right and circle the odd one out.</p>		
475	288	139
<p>Even if you do not perceive any difference, you have to make a choice.</p>		

APPENDICES TO CHAPTER 3

Appendix 3.1: Results of saltiness perception of Study B in multiple paired comparisons between a) the samples A, B and C b) the samples C, D and E (22 panellists).

a)

Row sample (saltier)	Column sample (less salty)		
	A	B	C
A		9	6
B	13		8
C	16	14	

b)

Row sample (saltier)	Column sample (less salty)		
	C	D	E
C		5	4
D	17		5
E	18	17	

Appendix 3.2: Results of saltiness perception of Study C3 in multiple paired comparisons between the dextran samples D_H, D_M and D_L salted at 0.6% w/v (viscosity 30 mPa.s, 33 panellists).

Row sample (saltier)	Column sample (less salty)		
	D _H	D _M	D _L
D _H		12	8
D _M	21		12
D _L	25	21	

Appendix 3.3: Results of sweetness perception of Study C4 in multiple paired comparisons between the dextran samples D_H, D_M and D_L sweetened at 5% w/v sucrose (viscosity 30 mPa.s, 27 panellists).

<i>Row sample (more sweet)</i>	<i>Column sample (less sweet)</i>		
	D _H	D _M	D _L
D _H		10	12
D _M	17		8
D _L	15	19	

Appendix 3.4: Results of thickness perception of Study B in multiple paired comparisons between a) the samples A, B and C b) the samples C, D and E (22 panellists).

a)

<i>Row sample (thicker)</i>	<i>Column sample (thinner)</i>		
	A	B	C
A		15	18
B	11		18
C	8	8	

b)

<i>Row sample (thicker)</i>	<i>Column sample (thinner)</i>		
	C	D	E
C		18	25
D	8		17
E	1	9	

APPENDICES TO CHAPTER 4

Appendix 4.1: Multiple paired comparison between Boger fluid and inelastic control salted at 0.6% w/w and 0.7% w/w NaCl for a) maltodextrins-based samples and b) glucose syrup-based samples (7 panellists).

a) Maltodextrine-based

Row samples (saltier)	Column samples (less salty)			
	Boger 0.6% NaCl	Boger 0.7% NaCl	Inelastic control 0.6% NaCl	Inelastic control 0.7% NaCl
Boger 0.6% NaCl		2	3	0
Boger 0.7% NaCl	5		5	3
Inelastic control 0.6% NaCl	4	2		2
Inelastic control 0.7% NaCl	7	4	5	

b) Glucose syrup-based

Row samples (saltier)	Column samples (less salty)			
	Boger 0.6% NaCl	Boger 0.7% NaCl	Inelastic control 0.6% NaCl	Inelastic control 0.7% NaCl
Boger 0.6% NaCl		5	4	3
Boger 0.7% NaCl	2		1	4
Inelastic control 0.6% NaCl	3	6		5
Inelastic control 0.7% NaCl	4	3	2	

APPENDICES TO CHAPTER 5

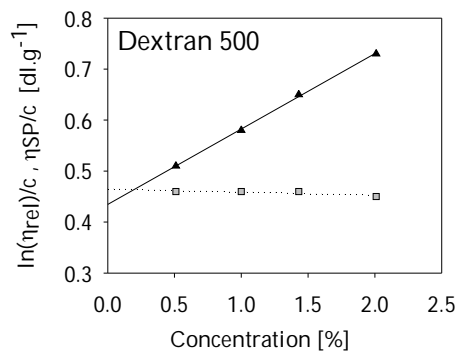
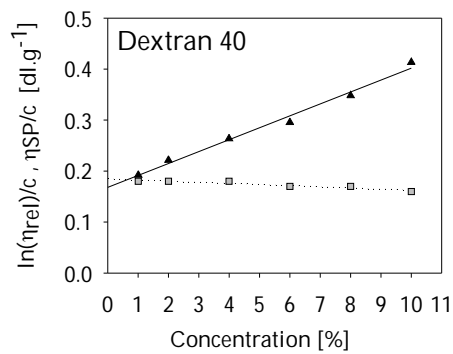
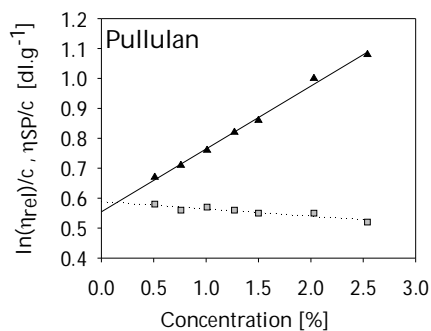
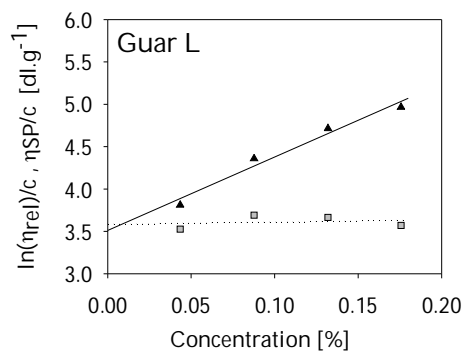
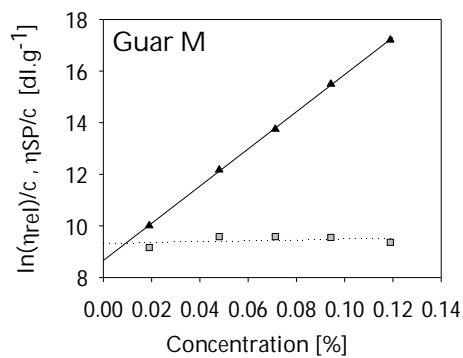
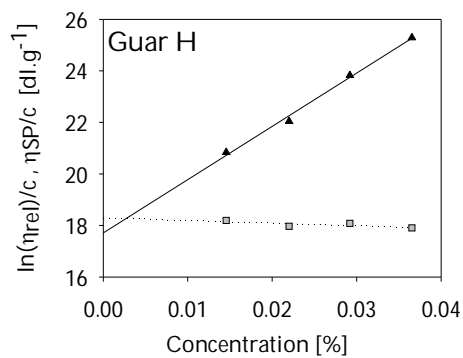
Appendix 5.1: Density of the samples at 20°C.

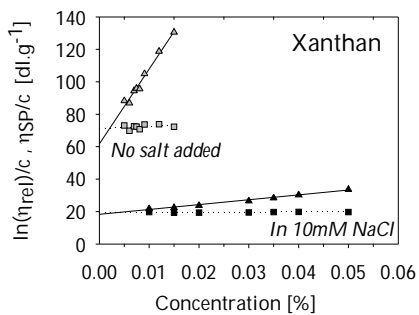
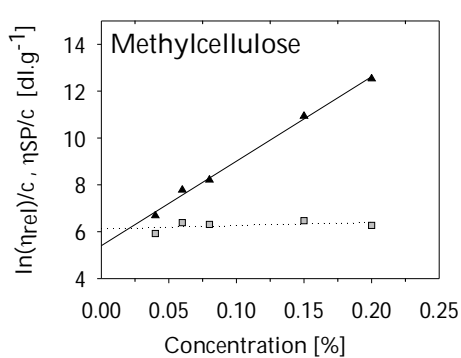
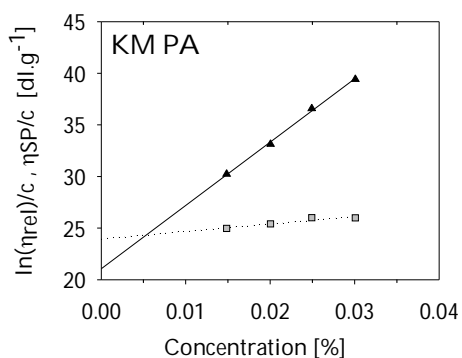
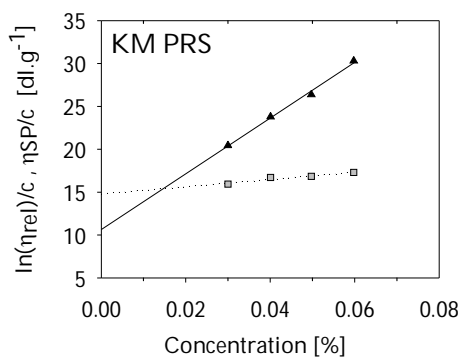
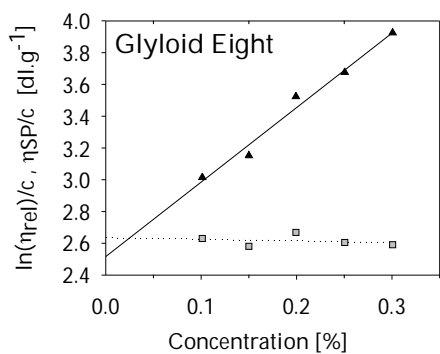
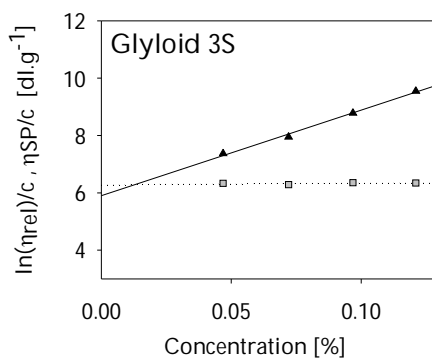
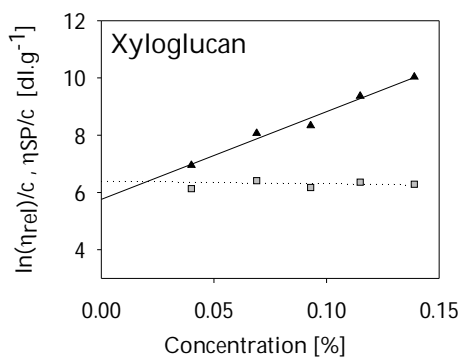
	Polymer	Concentration [% w/w]	ρ [g.cm ⁻³]
Galactomannans	Guar H	0.35%	1.0039
		0.50%	1.0051
	Guar L	0.50%	1.0038
		1.50%	1.0084
	LBG	0.45%	1.0019
		0.50%	1.0020
Xyloglucans	PXylo	0.50%	1.0021
		0.85%	1.0032
	Gly3S	0.50%	1.0022
		0.82%	1.0032
	Gly8	0.50%	1.0024
		2.07%	1.0081
Konjac Mannans	KM-LM	0.50%	1.0022
	KM-PA	0.13%	1.0007
		0.50%	1.0021
	KM-RS	0.21%	1.0018
0.50%		1.0021	
Dextrans	500	14.50%	1.0639
	40	20.50%	1.0875
	Methylcellulose	0.50%	1.0016
		0.72%	1.0022
	Xanthan	0.08%	1.0005
		0.50%	1.0025
	Pullulan	9.33%	1.0376

Appendix 5.2: Surface tension of the samples. For some samples (indicated by n/a, non available), the surface tension could not be successfully measured. An estimation is given between brackets.

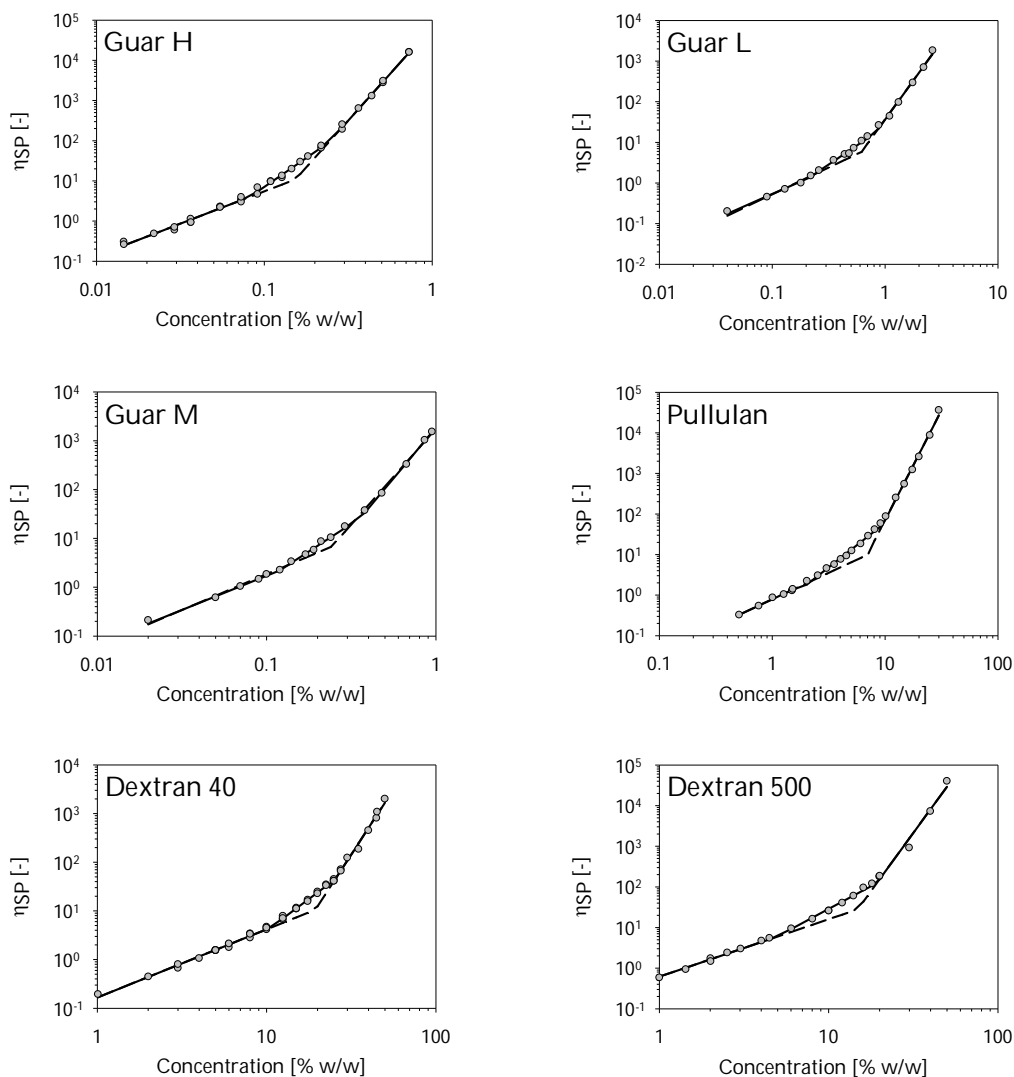
		All matched at zero shear viscosity		All at 0.5%
		concentration	surface tension	surface tension
<i>Galactomannans</i>	Guar L	1.50%	46.11 ± 0.11	51.61 ± 0.30
	Guar H	0.35%	58.83 ± 0.42	55.39 ± 0.24
	LBG	0.45%	55.53 ± 0.66	54.49 ± 0.78
<i>Xyloglucans</i>	3S	0.82%	71.39 ± 0.09	69.96 ± 0.85
	PXylo.	0.85%	66.64 ± 1.00	67.56 ± 0.15
	GlyEight	2.11%	58.37 ± 0.06	67.36 ± 1.03
<i>Konjac mannan</i>	KM PA	0.13%	59.94 ± 0.71	n/a (55)
	KM PRS	0.21%	67.22 ± 0.07	n/a (62)
	KM LM		-	65.44 ± 0.11
<i>Dextrans mannan</i>	40	28.00%	63.18 ± 1.20	-
	500	15.50%	n/a (65)	-
	Pullulan	9.33%	65.05 ± 1.07	-
	MCellulose	0.72%	53.14 ± 1.16	60.71 ± 0.81
	Xanthan	0.08%	64.83 ± 1.79	60.12 ± 0.16

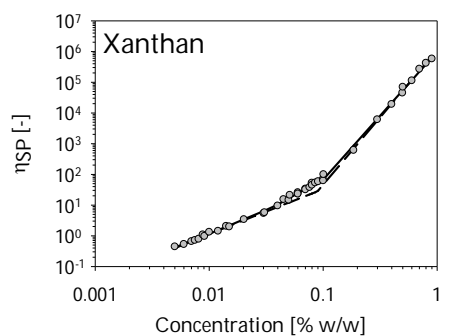
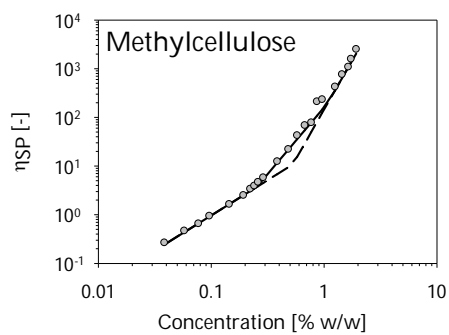
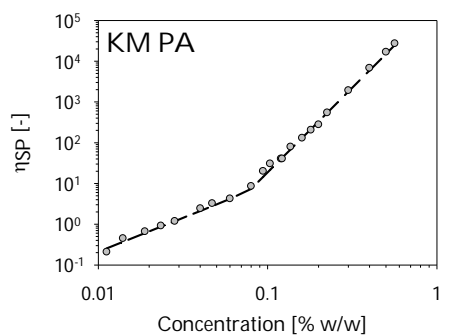
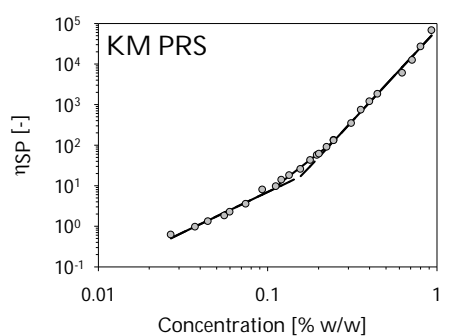
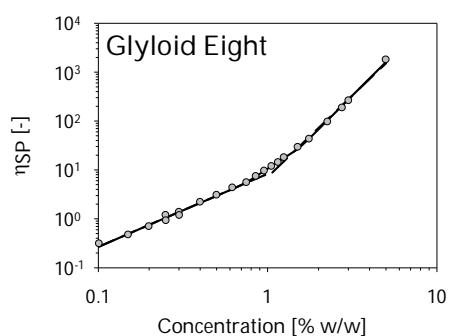
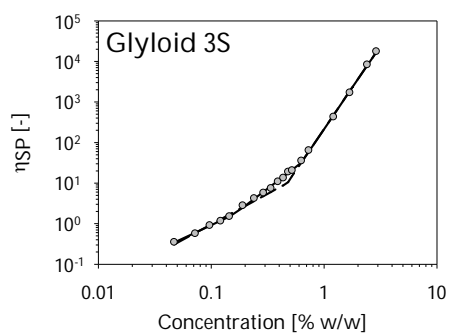
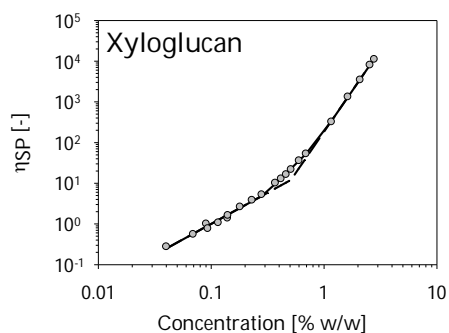
Appendix 5.3: Combined Huggins (▲) and Kraemer (■) extrapolation to intrinsic viscosity for all the polymers studied here.



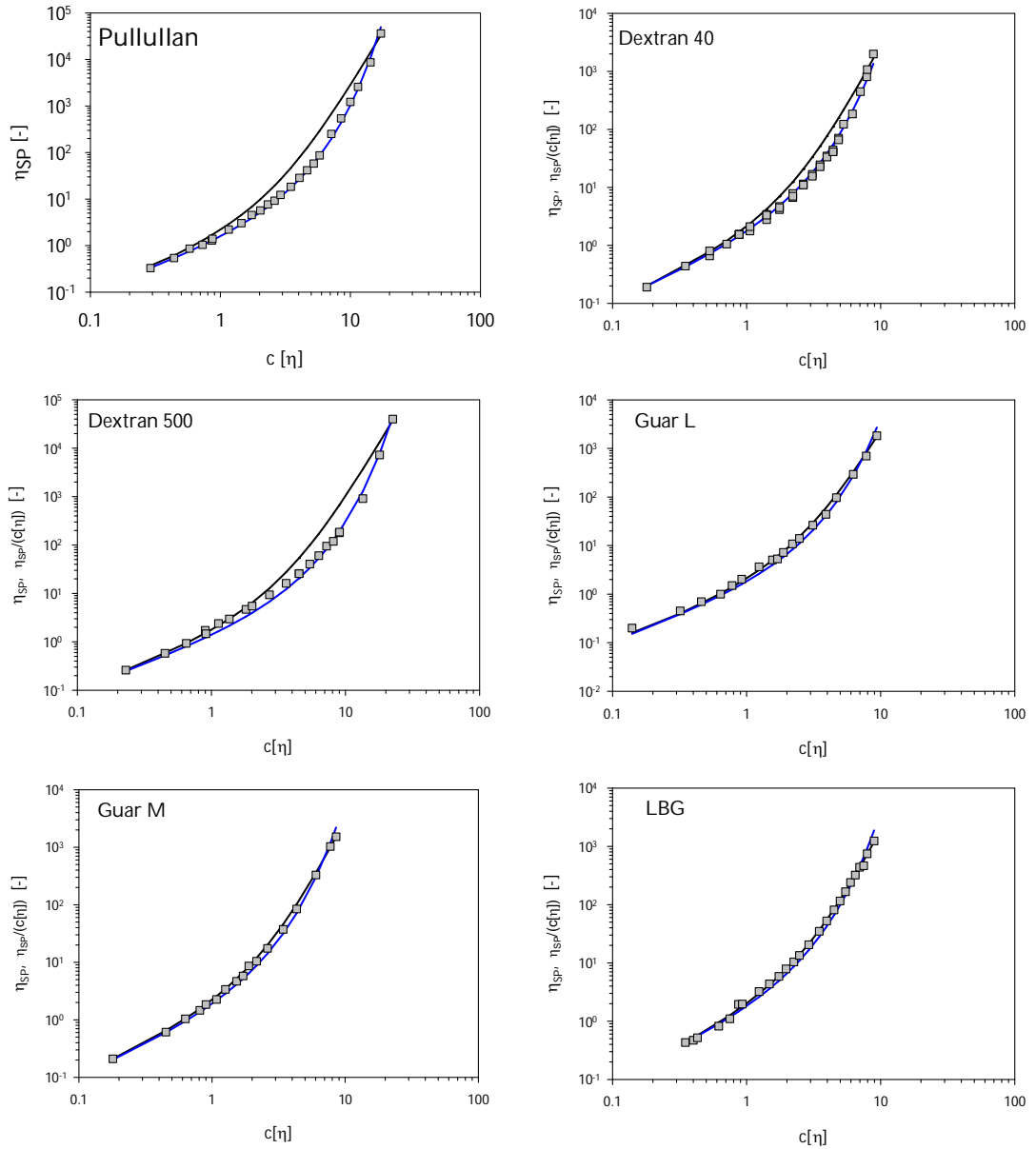


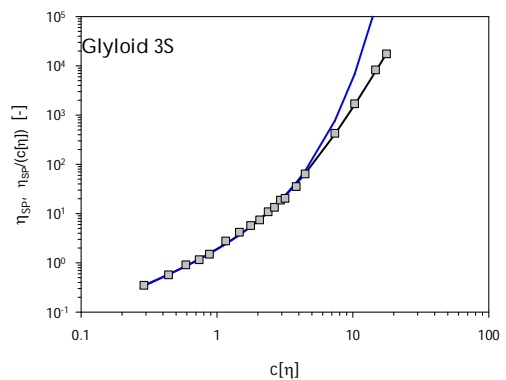
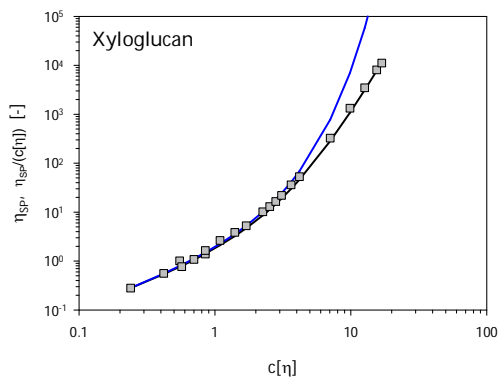
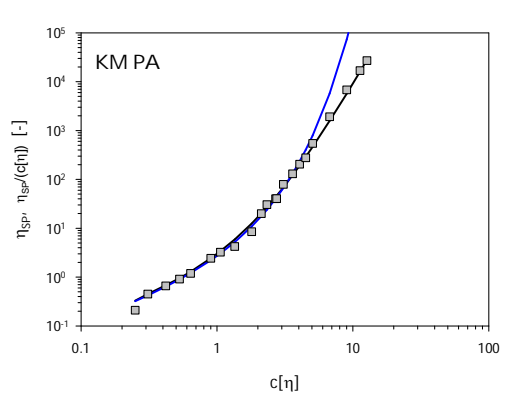
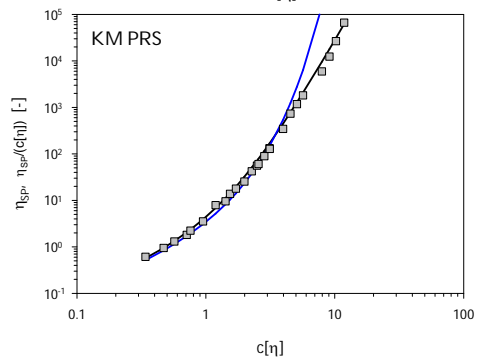
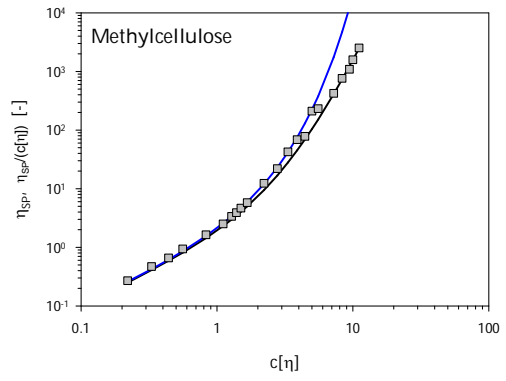
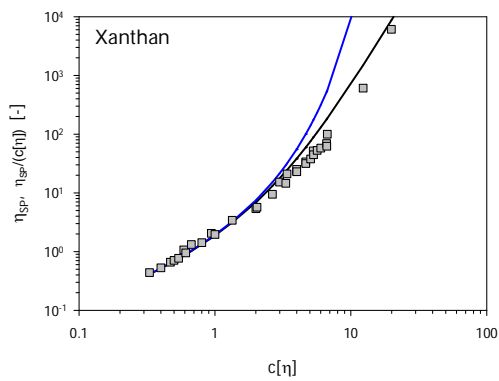
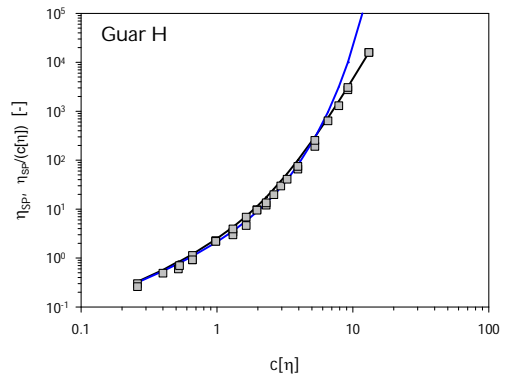
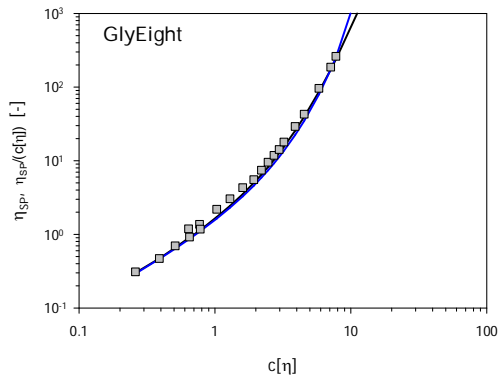
Appendix 5.4: C^* plot for all the polymers studied. The grey dots are experimental data point, the continuous black line corresponds to the linear fit with two critical concentrations (c^* , c^{}) and the dashed line corresponds to the linear fit with one critical concentration (c^*).**





Appendix 5.5: Fit of the Martin equation (in blue, considering infinite neighbours) and the modified Martin Equation (in black, considering 4 neighbours) to experimental data (■).





Appendix 5.6: Cross model parameters. The Cross model equation is defined as:

$$\eta = \frac{\eta_0 - \eta_\infty}{1 + k\dot{\gamma}^n} + \eta_\infty$$

where η is the apparent viscosity (Pa.s), $\dot{\gamma}$ is the shear rate (s⁻¹), η_0 is the zero shear viscosity (Pa.s), η_∞ is the infinite shear rate viscosity (Pa.s), k is a time constant (s) and n a dimensionless constant.

		η_0	η_∞	n	k	$\eta(10000s^{-1})$
Guar L	0.50%	0.008	0.004	0.687	0.001	0.006
	1.00%	0.034	0.001	0.043	0.427	0.011
	1.50%	0.109	0.005	0.534	0.039	0.022
Guar H	0.22%	0.035	0.003	0.033	0.650	0.005
	0.35%	0.100	0.004	0.724	0.044	0.007
	0.50%	0.947	0.010	0.775	0.185	0.012
	0.70%	2.887	0.010	0.306	0.768	0.015
LBG	0.50%	0.162	0.006	0.785	0.017	0.013
	1%	0.113	0.007	0.818	0.011	0.012
PXylo	0.50%	0.025	0.004	0.746	0.003	0.010
	0.85%	0.099	0.006	0.837	0.005	0.015
Gly 3S	0.50%			Not fitting		
	0.83%	0.100	0.005	0.821	0.006	0.014
GlyEigth	0.50%	0.006		Not fitting (Newtonian)		
	2.11%	0.107	0.004	0.700	0.003	0.041
KM LM	0.50%	0.010	0.001	0.017	5.280	0.002
KM PA	0.13%	0.112	0.004	0.704	0.054	0.007
	0.50%	23.233	0.001	0.774	0.856	0.023
KM PRS	0.21%	0.146	0.001	0.431	0.335	0.008
	0.50%	4.958	0.001	0.691	0.460	0.019
Dextran 500kDa	15.50%	0.104		Not fitting (Newtonian)		
Dextran 40kDa	28%	0.107		Not fitting (Newtonian)		
Pullulan	9.33%	0.104	0.026	0.827	0.000	0.072
Methylcellulose	0.50%	0.042	0.001	0.454	0.026	0.013
	0.72%	0.105	0.004	0.643	0.012	0.021
Xanthan	0.08%			Not fitting		
	0.50%			Not fitting		

